

**Functional analysis of mitochondrial sirtuins in
C. elegans and mammalian cells**

PhD Thesis

in partial fulfillment of the requirements
for the degree “Doctor rerum naturalium”
in the Molecular Biology Program
at the Georg August University Göttingen,
Faculty of Biology

submitted by

Martina Wirth

born in

Lauingen a.d. Donau, Germany

2010

Affidavit

I hereby declare that the presented thesis “Functional analysis of mitochondrial sirtuins in *C. elegans* and mammalian cells” has been written independently and with no other sources and aids than quoted.

Göttingen, September 30, 2010

List of publications

Wirth, M., and Jedrusik-Bode, M. (2009). Interplay between histone deacetylase SIR-2, linker histone H1 and histone methyltransferases in heterochromatin formation. *Epigenetics* 4:6, 1-4.

Wirth, M., Paap, F., Fischle, W., Wenzel, D., Agafonov, D.E., Samatov, T.R., Wisniewski, J.R., and Jedrusik-Bode, M. (2009). HIS-24 linker histone and SIR-2.1 deacetylase induce H3K27me3 in the *Caenorhabditis elegans* germ line. *Mol Cell Biol* 29, 3700-3709.

Illarionov B., Eisenreich W., Wirth M., Yong Lee C., Eun Woo Y., Bacher A., Fischer M. (2007). Lumazine proteins from photobacteria: localization of the single ligand binding site to the N-terminal domain. *Biol Chem.* 388(12), 1313-23.

Vutova, P., Wirth, M., Hippe, D., Gross, U., Schulze-Osthoff, K., Schmitz, I., and Luder, C.G. (2007). *Toxoplasma gondii* inhibits Fas/CD95-triggered cell death by inducing aberrant processing and degradation of caspase 8. *Cell Microbiol* 9, 1556-1570.

Table of contents

Acknowledgements	IV
Abstract	V
List of figures	VI
List of tables	VII
Abbreviations	VIII
1 Introduction	1
1.1 Discovery of sirtuins	1
1.2 Biochemical function and structural features of sirtuins.....	1
1.2.1 Enzymatic activity of sirtuins - Deacetylase vs. ADP-ribosyltransferase activity	1
1.2.2 Catalytic reaction mechanism of NAD ⁺ -dependent deacetylation	2
1.2.3 Structural properties of sirtuins	5
1.3 Mammalian sirtuins.....	8
1.3.1 The nuclear sirtuins SIRT1, SIRT6, SIRT7	9
1.3.1.1 SIRT1	9
1.3.1.2 SIRT6 and SIRT7	10
1.3.2 The cytoplasmic sirtuin SIRT2.....	11
1.3.3 The mitochondrial sirtuins SIRT3, SIRT4, SIRT5.....	11
1.3.3.1 SIRT3	11
1.3.3.2 SIRT4	12
1.3.3.3 SIRT5	13
1.4 <i>Caenorhabditis elegans</i> sirtuins	14
1.5 Modulation of sirtuin activity by NAD ⁺ metabolism.....	16
1.6 Reversible mitochondrial protein acetylation	17
1.7 Open questions and objective of this PhD thesis	18
2 Material and Methods	20
2.1 Material and Reagents	20
2.1.1 Laboratory equipment	20
2.1.2 Chemicals	21
2.1.3 Kits	22
2.1.4 Consumables and reagents	23
2.1.5 Enzymes	23
2.1.6 Antibodies	24
2.1.7 Peptides	24
2.1.8 Oligonucleotides.....	24
2.1.9 Plasmids	25
2.1.10 Bacterial Strains	26
2.1.11 <i>C. elegans</i> strains.....	26
2.1.12 Cell lines.....	27
2.2 Molecular biological methods.....	27
2.2.1 Plasmid DNA preparation	27
2.2.2 DNA digestion with restriction endonucleases	28

2.2.3	Polymerase chain reaction (PCR).....	28
2.2.4	Site-directed mutagenesis.....	28
2.2.5	Separation and isolation of DNA fragments	28
2.2.6	Transformation of plasmids into chemically competent bacteria.....	29
2.2.7	General cloning procedure	29
2.2.8	Summary of cloned plasmid constructs.....	30
2.2.8.1	pET11a based expression vector construct.....	30
2.2.8.2	pEU3-NII-StrepII based expression vector constructs	30
2.2.9	pCDNA3.1(+)-FLFL-HAHA-N mammalian expression vector based constructs	30
2.2.10	pCDNA3.1(+)-FLFL-HAHA-C mammalian expression vector based constructs	32
2.2.11	pEGFP-N1 mammalian expression vector based constructs	33
2.2.11.1	L4440 based constructs	33
2.2.11.2	pPD115.62 based constructs.....	33
2.3	Protein biochemical methods	34
2.3.1	SDS polyacrylamide gel electrophoresis (SDS-PAGE)	34
2.3.2	Protein detection techniques.....	34
2.3.2.1	Coomassie Blue staining	34
2.3.2.2	Western blotting	34
2.3.3	Mass spectrometry and data analysis	35
2.3.4	Generation of SIR-2.2-specific antibodies using recombinant protein for immunization. 35	
2.3.4.1	Expression of recombinant SIR-2.2 in <i>E. coli</i>	35
2.3.4.2	Purification of recombinant SIR-2.2 from inclusion bodies.....	35
2.3.4.3	Gelfiltration and ion exchange chromatography	36
2.3.4.4	High-performance liquid chromatography (HPLC)	36
2.3.4.5	Immunization, purification and characterization of SIR-2.2-specific antibodies from antiserum.....	36
2.4	<i>C. elegans</i> based methods	37
2.4.1	Culturing <i>C. elegans</i> on agar plates.....	37
2.4.2	Liquid culture of <i>C. elegans</i>	38
2.4.3	Axenization to synchronize or decontaminate <i>C. elegans</i>	38
2.4.4	Freezing and recovery of <i>C. elegans</i> stocks	38
2.4.5	Single worm PCR.....	38
2.4.6	Isolation of Mitochondria for cellular subfractionation	39
2.4.7	Preparation of <i>C. elegans</i> protein extracts.....	40
2.4.7.1	Preparation of total worm protein extracts	40
2.4.7.2	Preparation of mitochondrial protein extracts	40
2.4.7.3	Preparation of crude <i>C. elegans</i> lysate for Western blot analysis	41
2.4.8	Immunoprecipitation of proteins from <i>C. elegans</i> extract.....	41
2.4.9	Crossing of <i>C. elegans</i>	41
2.4.10	Isolation of RNA from <i>C. elegans</i> and reverse transcription	42
2.4.11	Microinjection of <i>C. elegans</i>	42
2.4.12	Generation of GFP/mCherry reporters using a PCR fusion-based approach	43
2.4.13	RNA interference (RNAi) by microinjection and feeding	45
2.4.14	Integration of extrachromosomal arrays by UV radiation.....	46
2.4.15	DiI staining.....	46
2.4.16	Microscopic analysis of <i>C. elegans</i>	46
2.4.17	Oxidative stress assay.....	47
2.5	Tissue culture based methods.....	47
2.5.1	Cultivation of cells	47
2.5.2	Transfection of cells	47
2.5.3	Immunoprecipitation of proteins from transfected cells.....	47
2.5.4	Analysis of protein acetylation using acetyllysine-specific antibodies	48

2.6	Enzymatic activity assays.....	48
2.6.1	Histone deacetylase (HDAC) activity assay.....	48
2.6.2	Spectrophotometric pyruvate carboxylase activity assay	49
2.6.3	Deacetylase activity assay in combination with mass spectrometry	49
3	Results	51
3.1	Analysis of SIR-2 protein expression and localization in <i>C. elegans</i>	51
3.1.1	SIR-2.2 and SIR-2.3 do not localize to the cell nucleus.....	51
3.1.2	SIR-2.2 and SIR-2.3 expression and localization patterns partially overlap.....	53
3.1.3	Analysis of SIR-2.3 expression in head neurons by DiI staining.....	54
3.1.4	SIR-2.2 and SIR-2.3 localize to mitochondria	56
3.2	Characterization of <i>sir-2.2</i> and <i>sir-2.3</i> deletion mutant <i>C. elegans</i> strains.....	58
3.2.1	<i>Sir-2.2</i> and <i>sir-2.3</i> deletion mutant worms used in this study	58
3.2.2	Knockdown of <i>sir-2.2</i> in a <i>sir-2.3</i> mutant background leads to a very mild phenotype ...	62
3.2.3	Sensitivity towards oxidative stress.....	63
3.3	Identification of SIR-2.2 and SIR-2.3 interaction partners	65
3.3.1	Identification of mitochondrial biotin carboxylases as factors interacting with SIR-2.2 and SIR-2.3	65
3.3.2	Evolutionarily conserved interaction of mammalian SIRT4 with mitochondrial biotin-dependent carboxylases	69
3.3.3	Analysis of the interaction specificity of <i>C. elegans</i> and mammalian sirtuins with mitochondrial biotin-dependent carboxylases	70
3.3.4	Mapping of the biotin carboxylase domain mediating interaction with SIRT4	72
3.4	Regulation of biotin carboxylase function by mitochondrial sirtuins	75
3.4.1	Mitochondrial biotin carboxylases are acetylated proteins	75
3.4.2	Analysis of the enzymatic activities of <i>C. elegans</i> SIR-2.2, SIR-2.3 and mammalian SIRT4.....	78
3.4.2.1	<i>In vitro</i> histone deacetylase activity (HDAC) assay.....	80
3.4.2.2	Mass spectrometry based <i>in vitro</i> deacetylase activity assay	81
3.4.3	Analysis of bovine PC activity after deacetylase reaction with <i>C. elegans</i> sirtuins.....	84
3.4.4	Reduced acetylation levels of MCCC1 and PCCA in cells overexpressing SIRT4.....	85
4	Discussion.....	87
4.1	SIR-2.2 and SIR-2.3 are mitochondrial proteins strongly expressed in tissue with high metabolic demand	87
4.2	Is there genetic redundancy between SIR-2.2 and SIR-2.3 in <i>C. elegans</i> ?.....	88
4.3	SIR-2.2 and SIR-2.3 mediate resistance to oxidative stress.....	89
4.4	Evolutionary conserved interaction with mitochondrial biotin carboxylases	91
4.5	Mitochondrial biotin-dependent carboxylases are acetylated proteins	92
4.6	Are mammalian SIRT4 and <i>C. elegans</i> SIR-2.2 and SIR-2.3 protein deacetylases?.....	92
4.7	Possible physiological role of interaction	94
5	Summary and Conclusion	101
Appendix		102
A.1	SIR-2.2 protein levels in <i>sir-2.2::gfp</i> and <i>sir-2.3(ok444); sir-2.2RNAi</i> worms	102
A.2	R programming for mass spectrometry analysis	102
A.3	Mass Spectrometry results	103
References		107
Curriculum vitae		119

Acknowledgements

Firstly, I would like to thank my two supervisors Dr. Monika Jedrusik-Bode and Dr. Wolfgang Fischle for giving me the chance to work on this project, for their support, encouraging ideas and patience over these years.

I am also very grate full to my PhD Thesis committee Prof. Herbert Jäckle and Prof. Frauke Melchior for their great interest, helpful comments and support in scientific and challenging non-scientific matters.

I am grateful for support from the Deutsche Forschungsgemeinschaft (DFG JE 505/1-1).

I want to thank Dr. Steffen Burkhardt, Ivana Bacakova and Kerstin Grüniger from the coordination office for their great support, help and commitment during all phases of my Master and PhD years.

I want to thank Jennifer Seefeldt for great work and commitment during her lab rotation.

I am grateful to all my collaborators:

Prof. Eric Verdin and Linh Ho for the analysis with the anti-acetyllysine antibodies and reagents;
Dr. Henning Urlaub and his group for their excellent mass spectrometry work and help;
Dr. Dirk Wenzel for the excellent electron microscopy analyses, his enthusiasm and helpful ideas;
Dr. Dmitry Agafonov and Dr. Timur Sumatov for wheat germ extract protein expressions.

I am very grateful to Dr. Dieter Klopfenstein and his group members for teaching me microinjection of *C. elegans*, sharing the microinjection aperture, reagents and helpful advice.

I also would like to thank Christian Wurm and Prof. Peter Rehling for helping me with reagents, protocols and advice when I started to explore the exciting field of mitochondrial research. In addition, I want to thank Mathias Beller for help with lipid assays, although I could not include them in this thesis.

I am grateful to Prof. Heidi Tissenbaum, the Caenorhabditis Genetics Center (CGC) and the Mitani Laboratory (National BioResource Project) for *C. elegans* strains.

Many thanks to all members of the Fischle group, for their help, friendship and assistance in the lab. I'm very grateful to Franziska, DingDing and Jenni for their help and essential constant support of the "worm folk". Moreover, a big thank you goes to my worm fellow Nora for sharing knowledge, reagents, Brezen, chocolate and especially the passion for Jonny Cash with me. Many big thanks also to Henriette, Kerstin, Nora and Sabi for their support, for great laughs, "Cisciscis's" and "Ha's", Cafe Kreuzberg and later on Gromo breakfast sessions, and the Bananenweizen or Bierle at the end of the day.

Many, many thanks also to the best flatmate ever, "ooooh Konstantina!", for supporting, feeding and spoiling me together with Christoph especially in the last three months. I'm also very grateful to Ieva and Achim for many funny moments and hopefully more to come.

I am grateful to my family, for their trust in me and their continued support.

Last but not least, I am most indebted to Stefan. Thank you for your love, trust, support, the many kilometers you drove for me,for keeping me sane and keeping my back clear especially in the last weeks.

Abstract

Silent information regulator 2 (SIR-2) proteins, also referred to as sirtuins, are highly conserved NAD⁺-dependent protein deacetylases that are emerging to be important energy sensors and regulators of metabolism, stress responses and aging. The mammalian sirtuin protein family is quite complex, comprising seven members (SIRT1 to SIRT7) with different subcellular localization (nucleus, cytoplasm, and mitochondria). The mitochondrial SIRT4 remains the only mammalian sirtuin of which ADP-ribosyltransferase activity, but no NAD⁺-dependent deacetylase activity could be detected. SIRT4 negatively regulates insulin secretion and might be a therapeutic target for treatment of diabetes. However, this requires a better understanding of its biological and enzymatic function as well as identification of novel substrates.

The simple multicellular organism *C. elegans* possesses only four SIR-2 variants (SIR-2.1 to SIR-2.4) that all show high sequence conservation to mammalian sirtuins. Overexpression of SIR-2.1 increases the life span of *C. elegans*, suggesting that these are also intriguing players in regulating longevity and in linking metabolism to aging-related processes. Whereas the majority of studies have focused on SIR-2.1, the variants SIR-2.2 and SIR-2.3, which are most homologous to mammalian SIRT4, remain by and large uncharacterized.

In this PhD thesis I showed that SIR-2.2 and SIR-2.3 are also localized to mitochondria and are predominantly expressed in *C. elegans* tissues with high energy demand, e.g. pharynx and body wall muscles. *Sir-2.2* and *sir-2.3* deletion mutant worms did not exhibit an obvious phenotype under normal growth conditions. However, overexpression and loss of SIR-2.2 and SIR-2.3 resulted in increased sensitivity to oxidative stress, suggesting that both proteins function in oxidative stress responses. Using immunoprecipitation experiments in combination with mass spectrometry, I was able to identify all three mitochondrial members of biotin-dependent carboxylases, pyruvate carboxylase (PC), propionyl-CoA carboxylase (PCC) and methylcrotonyl-CoA carboxylase (MCC), as factors interacting with SIR-2.2 and SIR-2.3. The interaction was evolutionarily conserved with mammalian SIRT4 and mediated by the homologous biotin carboxylation domain, which is present in all three proteins. Mitochondrial biotin carboxylases play an important role in gluconeogenesis, amino acid catabolism, β -oxidation and ketone body formation. Since all three proteins were found to be acetylated on multiple lysine residues, their enzymatic activity might be regulated by NAD⁺-dependent deacetylation through mammalian SIRT4 and *C. elegans* SIR-2.2 and SIR-2.3. SIRT4, SIR-2.2 and SIR-2.3 did not exhibit NAD⁺-dependent protein deacetylase activity on PC peptides containing the conserved acetylated lysine residues K273 and K741. However, overexpression of SIRT4 specifically reduced the acetylation levels of the α -subunits of PCC and MCC, indicating for the first time that SIRT4 might be indeed a NAD⁺-dependent deacetylase.

Overall, this study showed that *C. elegans* SIR-2.2 and SIR-2.3 and mammalian SIRT4 have conserved functions. Their interaction with mitochondrial biotin carboxylases indicates an important role as energy sensors and regulators of metabolic adaptation during nutrient deprivation.

List of figures

Figure 1-1: NAD ⁺ -dependent protein deacetylation reaction catalyzed by sirtuins.	2
Figure 1-2: Proposed chemical reaction mechanism of NAD ⁺ -dependent protein deacetylation catalyzed by sirtuins.	3
Figure 1-3: Multiple sequence alignment of the catalytic core domain region of sirtuins with known three-dimensional structures.	6
Figure 1-4: Three-dimensional crystal structures of different sirtuins.	7
Figure 1-5: Tissue-specific regulation of metabolism by SIRT1.	10
Figure 1-6: Metabolic functions of mitochondrial sirtuins.	14
Figure 2-1: Western blot analysis of generated SIR-2.2-specific antibodies.	37
Figure 2-2: PCR-fusion based approach for generating a C-terminal <i>gfp</i> reporter construct.	44
Figure 3-1: Expression and localization pattern of SIR-2 proteins in <i>C. elegans</i>	52
Figure 3-2: The expression and localization patterns of SIR-2.2 and SIR-2.3 partially overlap.	53
Figure 3-3: DiI staining of <i>sir-2.3::gfp</i> transgenic worms.	54
Figure 3-4: Analysis of SIR-2.2 and SIR-2.3 subcellular localization by electron microscopy.	56
Figure 3-5: Subcellular fractionation of N2 and <i>sir-2.3::gfp</i> transgenic worms by differential centrifugation.	58
Figure 3-6: RT-PCR analysis of the <i>sir-2</i> deletion mutant alleles.	59
Figure 3-7: Characterization of truncated proteins resulting from <i>sir-2</i> deletion mutant alleles.	60
Figure 3-8: Increased sensitivity to oxidative stress in worms overexpressing or deficient in SIR-2.2 and SIR-2.3.	64
Figure 3-9: Identification of mitochondrial biotin carboxylases as factors interacting with SIR-2.2.	66
Figure 3-10: Role of mitochondrial biotin-dependent carboxylases in anaplerosis and generation of ketone bodies.	67
Figure 3-11: Verification of mitochondrial biotin-dependent carboxylases as interaction partners of <i>C. elegans</i> SIR-2.2 and SIR-2.3.	68
Figure 3-12: Identification of endogenous mitochondrial biotin-dependent carboxylases as interacting factors of SIR-2.3.	69
Figure 3-13: Evolutionarily conserved interaction of mammalian SIRT4 with mitochondrial biotin carboxylases.	70
Figure 3-14: Analysis of specificity of interaction with <i>C. elegans</i> SIR-2.1, SIR-2.2 and SIR-2.3.	71
Figure 3-15: Interaction specificity of human mitochondrial sirtuins with mitochondrial biotin-dependent carboxylases.	72
Figure 3-16: Mapping of the domain of PC, PCCA and MCCC1 mediating interaction with SIRT4.	75
Figure 3-17: Lysine acetylation sites identified in PC, PCCA and MCCC1 by different mass spectrometric approaches.	77
Figure 3-18: Analysis of protein acetylation levels by Western blotting with anti-acetyllysine-specific antibodies.	78
Figure 3-19: Highly conserved catalytic core domain of <i>C. elegans</i> sirtuins.	78
Figure 3-20: Analysis of NAD ⁺ -dependent HDAC activity.	81
Figure 3-21: Mass spectrometric analysis of <i>in vitro</i> deacetylase reactions using acetylated peptides.	82
Figure 3-22: No changes in bovine PC activity after treatment with <i>C. elegans</i> SIR-2.2 and SIR-2.3.	84
Figure 3-23: Overexpression of SIRT4 specifically reduces the acetylation levels of PCCA and MCCC1 <i>in vivo</i>	86
Figure 4-1: Working hypothesis I.	96
Figure 4-2: Role of mitochondrial biotin carboxylases in insulin secretion.	98
Figure 4-3: Working hypothesis II.	99
Figure A-1: Analysis of SIR-2.2 protein levels in <i>sir-2.2::gfp</i> and <i>sir-2.3(ok444); sir-2.2RNAi</i> worms.	102

List of tables

Table 1-1: Diversity of mammalian sirtuins.	8
Table 1-2: Diversity of <i>C. elegans</i> SIR-2 proteins.	16
Table 2-1: Generally used laboratory equipment.	20
Table 2-2: Generally used chemicals.	21
Table 2-3: Generally used kits.	22
Table 2-4: Generally used consumables and reagents.	23
Table 2-5: Generally used enzymes.	23
Table 2-6: Generally used antibodies.	24
Table 2-7: Peptides used for deacetylase activity assays.	24
Table 2-8: Generally used plasmids.	25
Table 2-9: Generally used bacterial strains.	26
Table 2-10: <i>C. elegans</i> strains used in this study.	26
Table 2-11: Molecular details for genotyping.	27
Table 2-12: Cell lines used in this study.	27
Table 3-1: Overview on available <i>sir-2</i> mutant deletion strains.	59
Table 3-2: Knock down of <i>sir-2.2</i> in <i>sir-2.3(ok444)</i> mutant worms did not cause an obvious phenotype.	63
Table 3-3: Summary on observed NAD ⁺ -dependent deacetylase activity on acetylated peptides analyzed by mass spectrometry.	82

Abbreviations

α	anti- (antibody)	MCC	Methylcrotonyl-coenzyme A carboxylase
Δ	delta = deletion	MCCC1	Methylcrotonyl-coenzyme A α -subunit
aa	amino acid(s)	M	molar
ac	acetylation	min	minute(s)
ATP	adenosine triphosphate	Met	methionine
bp	base pair(s)	MNase	Micrococcus nuclease
BC	biotin carboxylase	mRNA	messenger ribonucleic acid
BCCP	biotin carboxyl carrier protein	MS	mass spectrometry
C	Celsius	n	nano
cDNA	complementary DNA	NAD ⁺	nicotinamide adenine dinucleotide
<i>C. elegans</i>	<i>Caenorhabditis elegans</i>	NADH	nicotinamide adenine dinucleotide (reduced form)
CoA	Coenzyme A	NAM	nicotin amide
cpm	count(s) per minute	NGM	Nematode growth medium
CGC	Caenorhabditis Genetics Center	PBS	phosphoate buffered saline
CR	Caloric restriction	PC	Pyruvate carboxylase
CT	carboxyltransferase	PCC	Propionyl-coenzyme A carboxylase
DMEM	Dulbeccos Modified Eagle's Medium	PCCA	Propionyl coenzyme A carboxylase α -subunit
DMSO	Dimethyl sulfoxide	PCR	polymerase chain reaction
DNA	deoxyribonucleic acid	PCT	pyruvate carboxyltransferase
DNase	deoxyribonuclease	PTM	post-translational modification
dNTP	deoxyribonucleic acid	rDNA	ribosomal deoxyribonucleic acid
DIC	differential interference contrast	RNA	ribonucleic acid
DiI	1,1'-dioctadecyl-3,3',3'-tetramethylindocarbocyanine perchlorate	RNAi	RNA interference
dsRNA	double-stranded ribonucleic acid	ROS	reactive oxygen species
DTT	DL-1,4-dithiothreitol	rpm	rotations per minute
EDTA	ethylenediaminetetraacetic acid	RT	room temperature
<i>E. coli</i>	<i>Escherichia coli</i>	RT-PCR	reverse transcriptase polymerase chain reaction
g	gram	SDS-PAGE	sodium dodecyl sulfate polyacrylamide gel electrophoresis
GDH	glutamate dehydrogenase	sec	second(s)
GFP	green fluorescent protein	S.E.M.	standard error of mean
h	hour(s)	SIR-2	silent information regulator-2
HDAC	histone deacetylase	SIRT	sirtuin
HEK293	human embryonic kidney 293 cell line	TCA	Tricarboxylic acid
HP1	heterochromatin protein 1	Thr	Threonine
HRP	horse-radish peroxidase	U	unit(s)
Ile	isoleucine	UTR	untranslated regions
IP	immunoprecipitation	UV	ultraviolet
IPTG	isopropyl β -D-thiogalactopyranoside	v/v	volume per volume
kb	kilo bases	Val	valine
kDa	kilo Dalton	w/o	without
l	liter	w/v	weight per volume
LB	Luria-Bertani (broth)	wt	wild type
m	milli	μ	micro

1 Introduction

1.1 Discovery of sirtuins

Silent information regulator 2 (SIR-2) proteins, also referred to as sirtuins, are a family of NAD⁺-dependent protein deacetylases [1], which are highly conserved and are found in all three domains of life (eubacteria, archaea and eukaryotes) [2, 3]. Unlike other protein deacetylases, SIR-2 requires NAD⁺ as a cofactor [4-6]. Deacetylation of a substrate is coupled to hydrolysis of NAD⁺ and the acetyl group is transferred from its substrate to a NAD⁺ cleavage product to form O-acetyl-ADP-ribose (Figure 1-1) [7, 8].

Saccharomyces cerevisiae SIR-2, the founding member of this large and diverse protein family, was originally identified as a factor necessary for epigenetic silencing of the mating type loci, telomeres and ribosomal DNA (rDNA) [9]. But it is also involved in DNA replication [10], DNA repair, suppression of recombination [11] and aging [12, 13]. Since increased dosage of SIR-2 and its orthologs leads to longevity in yeast [12, 14], worms [15] and flies [16-18], sirtuins have become intriguing players in regulating longevity and linking metabolism to aging and age-related diseases such as diabetes, neurodegenerative diseases and cancer [1, 19]. Mammalian sirtuins comprising seven members (SIRT1 to SIRT7, Table 1-1) are emerging to also have roles in regulating age-related processes. In recent years numerous target proteins of sirtuins, primarily of mammalian SIRT1, have been identified. Mammalian sirtuins are important regulators of diverse cellular processes such as cell survival, genome stability, stress responses and metabolism [20].

Although NAD⁺-dependent deacetylase activity has been demonstrated for SIR-2 proteins of many organisms, their physiological role in invertebrates and vertebrates has just begun to be investigated and therefore still remains largely elusive. Sirtuins might be critical regulators and novel targets for treating age-associated diseases [21]. However, a better understanding of sirtuins and the pathways regulated by them is required for that.

1.2 Biochemical function and structural features of sirtuins

1.2.1 Enzymatic activity of sirtuins - Deacetylase vs. ADP-ribosyltransferase activity

The first insight into the enzymatic activity of sirtuins provided the characterization of *Salmonella typhimurium* CobB, a bacterial SIR-2 protein. In the cobalamin biosynthesis pathway CobB was able to substitute CobT. As CobT is a known phosphoribosyltransferase catalyzing the transfer of phosphoribose from nicotinate mononucleotide to dimethylbenzimidazole, a pyridine nucleotide transfer reaction was also anticipated for SIR-2 proteins [22].

In 1999 Frye [23] showed that the *E. coli* SIR-2-like protein CobB and human SIRT2 were both able to transfer ³²P from [³²P]-NAD⁺ to bovine serum albumin (BSA). Shortly after this the group of Danesh Moazed reported that yeast SIR-2 transfers ADP-ribose from NAD⁺ to histones, which was thought to mediate gene silencing in yeast [24]. However, the weak

mono-ADP-ribosyl transferase activities described by both groups were soon attributed to non-enzymatic labeling, since a more robust NAD^+ -dependent deacetylase activity on acetylated histones was discovered for numerous SIR-2 proteins including yeast, mammals and bacterial CobB [4-6].

NAD^+ -dependent deacetylase activity has been demonstrated now for the majority of mammalian sirtuins (Table 1-1), except for mammalian SIRT4 where only mono-ADP-ribosyltransferase activity has been detected [25, 26]. Thus, it is still under debate whether sirtuins exhibit dual activities (NAD^+ -dependent deacetylases and mono-ADP-ribosyltransferase) or are true deacetylases.

1.2.2 Catalytic reaction mechanism of NAD^+ -dependent deacetylation

The fact that sirtuins require NAD^+ and catalyze a novel mechanism of histone/protein deacetylation distinguished them from known histone deacetylases and consequently sirtuins were classified as a new HDAC class, i.e. HDAC class III. Whereas class I and class II HDACs remove acetyl groups by hydrolysis, sirtuins catalyze protein deacetylation via an energetically costly mechanism consuming NAD^+ [27].

Deacetylation of an acetylated substrate is coupled to hydrolysis of NAD^+ generating deacetylated lysine, nicotine amide (NAM) and the unique compound O-acetyl-ADP-ribose (O-acetyl-ADPR) (Figure 1-1) [7, 8].

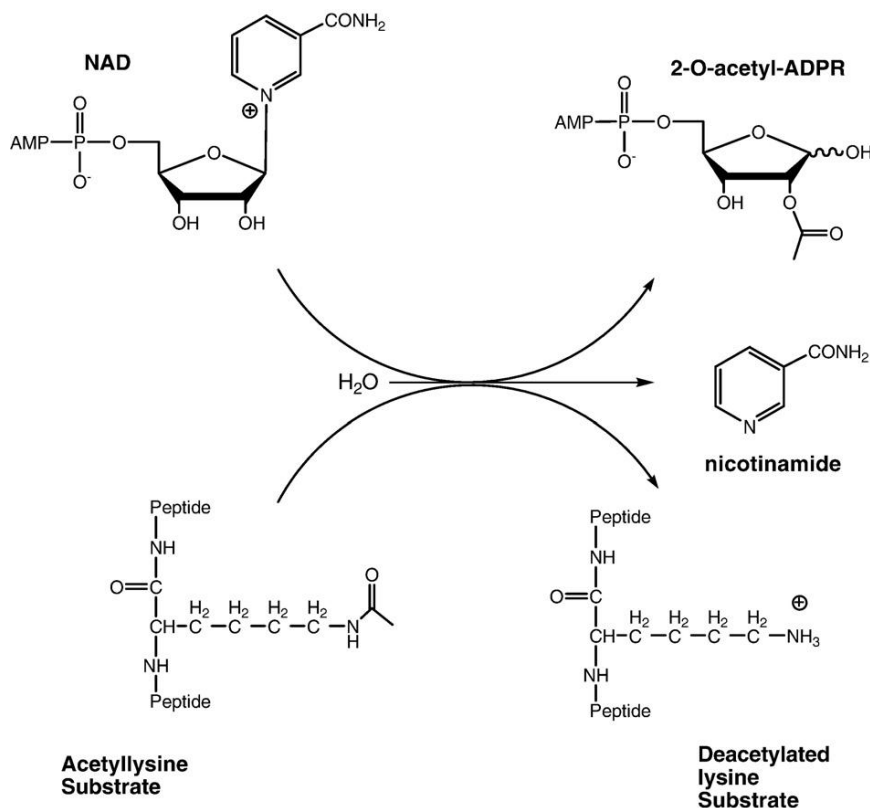


Figure 1-1: NAD^+ -dependent protein deacetylation reaction catalyzed by sirtuins.

Deacetylation of an acetylated lysine substrate is coupled to hydrolysis of NAD^+ . The acetyl group is transferred from its substrate to a NAD^+ cleavage product to form the novel compound O-acetyl-ADP-ribose. Figure taken from [21].

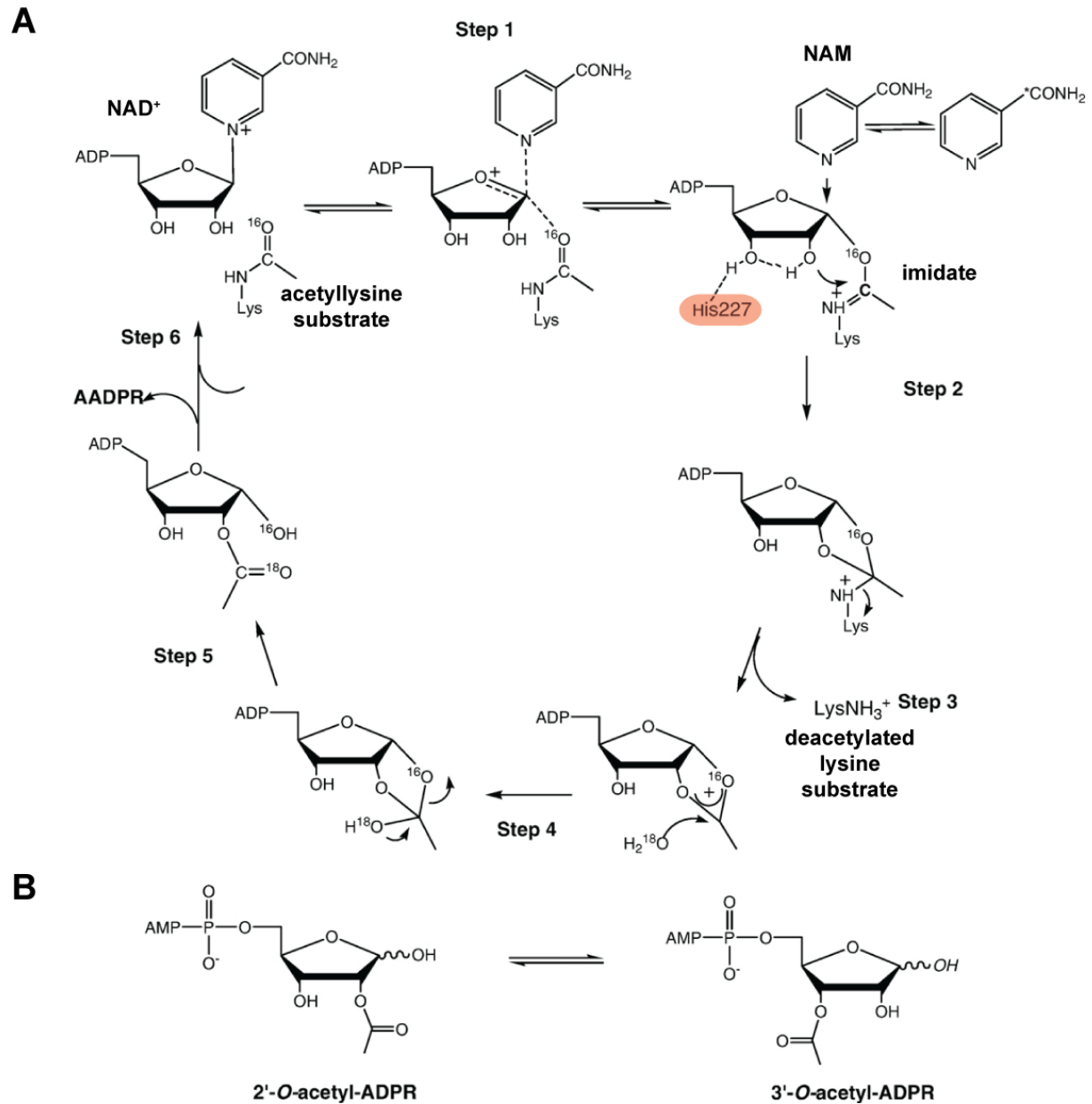


Figure 1-2: Proposed chemical reaction mechanism of NAD⁺-dependent protein deacetylation catalyzed by sirtuins.

A. The ADPR-peptidyl imidate mechanism proposes that the acetyl oxygen of the bound acetyllysine substrate undergoes a nucleophilic attack of the 1'-carbon of the ADP-ribose moiety of bound NAD⁺, forming NAM and a peptidyl imidate intermediate (Step 1). In step 2 the activated 2'-hydroxyl of the nicotinamide ribose attacks the imidate carbon generating the 1',2'-cyclic intermediate. Subsequently 2'-O-Acetyl-ADP-ribose (2'-OAAADPr) is formed via multiple reaction steps. An active site histidine is shown in red. **B.** In solution OAAADPr interconverts non-enzymatically between 2'-OAAADPr and 3'-OAAADPr. Figure adapted from [21].

A more detailed mechanism of the proposed deacetylation reaction referred to as ADPR-peptidyl-imidate mechanism is shown in Figure 1-2. After binding of NAD⁺ and the acetyllysine the acetyl oxygen undergoes in the first reaction step a nucleophilic attack of the 1'-carbon of the ADP-ribose moiety of NAD⁺ generating NAM and a peptidyl-imidate, a novel reactive intermediate. Next, the 2'-hydroxyl of the nicotinamide ribose is activated by an active site histidine and attacks the peptidylimidate carbon generating the 1',2'-cyclic intermediate. Multiple reaction steps including elimination of the deacetylated lysine followed

by addition of water lead to the formation of 2'-O-Acetyl-ADP-ribose (2'-OAADPr). OAADPr undergoes non-enzymatic interconversions between 2'-OAADPr and 3'-OAADPr after release from the active site [21, 28].

Although NAD^+ -dependent deacetylation is considered to be the primary enzymatic activity of sirtuins, not all sirtuins exhibit measurable protein deacetylase activity on histone substrates [25, 29]. For SIRT4 [25, 26] and SIRT6 [30] ADP-ribosyltransferase activity, transferring a single ADP-ribosyl group from NAD^+ to proteins or itself, was reported. Recently SIRT6 proved to be a histone 3 lysine 9 acetyl (H3K9ac)-specific deacetylase [31], implicating that SIRT4 might be as well a true deacetylase with very strict specificity for substrates that have not been identified yet.

Interestingly, some sirtuins such as yeast SIR-2 or the *Trypanosoma brucei* SIR-2 orthologue TbSIR2rp1 possess both NAD^+ -dependent protein deacetylase and mono ADP-ribosyltransferase activity [4, 7, 32], raising the question whether sirtuins have dual activities. ADP-ribosyltransferase activity was predominantly determined by detecting [^{32}P]-radiolabeled proteins after incubating them with sirtuins in the presence of [^{32}P]- NAD^+ . As none of the studies provided information on identities of the residues that were specifically ADP-ribosylated and ADP-ribosylation can also occur non-enzymatically [33, 34], the ADP-ribosyltransferase activity of sirtuins has been doubted. Currently relatively little is known about a potential reaction mechanism, since only few studies have been investigating the exact mechanism in more detail [21, 35-37]. Consistently, all studies reported that sirtuin-dependent ADP-ribosyltransferase activity is in general very weak compared to the protein deacetylase activity [30, 35, 36]. In the case of *T. brucei* SIR-2, it could be shown that to some extent the observed ADP-ribosylation results from non-enzymatic ADP-ribosylation by the deacetylation reaction product O-Acetyl-ADPR or ADPR (generated by hydrolysis of O-Acetyl-ADPR). However, to a larger extent the ADP-ribosylation seemed to be enzymatic via a proposed imidate-dependent reaction mechanism. The nucleophilic attack on the initially formed peptidyl-imidate intermediate (Figure 1-2) is probably intercepted by an exogenous nucleophile, such as the ϵ -amino of a lysine in the amino acid side chain instead of the acetylated lysine, yielding an ADP-ribosylated protein [35]. As the observed ADP-ribosylation was five orders of magnitude slower than the deacetylase reaction, it is questionable whether protein ADP-ribosylation by sirtuins is physiologically relevant. Although it is possible that the relative efficiencies not only of NAD^+ -dependent ADP-ribosylation but also deacetylation are modulated *in vivo* by accessory proteins, metabolites or posttranslational modifications in response to changes in cellular energy status or stress [35]. Sirtuin activity is inhibited by its reaction product nicotinamide (NAM) in a non-competitive manner, suggesting that NAM is an endogenous negative regulator of sirtuin activity and prevents intracellular NAD^+ depletion [5, 38]. NAM inhibits the catalytic activity of sirtuins probably via a process termed base exchange. The formed peptidyl-imidate intermediate (Figure 1-2) reacts with NAM reforming NAD^+ at the expense of deacetylation [39, 40].

O-AADPR, the reaction product of NAD^+ -dependent deacetylation, might act as a signaling molecule or serve as a substrate for downstream enzymatic processes [41]. In yeast O-AADPR seems to function in chromatin silencing by binding to SIR-3 and inducing conformational changes that promote the loading of the SIR-2/SIR-3/SIR-4 silencing complex

onto nucleosomes [42]. In mammals O-AADPR binds to the histone variant macroH2A [43], but apart from that the role of O-AADPR in mammals is still unresolved.

Since sirtuins have been implicated in life span determination, a lot of effort has been put into identifying small molecules and protein interactors modulating sirtuin activity. The mechanistic details of sirtuin activation by these factors still need to be resolved [21], but this area of research might provide potent therapeutic agents for treatment of age-associated diseases in the near future.

1.2.3 Structural properties of sirtuins

Next to biochemical analyses, determination of the three dimensional structures of several sirtuin proteins has provided important information for understanding the catalytic mechanism, substrate specificity and inhibitory mechanisms of sirtuins [44].

Sirtuin proteins from different organisms all contain a highly conserved catalytic core domain comprising approximately 275 amino acids (shown in multiple sequence alignment in Figure 1-3), but differ highly in length and amino acid composition in their N- and C-terminal flanking regions [2, 3]. In agreement, a high degree of structural superposition is found in the crystal structures of the catalytic core domains of different sirtuin proteins (Figure 1-4 A). The catalytic core region folds into two domains, a large domain structurally homologous to a Rossmann-fold domain, and a smaller, zinc-binding domain, which is structurally more diverse. The Rossmann-fold domain, which is commonly found in NAD^+/NADH binding proteins, features a typical NAD^+ -binding site comprising a conserved Gly-X-Gly motif for phosphate binding, a pocket for a NAD^+ molecule, and charged residues for the ribose group binding [45].

The small Zn^{2+} -binding domain is composed of two insertions within the Rossmann-fold domain. One of them contains a conserved Zn^{2+} -binding motif (Cys-X₂₋₄-Cys-X₁₅₋₄₀-Cys-X₂₋₄-Cys), coordinating a structurally important zinc ion [46]. As the small domain is structurally most diverse among different sirtuins in terms of primary sequence, three dimensional structure and relative position to the large domain, it might have an important function in determination of substrate specificity. In addition, the small Zn^{2+} -binding domain might provide binding sites for small molecules and proteins, modulating the enzymatic activity of sirtuins. It might also influence the subcellular location of sirtuins [44, 45, 47].

The large and the small domain are connected by several loops that form a pronounced, extended cleft. NAD^+ and the acetyl-lysine containing peptide substrates access the cleft from opposite sides to bind to the enzyme. Deacetylation is catalyzed by conserved amino acid residues and reactive groups of the bound substrate molecules in a hydrophobic tunnel buried in the cleft (Figure 1-4 B). The importance of this region for catalysis is also reflected by the fact that it has the highest sequence conservation within sirtuins (GAGISTSCGIPDFR in Hst2). Indeed, mutation of specific residues in this region disrupts protein deacetylase activity [44].

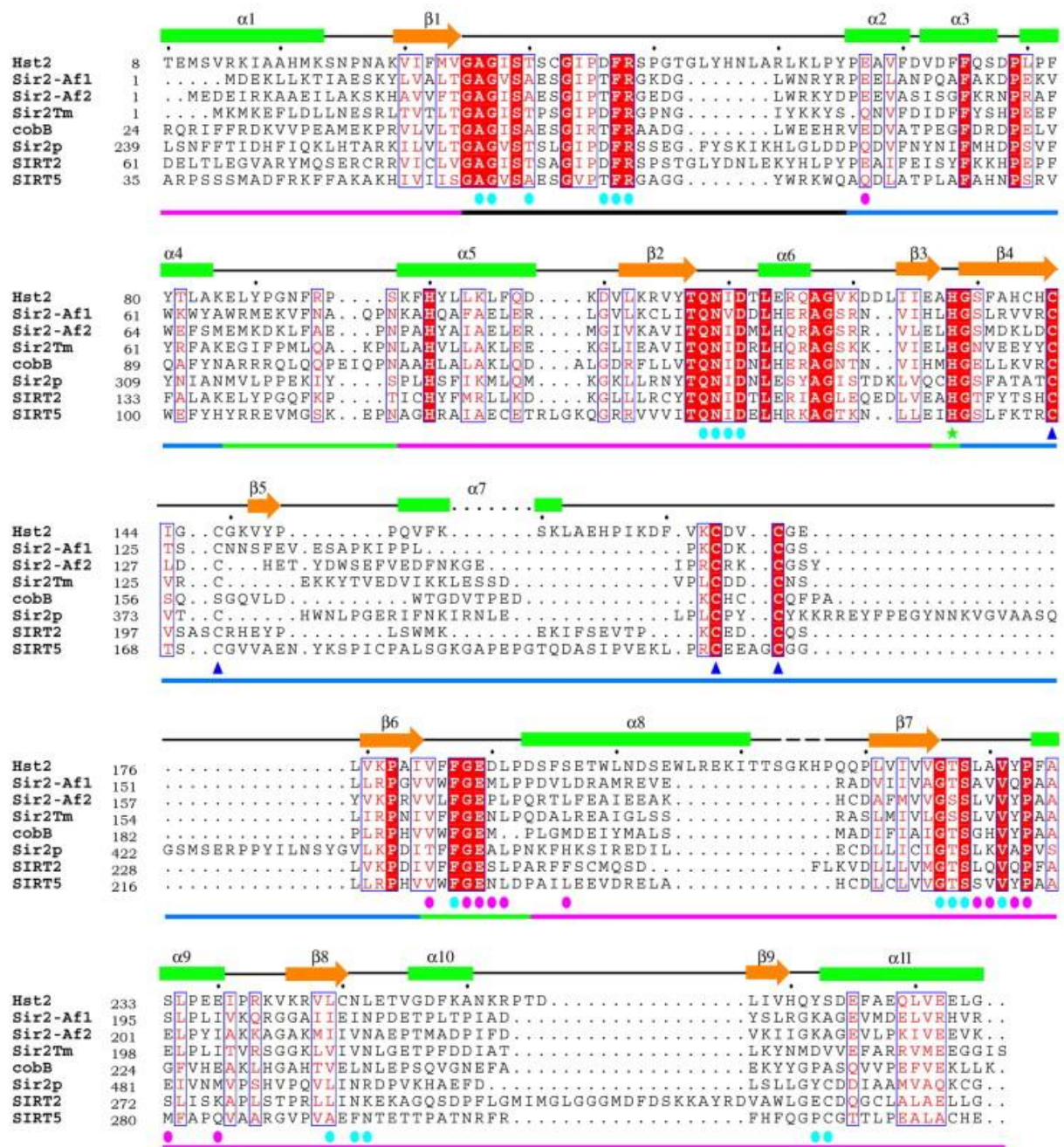


Figure 1-3: Multiple sequence alignment of the catalytic core domain region of sirtuins with known three-dimensional structures.

Multiple sequence alignment of *S. cerevisiae* Hst2 and Sir2p, *A. fulgidus* Sir2-Af1 and Sir2-Af2, *T. maritima* Sir2Tm, *E. coli* CobB, and *H. sapiens* SIRT2 and SIRT5. Cyan circles mark residues involved in NAD⁺ binding, purple circles indicate residues involved in acetyllysine binding, blue triangles label Zn²⁺-binding residues and a green asterisk marks the highly conserved catalytic histidine residue. Consensus is highlighted by red boxes and white boxes show similarities. Above the sequence alignment secondary structural elements of Hst2 are shown. Orange arrows: β sheets; green rectangles: α helices; black lines: loops; dashed lines: unstructured regions. Beneath the sequence alignment the color of the solid line indicates the Rossmann-fold domain (magenta), cofactor binding loop (black), small domain (blue), and loop regions (green) (also see **Figure 1-4**). Figure taken from [44].

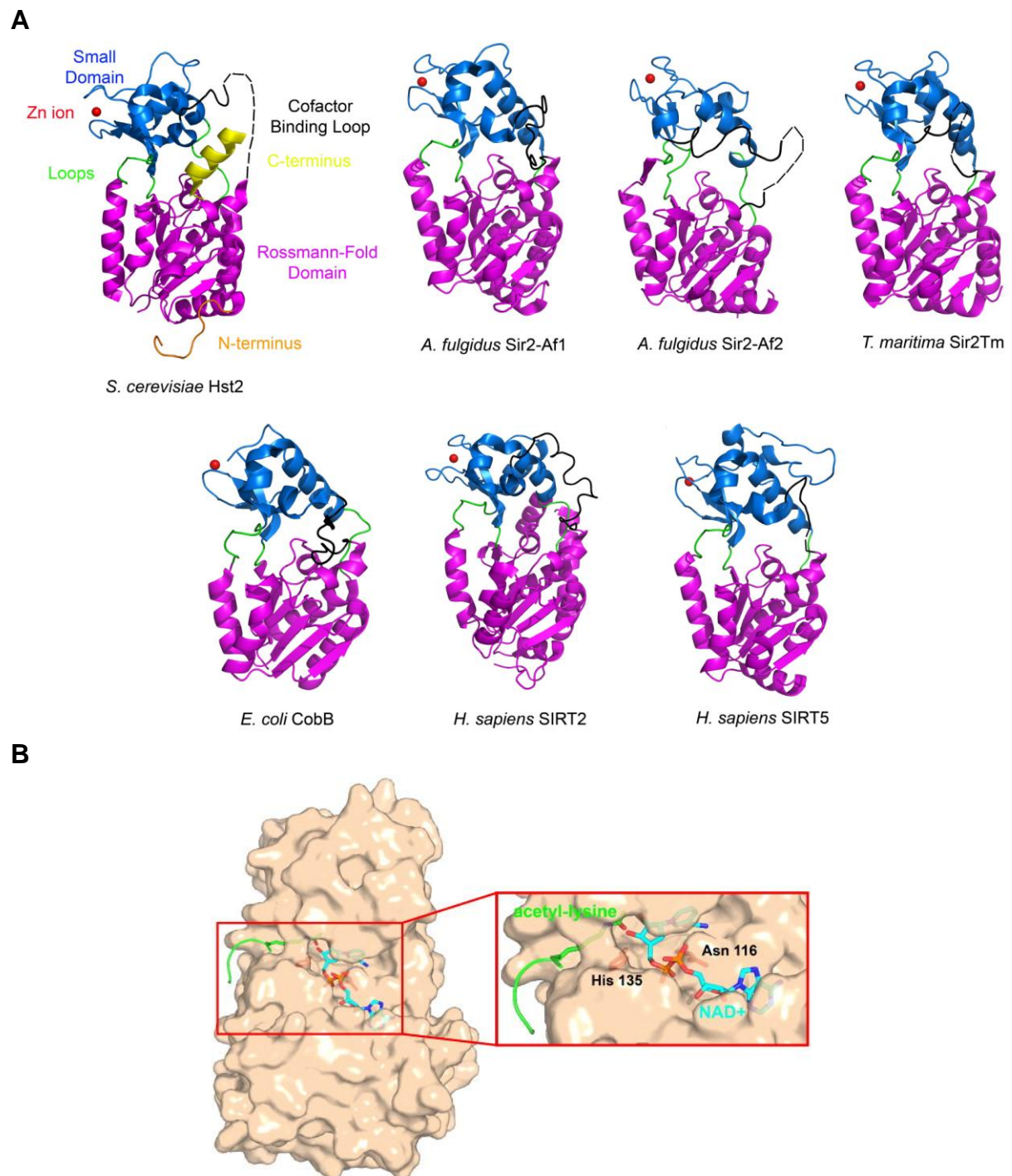


Figure 1-4: Three-dimensional crystal structures of different sirtuins.

A. The three-dimensional structure of each sirtuin is shown in a cartoon representation without bound ligand. The large magenta domain corresponds to the Rossmann-fold domain, the small blue domain to the Zn^{2+} -binding domain, the cofactor binding loop is depicted in black, other loops and the bound Zn^{2+} ion are shown in green and red, respectively. In the structure of Hst2 the N-terminal (orange) and C-terminal (yellow) regions are also included. **B.** Active site binding cleft of *S. cerevisiae* Hst2 shown in tan surface representation. In the close up view the backbone of the peptide substrate is shown in green, the acetyllysine side chain in green cpk stick representation, the conserved H135 and N116 in red cpk stick representation, and the bound NAD^+ in cyan cpk stick representation. Figures taken from [44]

The catalytic core domain of sirtuins is flanked by N- and C-terminal regions that are not conserved and vary in length and sequence between different protein family members. Relatively little is known about the function of these regions as they were not included in the majority of determined structures [44]. The structure of full-length yeast Hst2 showed that the protein forms a homotrimer and the 7 aa long N-terminal region is required for oligomerization. Interestingly, this N-terminal region binds the active side cleft in a similar conformation like an acetyl-lysine containing H4 peptide substrate. It gets displaced upon addition of acetylated peptide, which also disrupts trimer formation. The C-terminal region of Hst2 (yellow α -helical secondary structure in Figure 1-4 A) makes extensive interactions with aa residues within the cleft containing the catalytic core region. It also seems to affect NAD⁺ binding [48, 49]. As the catalytic core domain is highly conserved among different sirtuins and structures of peptide bound sirtuins provided little information on substrate discrimination, the N-terminal and C-terminal regions might also contribute significantly to substrate specification. However, to fully understand the catalytic mechanism, substrate specificity and inhibition of sirtuins further structural insights need to be complemented with more detailed biochemical analyses.

1.3 Mammalian sirtuins

The mammalian SIR-2 gene family named sirtuins (SIRTs) comprises seven members, SIRT1- SIRT7 [3], that all share a conserved sirtuin catalytic core domain. Their variable amino- and carboxyl-terminal extensions mediate diverse subcellular localization and might be also important for regulating their catalytic activity [50] (Table 1-1).

Table 1-1: Diversity of mammalian sirtuins.

Sirtuin	Enzymatic activity	Subcellular localization	Function	Homologues
SIRT1	Deacetylase	Nucleus, (Cytosol)	metabolism (gluconeogenesis, fatty acid oxidation, cholesterol regulation, insulin secretion), differentiation and development, stress responses and apoptosis	Sir2p (<i>S. cerevisiae</i>) Hst1p (<i>S. cerevisiae</i>) SIR-2.1 (<i>C. elegans</i>) dSIR2 (<i>D. melanogaster</i>)
SIRT2	Deacetylase	Cytosol (Nucleus)	tubulin deacetylation Cell cycle control	Hst2p (<i>S. cerevisiae</i>) SIRT2 (<i>D. melanogaster</i>)
SIRT3	Deacetylase	Mitochondria	mitochondrial protein deacetylation, Acetate metabolism, ATP production, fatty-acid oxidation	
SIRT4	ADP-ribosyltransferase	Mitochondria	insulin secretion (pancreatic β -cells)	SIR-2.2 (<i>C. elegans</i>) SIR-2.3 (<i>C. elegans</i>) SIRT4 (<i>D. melanogaster</i>)
SIRT5	Deacetylase	Mitochondria	Urea cycle (liver)	
SIRT6	Deacetylase/ADP-ribosyltransferase	Nucleus	Genome stability (Base excision repair), Telomeric chromatin structure, NF- κ B regulation	SIR-2.4 (<i>C. elegans</i>) SIRT6 (<i>D. melanogaster</i>)
SIRT7	Deacetylase	Nucleus (Nucleolus)	rDNA (PolI) transcription	SIRT7 (<i>D. melanogaster</i>)

SIRT1, SIRT6 and SIRT7 are predominantly nuclear, SIRT2 is cytoplasmic and SIRT3, SIRT4 and SIRT5 are mitochondrial proteins [51]. In the last ten years most of the sirtuins have been demonstrated to be NAD⁺-dependent deacetylases and a broad range of different target proteins regulated by sirtuins have been identified.

1.3.1 The nuclear sirtuins SIRT1, SIRT6, SIRT7

1.3.1.1 SIRT1

SIRT1 is the best characterized sirtuin as it is evolutionarily closest to the founding member of the sirtuin protein family, yeast SIR-2. Like yeast SIR-2, SIRT1 also functions in epigenetic silencing and chromatin organization by deacetylating acetylated lysine residues of histones (H1K9ac, H1K26ac, H3K9ac, H3K14ac, H4K16ac) [4, 52], but also other chromatin modifying factors such as the histone acetyltransferase p300 [53] or the H3K9me3 methyltransferase Suv39h1 [54]. Moreover, SIRT1 regulates transcription by deacetylating many transcription factors including p53 [55, 56], E2F1 [57], FOXO (Foxo1, Foxo3a, Foxo4) [58-61], NF- κ B [62], Hes1 [63], PPAR- γ [64], PGC-1 α [65], LXR [66] next to further factors. Based on the broad range of identified substrates, SIRT1 is implicated to function in chromatin organization, cell survival and stress responses, differentiation and development and metabolic regulation.

Most striking is SIRT1's ability to coordinate metabolic pathways in different tissues, facilitating appropriate physiological responses to changes in cellular energy levels and strongly supporting a key role of sirtuins as metabolic sensor (Figure 1-5). Human SIRT1 is expressed in all organs with strong expression in the major metabolic tissues liver, skeletal muscle, adipose tissue, pancreatic β -cells and brain [51]. In the liver SIRT1 regulates cholesterol flux. During fasting deacetylation of PGC1- α by SIRT1 activates transcription programs promoting fatty acid oxidation and glucose production by enhancing gluconeogenesis and repressing glycolysis in the liver. Mitochondrial fatty acid oxidation is also induced by SIRT1 in skeletal muscle upon fasting. In white adipose tissue, on the other hand, SIRT1 promotes lipolysis and fatty-acid mobilization by binding and repressing the nuclear receptor PPAR- γ . SIRT1 also modulates the production and secretion of adiponectin, which improves insulin sensitivity. In pancreatic β -cells SIRT1 positively regulates insulin secretion. There is increasing evidence that SIRT1 might have a protective function against type-2 diabetes, as mice overexpressing SIRT1 specifically in the pancreatic β -cells (BESTO) exhibit increased glucose-stimulated insulin secretion and improved glucose tolerance [67]. Interestingly, several SIRT1 activating compounds (including resveratrol and other non-polyphenolic substances) were shown to improve glucose homeostasis and insulin sensitivity in diet-induced and genetic type-2 diabetes animal models [68-72]. Thus, SIRT1 seems to be a key energy sensor linking NAD⁺-dependent protein deacetylation to energy metabolism and physiological responses during nutrient deprivation.

Since both resveratrol and SIRT1 orthologs have been shown to extend life span in yeast worms and flies, SIRT1 is also implicated in regulating aging and life-span extending effects of caloric restriction, a dietary regimen of low calorie intake without malnutrition [12, 14-18]. Particularly, SIRT1's potential function in the pathogenesis of age-associated diseases has

generated a lot of interest in developing sirtuin-targeted therapies to treat these metabolic disorders and to improve life quality.

Whereas the nuclear protein SIRT1 is quite well characterized, relatively little is known about the other mammalian sirtuin homologues.

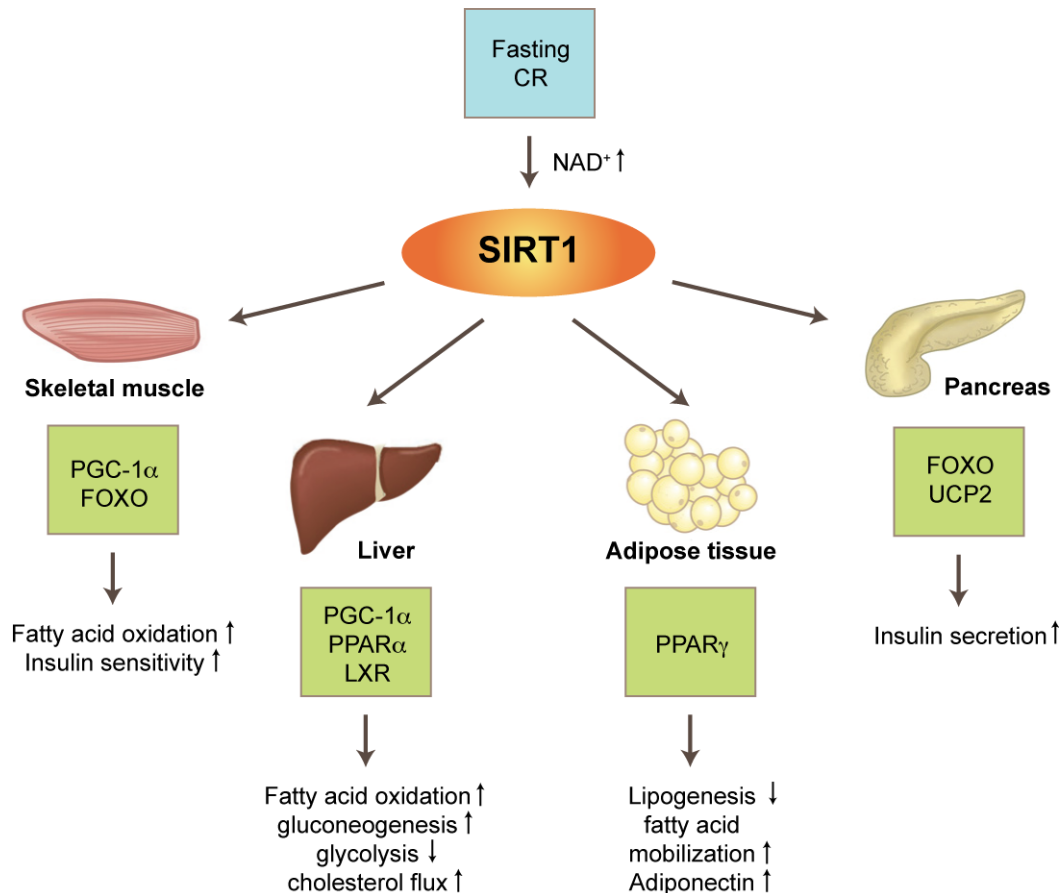


Figure 1-5: Tissue-specific regulation of metabolism by SIRT1.

Fasting or caloric restriction (CR) lead to an increase in intracellular NAD⁺ levels activating SIRT1. In the skeletal muscle, SIRT1 promotes fatty acid oxidation and improves insulin sensitivity via PGC-1 α and FOXO. In the liver, SIRT1 upregulates fatty acid oxidation, glucose synthesis, cholesterol flux and downregulates glycolysis through PGC-1 α , PPAR α and LXR. In adipose tissue (white adipose tissue), SIRT1 decreases lipogenesis and induces fatty acid mobilization by repressing PPAR γ function. In the pancreas (pancreatic β -cells) SIRT1 stimulates insulin secretion through FOXO and suppression of UCP2. Tissue icons taken from [25].

1.3.1.2 SIRT6 and SIRT7

SIRT6 and SIRT7 are also nuclear proteins but show different subnuclear localization compared to SIRT1. SIRT6 is highly associated with heterochromatic regions and SIRT7 is enriched in nucleoli.

SIRT6, which was initially described as a mono ADP-ribosyltransferase [30], functions primarily as a histone deacetylase specific for H3K9ac [31] and H3K56ac [73], maintaining telomere integrity and genome stability. Consistently, SIRT6 deficient mice show increased cellular sensitivity to genotoxic stress with defects in base excision repair (BER), a dramatically shortened life span and numerous progeroid and aging-like phenotypes [74].

Interaction of SIRT6 with the RelA/p65 component of the NF- κ B complex represses NF- κ B target genes. Increased NF- κ B transcription seems to contribute to the premature aging-like phenotype and degenerative symptoms observed in SIRT6 knockout mice [75]. Loss of SIRT7 also results in a reduced life span. SIRT7-deficient mice develop progressive cardiac hypertrophy along with inflammation and reduced stress resistance. SIRT7 seems to maintain tissue homeostasis in part by deacetylating p53 [76]. Moreover, SIRT7 interacts with RNA polymerase I and positively regulates rDNA transcription [77]. As SIRT1 also regulates p53 [78] and RNA polymerase I transcription [79], both sirtuins might act together. However, this needs to be further investigated.

1.3.2 The cytoplasmic sirtuin SIRT2

SIRT2 is predominantly located in the cytoplasm, but translocates to the nucleus during G2 to M transition [80, 81]. Various findings indicate that SIRT2 functions in controlling cell cycle progression. Overexpression of SIRT2 inhibits cell division in star fish oocytes [82] and SIRT2 expression is downregulated in different cancer types including gliomas, gastric carcinomas and melanomas [83-85]. Deacetylation of α -tubulin [29] and H4K16ac prior to mitosis [81] might also contribute to cell cycle regulation. Impaired microtubule stability and cytoskeleton organization due to SIRT2-mediated α -tubulin deacetylation has been implicated in promoting neuron degeneration and inhibition of oligodendrocyte differentiation [86-88]. In addition, SIRT2 is upregulated in white adipose tissue during caloric restriction (CR) and inhibits adipocyte differentiation by deacetylating FOXO1 [89, 90]. This further supports a critical role of sirtuins as energy sensors and key regulators of metabolic pathways in response to nutrient deprivation.

1.3.3 The mitochondrial sirtuins SIRT3, SIRT4, SIRT5

1.3.3.1 SIRT3

Among the mitochondrial sirtuins SIRT3 is currently the best characterized. SIRT3 is targeted to the mitochondrial matrix and possesses full protein deacetylase activity after proteolytic processing of the mitochondrial targeting sequence [91-93]. Both human and mouse SIRT3 are found in an approximately 44 kD long form (containing N-terminal mitochondrial targeting sequence) and a 28 kD short form. As full-length SIRT3 was also reported to be present in the nucleus and cytoplasm [94-96], controversy has arisen regarding its subcellular localization. It cannot be excluded that a small fraction of SIRT3 might be also present outside mitochondria.

In humans and mice SIRT3 is ubiquitously expressed with highest levels in metabolically active tissues, such as brown adipose tissue, muscle, liver, kidney, heart, and brain [91-93, 97]. Mice lacking SIRT3 are viable and fertile, and do not exhibit any obvious developmental or metabolic phenotype under normal physiological conditions [92]. However, SIRT3 deficient mice display significantly increased lysine acetylation of mitochondrial proteins [92]. There is growing evidence that lysine acetylation is an important posttranslational modification regulating mitochondrial energy metabolism and stress responses [98-100]. Notably, no differences in global protein acetylation levels were detected in SIRT4 and

SIRT5 null mice, suggesting that SIRT3 is the major protein deacetylase in mitochondria [92]. Nevertheless, only few SIRT3 substrates are known yet.

The first identified substrate of SIRT3 was the mitochondrial matrix protein acetyl-coenzyme A synthetase 2 (AceCS2), which forms acetyl-CoA from acetate, coenzyme A (CoA) and ATP (Figure 1-6) [101, 102]. Deacetylation of AceCS2 by SIRT3 upregulates its enzymatic activity. Increased AceCS2 activity is required during ketogenic conditions such as prolonged fasting or diabetes. AceCS2 is absent in liver, where acetate is released during fasting conditions, and abundant in the energy-expending tissues heart and muscle, where it converts acetate to acetyl-CoA for ATP production through the TCA cycle [103]. SIRT3 also regulates subunits of the electron transport chain and promotes mitochondrial ATP production by deacetylating several subunits of complex I [104], succinate dehydrogenase flavoprotein (SdhA) (subunit of complex II) [105], and ATP synthase alpha and beta subunits [105]. In addition, SIRT3 was shown to deacetylate and regulate the activity of isocitrate dehydrogenase 2 (IDH2), a key regulatory enzyme of the TCA cycle, as well as glutamate dehydrogenase (GDH), which is important for amino acid catabolism and anaplerosis [106]. Consistent with these findings reduced basal ATP levels were observed in heart, kidney, and liver of SIRT3 null mice [104]. However, SIRT3 knockout mice do not show any other obvious metabolic abnormalities under normal physiological conditions. There is growing evidence that SIRT3 function is important during metabolic stress conditions, e.g. fasting and caloric restriction. SIRT3 expression is upregulated during both starvation (liver and brown adipose tissue) [107] and caloric restriction (brown and white adipose tissue) [97]. SIRT3 knockout mice show defects in adaptive thermogenesis during fasting but not under the fed state [92, 107]. Reduced cold tolerance of starved SIRT3 null mice was recently shown to be caused by defects in β -oxidation of fatty acids. Deacetylation of long-chain acyl coenzyme A dehydrogenase (LCAD) by SIRT3 promotes fatty acid expenditure during fasting [107]. In summary, all these studies emphasize a central role of SIRT3 in regulating mitochondrial energy metabolism.

Besides this, SIRT3 has been implicated to function in mitochondrial stress responses and aging. In response to genotoxic stress both SIRT3 and SIRT4 are required for nicotinamide phosphoribosyltransferase (NAMPT)-mediated protection against cell death. Genotoxic stress or nutrient restriction upregulates the NAD^+ biosynthetic enzyme NAMPT, boosting mitochondrial NAD^+ levels and thereby facilitating this protection [108]. Moreover, SIRT3 was recently shown to act as tumor suppressor. In response to genotoxic and metabolic stress significantly increased reactive oxygen species (ROS) levels were observed in SIRT3 deficient mouse embryonic fibroblast (MEF) cells, which provided a tumor permissive environment in mammary gland cells [109].

SIRT3 might also be involved in life span determination. Genetic studies have linked polymorphisms in the SIRT3 gene to extended life span in male humans [110, 111].

1.3.3.2 SIRT4

SIRT4 is a mitochondrial matrix protein that is ubiquitously expressed. In human and in mice highest expression of SIRT4 is observed in major metabolic tissues including pancreatic beta cells, brain, liver, kidney and heart, and moderate expression of SIRT4 is found in skeletal

muscle [25, 26, 51]. In contrast to SIRT3 no NAD⁺-dependent protein deacetylase activity could be demonstrated for SIRT4 so far. But SIRT4 seems to exhibit ADP-ribosyltransferase activity [25, 26]. Only one SIRT4 substrate has been identified until now. SIRT4 interacts and down-regulates the activity of the mitochondrial matrix enzyme glutamate dehydrogenase (GDH) via ADP-ribosylation (Figure 1-6) [25]. GDH, converting glutamate into α -ketoglutarate and ammonia, plays an important role in generating ATP (through the TCA cycle) to promote insulin secretion in pancreatic islet cells [112]. Consistent with these findings, SIRT4 deficient mice show significantly increased blood insulin levels compared to wild type mice fed ad libitum or fasted overnight. Both GDH activity and insulin secretion in response to glucose and amino acids were higher in pancreatic islets isolated from SIRT4 knockout mice [25]. SIRT4 overexpression, on the other hand, suppressed insulin secretion in insulinoma cells [26], further supporting the function of SIRT4 as negative regulator of insulin secretion, which might also protect against diabetes. Furthermore, SIRT4 was reported to interact with insulin-degrading enzyme (IDE) and adenine nucleotide translocator 2 (ANT2/3) [26]. Since no enzymatic activity of SIRT4 on these proteins has been reported, the functional relevance of this interaction still needs to be determined. Interestingly, both IDE and ANT2 are implicated in the pathogenesis of type-2 diabetes. As loss of SIRT4 might contribute to diabetes, the physiological function of SIRT4 in pancreatic islets but also in other tissues needs to be further analyzed. Moreover, additional SIRT4 substrates need to be identified for a more comprehensive understanding of the physiological role of SIRT4 under normal and pathological conditions. This may also allow to ultimately clarify whether SIRT4 solely acts as ADP-ribosyltransferase or possesses NAD⁺-dependent protein deacetylase activity with very strict substrate specificity as well.

1.3.3.3 SIRT5

SIRT5 is localized to the mitochondrial matrix and exhibits NAD⁺-dependent protein deacetylase activity. In contrast to SIRT3, SIRT5 possesses only weak deacetylase activity on acetylated histones and BSA [47, 113]. However, robust enzymatic activity could be recently demonstrated on carbamoyl phosphate synthetase 1 (CPS1), the first identified substrate of SIRT5 (Figure 1-6) [114]. CPS1 catalyzes the first and rate-limiting step in the urea cycle [115, 116]. Deacetylation by SIRT5 increases CPS1 activity and promotes ammonia detoxification, which is important e.g. during fasting when amino acids have to be utilized as energy source generating excess ammonia [116, 117]. Accordingly, fasting leads to an activation of SIRT5 and results in severe hyper-ammonemia in SIRT5 deficient mice, demonstrating an important protective role of SIRT5 in adaption to food limitation [114]. SIRT5 was also reported to interact with cytochrome c, which is localized to the intermembrane space [106]. Although SIRT5 was shown to be targeted to the intermembrane space after overexpression or after mitochondrial import *in vitro* [96, 106], endogenous SIRT5 was exclusively present in the matrix of liver mitochondria [114]. Therefore, cytochrome c might not be a physiological substrate of SIRT5. Identification of novel SIRT5 substrates will provide more insights into mechanisms and pathways regulated by this sirtuin in order to adapt to food scarcity.

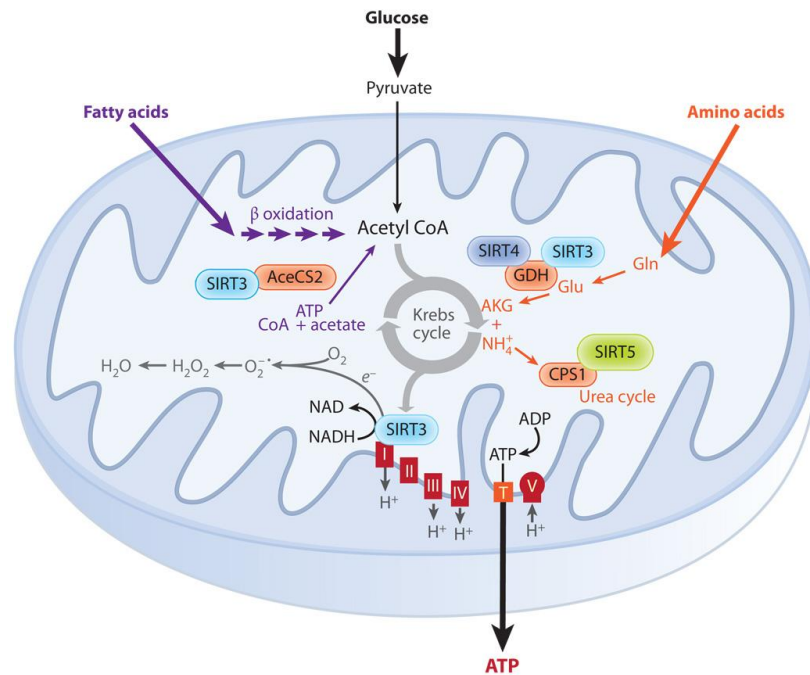


Figure 1-6: Metabolic functions of mitochondrial sirtuins.

Mitochondria are the central organelle for metabolism of fuels such as pyruvate (derived from glucose) fatty acids, and amino acids. SIRT3 regulates mitochondrial ATP production by deacetylating metabolic enzymes such as AceCS2 and complex I subunits. SIRT4 represses GDH activity by ADP-ribosylation and SIRT5 regulates the urea cycle by deacetylating CPS1. Figure taken from [19]

1.4 *Caenorhabditis elegans* sirtuins

Knowledge on SIR-2 protein function in lower eukaryotes such as yeast provided key insights into the biological pathways regulated by mammalian sirtuins. Whereas in lower eukaryotes the biological role of sirtuins is reasonably well understood, their function in simple multicellular organisms such as *C. elegans* has remained elusive.

C. elegans is well suited to study the function of sirtuins and aging-related processes. In contrast to mammals, the genome of *C. elegans* possesses only four *sir-2* gene variants, *sir-2.1* (R11A8.4), *sir-2.2* (F46G10.7), *sir-2.3* (F46G10.3) and *sir-2.4* (C06A5.11). All variants exhibit high sequence similarity to mammalian sirtuins (Table 1-2) [3]. Moreover, *C. elegans* has a relatively short life span of about two to three weeks and a rapid generation time of approximately 3.5 days (at 20°C). The entire cell lineage is relatively invariant and has been traced from single-celled zygote to adult [118]. The ability of generating mutant and transgenic worms as well as the ease of RNAi have made *C. elegans* a powerful system to analyze gene functions [119].

So far, relatively little is known about the functions of *C. elegans* sirtuins. The vast majority of the studies have focused on the role of SIR-2.1 in life span determination, after *sir-2.1* was identified as longevity factor in a genetic *C. elegans* screen [15].

SIR-2.1 is evolutionarily closest to yeast SIR-2 and mammalian SIRT1. Extra copies of the *sir-2.1* gene lead to an increase in *C. elegans* life span by up to 50% [15]. SIR-2.1 seems to extend life span by multiple pathways. One pathway depends on DAF-16, a forkhead

transcription factor of the FOXO family, which is negatively regulated by the conserved insulin/IGF-1 pathway [15]. Instead of a direct function in the insulin/IGF-1 pathway, recent studies indicate that SIR-2.1 acts in a parallel pathway, which converges on the level of DAF-16 regulation. 14-3-3 proteins (*C. elegans* PAR-5 and FTT-2), which are known to bind FOXO transcription factors in mammals, were identified as interaction partners of SIR-2.1. These seem to be required for SIR-2.1-induced activation of DAF-16 and stress resistance [120, 121]. Recently, SIR-2.1 was also reported to be required for life span extension by calorie restriction (CR) that does not depend on DAF-16, but the exact mechanism has not been determined yet [122].

SIR-2.1 localizes predominantly to the cell nucleus [122] and was shown to exhibit histone deacetylase activity [18]. Like its yeast and mammalian counterparts, SIR-2.1 functions in chromatin regulation and is involved in chromatin silencing of repetitive transgenes in the germline of *C. elegans* by a mechanism similar to SIR-2-dependent silencing of telomeres in yeast [123]. In addition, SIR-2.1 induces (next to the chromatin modifying *C. elegans* Polycomb group proteins (Mes-2, Mes-3, Mes-4, and Mes-6)) a partial cytoplasmatic localization of the linker histone HIS-24 (H1.1) in the germline [124]. Moreover, both SIR-2.1 and HIS-24 associate with subtelomeric regions, promote the modification of H3K27me3 and H3K9me3 and have synthetic effects on brood size, embryogenesis and fertility in *C. elegans* [125].

SIR-2.1 also functions in stress responses and was shown to be essential in DNA damage and repair signaling in the *C. elegans* germline. Translocation of SIR-2.1 from the nucleus to the cytoplasm and colocalization with the *C. elegans* Apaf-1 homologue CED-4 seems to induce a novel proapoptotic pathway of DNA-damage-induced apoptosis, which is independent of CEP-1 (*C. elegans* P53-like protein) and DAF-16 [126]. In neurons SIR-2.1 overexpression was shown to promote cell survival and protect against huntingtin polyglutamine [127] and prion neurotoxicity [128]. These studies further demonstrate a neuroprotective function of sirtuins and implicate a promising therapeutic potential of sirtuin activity modulators for treatment of neurodegenerative diseases.

Currently the analysis of *C. elegans* sirtuins has been focused on SIR-2.1, whereas the other three variants have been neglected and still need to be characterized.

SIR-2.2 and SIR-2.3 are most homologous to mammalian SIRT4 [3] and might be also mitochondrial proteins. A genome wide RNAi screen identified SIR-2.2 together with many chromatin related factors, DNA repair/replication proteins, and cell cycle/checkpoint proteins, to be required for genome stability in somatic and germline cells [129]. Next to SIR-2.1, SIR-2.2 was also able to protect *C. elegans* from neurodegeneration [127], suggesting that SIR-2.2 might function in the nucleus or cytoplasm. However, both SIR-2.2 and SIR-2.3 do not seem to function in life span extension [15, 130]. Moreover, no changes in life span were observed in worms overexpressing SIR-2.4, which is evolutionarily closest to mammalian SIRT6 [15]. As in the case of SIR-2.2 and SIR-2.3 the biological function of SIR-2.4 remains elusive.

Table 1-2: Diversity of *C. elegans* SIR-2 proteins.

SIR-2 variant	Function	Substrates	Homology
SIR-2.1	Life span determination, Chromatin silencing/regulation, DNA-damage induced apoptosis, protection against neurodegeneration	Histones, 14-3-3	SIRT1
SIR-2.2	Genome stability, protection against neurodegeneration	?	SIRT4
SIR-2.3	?	?	SIRT4
SIR-2.4	?	?	SIRT6

1.5 Modulation of sirtuin activity by NAD⁺ metabolism

Sirtuins were classified into a new class of HDACs (class III) because of their unique requirement of NAD⁺ as cofactor for protein deacetylation. NAD⁺ and its reduced form NADH are essential redox carriers, coupling the metabolism of biomolecules to ATP synthesis through the respiratory chain [131]. Therefore, the NAD⁺/NADH ratio is a key indicator of the cellular energy status and sirtuins, that are absolutely depending on NAD⁺ as cofactors for enzymatic activity, have become important sensors of the cellular metabolic state [132].

There is growing evidence that NAD⁺ biosynthetic pathways are critical regulators of sirtuin activity. Genetic studies in yeast have linked changes in NAD⁺ metabolism to sirtuin activity, as deficiencies in the NAD⁺ synthesis salvage pathway decrease SIR-2-mediated chromatin silencing [6, 133, 134], and increased NAD⁺ synthesis enhances silencing of SIR-2-regulated gene loci and life span extension [134].

In addition, there is growing evidence that metabolic stress such as prolonged fasting or caloric restriction (CR) induces NAD⁺ biosynthetic pathways increasing intracellular NAD⁺ levels [108, 114] and thereby upregulates sirtuin activity. In *C. elegans* overexpression of the nicotinamidase PNC-1, the first enzyme in the NAD⁺ salvage pathway of invertebrates, increases survival of *C. elegans* during oxidative stress in a SIR-2.1 dependent manner [135]. In mammals genotoxic stress and nutrient restriction upregulates NAMPT (catalyzing the first and rate-limiting step in NAD⁺ biosynthesis in vertebrates) and boosts mitochondrial NAD⁺ levels. Increased mitochondrial NAD⁺ promotes cell survival and requires not only an intact mitochondrial NAD⁺ salvage pathway but also SIRT3 and SIRT4 [108]. Interestingly, this protective function depends only on physiological NAD⁺ levels in mitochondria, but not in the cytoplasm and nucleus, suggesting that mitochondria dictate cell survival. Sirtuins and functional homologs of NAMPT are also present in prokaryotes [6]. The protective function of NAD⁺ for cell survival seems to be evolutionarily conserved and to induce ancient survival responses, as increased NAD⁺ levels also provide bacterial survival to heat, salt stress, and glucose restriction [136].

Sirtuin activity is inhibited by its reaction product NAM in a non-competitive manner, indicating that the catalytic activity of sirtuins is negatively regulated by intracellular NAM concentrations [38, 137, 138]. Notably, NAM is an agent with therapeutic potential as it was

shown to prevent type I diabetes, neurotoxicity and tissue damage in ischemia [132, 139, 140]. Nicotinamide (at high dose) seems to function by enhancing NAD⁺ biosynthesis and increasing NAD⁺ pools [141, 142].

NAD⁺ biosynthesis pathways and sirtuins are intimately connected and critical components in a regulatory network that contributes to metabolic robustness in response to nutritional and environmental cues that affect cell survival, tissue functionality, and ultimately life span. Therefore, next to drugs targeting sirtuins, NAD⁺ intermediates (nutriceuticals) promoting NAD⁺ biosynthesis and indirectly affecting sirtuin activity may be beneficial for treatment of age-associated diseases such as diabetes and neurodegenerative diseases [143].

1.6 Reversible mitochondrial protein acetylation

Mitochondria are the central organelle for important physiological processes including cellular energy (ATP) production, fatty acid and amino acid metabolism, biosynthesis of heme, pyrimidines and steroids, ion homeostasis, and apoptosis [144]. Mitochondria are also the major site for generation of reactive oxygen species (ROS) as a byproduct of oxidative phosphorylation, which damage macromolecules and can cause mitochondrial defects and dysfunction. Mitochondrial function must therefore be tightly linked to nutrient availability and be able to adapt to oxidative stress in order to avoid imbalances in metabolic homeostasis. Notably, defects in mitochondrial functions have been implicated in aging and age-associated diseases such as diabetes, neurodegenerative disorders, cardiovascular diseases and cancer [145].

Protein lysine acetylation is emerging to be a key posttranslational modification in regulating metabolic enzymes [98, 99, 146, 147]. Global proteomic approaches employing immuno-affinity purification of lysine-acetylated, tryptic peptides with anti-acetyllysine-specific antibodies and subsequent mass spectrometric analyses have shown that at least 20% of mitochondrial proteins are acetylated. Acetylation sites were identified in mitochondrial proteins of all major pathways of intermediate metabolism, including the tricarboxylic acid (TCA) cycle, oxidative phosphorylation, β -oxidation and the urea cycle. In addition, mitochondrial channel proteins, proteins acting in amino acid, carbohydrate and nucleotide metabolic pathways and antioxidant defense pathways are acetylated [98, 99, 146]. There is growing evidence that mitochondrial protein acetylation is dynamic, as it changes during fasting and calorie restriction and is an important posttranslational modification to regulate the catalytic activity of metabolic enzymes [98, 146, 148].

Mitochondria are double-membrane organelles that are derived from a eubacterial endosymbiont and still share many features with their prokaryotic ancestors [149]. Recent studies showed that lysine acetylation is also an abundant posttranslational modification in prokaryotic cells (*E. coli*) [100, 147, 150]. In these studies, more than 50% of the identified acetylated proteins are metabolic enzymes. A large number of proteins were lysine-acetylated orthologs between *E. coli* and mammals, suggesting an evolutionarily conserved function of lysine acetylation in energy metabolism, but also translation and stress responses from bacteria to mammals. Exposure to hypoxia (but not starvation) led to changes in acetylation

levels intimately linking reversible protein acetylation to regulatory mechanisms that allow cells to adjust to changes in cellular environment [50, 100].

The identification of lysine-acetylation as an abundant post-translational modification in mitochondria and sirtuins as mitochondrial deacetylases raises an interesting question. Are there mitochondrial lysine acetyltransferases? Up to now this question remains unresolved, as no mitochondrial protein acetyltransferase has so far been identified in mammals.

In *Salmonella enterica* the enzymatic activity of acetyl-CoA synthetase is regulated by acetylation through Pat [151], the only known bacterial acetyltransferase, and deacetylation through CobB, a bacterial SIR-2 homolog [152]. Interestingly, both human SIRT2 and yeast SIR-2 can substitute CobB function in CobB-deficient *S. enterica* strains, suggesting an evolutionarily conserved function of sirtuins in regulating cellular metabolism [153]. No orthologs of Pat have been found in mammalian cells and it is also not known whether there are other mitochondrial acetyltransferases existing in mammals [50]. However, the observation that proteins encoded by mitochondrial DNA, e.g. the ATP synthase F₀ subunit 8, are acetylated, argues against the possibility that lysine acetylation of mitochondrial proteins occurs in the cytoplasm prior to import, but not within mitochondria. It is therefore anticipated that there are also acetyltransferases existing in the mammalian mitochondrion [50]. Since it cannot be excluded that mitochondrial proteins also become acetylated in a non-enzymatic manner [154, 155], some acetylation sites of mitochondrial proteins might not have regulatory functions.

Taken together, these findings show that lysine acetylation is intimately linked to energy metabolism and stress responses in mitochondria. The mitochondrial sirtuins SIRT3, SIRT4 and SIRT5, requiring NAD⁺ for deacetylation, are potential energy and stress sensors and seem to contribute to coordination and regulation of mitochondrial energy homeostasis. Thus, identification of further sirtuin substrates as well as mitochondrial acetyltransferase will be crucial for a comprehensive understanding of the functional importance of protein lysine acetylation in mitochondria.

1.7 Open questions and objective of this PhD thesis

Sirtuin research has created an exciting field and revealed intriguing connections between protein acetylation and regulation of metabolic pathways, stress responses and life span [20]. The mammalian sirtuin protein family comprises seven members and is very complex. Three sirtuins, SIRT3, SIRT4 and SIRT5 are localized to mitochondria and are highly expressed in major metabolic tissues [51]. Although these proteins might function as important energy sensors, which couple metabolic pathways to nutrient availability, only few studies have investigated their biological functions so far.

The mitochondrion is the major organelle for ATP production, generation of ROS and apoptotic signaling events [144]. Dysfunction of mitochondrial metabolism has been associated to many age-related diseases such as diabetes, neurodegenerative disorders, cardiovascular diseases and cancer [145]. Interestingly, SIRT4 has been shown to negatively regulate insulin secretion and might be associated to the pathogenesis of diabetes [25, 26].

Therefore, SIRT4 itself, but also factors regulated by SIRT4, might be novel therapeutic targets in treatment of diabetes.

Only one SIRT4 substrate, glutamate dehydrogenase (GDH), has been identified so far. Many important questions regarding its biological function still need to be answered: Which other factors are substrates of SIRT4? Does SIRT4 regulate their activity in response to nutrient deprivation or stress? Is SIRT4 a regulator of energy homeostasis, which coordinates mitochondrial metabolism and adaption to metabolic stress in different tissues?

Reversible mitochondrial protein acetylation might switch metabolic pathways in response to changing nutrient levels. Until now, SIRT4 is the only mammalian sirtuin where no other activity than ADP-ribosylation has been detected, raising the question whether SIRT4 has protein deacetylase activity. Because of its high sequence conservation to the other mammalian sirtuins, it is very likely that SIRT4 also possesses NAD⁺-dependent protein deacetylase activity. However, the proof of this might be challenging, as SIRT4 seems to exhibit very strict substrate specificity.

Although analysis of SIR-2 proteins in lower eukaryotes has provided key insights into the biological function of mammalian sirtuins, the knowledge of sirtuins in the simple multicellular organism *C. elegans* is very limited and has been focused primarily on the variant *sir-2.1*, neglecting the other three variants (*sir-2.2* to *sir-2.3*). As discussed in section 1.4, *C. elegans* provides a less complex and powerful model system to analyze the biology of sirtuins on an organismal level. Interestingly, *C. elegans* SIR-2.2 and SIR-2.3 are most homologous to SIRT4 and there are no other SIR-2 proteins that share highest sequence homology to SIRT3 or SIRT5. Currently, it is not known whether SIR-2.2 and SIR-2.3 are mitochondrial proteins and several additional questions remain: Are SIR-2.2 and SIR-2.3 NAD⁺-dependent protein deacetylases? Do they function in regulation of energy metabolism and stress responses? Are these functions conserved for mammalian SIRT4?

Based on these questions the aim of my PhD thesis was to characterize the expression and localization of *C. elegans* SIR-2.2 and SIR-2.3. A further goal was to elucidate their role in regulation of metabolism and stress responses. This included the identification of novel interaction partners, which were also relevant for the analysis of the enzymatic activities of SIR-2.2 and SIR-2.3. Moreover, I investigated whether my findings are conserved from *C. elegans* to human in order to contribute to a better understanding of the biological function and enzymatic activity of mammalian SIRT4.

2 Material and Methods

2.1 Material and Reagents

2.1.1 Laboratory equipment

Generally used laboratory equipment is summarized in Table 2-1.

Table 2-1: Generally used laboratory equipment.

Equipment	Manufacturer	Equipment	Manufacturer
ÄKTA Explorer FPLC System	GE Healthcare, Buckinghamshire (UK)	Multitron shaker	HT Infors, Braunschweig
Balances	Mettler-Toledo, Giessen	Nanodrop® ND-1000	Peqlab, Erlangen
Bioruptor™	Diogenode, Liege (Belgium)	NuPAGE® Pre-cast system	Invitrogen, Karlsruhe
Branson Digital Sonifier	Heinemann Ultraschall- und Labortechnik, Schwaebisch Gmuend	Olympus IX70	Olympus, Hamburg
Cary 100 UV-Vis Spectrophotometer	Varian, Palo Alto (USA)	Olympus SZX10	Olympus, Hamburg
Centrifuges 5415R/5810R	Eppendorf, Hamburg	PCR machine Eppendorf Mastercycler eppgradientS	Eppendorf, Hamburg
ECLIPSE Ti-E, inverted research microscope	Nikon, Kingston (UK)	pH meter	Mettler-Toledo, Giessen
EmulsiFlex-C5 High Pressure Homogenizer	Avestin, Ottawa (Canada)	PlateChameleon	Hidex, Turku (Finland)
Eppendorf Transjector 5246	Eppendorf, Hamburg	Potter S	B. Braun Biotech International GmbH, Melsungen
Eppendorf TransferMan NK2	Eppendorf, Hamburg	Power Supply Power Pac Universal	Biorad, München
Freezer -20°C	Liebherr, Bulle (Switzerland)	Scanner Perfection V750 PRO	Epson
Freezer -80°C	Thermo Scientific, Braunschweig	Sorvall Evolution RC	Thermo Scientific, Braunschweig
Here Safe sterile hood	Heraeus, Hanau	Stratalinker® UV crosslinker 2400	Stratagene, La Jolla (USA)
Heraeus Kelvitron Incubator	Thermo Scientific, Braunschweig	Stuart Gyrorocker SSL3	Sigma, Steinheim
Kodak X OMAT 2000 processor	Caresream Health, New York	Sub-Cell-GT Agarose gel electrophoresis	Biorad, München
Leica TCS SP5	Leica, Wetzlar	Thermomixer comfort	Eppendorf, Hamburg
Liquid Scintillation Analyzer Tri-Carb 3110TR	PerkinElmer, Waltham (USA)	UV Transilluminator	Biorad, München
Mini-Protean 3 Cells	Biorad, München	Vortex Genie 2	Scientific Industries, New York (USA)
MiniTrans-Blot	Biorad, München	Waterbath TW12	Julabo, Seelbach

2.1.2 Chemicals

Chemicals generally used for buffers and media are listed in Table 2-2.

Table 2-2: Generally used chemicals.

Chemical	Manufacturer	Chemical	Manufacturer
Acetic acid	Merck, Mannheim	D-Mannitol	Sigma, Steinheim
Adenosine 5'-triphosphate (ATP)	Sigma, Steinheim	2-Mercaptoethanol	Sigma, Steinheim
Acetyl Coenzyme A	Roche, Mannheim	Methanol	Sigma, Steinheim
Acrylamide / Bisacrylamide (37.5:1)	Merck, Mannheim	D/L-Methionine	Sigma, Steinheim
Agar	Roth, Karlsruhe	Milk powder	Regilait, Saint-Martin-Belle-Roche (France)
Agarose	Serva, Heidelberg	β -Nicotinamide Adenine Dinucleotide, (β -NAD ⁺)	Sigma, Steinheim
Albumin, bovine (BSA)	New England Biolabs, Ipswich	β -Nicotinamide Adenine Dinucleotide, reduced form (β -NADH)	Sigma, Steinheim
Ammonium chloride (NH ₄ Cl)	Merck, Mannheim	Nickel chloride (NiCl ₂)	Riedel-de Haën, Seelze
Ammonium persulfate (APS)	AppliChem GmbH, Darmstadt	Nonidet P-40 (NP-40)	Roche, Mannheim
Ampicillin	AppliChem GmbH, Darmstadt	Paraquat (Methylviologen-dichloride hydrat)	Sigma, Steinheim
Bovine growth serum (BGS)	Sigma, Steinheim	Penicillin Streptomycin 100x	Gibco, München
Bovine Serum Albumin (BSA)	Sigma, Steinheim	Peptone	Roth, Karlsruhe
Bromophenol blue	Serva, Heidelberg	Phenol/Chloroform/Isoamylalcohol	Roth, Karlsruhe
Calcium chloride (CaCl ₂)	Roth, Karlsruhe	Phenylmethylsulfonyl fluorid (PMSF)	Serva, Heidelberg
Chloramphenicol	Amresco, Solon (USA)	Ponceau S	Sigma, Steinheim
Chloroform	Merck, Mannheim	Potassium bicarbonate	Sigma, Steinheim
Cobalt chloride (CoCl ₂)	Riedel-de Haën, Seelze	Potassium chloride (KCl)	Roth, Karlsruhe
Coomassie brilliant blue	BIO-RAD, München	Potassium dihydrogen phosphate (KH ₂ PO ₄)	Roth, Karlsruhe
Copper chloride (CuCl ₂)	Merck, Mannheim	Potassium monohydrogen phosphate (K ₂ HPO ₄)	Merck, Mannheim
Dimethylsulfoxid (DMSO)	Sigma, Steinheim	Protease inhibitor (Complete EDTA-free)	Roche, Mannheim
1,1'-dioctadecyl-3,3',3'-tetramethylindocarbocyanine perchlorate (DiI; DiI ₁₈ (3))	Molecular Probes [®] , Invitrogen, Karlsruhe	Sodium acetate	Roth, Karlsruhe
DL-Dithiothreitol (DTT)	Alexis Biochemicals	Sodium azide (NaN ₃)	Alfar Aesar, Karlsruhe
dNTPs	Invitrogen, Karlsruhe	[¹⁴ C] Sodium Bicarbonate (specific activity of 52 mCi/mmol, 1 mCi)	PerkinElmer, Waltham (USA)

Ethanol	Merck, Mannheim	Sodium chloride (NaCl)	Merck, Mannheim,
Ethidium bromide	Roth, Karlsruhe	Sodium dihydrogen phosphate (NaH ₂ PO ₄)	Merck, Mannheim
Ethylenediaminetetraacetate (EDTA)	Roth, Karlsruhe	Sodium dodecyl sulfate (SDS)	VWR, Poole
Ethylene glycol tetraacetic acid (EGTA)	Roth, Karlsruhe	Sodium hydroxide	Merck, Mannheim
Glucose	Merck, Mannheim	Sodium monohydrogen phosphate (Na ₂ HPO ₄)	Merck, Mannheim
Glycerol	Merck, Mannheim	Sodium pyruvic acid	Sigma, Steinheim
Glycine	Merck, Mannheim		
Halocarbon oil 700	Sigma, Steinheim	Sodium sulfate (Na ₂ SO ₄)	Merck, Mannheim
Hydrochloric acid (HCl)	Merck, Mannheim	Sucrose	Serva, Heidelberg
4-(2-Hydroxyethyl)-1-piperazineethanesulfonic acid (HEPES)	VWR, Poole	Tetramethyl ethylenediamine (TEMED)	Sigma, Steinheim
Iron chloride (FeCl ₃)	Roth, Karlsruhe	Trichostatin A	Cell Signaling (NEB, Ipswich, USA)
Isopropyl β-D-thiogalactopyranoside (IPTG)	AppliChem GmbH, Darmstadt	Triethanolamine	VWR, Poole
L-Glutamine 100x	Gibco, München	Tris (hydroxymethyl) amino ethane (Tris)	Roth, Karlsruhe
Lumasafe™ Plus	Lumac, Groningen (Netherlands)	Triton X-100	Merck, Mannheim
Isoamylalcohol	Sigma, Steinheim	Trypsin solution	Gibco, München
α-Lactose	Roth, Karlsruhe	Tween 20	Sigma, Steinheim
Magnesium chloride (MgCl ₂)	Merck, Mannheim	Urea	Merck, Mannheim
Magnesium sulfate (MgSO ₄)	Roth, Karlsruhe	Yeast extract	MOBIO, Hamburg
Manganese chloride (MnCl ₂)	Roth, Karlsruhe	Zinc sulfate (ZnSO ₄)	AppliChem GmbH, Darmstadt

2.1.3 Kits

Generally used kits are listed in Table 2-3.

Table 2-3: Generally used kits.

Kits	Supplier
Coomassie Plus (Bradford) Protein Assay	Thermo Fisher Scientific, Rockford (USA)
CalPhos™ Mammalian Transfection Kit	Clontech, Mountain View (USA)
MEGAscript® T7 Kit	Ambion, Wiesbaden
Micro BSA Protein Assay Kit	Thermo Fisher Scientific, Rockford (USA)
NucleoBond® Xtra Midi	Macherey & Nagel, Dueren
NucleoBond® Plasmid	Macherey & Nagel, Dueren
SuperScript™ III First-Strand Synthesis System for RT-PCR	Invitrogen, Karlsruhe
Zymoclean™ DNA Clean & Concentrator™-5	Zymo Research, Orange (USA)
Zymoclean™ Gel DNA Recovery Kit	Zymo Research, Orange (USA)

2.1.4 Consumables and reagents

Generally used consumables and reagents are listed in Table 2-4.

Table 2-4: Generally used consumables and reagents.

Consumables / Others	Supplier
9 cm, 6 cm, 3.5 cm Petri dish	Greiner, Solingen
1 kb Plus DNA Ladder	Invitrogen, Karlsruhe
Amersham Hyperfilm ECL (18 x 24 cm)	GE Healthcare, Buckinghamshire (UK)
Amicon Ultra-15 Centrifugal Filter Units	Millipore, Billerica (USA)
Amylose Resin	New England Biolabs, Ipswich (USA)
Anti-FLAG [®] M2 affinity gel	Sigma, Steinheim
Cryotubes	Greiner, Solingen
DMEM GlutaMAXII [-Pyruvate]	Gibco, München
Dynabeads [®] M280 sheep anti mouse IgG	Invitrogen, Karlsruhe
ECL plus [™] Western Blotting Detection Reagent	GE Healthcare, Buckinghamshire (UK)
Femtotip [®] II	Eppendorf, Hamburg
GFP-Trap [®] -A	Chromotek, Planegg-Martinsried
jetPEI [™] Transfection Reagent	Polyplus-transfection SA, Illkirch (France)
Microloader	Eppendorf, Hamburg
Mono Q [™] 5/50 GL	GE Healthcare, Buckinghamshire (UK)
Ni-NTA resin	Qiagen, Hilden
Nitrocellulose membrane	GE Healthcare, Buckinghamshire (UK)
Phase Lock Gel [™] (2 ml, heavy)	Eppendorf, Hamburg
Pierce [®] Avidin Agarose Resin	Thermo Fisher Scientific, Rockford (USA)
Protein G Sepharose [™] 4 Fast Flow	GE Healthcare, Buckinghamshire
Complete, EDTA-free, Protease Inhibitor Cocktail tablets	Roche, Mannheim
SeeBlue [®] Plus2 Pre-Stained protein standard	Invitrogen, Karlsruhe
Superdex 200 10/30 GL	GE Healthcare, Buckinghamshire (UK)
TRIzol [®] Reagent	Invitrogen, Karlsruhe

2.1.5 Enzymes

Generally used enzymes are listed in Table 2-5.

Table 2-5: Generally used enzymes.

Enzyme	Supplier
Antarctic phosphatase	New England Biolabs (NEB), Ipswich (USA)
BamHI, BglII, EcoRI, KpnI, MluI, NdeI, NotI, PstI, XhoI	New England Biolabs (NEB), Ipswich (USA)
DNaseI	New England Biolabs (NEB), Ipswich (USA)
DpnI	New England Biolabs (NEB), Ipswich (USA)
Expand High Fidelity DNA polymerase mix	Roche, Mannheim
Malate Dehydrogenase (EC 1.1.1.37), porcine heart mitochondria	Serva, Heidelberg
Micrococcal nuclease (MNase)	Calbiochem [®] , Merck, Darmstadt
PfuUltra [™] II Fusion HS DNA Polymerase	Stratagene, La Jolla (USA)
Pfu DNA polymerase	Fermentas, St. Leon-Rot
Proteinase K	Invitrogen, Karlsruhe
Pyruvate Carboxylase (EC 6.4.1.1), bovine liver	Sigma, Steinheim
T4 DNA Ligase	New England Biolabs (NEB), Ipswich (USA)
Taq DNA Polymerase (recombinant), LC	Fermentas, St. Leon-Rot

2.1.6 Antibodies

Used antibodies for Western blotting and immunoprecipitation are listed in Table 2-6.

Table 2-6: Generally used antibodies.

Name	Host	Manufacturer, catalog number	Application	Dilution for WB
Primary antibodies:				
anti-acetylated-Lysine	rabbit, polyclonal	Cell signaling, #9441	WB	1:1000
anti-acetylated-Lysine	mouse, monoclonal	Cell signaling, #9681	WB	1:1000
anti-ATP synthase (Complex V) subunit alpha	mouse, monoclonal	Mitosciences, MS507		
anti-Complex I subunit NDUFS3 (<i>C. elegans</i> NUO-2)	mouse monoclonal	Mitosciences, MS112	WB	1:1000
anti-cytochrome c	mouse, monoclonal	Mitosciences, MSA06	WB	1:1000
anti-Flag M2	mouse, monoclonal	Sigma, F3165	WB, IP	1:1000
anti-GFP	mouse monoclonal (clones 7.1 and 13.1)	Roche, 11814460001	WB, IP	1:1000
anti-H3	rabbit, polyclonal	Abcam, ab1791	WB	1:30000
anti-Myc	mouse monoclonal (clone 4A6)	Millipore, Temecula (USA)	WB, IP	1:1000
anti-SIR-2.2			WB, IP	
Secondary antibodies:				
anti-mouse-HRP	goat, polyclonal	DakoCytomation, P0447	WB	1:5000
anti-rabbit-HRP	swine, polyclonal	DakoCytomation, P0399	WB	1:5000

WB: Western blotting; IP: immunoprecipitation

2.1.7 Peptides

Peptides used as substrates for deacetylase activity assays are listed in Table 2-7.

Table 2-7: Peptides used for deacetylase activity assays.

Name	Peptide	Amino acid sequence	Acetylated lysine	Supplier
MPIG-47	Human PC (265-280)	CSIQRRHQK ₂₇₃ (ac)VVEIAPA-CONH2	K ₂₇₃ ac	Charite-Universitätsmedizin Berlin
MPIG-48	Human PC (733-749)	AGTHILCIK ₇₄₁ (ac)DMAGLLKP-CONH2	K ₇₄₁ ac	Charite-Universitätsmedizin Berlin
H3K9ac	H3 (1-20C)	ARTKQTARK ₉ (ac)STGGKAPRKQLC	K ₉ ac	Baylor
H3K14ac	H3 (1-20C)	ARTKQTARKSTGGK ₁₄ (ac)APRKQLC	K ₁₄ ac	Baylor

2.1.8 Oligonucleotides

Primer sequences were designed using the DNASTAR Lasergene 7 program and purchased from Invitrogen (Karlsruhe) or MWG (Ebersberg). The oligonucleotide sequences are described in the corresponding method sections (2.2.8, 2.4.5, 2.4.12) (underlined sequences indicate restriction sites, mutated nucleotides are lowercased).

2.1.9 Plasmids

Vectors used for cloning are listed in Table 2-8.

Table 2-8: Generally used plasmids.

Name	Type	Promoter	Selection	Tags	Source
pCDNA3.1(+)-FLFL-HAHA-C	mammalian expression vector	T7/CMV	Ampicillin	Double FLAG and double HA-tag N-terminal	[156], Chromatin Biochemistry group, Dr. W. Fischle, Max Planck Institute for Biophysical Chemistry, Göttingen
pCDNA3.1(+)-FLFL-HAHA-C	mammalian expression vector	T7/CMV	Ampicillin	Double FLAG and double HA-tag C-terminal	[156]
pET11a	bacterial expression vector	T7	Ampicillin	-	New England Biolabs (NEB), Ipswich (USA)
pEU3-NII-StrepII	Cell-free protein synthesis	T7	Ampicillin	C-terminal StrepII-tag	Department of Cellular Biochemistry, Prof. R. Luehrmann, Max Planck Institute for Biophysical Chemistry, Göttingen
pEGFP-N1	Mammalian expression vector	CMV	Kanamycin	C-terminal EGFP-tag	Clontech, Mountain View (USA)
pPD115.62 (L3570)	worm expression	<i>myo-3</i>	Ampicillin	C-terminal GFP-tag, (<i>unc-54</i> 3'UTR)	Andrew Fire, Stanford School of Medicine (USA)
L4440 (pPD129.36)	Worm expression, RNAi	T7	Ampicillin	-	Andrew Fire, Stanford School of Medicine (USA)

The following plasmids were provided by other group members or collaborators:

The plasmid pRF4 [157] used as selection marker for microinjection of *C. elegans* as well as the cosmid F46G10 (F46G10.7 and F46G10.3), originally generated by the Wellcome Trust Sanger Institute (Cambridge, UK), were kindly provided by Dr. Monika Jedrusik-Bode (Max Planck Institute for Biophysical Chemistry, Göttingen). Szabolcs Soeroes and Nora Köster-Eiserfunke (Max Planck Institute for Biophysical Chemistry, Göttingen) kindly provided the plasmids pEU3-NII-Strep and pCDNA3.1(+)-FLFL-HAHA, respectively, containing both the cDNA of HP1 β . Mammalian expression plasmids pCDNA3.1 encoding human SIRT3, SIRT4, SIRT5, and CDYL1c with a C-terminal Myc-HIS-tag were kindly provided by the laboratory of Prof. Eric Verdin (Gladstone Institute of Virology and Immunology, University of California, San Francisco, USA) and Henriette Franz (Max Planck Institute for Biophysical Chemistry, Göttingen).

2.1.10 Bacterial Strains

Table 2-9 summarizes all bacterial strains used for cloning, expression of recombinant protein or as food source for *C. elegans*.

Table 2-9: Generally used bacterial strains.

Strain	Genotype/description	Application	Source
DH5a	<i>E. coli</i> F- f80lacZDM15 D(lacZYA-argF) U169 <i>deoR recA1 endA1 hsdR17</i> (r _k ⁻ , m _k ⁺) <i>phoA supE44 l^{thi}-1 gyrA96 relA1</i>	plasmid amplification; cloning	Invitrogen, Karlsruhe
BL21-CodonPlus (DE3)-RIL	<i>E. coli</i> B F- <i>ompT hsdS</i> (r _B ⁻ m _B ⁻) <i>dcm</i> ⁺ Tet ^r <i>gal l</i> (DE3) <i>endA Hte [argU ileY leuW Cam^r]</i>	protein expression	Stratagene, La Jolla (USA)
OP50-1	Uracil auxotroph. <i>E. coli</i> B, streptomycin resistant, useful for growing <i>C. elegans</i> in bulk	<i>C. elegans</i> food	CGC (Caenorhabditis Genetics Center, University of Minnesota, USA)
HB101	<i>E. coli</i> [supE44 <i>hsdS20</i> (r _B -m _B -) <i>recA13 ara-14 proA2 lacY1 galK2 rpsL20 xyl-5 mtl-1</i>]. Contains a mutation (<i>rpsL20</i>) in a ribosomal subunit gene that confers streptomycin resistance	<i>C. elegans</i> food	CGC (Caenorhabditis Genetics Center, University of Minnesota, USA)
HT115(DE3)	<i>E. coli</i> F-, <i>mcrA</i> , <i>mcrB</i> , IN(<i>rrnD</i> - <i>rrnE</i>)1, <i>rnc14::Tn10</i> (DE3 lysogen: <i>lavUV5</i> promoter - T7 polymerase) (IPTG-inducible T7 polymerase) (RNAse III minus), tetracycline resistant	RNAi feeding	CGC (Caenorhabditis Genetics Center, University of Minnesota, USA)

2.1.11 *C. elegans* strains

C. elegans strains I generated in this study (MAJ13 to MAJ16) or obtained from different sources are listed in Table 2-10.

Table 2-10: *C. elegans* strains used in this study.

Strain	Genotype	Source/CGC lab designation	Reference
N2	wild-type	Hodkin J, Oxford University, Oxford (UK); distributed by the CGC	[158]
VC199	<i>sir-2.1(ok434)IV</i>	<i>C. elegans</i> Gene Knockout Project (OMRF), Robert Barstead (RB), Oklahoma Medical Research Foundation, Oklahoma City, USA)	
MAJ11	<i>sir-2.2(tm2648)X</i>	National BioResource Project NBRP, Mitani	
MAJ12	<i>sir-2.2(tm2673)X</i>	National BioResource Project NBRP, Mitani	
RB654	<i>sir-2.3(ok444)X</i>	<i>C. elegans</i> Gene Knockout Project (OMRF), Robert Barstead (RB), Oklahoma Medical Research Foundation, Oklahoma City, USA)	
BC14289	<i>sEX14289[sir-2.2_{pr}::gfp]</i> , transcriptional fusion	David Baillie (BC), Simon Fraser University, Vancouver, Canada	[159, 160]
BC15074	<i>sEX15074[sir-2.2_{pr}::gfp]</i> , transcriptional fusion	David Baillie (BC), Simon Fraser University, Vancouver, Canada	[159-161]
HT822	<i>lpIs[sir-2.1_{pr}::sir-2.1::gfp rol-6(su1006)]</i> , translational fusion	Heidi Tissenbaum (HT), Univ. of Massachusetts Medical School, Worcester, USA	[122]
MAJ13	<i>mpgIs13[sir-2.2_{pr}::sir-2.2::strep::gfp rol-6(su1006)]</i> , translational fusion	Monika Jedrusik-Bode (MAJ), MPI for Biophysical Chemistry, Göttingen	

Strain	Genotype	Source	Reference
MAJ14	<i>mpgIs14[sir-2.3_{pr}::sir-2.3::ha::gfp rol-6(su1006)]</i> , translational fusion	Monika Jedrusik-Bode (MAJ), MPI for Biophysical Chemistry, Göttingen	
MAJ15	<i>mpgEx15[sir-2.4_{pr}::sir-2.3::ha::gfp rol-6(su1006)]</i> , translational fusion	Monika Jedrusik-Bode (MAJ), MPI for Biophysical Chemistry, Göttingen	
MAJ16	<i>mpgIs13[sir-2.2_{pr}::sir-2.2::strep::gfp rol-6(su1006)]; mpgEx16 [sir-2.3_{pr}::sir-2.3::ha::mcherry]</i> , translational fusion	Monika Jedrusik-Bode (MAJ), MPI for Biophysical Chemistry, Göttingen	
SJ4103	<i>zcls14[myo-3_{pr}::gfp(mit)]</i> , transcriptional fusion, mitochondrial GFP expression	David Ron (SJ), Skirball Institute, New York, USA	[162]
SJ4143	<i>zcls17[ges-1_{pr}::gfp(mit)]</i> , transcriptional fusion, mitochondrial GFP expression	David Ron (SJ), Skirball Institute, New York, USA	[162]

Sequence context specifying the localization of the different deletion mutations is summarized in Table 2-11. Flanking sequences are reported on the plus strand.

Table 2-11: Molecular details for genotyping.

Genotype	Molecular details (taken from wormbase)
<i>sir-2.1(ok434)IV</i>	...gcagaaatctgaagaaaaaa --[768 bp deletion] ttttgcacaacgtgtac... – wild type ...gcagaaatctgaagaaaaaaTT----- ttttgcacaacgtgtac... – <i>ok434</i>
<i>sir-2.2(tm2648)X</i>	...atataaaattcaaaacaata [419 bp deletion] catattggatttaaaaaaaa... – wild type ...atataaaattcaaaacaata ----- catattggatttaaaaaaaa... – <i>tm2648</i>
<i>sir-2.2(tm2673)X</i>	...ctagctgagccttcaaaaaat [548 bp deletion] tcttctaattgataatgttt... – wild type ...ctagctgagccttcaaaaaat ----- tcttctaattgataatgttt... – <i>tm2673</i>
<i>sir-2.3(ok444)X</i>	...taaaatgcacatcatgtgaat [839 bp deletion] gcaaaacaaccaattttcat... – wild type ...taaaatgcacatcatgtgaat ----- gcaaaacaaccaattttcat... – <i>ok444</i>

2.1.12 Cell lines

Cell lines used for protein expression are listed in Table 2-12.

Table 2-12: Cell lines used in this study.

Cell line	Origin	Organism	Medium	Source
HEK293	Embryonic Kidney	human	DMEM	ATCC
HEK293T	Embryonic Kidney	human	DMEM	ATCC

2.2 Molecular biological methods

2.2.1 Plasmid DNA preparation

DH5 α bacteria transformed with the plasmid of interest were grown in 5 ml or 100 ml LB medium (1% (w/v) peptone, 0.5% (w/v) yeast extract, 0.5% (w/v) NaCl) at 37°C overnight. Plasmid DNA was isolated using either the NucleoBond® Plasmid or NucleoBond® Xtra Midi (Macherey & Nagel, Dueren) according to manufacturer's description. The plasmid DNA concentration was determined photometrically with the NanoDrop® ND-1000 at 260 nm.

2.2.2 DNA digestion with restriction endonucleases

PCR products and plasmids were digested with restriction endonucleases (New England Biolabs (NEB), Frankfurt am Main) according to NEB protocols [163].

2.2.3 Polymerase chain reaction (PCR)

Specific DNA sequences were amplified by PCR based on standard protocols [164]. A 50 µl reaction mix contained 50 ng of template DNA, 500 nM of each primer, 300 µM of each dNTP (Roche, Mannheim), 1 unit PfuUltraTM II Fusion HS DNA Polymerase (Stratagene, Agilent Technologies, Waldbronn), 1x reaction buffer (provided by the manufacturer) and 2 µl DMSO. PCR reactions were performed in the Mastercycler ep gradient S (Eppendorf) using the following program: 5 min at 94°C; [1 min at 94°C, 1min at 55°C, 1 min/kb at 72°C] 8x; [30 sec at 94°C, 30 sec at 60°C, 1 min/kb at 72°C] 22x; 10 min at 72°C.

2.2.4 Site-directed mutagenesis

For site-directed mutagenesis the primers were designed according to the “Quick Change Site-directed mutagenesis” protocol (Stratagene). Briefly, the length of the two complementary primers was 25-45 bp and the mutated nucleotides were located in the middle of the primers with 10-15 bp of correct sequence on both sides. The template plasmid was amplified with PfuUltraTM II Fusion HS DNA Polymerase (Stratagene) as described in (2.2.3) or with Pfu DNA Polymerase (Fermentas), using the following reaction conditions and thermocycler program: 1x buffer w/o MgSO₄ (provided by the manufacturer), 3 mM MgSO₄, 200 nM of each primer, 300 µM of each dNTP (Roche, Mannheim), 200 ng template DNA, 1 µl Pfu DNA Polymerase in a total volume of 50 µl. 3 min at 95°C; [30 sec at 95°C, 45 sec at 65°C, 2 min/kb at 72°C] 19x; 20 min at 72°C. If two sites were mutated, both primer pairs were included in the PCR reaction.

The obtained PCR product was separated by agarose gel electrophoresis, purified from the gel (2.2.5) and digested with DpnI (NEB) according to manufacturer’s instructions [163]. After transformation into DH5α the DNA was isolated (2.2.1) and sequenced by MWG (Ebersberg) or Seqlab (Göttingen).

2.2.5 Separation and isolation of DNA fragments

Agarose gel electrophoresis was used to separate DNA fragments according to their size [164]. To load the DNA solution into the gel pockets, 10x loading dye (10 mM EDTA, 30% (w/v) glycerol, 100 µg/ml bromphenol blue) was added and the DNA samples were separated in 0.7% to 2% agarose gels (0.7% (w/v) agarose, 89 mM Tris, 89 mM boric acid, 2 mM EDTA, 0.01% (v/v) ethidium bromide, pH 8.0) and TBE buffer (89 mM Tris, 89 mM boric acid, 2 mM EDTA), using the Sub-Cell-GT Agarose gel electrophoresis system (Biorad, München) at a setting of 120 V for 30 min. The DNA was visualized with UV light (320 nm) and the sizes of the DNA fragments were determined by comparing with the bands of the 1 kb Plus DNA ladder (Invitrogen). DNA bands of interest were cut out of the gel and purified from the agarose gel with the ZymocleanTM Gel DNA Recovery Kit (Zymo Research) according to the manufacturer’s protocol.

The DNA Clean & ConcentratorTM-5 Kit (Zymo Research) or phenol/chloroform extraction was used as well to isolate and purify DNA samples. Phenol/chloroform extraction was

performed in Phase Lock Gel™ (2 ml, heavy) tubes (Eppendorf, Hamburg). Briefly, samples were mixed with an equal volume of phenol:chloroform:isoamyl alcohol (25:24:1) and centrifuged at 14000 rpm for 5 min. The upper aqueous phase containing the DNA was then mixed with an equal volume of chloroform:isoamyl alcohol (24:1), centrifuged again and then transferred to new tube.

If necessary, DNA was further purified or concentrated by ethanol precipitation. 1/10 volume of 3 M sodium acetate pH 5.2 and a 2.5-fold volume of ethanol were mixed with the DNA sample and incubated for 1 h to overnight at -20°C. After centrifugation at 16000 x g, 30 min at 4°C the DNA pellet was washed once with 75% ethanol, air dried and then resolved in 20-50 µl of sterile H₂O.

2.2.6 Transformation of plasmids into chemically competent bacteria

Plasmid DNA was transformed into chemically competent DH5α or BL21-CodonPlus®(De3)-(RIL) bacteria via heat shock treatment [164]. A 50 µl aliquot of bacteria was thawed on ice, DNA was added and the sample was incubated on ice for further 20 min. After heat shock treatment at 42°C for 1 min the sample was put immediately on ice for 2 min. Next, 500 µl of SOC medium (2% (w/v) tryptone, 0.5% (w/v) yeast extract, 10 mM NaCl, 2.5 mM KCl, 10 mM MgCl₂, 20 mM glucose) was added and the mixture was incubated at 37°C for 60 min with shaking. Bacteria were pellet by centrifugation at 1500 x g for 2 min and then spread on a LB-agar plate (1% (w/v) tryptone, 0.5% (w/v) yeast extract, 1% (w/v) NaCl, 1% (w/v) agar), containing the required antibiotic (100 µg/ml ampicillin or 50 µg/ml kanamycin). The bacterial growth plate was incubated at 37°C overnight. A single colony was picked to inoculate growth media.

2.2.7 General cloning procedure

For cloning of cDNA or genomic DNA fragments into target vectors [164] the DNA sequence was amplified by PCR (2.2.3) with primers described in Section 2.2.8. The amplified DNA was purified from an agarose gel (2.2.4) and digested with the same restriction endonucleases used for the target vector. After restriction digest the DNA fragments were separated by agarose gel electrophoresis and purified by gel extraction (2.2.4). The vector sequence was dephosphorylated with Antarctic phosphatase [163]. Ligation was performed in a total reaction volume of 20 µl containing 100 ng vector, 3- to 8-fold molar excess of insert DNA, 1 µl of T4 DNA ligase (NEB) and 1x reaction buffer (provided by the manufacturer). After incubation at RT for 2 h or 15°C overnight 10 µl of the reaction were transformed into DH5α (2.2.6), plated on agar plates with the corresponding antibiotic and incubated at 37°C overnight. Single colonies were picked and grown in 5 ml LB medium (containing the antibiotic corresponding to the used cloning vector) at 37°C overnight. 500 ng of plasmid DNA purified from these cultures (2.2.1) was digested with the restriction enzymes used for cloning and separated by agarose gel electrophoresis. Plasmids exhibiting the correct insert sizes were sequenced by MWG (Ebersberg) or Seqlab (Göttingen).

2.2.8 Summary of cloned plasmid constructs

2.2.8.1 pET11a based expression vector construct

To generate a SIR-2.2-specific antibody directed against the whole protein, the cDNA sequence of SIR-2.2 was cloned into the bacterial expression vector pET11a using NdeI and BamHI restriction sites. The sequence of SIR-2.2 was amplified by PCR (2.2.3) using cDNA isolated from wild type N2 worms (2.4.9) as template.

The following primers were used:

MJ75_sir-2.2cDNA_pet11a_for_NdeI: GGAATTCCATATGATGGCTCAAAAGTTTGTACCGG
 MJ76_sir-2.2cDNA_pet11a_rev_BamHI: CGGGATCCCTACATTTCTTTTAAAACGTCAGAG

2.2.8.2 pEU3-NII-StrepII based expression vector constructs

The cDNA of SIR-2.1, SIR-2.2, SIR-2.3 and SIR-2.4 was cloned into the pEU3-NII-StrepII vector for recombinant protein expression using wheat germ extract, a cell-free *in vitro* transcription and translation system [165]. The construct containing the cDNA of HP1 β was kindly provided by Szabolcs Sörös (Max Planck Institute for Biophysical Chemistry, Göttingen).

The following primers were used:

MW09_sir-2.1cDNA_for_XhoI: CCGCTCGAGATGTCACGTGATAGTGGCAACG
 MW10_sir-2.1cDNA_rev_NotI: ATAAGAATGCGGCCGGATACGCATTTCTTCACACAAATGC
 MJ130_sir-2.2cDNA_for_XhoI: CCGCTCGAGATGGCTCAAAAGTTTGTACCG
 MJ131_sir-2.2cDNA_rev_NotI: ATAAGAATGCGGCCGCCATTTCTTTTAAAACGTCAGAG
 MW13_sir2.3cDNA_for_XhoI: CCGCTCGAGATGGCACGAAAGTATGTACC
 MW14_sir2.3cDNA_rev_NotI: ATAAGAATGCGGCCGCCATTTCTTTCAAAAACATCCG
 MW11_sir2.4cDNA_for_XhoI: CCGCTCGAGATGAAATCTGCAAAATACAAAACCG
 MW12_sir2.4cDNA_rev_NotI: ATAAGAATGCGGCCGCGCTAATTTTCAATGGAATAGGCAC

2.2.9 pCDNA3.1(+)-FLFL-HAHA-N mammalian expression vector based constructs

To express *C. elegans* and mammalian proteins with an N-terminal FLAG-tag in mammalian cells cDNA sequences were cloned into the mammalian expression vector pCDNA3.1(+)-FLFL-HAHA-N, kindly provided by Nora Köster-Eiserfunke (Max Planck Institute for Biophysical Chemistry, Göttingen) [156].

The sequences of *C. elegans* proteins were amplified by PCR (2.2.3) using cDNA isolated from wild type N2 worms (2.4.9) as template. The DNA sequences of the mammalian proteins were obtained by PCR from cDNA of NIH3T3 cells, kindly provided by Nils Kost (Max Planck Institute for Biophysical Chemistry, Göttingen). Mouse SIRT5 cDNA was amplified from the plasmid pCAGGS-SIRT5 kindly provided by the laboratory of Leonard Guarente (Massachusetts Institute of Technology, Cambridge, USA).

The following primers were used:

C. elegans SIR-2 proteins:

MW24_sir-2.1cDNA_for_NotI: ATAAGAATGCGGCCGCATGTCACGTGATAGTGGCAACG
 MW10_sir-2.1cDNA_rev_NotI: ATAAGAATGCGGCCGCGATACGCATTTCTTACACAAATGC

MJ94_sir_2.2_cDNA_for_BamHI: CGCGGATCCATGGCTCAAAAGTTTGTACCGG
 MJ131_sir-2.2cDNA_rev_NotI: ATAAGAATGCGGCCGCCATTTCTTTTAAAACGTCAGAG

MW25_sir2.3cDNA_for_NotI: ATAAGAATGCGGCCGCATGGCACGAAAGTATGTACC
 MW14_sir2.3cDNA_rev_NotI: ATAAGAATGCGGCCGCCATTTCTTTCAAAACATCCG

C. elegans ACDH-3:

MW79_acdh-3cDNA_for_NotI: ATAAGAATGCGGCCGCATGTCTTCTTGTCTCGGTCTC
 MW80_acdh-3cDNA_rev_NotI: ATAAGAATGCGGCCGCAGCCTTTTGTGATATTTCGATGTC

C. elegans CYC-1:

MW62_cyc-2.1cDNA_for_NotI: ATAAGAATGCGGCCGCATGTCCGATATCCCAGCTGGAG
 MW63_cyc-2.1cDNA_rev_NotI: ATAAGAATGCGGCCGCGAGGGACTTGCGGATTCAACC

C. elegans biotin carboxylases:

MW75_mccc-1cDNA_for_NotI: ATAAGAATGCGGCCGCATGCTTGGTGTATTCCAAAAACGATGTGC
 MW76_mccc-1cDNA_rev_NotI: ATAAGAATGCGGCCGCTGCGAATTGAACCAAAACTGC

MW83_pcca-1cDNA_for_NotI: ATAAGAATGCGGCCGCATGCTCCGTGCTGCATCCAG
 MW84_pcca-1cDNA_rev_NotI: ATAAGAATGCGGCCGCCTCGAGCTCAACGAGCACCTC

MW121_pyc-1cDNA_for_NotI: ATAAGAATGCGGCCGCATGCGGTTCTCCCGCATCCCACC
 MW122_pyc-1cDNA_rev_NotI: ATAAGAATGCGGCCGCTGGTTCAACTTCAACTACCAAGTCTCCGG
 C

Mouse biotin carboxylases:

MW106_mMCCC1cDNA_for_NotI: ATAAGAATGCGGCCGCATGGCGGGCGGGCGGCGTTG
 MW107_mMCCC1cDNA_rev_NotI: ATAAGAATGCGGCCGCTTTGTGAGACTCCTCCTCCTCAA
 TTCC

MW103_mPCCA1cDNA_for_NotI: ATAAGAATGCGGCCGCATGGCGGGGAGTGGGTCAGG
 MW104_mPCCA1cDNA_rev_NotI: ATAAGAATGCGGCCGCTCCAGCTCCACAAGCAGGTCTCC

MW132_mPCcDNA_for_NotI: ATAAGAATGCGGCCGCATGCTGAAGTTCCAAACAGTTCGA
 GG

MW133_mPCcDNA_rev_NotI: ATAAGAATGCGGCCGCCTCAATCTCTAGGATGAGGTGTC
 GC

Site-directed mutagenesis PCR (2.2.4) was performed to generate a SIR-2.2 construct that contains two point mutations in amino acid residues that are important for the enzymatic activity of sirtuins. The histidine (H) residue 134 and the asparagine (N) residue 117 were mutated to a tyrosine (Y) and alanine (A) residue, respectively, using the following primers:

MW181_sir-2.2cDNA_H134Y_for: GGTAACGGAACCTtATGGCAGTGCTCTTCAAGTAAAATGT
 ACAACATG
 MW182_sir-2.2cDNA_H134Y_rev: CATTTTACTTGAAGAGCACTGCCATaAAGTTCCGTTACCAT
 TTTTGAGC
 MW183_sir-2.2cDNA_N117A_for: CCAATGGTTAATCACACAAgcCGTGGATGGGCTTCACTTA
 AAAGCGG
 MW184_sir-2.2cDNA_N117A_rev: GTGAAGCCCATCCACGgcTTGTGTGATTAACCATTGGAAT
 CTATCGG

2.2.10 pCDNA3.1(+)-FLFL-HAHA-C mammalian expression vector based constructs

To map the domain mediating the interaction with mouse SIRT4 the sequences of the different biotin carboxylase domains were cloned with an C-terminal FLAG-tag into the mammalian expression vector pCDNA3.1(+)-FLFL-HAHA-C kindly provided by Nora Koester-Eiserfunke (Max Planck Institute for Biophysical Chemistry, Göttingen) [156].

The following primers were used:

Mouse pyruvate carboxylase:

MW132_mPCcDNA_for_NotI:	ATAAGAATGCGGCCGCATGCTGAAGTTCCAAACAGTTCGAGG
MW134_mPCcDNA_rev_XhoI:	GGCCGCTCGAGTCACTCAATCTCTAGGATGAGGTCGTCCG
MW132_mPC_BC_for_NotI:	ATAAGAATGCGGCCGCATGCTGAAGTTCCAAACAGTTCGAGG
MW141_mPC_BC_rev_XhoI:	GGCCGCTCGAGTTAAACAGCAGGATCCACAGGACTGG
MW142_mPC_ATP_for_NotI:	ATAAGAATGCGGCCGCGGTCCAAGCCCAGAGGTGGTCCGC
MW143_mPC_ATP_rev_XhoI:	GGCCGCTCGAGTTAGTTCTCCTGCCGCAGGCCAGG
MW144_mPC-PCT_for_NotI:	ATAAGAATGCGGCCGCCCTGTGGTGCCCATAGGCC
MW145_mPC-PCT_rev_XhoI:	GGCCGCTCGAGTTAGTTGCCAGACTTCATGGTAGCCG
MW146_mPC_BCCPL_for_NotI:	ATAAGAATGCGGCCGCTCCGACGTGTATGAGAATGAGATTCC
MW134_mPCcDNA_rev_XhoI:	GGCCGCTCGAGTCACTCAATCTCTAGGATGAGGTCGTCCG
MW147_mPC_BCCP_for_NotI:	ATAAGAATGCGGCCGCAAGGCTTTGAAGGATGTGAAGGGCC
MW134_mPCcDNA_rev_XhoI:	GGCCGCTCGAGTCACTCAATCTCTAGGATGAGGTCGTCCG

Mouse propionyl carboxylase α -subunit:

MW103_mPCCA1cDNA_for_NotI:	ATAAGAATGCGGCCGCATGGCGGGGCAGTGGGTCAGG
MW105_mPCCA1cDNA_rev_XhoI:	GGCCGCTCGAGTCATTCCAGCTCCACAAGCAGGTCTCC
MW103_mPCCA1_BC_for_NotI:	ATAAGAATGCGGCCGCATGGCGGGGCAGTGGGTCAGG
MW174_mPCCA1_BC_rev_XhoI:	GGCCGCTCGAGTCACACATCAGGCCTAATAACTGGTACTC
MW175_mPCCA1_Cterm_for_NotI:	ATAAGAATGCGGCCGCGCTAAGTGGGAGCTCTCGGTAAAGTTAC
MW105_mPCCA1_Cterm_rev_XhoI:	GGCCGCTCGAGTCATTCCAGCTCCACAAGCAGGTCTCC

Mouse methylcrotonyl-CoA carboxylase α -subunit:

MW106_mMCCC1cDNA_for_NotI:	ATAAGAATGCGGCCGCATGGCGGCGGCGGCGTTG
MW108_mMCCC1cDNA_rev_XhoI:	GGCCGCTCGAGTCATTTGTCAGACTCCTCCTCCTCAAATTC
MW106_mMCCC1_BC_for_NotI:	ATAAGAATGCGGCCGCATGGCGGCGGCGGCGTTG
MW176_mMCCC1_BC_rev_XhoI:	GGCCGCTCGAGTCAACTGCTGAATGAAAACGGAGAGAATTGATC
MW177_mMCCC1_Cterm_for_NotI:	ATAAGAATGCGGCCGCGGGAGAAGACTGAATATCTCTTACACCAGG
MW108_mMCCC1_Cterm_rev_XhoI:	GGCCGCTCGAGTCATTTGTCAGACTCCTCCTCCTCAAATTC

2.2.11 pEGFP-N1 mammalian expression vector based constructs

To express *C. elegans* and mouse sirtuins with an N-terminal GFP-tag in HEK293 cells, the sequences were cloned into the mammalian expression vector pEGFP-N1 using the following primers:

C. elegans SIR-2 proteins:

MW09_sir-2.1cDNA_for_XhoI:	CCGCTCGAGATGTCACGTGATAGTGGCAACG
MW131_sir-2.1cDNA_rev_KpnI:	CGGGGGTACCCCGATACGCATTTCTTCACACAAATGCG
MJ130_sir-2.2cDNA_for_XhoI:	CCGCTCGAGATGGCTCAAAAGTTTGTACCG
MW17_sir-2.2cDNA_rev_BamHI:	GGGATCCGCGCGCATTTCTTTTAAAACGTCAGAG
MJ88_sir-2.3cDNA_for_XhoI:	CCGCTCGAGTGTATGGCACGAAAGTATGTACC
MW130_sir-2.3cDNA_rev_BamHI:	GGGATCCGCGCGCGATGAAAATTGGTTTGTTTTGC

Mitochondrial mouse sirtuins:

MW137_mSIRT3cDNA_for_XhoI:	GGCCGCTCGAGATGGCGCTTGACCCTCTAGGCG
MW156_mSIRT3cDNA_rev_KpnI:	CGGGGGTACCCCTCTGTCCTGTCCATCCAGCTTGCC
MW101_mSIRT4cDNA_for_XhoI:	CCGCTCGAGATGAGCGGATTGACTTTCAGGCCG
MW102_mSIRT4cDNA_rev_BamHI:	GGGATCCGCGCGGGGATCTTGAGCAGCGGAACCTCAG
MW139_mSIRT5cDNA_for_XhoI:	GGCCGCTCGAGATGCGACCTCTCCTGATTGCTCC
MW157_mSIRT5cDNA_rev_KpnI:	CGGGGGTACCCAGAAAGTCCTTTTCAGTTTCATGAGGAGC

2.2.11.1 L4440 based constructs

For knockdown of SIR-2.2 and SIR-2.3 by RNAi feeding the cDNA sequences were cloned into the vector L4440 using the following primers:

MJ39_sir-2.2cDNA_for_KpnI:	GGGGTACCCCGCCGAGCTCTGTGAAAATTCC
MJ40_sir-2.2cDNA_rev_BglII:	GAAGATCTTTTATTAACCTTCATCGTCGCCATGT
MJ88_sir-2.3cDNA_for_XhoI:	CCGCTCGAGTGTATGGCACGAAAGTATGTACC
MJ89_sir-2.3cDNA_rev_XhoI:	CCGCTCGAGCTTCATTGTTGCCATCTG

2.2.11.2 pPD115.62 based constructs

To generate transgenic *C. elegans* strains that express GFP-tagged (C-terminal) SIR-2.2 under control of the endogenous promoter, the genomic sequence of SIR-2.2 was cloned into the vector pPD115.62 (Andrew Fire, Stanford University, Stanford, USA) using PstI and MluI restriction sites. The myo-3 promoter was removed and at the C-terminus a Strep-tag and a TEV protease cleavage site were introduced. The promoter and genomic sequence of SIR-2.2 was amplified by PCR from the cosmid F46G10 using the following primers:

MW18_sir-2.2promoter&genomic_for_PstI:	GCGGGCTGCAGGCACATTTTGAACATGTGAGCC
MW19_sir-2.2promoter&genomic_rev_MluI:	CGGGACGCGTGGCGCCCTGAAAATACAGGTTTTCCTTCTC GAATTGTGGGTGGGACCAGGATCCCATTTCTTTTAAAACG TCAGAG

To generate mCherry-tagged transgenic worm strains the sequence of *gfp* was replaced by the sequence of *mcherry* using the following primer pair:

MW53_mCherry_for_MluI:	CGGG <u>ACGCGT</u> GGCATGGTGAGCAAGGGCGAGGAGG
MW54_mCherry_rev_EcoRI:	GCGCG <u>GAAATTC</u> TACTTGTACAGCTCGTCCATGCCG

2.3 Protein biochemical methods

2.3.1 SDS polyacrylamide gel electrophoresis (SDS-PAGE)

Separation of proteins according to their molecular weight was performed by SDS polyacrylamide gel electrophoresis [166] based on standard protocols [167]. Tris-glycine gels with a 10%, 12% or 15% separating gel (10-15% acrylamide/bisacrylamide (37.1:1), 0.4 M Tris, 0.1% (w/v) SDS, 5% (v/v) glycerol, 0.1% (w/v) APS, 0.04% (v/v) TEMED, pH 8.8) and a 4% stacking gel (4% acrylamide/bisacrylamide (37.1:1), 0.68 M Tris, 0.1% (w/v) SDS, 0.1% (w/v) APS, 0.1% (v/v) TEMED, pH 6.8) were poured and run using the Mini-Protean electrophoresis system (Bio-Rad, München). After boiling for 5 min in protein sample buffer (62.5 mM Tris, 8.5% (v/v) glycerol, 2% (w/v) SDS, 100 µg/ml bromphenol blue, 150 mM 2-mercaptoethanol) the samples were loaded onto the gels and separated at a constant voltage of 150-200 V in SDS-PAGE running buffer (25 mM Tris, 200 mM glycine, 0.1% (w/v) SDS) until the tracking dye reached the bottom of the gel. SeeBlue[®] Plus2 Pre-Stained protein standard (Invitrogen, Karlsruhe) was used as size reference.

For mass spectrometric analysis of protein samples the NuPAGE[®] Pre-cast system (Invitrogen, Karlsruhe) was used according to manufacturer's instructions.

2.3.2 Protein detection techniques

2.3.2.1 Coomassie Blue staining

Coomassie Blue staining was used to stain proteins in SDS-PAGE gels. The gel was incubated in Coomassie staining solution (0.05% (w/v) Coomassie brilliant blue, 10% (v/v) acetic acid, 50% (v/v) methanol) for 20-30 min at RT and then destained in destaining solution (10% (v/v) acetic acid, 7.5% (v/v) methanol) for at least 60 min at RT.

2.3.2.2 Western blotting

For antibody-specific detection of proteins samples were separated by SDS-PAGE and transferred to a nitrocellulose membrane in transfer buffer (25 mM Tris, 200 mM glycine, 20% (v/v) methanol, 0.1% (w/v) SDS) for 60 min at 4°C and constant voltage of 100 V with the Mini-Trans-Blot blotting system (Bio-Rad, München). After transfer the membrane was blocked in PBS-T milk (137 mM NaCl, 2.7 mM KCl, 10 mM Na₂HPO₄, 2 mM KH₂PO₄, 0.1% (v/v) Tween[®]-20, 5% (w/v) low-fat dry milk, pH 7.4) for 30-60 min with gentle rocking. To detect the protein of interest the membrane was incubated with the primary antibody diluted in PBS-T milk (for dilutions see 2.1.6) for 60 min at RT or overnight at 4°C. The membrane was washed four times with PBS-T (137 mM NaCl, 2.7 mM KCl, 10 mM Na₂HPO₄, 2 mM KH₂PO₄, 0.1% (v/v) Tween[®]-20, 5% (w/v), pH 7.4) for 15 min each and then incubated with the respective horseradish peroxidase (HRP) conjugated secondary antibodies (1:5000 dilution) in PBS-T milk for 60 min at RT. The membrane was washed

again with PBS-T four times for 15 min each. To detect the protein of interest chemiluminescently ECL or ECL Plus Western Blotting Detection Reagents (GE Healthcare) and Amersham Hyper ECL films (GE Healthcare) were used according to manufacturer's instructions. Films were developed with the Kodak X OMAT 2000 processor.

2.3.3 Mass spectrometry and data analysis

Protein samples were analyzed by mass spectrometry (MS) in the group of Dr. Henning Urlaub at the Max Planck Institute for Biophysical Chemistry (Göttingen). Proteins were separated on NuPAGE[®] gels (2.3.1) and stained with Coomassie (2.3.2.1). Entire individual lanes were cut into 23 slices of equal size and digested according to Shevchenko et al. [168]. After extraction peptides were analyzed by LC-coupled tandem MS on an Orbitrap XI mass spectrometer (Thermo Fisher Scientific). The MASCOT search engine (with the taxonomy filter *C. elegans*) was used to search CID fragment spectra against the NCBI database. The statistical program R was used to analyze output files and subtract output files from each through their gi-numbers (NCBI).

2.3.4 Generation of SIR-2.2-specific antibodies using recombinant protein for immunization

2.3.4.1 Expression of recombinant SIR-2.2 in *E. coli*

To express non-tagged SIR-2.2 protein the plasmid pET11a containing the cDNA sequence of SIR-2.2 (2.2.8) was transformed into *E. coli* BL21 (DE3) RIL cells (2.2.6) and a single colony was picked to inoculate 100 ml pre-culture (LB medium) and finally 6 l of ZYM-5052 auto-inducing medium (1% (w/v) N-Z-amine (enzymatic digested casein from bovine milk), 0.5% (w/v) yeast extract, 0.5% (w/v) glycerol, 0.05% (w/v) glucose, 0.2% (w/v) α -lactose, 25 mM Na₂HPO₄, 25 mM KH₂PO₄, 50 mM NH₄Cl, 5 mM Na₂SO₄, 2 mM MgCl₂, 50 μ M FeCl₃, 20 μ M CaCl₂, 10 μ M MnCl₂, 10 μ M ZnSO₄, 2 μ M CoCl₂, 2 μ M CuCl₂, 2 μ M NiCl₂, 2 μ M Na₂MoO₄, 2 μ M Na₂SeO₃, 2 μ M H₃BO₃) both containing 100 μ g/ml ampicillin [169]. After shaking 24 h at 25°C bacteria were harvested by centrifugation at 6000 x g for 15 min at 4°C. Expression of protein was checked by analyzing an aliquot of bacteria by SDS-PAGE (2.3.1) and Coomassie Blue staining (2.3.2.1).

2.3.4.2 Purification of recombinant SIR-2.2 from inclusion bodies

Since full-length non-tagged SIR-2.2 was not soluble when expressed in *E. coli*, it was purified from inclusion bodies analog to Luger et al. [170] with some modifications. The bacterial pellet from 2.3.4.1 was resuspended in 30 ml washing buffer (50 mM Tris, 100 mM NaCl, 1 mM EDTA, 1 mM PMSF, 1mM benzamidine, 1 mM DTT, pH 7.5) and lysed with the EmulsiFlex-C5 cell disruptor (Avestin) at 4°C until homogeneity was reached. After centrifugation at 23000 x g and 4°C for 20 min the pellet containing the SIR-2.2 inclusion bodies was resuspended and washed twice with 150 ml TW buffer (50 mM Tris, 100 mM NaCl, 1 mM EDTA, 1 mM PMSF, 1mM benzamidine, 1 mM DTT, 1% (v/v) Triton X-100, pH 7.5) followed by two washes with 150 ml wash buffer. To extract the inclusion bodies 1 ml DMSO was added and the pellet was incubated at RT for at least 30 min. 10 ml unfolding buffer (7 M guanidinium-HCl, 20 mM Tris-HCl, 10 mM DTT, pH 8.0) were added and the

pellet was shaken gently for 1 h at RT. To remove non-dissolved material the suspension was centrifuged for 20 min at 23000 x g and 4°C. The supernatant was saved and subjected to further purification by gel-filtration.

2.3.4.3 Gelfiltration and ion exchange chromatography

Gelfiltration and ion exchange chromatography were performed on the ÄKTA Explorer FPLC instrument (GE Healthcare). The protein extract was first purified using an XK50/100 Sephacryl S-200 high-resolution gel-filtration column (GE Healthcare) that had been equilibrated with SAU1000 buffer (7 mM deionized urea (passed over Amberlite MB3 ion exchange resin prior to use), 20 mM Tris-HCl, 1 mM EDTA, 1 M NaCl, 2 mM DTT, pH 8.0). Eluted peak fractions that contained SIR-2.2 were combined, diluted 1:20 in SAU-0 buffer (7 mM deionized urea, 20 mM Tris-HCl, 1 mM EDTA, 2 mM DTT, pH 10.5) and applied to a MonoQ™ 5/50 GL Anion exchange column (GE Healthcare) equilibrated in SAU-0 buffer. SIR-2.2 was eluted with a linear gradient from 50 mM to 1 M NaCl in 20 column volumes. Fractions containing SIR-2.2 were pooled and analyzed for purity by SDS-PAGE (2.3.1) and Coomassie Blue staining (2.3.2.1).

2.3.4.4 High-performance liquid chromatography (HPLC)

To further improve the purity of the SIR-2.2 sample (2.3.4.3) HPLC was performed using the HPLC Prominence system (Shimadzu) and a VYDAC® 208TP C8 reverse phase column (Grace, Deerfield, USA). Peak fractions containing highly pure SIR-2.2 were pooled and lyophilized in the SpeedVac Savant SPD131DDA (Thermo Scientific, Braunschweig).

2.3.4.5 Immunization, purification and characterization of SIR-2.2-specific antibodies from antiserum

Two rabbits were immunized with recombinant SIR-2.2 protein by the Charles River Laboratory according to their proprietary protocol. For immunization of each rabbit 1.6 mg protein at a concentration of 1 mg/ml in 3 M urea and 50 mM NaPhosphate buffer pH 6.8 were forwarded to the company.

The serum of both rabbits was tested on crude *C. elegans* lysates (2.4.7.3) of N2 and *sir-2.2(tm2648)X* and *sir-2.2(tm2673)X* mutant worms by Western blot analysis (2.3.2.2). Sir-2.2-specific antibodies present in the serum of one rabbit were affinity purified using SIR-2.2 protein bound to nitrocellulose membranes [171, 172]. Briefly, 1 mg of recombinant SIR-2.2 (protein also used for immunization) was loaded onto 4 SDS-PAGE gels and transferred onto nitrocellulose membranes (GE Healthcare) by Western blotting. After staining the membranes with Ponceau-S solution (5% (v/v) acetic acid, 0.1% (w/v) Ponceau-S), the bands of SIR-2.2 were cut out, destained by washing with PBS-T and dried. The membrane stripes containing SIR-2.2 protein were blocked with PBS-T milk for 1 h at RT and then washed three times with PBS-T. 2 ml serum were diluted with 8 ml PBS (1:5) and incubated with the membrane stripes for 2-3 h at RT or overnight at 4°C. After washing four times 10 min each with PBS-T SIR-2.2-specific antibodies were eluted from the membrane stripes with glycine elution buffer (5 mM glycine, 0.01% BSA, 0.05% Tween, 500 mM NaCl, pH 2.6). One membrane stripe at a time was swirled for 30 sec with 2 ml glycine elution buffer. The buffer was then immediately transferred to a 15 ml tube with 600 µl 1M Tris pH 8.0. The glycine elution step

was repeated twice and the eluates were all pooled in the same tube. The pH of the eluate was checked with pH stripes and was between pH 7-8. The eluates of all four membrane stripes were pooled, dialyzed against PBS at 4°C overnight and concentrated to a volume of approximately 1 ml with an Amicon Ultra centrifugal filter (Millipore). For long-term storage of the SIR-2.2-specific antibodies sodium azide was added to a final concentration of 0.05% (w/v) and the aliquots were stored at 4°C for further use.

The specificity of the SIR-2.2 antibodies was analyzed on crude *C. elegans* lysate (2.4.7.3) of wild type N2 and *sir-2.2 deletion* mutant worm strains (*sir-2.2(tm2648)* and *sir-2.2(tm2673)*) by Western blotting (2.3.2.2). The antibodies of one rabbit specifically detected SIR-2.2 and are referred to as anti-SIR-2.2 antibodies in this study. These antibodies were used for Western blot and immunoprecipitation experiments (2.4.8).

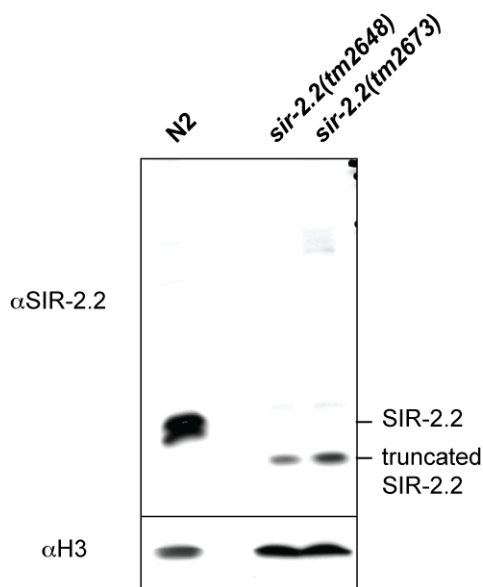


Figure 2-1: Western blot analysis of generated SIR-2.2-specific antibodies.

Crude extracts of wild type N2, *sir-2.2(tm2648)* and *sir-2.2(tm2673)* mutant worms were separated by SDS PAGE and analyzed by Western blotting using the anti-SIR-2.2 antibodies in a dilution of 1:1000. Western blot analysis with anti-H3 antibodies was used to confirm equal loading. Running positions of the full-length and truncated SIR-2.2 protein are indicated on the right.

2.4 *C. elegans* based methods

2.4.1 Culturing *C. elegans* on agar plates

C. elegans strains were maintained on Nematode Growth Medium (NGM) agar plates (0.3% (w/v) NaCl, 0.25% (w/v) peptone, 1.7% (w/v) agar, 5 mg/l cholesterol, 1 mM CaCl₂, 1 mM MgSO₄, 25 mM K-phosphate buffer, pH 6.0, 100 µg/ml streptomycin, 10 µg/ml nystatin) seeded with *E. coli* OP50-1 at 15°C, 20°C or 24.5°C [158, 173]. Larger quantities of worms were obtained on Super NGM plates (0.3% (w/v) NaCl, 2% (w/v) peptone, 1.7% (w/v) agar, 15 mg/l cholesterol, 1 mM CaCl₂, 1 mM MgSO₄, 25 mM K-phosphate buffer, pH 6.0, 100 µg/ml streptomycin, 10 µg/ml nystatin) which produced a much thicker bacterial lawn and allowed the worms to grow to higher densities [174].

Worms were transferred from an old plate to a new plate either by cutting out a chunk of agar with a spatula and putting it on a new plate, or by picking individual worms with a platinum wire mounted to a pasteur pipette.

2.4.2 Liquid culture of *C. elegans*

For biochemical analyses large quantities of *C. elegans* were generated by growing worms in liquid culture [175]. Worms of approximately 5 (9 mm) NGM plates were washed off with dH₂O. After washing three times with dH₂O the worms or axenic eggs (obtained from hypochloride treatment (2.4.3)) were used to inoculate 200 ml S basal Medium (0.1 M NaCl, 50 mM K-phosphate buffer pH 6.0, 5 mg/ml (w/v) cholesterol, 10 mM K-citrate pH 6.0, 6.4 mM EDTA, 2.5 mM FeSO₄, 1 mM MnCl₂, 1 mM ZnSO₄, 0.1 mM CuSO₄, 3 mM CaCl₂, 3 mM MgSO₄, 1x Penicillin/Streptomycin/Neomycin (PNS, Gibco), 1x Steptomycin (Sigma)) supplemented with 2 ml concentrated HB101 bacterial solution. The worm cultures were incubated at 15°C, 20°C or 25°C while shaking (120 rpm) for 3 to 6 days until a high worm density had been reached with the majority of worms being adults. The growth of the worms was monitored daily by inspecting small aliquots of worm culture with a dissecting microscope. More bacterial solution was added to the culture if required. For harvesting, the worm suspension was transferred to 50 ml falcon tubes and centrifuged at 1500 x g and 4°C for 3 min. The worm pellet was washed several times with dH₂O until the supernatant was clear. Depending on further experiments the worm pellet was either flash frozen in liquid N₂ and stored at -80°C or directly lysed for preparation of mitochondria (2.4.7.2).

2.4.3 Axenization to synchronize or decontaminate *C. elegans*

Worms were harvested when the plates contained many gravid hermaphrodites and washed several times with dH₂O. Worms were resolved by treatment with bleach solution (0.5 M NaOH, 1.2% NClO) for 10 min with frequent vortexing in between. The released axenized eggs were collected by centrifugation at 1500 x g, 4°C for 3 min and washed three times with dH₂O. The eggs were either directly transferred to fresh NGM plates or further staged by incubation in M9 buffer overnight at 20°C. In the absence of food hatched larvae arrested in L1 stage and resumed growth after transferring them onto fresh NGM plates the next day. If worms were severely contaminated gentamycin (10 mg/l) was added to the M9 buffer for overnight incubation [173].

2.4.4 Freezing and recovery of *C. elegans* stocks

For indefinite storage *C. elegans* strains were frozen and kept at -80°C. Worms of 2-3 freshly starved 90 mm plates (containing many L1-L2 stage larvae) were washed off plates with dH₂O and collected in a 15 ml falcon tube. The tube was incubated on ice until worms had settled to the bottom of the tube. The supernatant was removed and the volume of the worm suspension was adjusted to 3-4 ml with dH₂O. After adding an equal volume of freezing solution (0.3% (w/v) KH₂PO₄, 0.6% (w/v) Na₂HPO₄, 0.5% (w/v) NaCl, 1 mM MgSO₄, 30% glycerin (v/v)), the worm suspension was mixed and aliquoted into cryotubes (1 ml/tube). The cryotubes were packed in a styrofoam box and frozen at -80°C. For recovery of a *C. elegans* stock, a frozen aliquot was thawed at RT and transferred onto a fresh NGM plate [158, 173].

2.4.5 Single worm PCR

To determine whether a worm is homozygous or heterozygous for a particular deletion allele, single worm duplex PCR genotyping was performed [119]. A single hermaphrodite was picked into 2.5 µl single worm PCR lysis buffer (10 mM Tris, 50 mM KCl, 2.5 mM MgCl₂,

0.45% (v/v) NP-40, 0.45% (v/v) Tween 20, 0.01% (w/v) gelatin, 100 µg/ml Proteinase K, pH 8.3) of a PCR tube. The tube was frozen at -80°C for 30 min. Worms were lysed in the PCR machine by incubating them at 60°C for 60 min followed by 15 min at 95°C to inactivate the Proteinase K. The PCR reaction was then performed with three primers that can amplify two different-sized PCR products, each arising only from the wild type or deletion allele, respectively. Primer F1 (forward primer) and primer R1 (reverse primer) were placed outside and primer F2 (forward primer) within the deletion mutation. Due to a relatively short elongation time primers F2 and R1 produced a ~250-400 bp long wild type amplicon and primers F1 and R1 a ~100 bp larger deletion allele amplicon.

To each lysed worm 22.5 µl PCR reaction buffer (2.2 mM MgCl₂, 250 µM of each dNTP (Roche), 0.7 µM of each primer, 0.5 unit Taq DNA polymerase (Fermentas), 1x reaction buffer (provided by the manufacturer)) and the PCR was performed using the following protocol: 3 min at 94°C; [40 sec at 94°C, 40 sec at 55°C, 40 sec at 72°C] 8x; [40 sec at 94°C, 40 sec at 56°C, 40 sec at 72°C] 22x; 5 min at 72°C.

The following primers were used to genotype *sir-2.2(tm2648)* and *sir-2.2(tm2673)* deletion mutant worms:

MW27_sir-2.2_F1	GCAGGAATATCTACAGAATCTGG
MW28_sir-2.2_R1	AGAGGCGTCCATACTCTCTTAG
MW29_sir-2.2_F2	GGTACATTGGACTGAATCAACTC

The following primers were used to analyze *sir-2.3(ok444)* deletion mutant worms:

MW34_sir-2.3_R1	CTGATCAGCTCTAGTAGGTCCA
MW35_sir-2.3_F2	CCGACTTACTTAATCATACCAC
MW36_sir-2.3_F1	GGCTCATAACTGCTCTCACG

2.4.6 Isolation of Mitochondria for cellular subfractionation

Mitochondria were isolated based on the protocol of Li et. al. [176] with minor modifications. Synchronized worms were obtained from axenic eggs by treatment with hypochloride (2.4.3) and harvested when grown to adult stage on Super NGM plates.

Worms were washed of plates with dH₂O and collected by centrifugation at 3000 rpm at 4°C for 3 min. After washing three to four times worms were resuspended in M9 buffer (0.3% KH₂PO₄, 0.6% Na₂HPO₄, 0.5% NaCl, 1mM MgSO₄) and incubated 30 min at RT to allow them to digest remaining bacteria in the gut. The isolation of mitochondria was performed in the cold room and throughout the purification procedure all samples were kept on ice. For isolation of mitochondria five to 10 g of worms were resuspended in 20 ml lysis buffer (250 mM sucrose, 10 mM HEPES pH 7.5, 1 mM EGTA) containing protease inhibitor cocktail (complete EDTA-free, Roche, Mannheim) and homogenized in a glass tissue grinder using 20 strokes. The homogenate was centrifuged at 800 x g for 10 min at 4°C. The supernatant was saved and the pellet was resuspended in another 20 ml of lysis buffer. To achieve disruption of more than 90% of the worms the homogenization procedure and 800 x g centrifugation step were repeated four times. Afterwards, supernatants were pooled (corresponding to the postnuclear supernatant) and centrifuged at 12000 x g for 10 min at 4°C. The resulting supernatant, which is referred to the postmitochondrial supernatant, was

saved. To increase the purity of the crude mitochondria, the pellet was gently resuspended in 10 ml lysis buffer and subsequently centrifuged at 800 x g. The pellet was discarded and the collected supernatant was centrifuged at 12000 x g for 10 min at 4°C. The final crude mitochondrial pellet was resuspended in LB buffer. After adjusting the protein concentration to 5-10 mg/ml with LB, aliquots were flash frozen in liquid N₂ and stored at – 80°C.

During the purification procedure aliquots of the postnuclear supernatant, postmitochondrial supernatant and final crude mitochondrial pellet were taken and analyzed by SDS-PAGE and Western blotting (2.3.2.2).

2.4.7 Preparation of *C. elegans* protein extracts

2.4.7.1 Preparation of total worm protein extracts

Total worm protein extract was prepared according to Cheeseman et al. [177] with some modifications. Sufficient amounts of worms were obtained by liquid culture (2.4.2). Approximately 5 g of frozen worm pellet was grounded in liquid N₂ with a pre-chilled mortar and pestle. An equal volume of 2x Cheeseman buffer (50 mM Hepes, 2 mM EGTA, 2 mM MgCl₂, 200 mM KCl, 20% (v/v) glycerol, 0.1% (v/v) NP-40, pH 7.4) containing 2x protease inhibitor cocktail (Complete EDTA-free Protease inhibitor, Roche) was added to the grounded worms, thawed on ice and then sonicated with a Branson Digital Sonifier using the following settings: 30% amplitude for 3 min total (15 sec on, 59 sec off), 40% amplitude for 30 sec total (15 sec on, 59 sec off). After centrifugation at 22000 x g and 4°C for 10 min the supernatant was transferred to a fresh ultracentrifuge tube and further clarified by centrifugation at ~105000 g and 4°C for 20 min. The supernatant was collected in a fresh tube and protein concentration of the extract was determined using the Coomassie Plus (Bradford) Protein Assay (Thermo Scientific) according to manufacturer's instructions.

2.4.7.2 Preparation of mitochondrial protein extracts

For mitochondrial protein extract preparation mitochondria were isolated according to the protocol described by Gandre and van der Blik [178] with some modifications. 5 g of worms grown in liquid culture (2.4.2) were resuspended in 10 ml ice-cold isolation buffer (IB) (210 mM mannitol, 70 mM sucrose, 10 mM Hepes, 0.1 mM EDTA, 0.4% (w/v) BSA, 1x Complete EDTA-free protease inhibitor (Roche), pH 7.6) and homogenized in a chilled Glass-Teflon Potter (Size S) attached to a Potter homogenizer (Potter S, B. Braun Biotech) with 15 strokes at 1200 rpm. The homogenate was transferred to a 50 ml falcon tube and centrifuged at 750 x g and 4°C for 10 min. The supernatant (corresponding to the postnuclear supernatant (PNS)) was collected in a fresh tube and the pellet was resuspended in 10 ml IB. To disrupt the majority of worms, the homogenization procedure and 750 x g centrifugation step were repeated four times. All postnuclear supernatants were pooled and then centrifuged at 12000 x g, 4°C for 10 min. The resulting supernatant referred to as postmitochondrial supernatant (PMS) was discarded, the mitochondrial pellet was resuspended carefully in 12 ml IB and centrifuged at 12000 x g, 4°C for 10 min. The supernatant was discarded and the crude mitochondrial pellet was resuspended in IB buffer. After adjusting the protein concentration to 5-10 mg/ml with IB, the sample was aliquoted, flash frozen in liquid N₂ and stored at – 80°C.

1 ml crude mitochondria were thawed on ice and centrifuged at 12000 x g and 4°C for 10 min. The mitochondrial pellet was resuspended in 750 µl lysis buffer (25 mM Hepes, 1 mM EGTA, 1 mM MgCl₂, 500 mM KCl, 10% (v/v) glycerol, 0.5% (v/v) NP-40, pH 7.6) containing Complete EDTA-free protease inhibitor (Roche) and incubated on a rotating platform for ~ 1h in the cold room. The sample was centrifuged at 16000 x g and 4°C for 30 min and the supernatant was transferred to a fresh tube. The pellet was resuspended in 1 ml lysis buffer, rotated again for ~ 1h in the cold room before recentrifugation. Supernatants were combined and subjected to immunoprecipitation experiments.

2.4.7.3 Preparation of crude *C. elegans* lysate for Western blot analysis

Worms were washed off NGM plates with dH₂O and transferred to a 1.5 ml tube. After centrifugation at 1500 x g for 3 min the worm pellet was washed with dH₂O several times until the supernatant was clear. The worm pellet was weighed and an equal volume of nematode solubilization buffer (0.3% (v/v) ethanolamine, 2 mM EDTA, 1 mM PMSF, 5 mM DTT) [179] and 2x SDS sample buffer were added. The sample was boiled for 10 min, sonicated for 20 min (at 30 sec on, 30 sec off intervals) in the BioruptorTM (Diogenode, Belgium) and boiled again for another 5 min. After centrifugation at 16000 x g and 4°C for 10 min 15-20 µl of the supernatant were loaded onto a SDS-PAGE gel (2.3.1) for Western blot analysis (2.3.2.2).

2.4.8 Immunoprecipitation of proteins from *C. elegans* extract

Immunoprecipitation experiments were performed with total worm protein extracts (2.4.7.1) or mitochondrial protein extracts (2.4.7.2) obtained from *sir-2.2::gfp* (MAJ13), *sir-2.3::gfp* (MAJ14), BC14289/BC15074 (negative control for total worm extracts) or SJ4103/SJ4143 (negative control for mitochondrial worm extracts) transgenic worms.

60 µl ProteinG-Sepharose beads (50% slurry) or 40 µl GFP-Trap[®]-A beads were equilibrated by washing three times each with 1 ml ice-cold PBS and centrifugation at 500 x g and 4°C for 5 min. 7.5 µl anti-GFP (Roche) or 25 µl of the anti-SIR-2.2 antibody were bound to the ProteinG-Sepharose beads for at least 1 h at 4°C with rotation. Beads were blocked with 0.1% (w/v) BSA for 1h at 4°C with rotation and then washed three times each with 1 ml 1x Cheeseman buffer (2.4.7.1) before adding 1 ml Cheesemann extract or 0.7 ml mitochondrial extract to the beads.

For immunoprecipitation the beads were incubated at 4°C over night with constant rotation and washed three times each with 1 ml 1x Cheeseman buffer containing 1x Complete EDTA-free protease inhibitor (Roche). After the last wash beads were drained using a gel loading tip and boiled in 40 µl SDS sample buffer.

2.4.9 Crossing of *C. elegans*

The *sir-2.2(tm2648)* and *sir-2.2(tm2673)* deletion mutant worms as well as the stable integrated *sir-2.2::gfp* and *sir-2.3::gfp* transgenic worms (2.4.14) were crossed back to wild type N2 worms to eliminate any potential background mutation. Crosses were set up by placing 1-4 hermaphrodites of the corresponding strain together with 10-15 N2 males on the same NGM plate for 2 days at 20°C. Due to their roller phenotype the *sir-2.2::gfp* and *sir-2.3::gfp* transgenic worms were crossed with 20-30 N2 males. If mating was successful

(~50% occurrence of male progeny), L4 stage hermaphrodites of the F1 generation were singled on new NGM plates and allowed to lay eggs. In the case of the *sir-2.2(tm2648)* and *sir-2.2(tm2673)* mutant worms the F1 hermaphrodites were picked and analyzed by single worm PCR (2.4.5) to confirm the heterozygosity of the particular deletion alleles. F2 L4 hermaphrodites of heterozygous animals were again singled on NGM plates to lay eggs and analyzed by single worm PCR. The progeny of homozygous F2 hermaphrodites were used to set up the next backcross with N2 males. In the case of the *sir-2.2::gfp* and *sir-2.3::gfp* transgenic worm strains single worm PCR could not be applied and homozygosity of the F2 generation hermaphrodites was determined by 100% propagation of the GFP expression signal. The *sir-2.2(tm2648)* and *sir-2.2(tm2673)* deletion strains were crossed back to N2 worms six times and five times, respectively, the *sir-2.2::gfp* and *sir-2.3::gfp* transgenic worms were backcrossed three times. The *sir-2.3(ok444)* deletion mutant strain was crossed back to wild type twice by Dr. Monika Jedrusik-Bode (Max Planck Institute for Biophysical Chemistry, Göttingen).

2.4.10 Isolation of RNA from *C. elegans* and reverse transcription

RNA was isolated from *C. elegans* with TRIzol[®] Reagent (Invitrogen) extraction. To 0.25 g worms 1 ml TRIzol[®] Reagent and 12.5 μ l β -mercaptoethanol were added. The sample was vortexed for several minutes, frozen in liquid N₂, and thawed again with intensive vortexing. After repeating twice the freeze-thaw procedure the tube was incubated at RT for 5 min and then centrifuged at 16000 x g for 10 min at 4°C to pellet insoluble material. The supernatant was transferred into a Phase Lock Gel[™] (2 ml, heavy) tube, 200 μ l chloroform/isoamylalcohol (49:1, (v/v)) were added and mixed well. The sample was incubated at RT for 3 min, followed by centrifugation at 16000 x g for 10 min at 4°C to separate phases. The upper aqueous phase was transferred to a fresh tube and mixed with 500 μ l isopropanol. To precipitate the RNA the sample was incubated at RT for at least 10 min and then centrifuged at 16000 x g for 10 min at 4°C. The RNA pellet was washed once with 1 ml 75% EtOH, dried at 37°C for 5-10 min and finally dissolved in RNase-free H₂O. The RNA concentration was determined using the Nanodrop[®] ND-1000.

To remove contaminating genomic DNA, 3 μ g of RNA was digested with DNaseI at 37°C for 30 min using the following DNaseI reaction mix: 0.8 μ l DNaseI buffer (100 mM Tris, 25 mM MgCl₂, 5 mM CaCl₂, pH 7.6), 1 μ l RNase-out, and 0.8 μ l DNaseI in a total volume of 8 μ l. The reaction was stopped by adding 0.4 μ l 100 mM EDTA and DNaseI was inactivated by incubation at 75°C for 10 min. The 8 μ l RNA solution was then used for the synthesis of first-strand cDNA, which was performed using the Superscript II Kit (Invitrogen) and provided Oligo(dT) primers according to manufacturer's instructions. After digesting RNA with 1 μ l RNase H at 37°C for 30 min, the cDNA was stored at -80°C for further use.

2.4.11 Microinjection of *C. elegans*

Transgenic *C. elegans* strains were generated by microinjection of DNA mixtures into the distal gonad arms of young adult hermaphrodites [157, 180, 181]. As a marker for successful transformation the plasmid pRF4, carrying the dominant mutant *rol-6(su1006)* allele of the collagen gene *rol-6*, was co-injected. Expression of *rol-6(su1006)* causes worms to move in circles and rotate around their body axis (roller phenotype) allowing an easy identification of

transgenic animals [182, 183]. To generate *sir-2.2::gfp* transgenic worms, 25 ng/μl of the plasmid pPD115.62 encoding the promoter and genomic sequence of *sir-2.2* fused to a C-terminal Strep-GFP-tag (2.2.11.2) were injected together with 100 ng/μl pRF4 into N2 worms according to Mello and Fire [181] with some modifications. The *gfp* reporter gene construct of *sir-2.3* was created by a PCR fusion-based approach and is described in section (2.4.12).

For injection worms were mounted in a drop of halocarbon oil on a 2% agarose pad. 2-5 μl of DNA solution was loaded into a Femtotip[®]II microinjection needle using a Microloader tip. The needle was connected to a pressurized Eppendorf transjector 5246 (Eppendorf, Hamburg) controlled by a micromanipulator (TransferMan NK2, Eppendorf) and the agar pad with the worm was placed on the inverted Olympus IX70 microscope (Olympus, Hamburg). A 40x magnification was used to focus and inject the needle into the syncytial region of one gonad arm. Pressure was applied until a flow of DNA solution could be seen and the gonad swelled considerably. After retracting the needle the second gonad arm was injected or the worm was immediately recovered by putting a drop of M9 buffer on top of it. The worm was allowed to rehydrate for 5 min and was then transferred to a new NGM plate. Surviving worms were singled on NGM plates and their progeny were screened for a roller phenotype. Transgenic animals displaying a roller phenotype were analyzed for GFP-expression on a dissecting microscope (Olympus SZX10, Olympus, Hamburg) equipped with a GFP filter. Worms exhibiting GFP-expression were again singled to obtain individual transgenic lines with a good transmission rate of the extrachromosomal array.

2.4.12 Generation of GFP/mCherry reporters using a PCR fusion-based approach

The reporter gene constructs *sir-2.3_{pr}::sir-2.3::ha::gfp*, *sir-2.3_{pr}::sir-2.3::ha::mcherry* and *sir-2.4_{pr}::sir-2.4::ha::gfp* were generated by a PCR fusion-based approach according to the protocol described by Hobert [184] and as outlined in Figure 2-2. In PCR #1 the promoter and genomic sequence of *sir-2.3* was amplified from the cosmid F46G10 using the following reaction conditions and the following thermocycler protocol: 50 ng of template DNA, 500 nM of each primer, 300 μM of each dNTP (Roche, Mannheim), 0.5 μl Expand High Fidelity DNA polymerase mix (Roche, Mannheim), 1x reaction buffer (provided by the manufacturer), 3 mM MgCl₂; 5 min at 94°C; [1 min at 94°C, 1min at 48°C, 3 min 30 sec at 68°C] 8x; [30 sec at 94°C, 30 sec at 55°C, 3 min 30 sec at 72°C] 22x; 10 min at 72°C. In parallel, the *gfp* or *mcherry* coding sequence and the 3' untranslated region (UTR) of the *unc-54* gene were amplified by PCR #2 using the same reaction conditions (except for pPD115.62-*sir-2.2_{pr}::sir-2.2::strep::gfp* being the template for the *gfp* coding sequence and pPD115.62-mCherry (2.2.11.2) for the *mcherry* coding sequence) and the following thermocycler protocol: 5 min at 94°C; [1 min at 94°C, 1min at 50°C, 4 min at 68°C] 8x; [30 sec at 94°C, 30 sec at 55°C, 4 min at 72°C] 22x; 10 min at 72°C. Primer B (reverse primer of PCR #1) introduced a C-terminal HA-tag and TEV-protease cleavage site. The sequence of the TEV-protease cleavage site was also present in primer C (forward primer of PCR #2) producing an overlap of more than 24 nucleotides between amplicon #1 and amplicon #2. The DNA concentration of each PCR product was roughly estimated by agarose gel electrophoresis and an aliquot of each reaction was diluted to a concentration of ~10-50 ng/μl with dH₂O. In the fusion PCR reaction both products are fused with nested primers (Primer

A* and Primer D*). The same PCR reaction conditions and thermocycler protocol were used as described above except for using 1 μ l of each PCR product as template, 55°C and 60°C as annealing temperatures and 4 min 30 sec as elongation time. The DNA concentration of the fusion PCR product was again estimated by agarose gel electrophoresis. Without any further purification the reaction was diluted with dH₂O to a final concentration of ~50 ng/ μ l and microinjected into worms together with the marker plasmid pRF4 (100 ng/ μ l) (2.4.11).

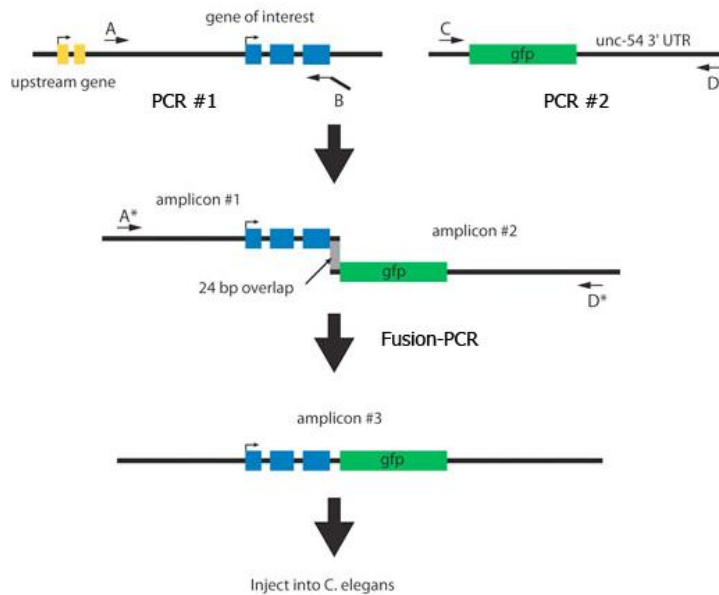


Figure 2-2: PCR-fusion based approach for generating a C-terminal *gfp* reporter construct.

In PCR reaction #1 primer A and B amplify the promoter and genomic region of a gene of interest. In parallel, primer C and D amplify in PCR reaction #2 the *gfp* reporter gene sequence and 3'UTR of *unc-54*. Primer B and C introduce a 24 bp overlap into amplicon #1 and amplicon #2 allowing fusion of both fragments in the fusion-PCR reaction using the nested primer A* and D*. The resulting PCR product (amplicon #3) can be directly microinjected into *C. elegans* without further purification. Figure taken from Boulin et al. [185].

The following primer sequences were used:

SIR-2.3:

MW50_sir-2.3_PrimerA: CGTGTAGTTTTGGAATTTGATAATATTGTG
 MW51_sir-2.3_PrimerA*: GCGGGCTGCAGGGAATTTGATAATATTGTGTTGACGACAG
 MW52_sir-2.3_gfp_PrimerB: GCGTAGTCTGGGACGTCGTATGGGTACGCGGCCGCCATTTCTTTCA
 AAACATCCGAAATTCTG
 MW41_sir-2.3_gfp_PrimerC: CGTACCATAACGACGTCCAGACTACGCTGAAAACCTGTATTTTCA
 GGGCGCCACGCG
 MW42_sir-2.3_unc-54_PrimerD: AAGGGCCCGTACGGCCGACTAGTAGG
 MW43_sir-2.3_unc-54_PrimerD*: CGACTAGTAGGAAACAGTTATGTTTGGTATATTGGG
 MW58_sir23_mCherry_PrimerB: GCCCTGAAAATACAGGTTTTTCAGCGTAGTCTGGGACGTCGTATGG
 GTACGCGGCC
 MW59_sir23_mCherry_PrimerC: CCAGACTACGCTGAAAACCTGTATTTTCAGGGCGCCACGCGTGCC
 ATGGTGAGCAAGGGCGAGGAGG

SIR-2.4:

MW47_sir-2.4_gfp_PrimerA: GCAGCTAAAAATGCTAAAAAAGGTGC
 MW48_sir-2.4_gfp_PrimerA*: GCGGGCTGCAGGGTGTCTAAATATTGAAAATCCTTTCGACC
 MW49_sir-2.4_gfp_PrimerB: GCGTAGTCTGGGACGTCGTATGGGTACGCGGCCGCGCTAATTTTC
 AATGGAATAGGCAC

2.4.13 RNA interference (RNAi) by microinjection and feeding

RNAi was induced by microinjecting dsRNA into the gonad of *C. elegans* and further enhanced by feeding injected worms with *E. coli* HT115 (DE3) expressing the specific dsRNA [186].

In vitro synthesis and microinjection of dsRNA

To generate dsRNA, the cDNA sequences of *sir-2.2* and *sir-2.3* were cloned into the feeding vector L4440 (2.2.11.1), which contains two convergent T7 polymerase promoters in opposite orientations separated by a multicloning site [187]. Subsequently, the cDNA sequence of *sir-2.2* was PCR amplified with a primer specific for the flanking T7 promoter sequences (5'-GTAATACGACTCACTATAGGG-3'). The following 50 µl reaction mix and PCR protocol were used: 50 ng plasmid DNA, 1 µM T7 primer, 300 µM of each dNTP (Roche, Mannheim), 0.5 µl Expand High Fidelity DNA polymerase mix (Roche, Mannheim), 1 x reaction buffer (provided by the manufacturer), 3 mM MgCl₂; 3 min at 94°C, [1 min at 94°C, 40 sec at 55°C, 1 min at 72°C] 5x; [40 sec at 94°C, 40 sec at 60°C, 1 min at 72°C] 25x, 10 min at 72°C. The PCR product was extracted with chloroform:isoamylalcohol (24:1) and ethanol precipitated (2.2.1). The DNA pellet was resuspended in RNase-free H₂O and DNA concentration was measured using the Nanodrop[®] ND-1000 (Pepqlab).

The DNA was *in vitro* transcribed by T7 RNA polymerase using the MEGAscript[®] T7 kit (Ambion) according to manufacturer's instructions. The generated dsRNA was isolated by phenol/chloroform extraction and ethanol precipitation. The RNA pellet was resuspended in RNase-free H₂O and the concentration was determined by Nanodrop[®] ND-1000 (Pepqlab). In addition the integrity of the dsRNA was checked on a 1% agarose gel. The *sir-2.2* dsRNA was microinjected (2.4.11) into *sir-2.3(ok444)* mutant worms at a concentration of 2 µg/µl. As control M9 buffer was injected into wild type N2 worms.

RNAi mediated by feeding

The feeding construct L4440-*sir-2.2*(cDNA) was transformed into the *E. coli* strain HT115 (DE3), a RNaseIII-deficient strain of *E. coli* with an isopropyl-β-D-thiogalactopyrynoside (IPTG) inducible T7 polymerase [188]. 5 ml LB medium containing ampicillin (100 µg/ml) was inoculated with a single bacterial colony and incubated at 37°C for 8 h with constant shaking. 100 µl of the bacterial culture were spread on 50 mm NGM feeding plates (NGM plates with 100 µg/ml ampicillin, 12.5 µg/ml tetracycline, 1 mM IPTG and without streptomycin) and incubated overnight at RT to grow bacterial lawn and induce dsRNA expression.

After microinjection of *sir-2.2* dsRNA, *sir-2.3(ok444)* mutant worms were singled to *sir-2.2* feeding plates and incubated at 25°C. Every 12 h, 24 h, 36 h and 48 h the hermaphrodites were transferred to fresh feeding plates. Control worms injected with M9 buffer were transferred to feeding plates seeded with *E. coli* HT115 (DE3) carrying the empty L4440 vector. The F1 generation was screened for phenotypic alterations with a dissecting microscope and differential interference contrast (DIC), using the confocal laser scanning microscope Leica TCS SP5 (Leica, Wetzlar).

2.4.14 Integration of extrachromosomal arrays by UV radiation

Extrachromosomal arrays were integrated into chromosomal DNA of *sir-2.2::gfp* and *sir-2.3::gfp* transgenic worms by treatment with UV radiation [174]. L4 hermaphrodites of the *sir-2.2::gfp* and *sir-2.3::gfp* extrachromosomal transgenic lines that expressed the corresponding *gfp* construct were picked on 5-9 50 mm NGM plates (~40 worms/plate) that were not seeded with bacteria. The worms were UV radiated in a Stratlinker[®] UV crosslinker 2400 using an energy setting of 30,000 $\mu\text{J}/\text{cm}^2$ and a wavelength of 254 nm. The agar plate was transferred completely to a large NGM plate and worms were grown for at least two generations at RT. This allowed potential integrants to become homozygous by self-fertilization. After ~10 days two large pieces of agar were cut out from each plate and transferred to fresh 90 mm NGM plates. The next day 15-20 hermaphrodites of each plate (exhibiting GFP expression without mosaicism) were singled on 50 mm NGM plates. The progeny of these hermaphrodites were then screened for 100 % transmission of the transgene. Obtained stable transgenic lines were crossed back three times to wild type N2 worms to eliminate potential background mutations (2.4.9).

2.4.15 DiI staining

Dye-filling with the lipophilic fluorescent dye 1,1'-dioctadecyl-3,3,3',3'-tetramethylindocarbocyanine perchlorate (DiI) was performed to stain the sensory neurons of *C. elegans in vivo* based on the method described by Hedgecock [189]. After washing *sir-2.3::gfp* transgenic worms several times with M9 buffer the worm pellet was resuspended in M9 buffer containing 2 $\mu\text{g}/\text{ml}$ DiI (Molecular Probes, 1:1000 dilution of 2 mg/ml DiI dissolved in DMSO) and incubated in the dark at 23°C with shaking. For recovery and destaining worms were transferred to fresh NGM plates and allowed to crawl for at least 1 h. To analyze the staining of sensory neurons worms were mounted on 2% agarose pads and immobilized with 2% sodium azide in M9 buffer. Pictures were taken on a Leica TCS SP5 confocal laser-scanning microscope (Leica).

2.4.16 Microscopic analysis of *C. elegans*

For standard handling and phenotypic analyses worms were monitored on NGM plates (Olympus SZX10 equipped with filters for green and red fluorescence). Differential interference contrast microscopy and fluorescence microscopy were performed on a Leica TCS SP5 confocal laser-scanning microscope (using 40 x and 63 x object lenses). Specimens were prepared by mounting worms on 2% agarose pads (2% (w/v) agarose in H₂O) with a drop of 2% sodium azide to immobilize worms. Agarose pads were prepared by spotting a drop of molten 2% agarose on a coverslip, placing a second coverslip on top and flattening the drop with mild pressure to a thin film of agarose.

Immunoelectron microscopy of ultrathin cryosections was performed by Dirk Wenzel at the Electron Microscopy group of the Max Planck Institute for Biophysical Chemistry, Göttingen. Briefly, worms were cut, fixed with 2% paraformaldehyde in 0.1 M Na-phosphate buffer (pH 7.4) for 24 h at 4°C, and postfixed with 4% paraformaldehyde-0.1% glutaraldehyde for 2 h on ice. Cryosections were prepared as previously described [190, 191], labeled for the indicated antigens, and examined with a Philips CM120 electron microscope and a TVIPS charge-coupled device camera system.

2.4.17 Oxidative stress assay

Sensitivity towards oxidative stress was analyzed as described by Masse et al. [192] with some modifications. Worm strains were cultured synchronously for two generations on RNAi feeding plates (2.4.13) at 25°C. N2, *sir-2.2::gfp* and *sir-2.3::gfp* transgenic worms were grown on control feeding plates seeded with *E. coli* HT115(DE3), transformed with the empty L4440 vector, *sir-2.3(ok444)* and *sir-2.2(tm2648)* mutant worms were maintained on *sir-2.2* RNAi and *sir-2.3* RNAi feeding plates, respectively. 200 µl 250 mM paraquat solution (methylviologen-dichloride hydrat, Sigma, dissolved in dH₂O) were spread on top of already seeded RNAi feeding plates. Of each strain five plates with 20 worms (L4 larvae) per plate were prepared and survival of worms was checked every day. Worms were scored as dead when they did not respond to prodding with a pick. The mean life spans and average survival curves were determined from at least three independent experiments. A two-tailed Student's t-test was used to calculate the significance of differences in mean life span to wild type worms.

2.5 Tissue culture based methods

2.5.1 Cultivation of cells

HEK293 and HEK293T cells were grown in DMEM medium (supplemented with 10% bovine growth serum (BGS), L-glutamine and Penicillin/Streptomycin) at 37°C and 5% CO₂. After reaching 90% confluence cells were split by washing them once with PBS and treating them with 0.05% Trypsin-EDTA for 5 to 10 min. Trypsin digestion was stopped by addition of medium and the cells were plated in a dilutions appropriate for further maintenance or transfection.

2.5.2 Transfection of cells

HEK293 and HEK293T cells were transfected with plasmid DNA by CaPO₄ precipitation using the CalPhosTM Mammalian Transfection Kit (Clontech, Mountain View, USA) according to manufacturer's protocol. To express *C. elegans* proteins in HEK293 cells transfection was performed with the jetPEITM Transfection Reagent (Polyplus-transfection SA, Illkirch, France) as described in the instructions of the manufacturer.

2.5.3 Immunoprecipitation of proteins from transfected cells

Immunoprecipitation (IP) experiments were performed as described by Ahuja et al. [26] with some modifications. For each IP reaction HEK293 or HEK293T cells of 1-2 15 mm cell culture dishes were co-transfected (2.5.2) with the plasmids of interest, harvested after 24-48 h and washed once with ice-cold PBS buffer (137 mM NaCl, 2.7 mM KCl, 4.3 mM Na₂HPO₄, 1.47 mM KH₂PO₄, pH 7.4). The cell pellet was lysed with 500 µl buffer A (50 mM Tris-HCl, 500 mM NaCl, 10 mM CaCl₂, 0.5% (v/v) NP-40, 0.5 mM EDTA, 10% (v/v) glycerol, 1x Complete Protease inhibitor (EDTA free, Roche), pH 7.5) containing 20 U/ml micrococcal nuclease (MNase, Calbiochem). The chromatin fraction of the lysates was digested for 30 min at 30°C with agitation. 500 µl buffer B (50 mM Tris-HCl, 150 mM NaCl, 0.5% (v/v) NP-40, 0.5 mM EDTA, 10% (v/v) glycerol, 1x Complete Protease inhibitor (EDTA free, Roche), pH

7.5) were added and the lysate was clarified by centrifugation at 16000 x g for 30 min at 4°C. The supernatant was added to equilibrated beads.

For equilibration beads were washed three times each with 1 ml buffer B or PBS and then blocked for at least 1 h with 0.1% (w/v) BSA at 4°C with rotation. Beads were washed three times before adding the cellular extract. To immunoprecipitate GFP-tagged proteins 5 µl GFP-Trap[®] A agarose beads (Chromotek) were used. Anti-FLAG-IPs were performed either with 15 µl anti-FLAG[®] M2 agarose beads (Sigma) or with 30 µl magnetic Dynabeads[®] M-280 Sheep anti-mouse (Invitrogen) and 4 µl anti-FLAG[®] M2 antibody (Sigma). For anti-Myc IP experiments 4 µl anti-Myc antibody (Millipore) was bound to 20 µl Dynabeads[®] M-280 Sheep anti-mouse (Invitrogen) for 3 h at 4°C prior to blocking.

To immunoprecipitate tagged-proteins the beads were rotated at 4°C overnight. The beads were washed six times each with 1 ml buffer A and then boiled in 40-60 µl SDS sample buffer. Proteins were separated by SDS-PAGE (2.3.1) and analyzed by Western blotting (2.3.2.2).

2.5.4 Analysis of protein acetylation using acetyllysine-specific antibodies

Protein acetylation levels were analyzed by Linh Ho from the laboratory of our collaborator Prof. Eric Verdin (Gladstone Institute of Virology and Immunology, San Francisco, USA) as previously described [102, 193].

2.6 Enzymatic activity assays

2.6.1 Histone deacetylase (HDAC) activity assay

Histone deacetylase assays were essentially performed as described by Verdin et al. [194] using a chemically acetylated H4 peptide as a substrate. Recombinant *C. elegans* SIR-2 proteins as well as HP1β (negativ control) were translated *in vitro* using wheat germ extract [165] by Dimitry Agafonov and Timur Sumatov (Department of Cellular Biochemistry, Max Planck Institute for Biophysical Chemistry, Göttingen). For protein expression with wheat germ extract full-length *sir-2.1*, *sir-2.2*, *sir-2.3* and *sir-2.4* were cloned into pEU3-NII-StrepII. pEU3-NII-StrepII containing the cDNA of HP1β was kindly provided by Szabolcs Sörös (Max Planck Institute for Biophysical Chemistry, Göttingen). Since wheat germ extract does not exhibit intrinsic deacetylase activity, *in vitro*-translated proteins were directly used for the enzymatic assay without further purification. The total reaction volume was 100 µl containing 5 µl of *in vitro*-translated protein, 1 µl [³H] peracetylated H4 peptide and 1x HDAC buffer (50 mM Tris, 4 mM MgCl₂, 1 mM NAD⁺, pH 9.0). Reactions were incubated at 25°C for 2 h or overnight with shaking. For quantification acetate was released from O-acetyl-ADP-ribose by addition of 25 µl Stop-mix (1 M HCl, 0.16 M HAc) and extracted with 600 µl organic solvent (Ethyl acetate). 550 µl of the upper organic phase were analyzed by scintillation counting. The protein concentrations of the *in vitro*-translated proteins were determined by quantifying the incorporation of [¹⁴C]leucine into full-length protein bands using SDS-PAGE gel electrophoresis and autoradiography.

2.6.2 Spectrophotometric pyruvate carboxylase activity assay

To analyze whether treatment of bovine pyruvate carboxylase (PC) with *C. elegans* or mammalian sirtuins changes its enzymatic activity, a photospectrometric pyruvate carboxylase activity assay [195] was used.

For the deacetylation assay of PC FLAG-tagged *C. elegans* proteins and Myc-tagged human proteins were expressed in HEK293T cells (2.5.2). Cells were lysed in 750 μ l buffer C (50 mM Tris-HCl, 150 mM NaCl, 10 mM CaCl₂, 0.5% (v/v) NP-40, 0.5 mM EDTA, 10% (v/v) glycerol, 1x Complete Protease inhibitor (EDTA free, Roche), 20 U/ml MNase (Calbiochem), pH 8.0), incubated for 30 min at 30°C with agitation and sonicated 30 min (30 sec on, 30 sec off). Then 200 μ l buffer C (without CaCl₂ and MNase) was added and the lysate was centrifuged at 16000 x g for 30 min at 4°C. The supernatant was added to equilibrated magnetic Dynabeads[®] M-280 Sheep anti-mouse (Invitrogen) bound with anti-FLAG[®] M2 (Sigma) or anti-Myc (Millipore) antibody (2.5.3) and rotated at 4°C overnight. Beads were washed three times with buffer C (without CaCl₂ and MNase) and once with 1x DAC buffer (50 mM Tris, 4 mM MgCl₂, 1 mM NAD⁺, pH 8.0).

For the DAC assay beads were split into two reactions. Each reaction was incubated with 110 μ l DAC buffer containing 0.55 μ g bovine pyruvate carboxylase (Sigma) at 25°C (*C. elegans* proteins) or 37°C (human proteins) for 1 h with shaking. The supernatant of each reaction was then immediately used for the photospectrometric pyruvate carboxylase assay.

The activity of pyruvate carboxylase was determined with a malate dehydrogenase coupled assay for oxaloacetate measuring the decrease in absorbance at 340 nm due to NADH oxidation. The assay was performed at 30°C in a total volume of 500.5 μ l PC reaction buffer containing 134 mM triethanolamine hydrochloride-KOH buffer, pH 8.0, 5 mM MgSO₄, 7 mM pyruvic acid, 0.12% (w/v) BSA, 0.23 mM NADH, 0.05 mM acetyl-coenzyme A, 2.63 units malate dehydrogenase, 1 mM ATP, 15 mM KHCO₃, 10 mM Tris-HCl, pH 8.0, 0.8 mM MgCl₂, 0.2 mM NAD⁺ and 0.5 μ g bovine pyruvate carboxylase (Sigma). 100 μ l supernatant of the DAC reaction were mixed with 384 μ l 1.3x PC reaction buffer (without ATP and KHCO₃) in a quartz cuvette and equilibrated to 30°C in a thermostatted Cary 100 UV-Vis Spectrophotometer (Varian, Palo Alto, USA). The reaction was started by addition of 16.5 μ l ATP/KHCO₃ solution and decrease in absorbance at 340 nm was recorded for 15 min. Measured linear range reaction velocities were used to calculate the enzymatic activities of bovine PC using the following formula:

$$\text{units}[\mu\text{mol}/\text{min}] = \frac{\Delta A}{\Delta t \cdot \epsilon_{\text{NADH}} \cdot d} \cdot V$$

(A = absorbance, t = time, ϵ = extinction coefficient (ϵ_{NADH} at 340 nm = 6220 L M⁻¹ cm⁻¹), d = path length (1 cm), V = reaction volume).

2.6.3 Deacetylase activity assay in combination with mass spectrometry

In vitro deacetylase activity assays were performed with immunoprecipitated protein (for details see (2.6.2)) expressed in HEK293T cells. Proteins bound to beads were incubated with 1 μ g acetylated peptide in DAC buffer II (50 mM Tris, 150 mM NaCl, 4 mM MgCl₂, 2 mM NAD⁺, pH 8.0) at 25°C (*C. elegans* proteins) or at 37°C (mammalian proteins) overnight while shaking. The supernatant of the DAC reactions was analyzed by mass spectrometry in

the group of Dr. Henning Urlaub (Max Planck Institute for Biophysical Chemistry, Göttingen) on a 4800 MALDI TOF/TOFTM Analyzer (Applied Biosystems, Darmstadt).

3 Results

3.1 Analysis of SIR-2 protein expression and localization in *C. elegans*

3.1.1 SIR-2.2 and SIR-2.3 do not localize to the cell nucleus

To analyze the expression and localization of the different SIR-2 proteins I generated transgenic worms, expressing C-terminally GFP-tagged SIR-2 proteins under control of the endogenous promoter. The *sir-2.1::gfp* (HT822) strain was already existing and kindly provided by Heidi Tissenbaum [122]. To generate *sir-2.2::gfp* transgenic worms, the entire 5' untranslated region (UTR, 1.8 kb) and genomic region of *sir-2.2* were fused to a C-terminal Strep::GFP-tag and the 3' UTR of *unc-54* in the vector pPD115.62. Transgenic worms were generated by microinjection into wild type N2 worms. *Sir-2.3::gfp* and *sir-2.4::gfp* transgenic worms were obtained by a PCR fusion-based approach, omitting time consuming cloning [184]. The 5' UTRs (*sir-2.3*: 0.9 kb; *sir-2.4*: 0.7 kb) and genomic sequences of *sir-2.3* and *sir-2.4* were fused via PCR to a C-terminal HA::GFP-tag and *unc-54* 3' UTR via PCR and the linear fragments were injected into N2 worms. Extrachromosomal arrays of *sir-2.2::gfp* and *sir-2.3::gfp* transgenic worms were integrated by UV radiation resulting in one integrated transgenic line for *sir-2.2* and in four integrated lines for *sir-2.3*. In *sir-2.4::gfp* transgenic worms protein expression was only observed in few generations after microinjection and no transgenic line stably propagating the extrachromosomal array could be established.

In accordance to the observations of Wang and Tissenbaum [122] SIR-2.1 is primarily a nuclear protein. It was expressed in most if not all neurons in the head and tail, in many pharyngeal cells, in the hypodermis and in body wall muscles. Interestingly, no SIR-2.1::GFP signal was observed in the intestine (Figure 3-1 A to C).

SIR-2.2 was expressed in many tissues (muscles, neurons, intestine, somatic gonad) of *C. elegans* and exhibited a particularly high expression in the pharynx, bodywall muscle cells and the posterior part of the intestine (Figure 3-1 D, E). Like SIR-2.1 [122] SIR-2.2::GFP expression was first seen in the three-fold stage of embryogenesis. However, SIR-2.2 was not targeted to the nucleus, but found localized to filamentous subcellular structures (Figure 3-1 F). The expression pattern of SIR-2.3::GFP was very similar to that of SIR-2.2 as it also did not localize to nuclei and showed prominent GFP-signals in the pharynx and bodywall muscles (Figure 3-1 G). In addition, strong SIR-2.3::GFP expression was detected in unidentified cells in the head (indicated by arrows) and in somatic cells of the gonad (Figure 3-1 G, H). Interestingly, I observed that expression of SIR-2.3::GFP started earlier in embryogenesis (approximately at the 100 cell stage) than expression of SIR-2.1 and SIR-2.2 (Figure 3-1 I). No SIR-2.2::GFP or SIR-2.3::GFP expression was detected in the germline, which might be due to transgene silencing effects [181, 196]. SIR-2.4::GFP localized to the nucleus in intestinal cells of embryos and L1 stage larvae (Figure 3-1 J, K). In young adult worms I detected SIR-2.4::GFP in the spermatheca, but it exhibited no nucleus-specific localization (Figure 3-1 L).

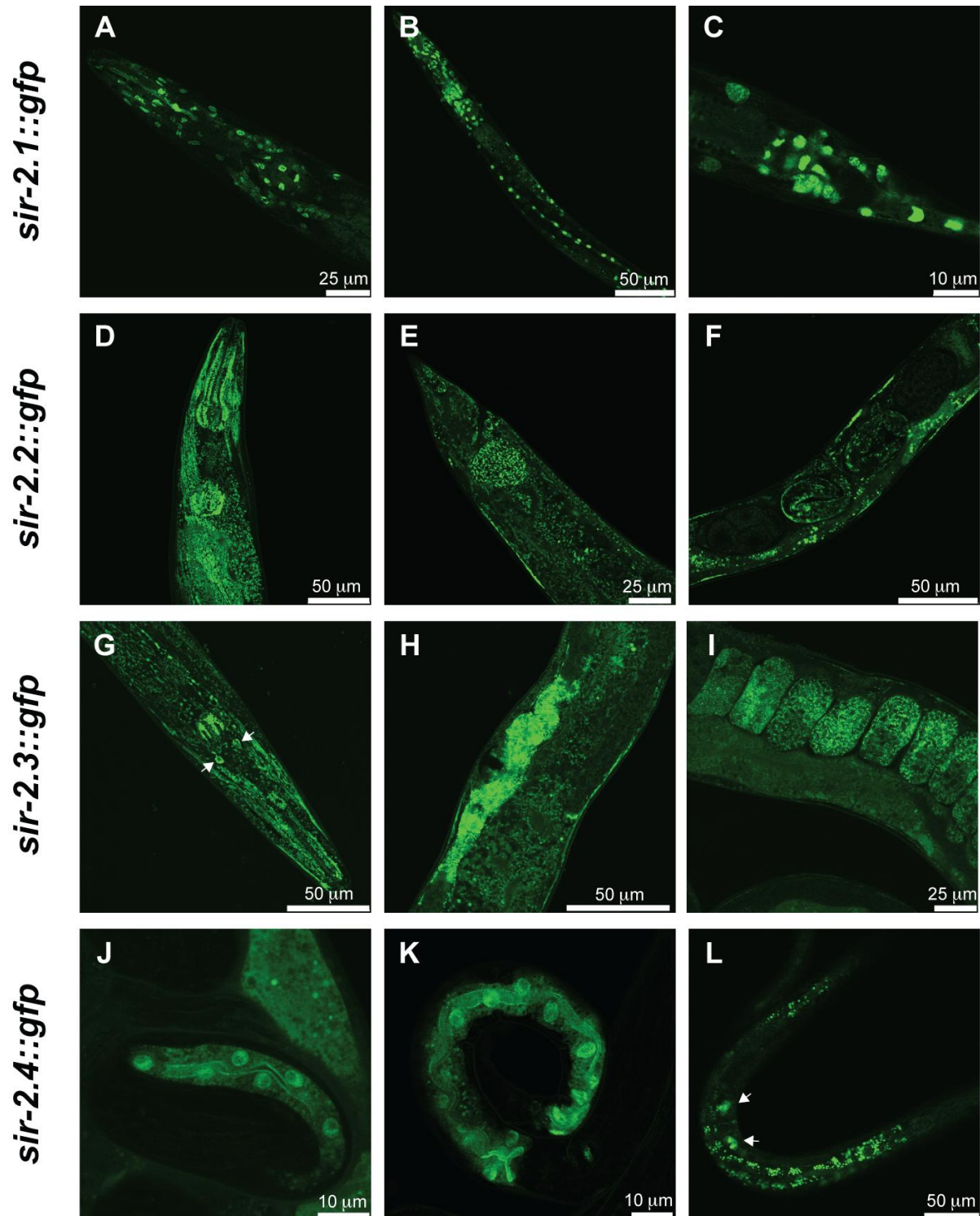


Figure 3-1: Expression and localization pattern of SIR-2 proteins in *C. elegans*.

GFP was fused C-terminally to the promoter and genomic sequence of each *sir-2* variant. Transgenic strains were generated by microinjection. For *sir-2.2* and *sir-2.3* extrachromosomal arrays were integrated by treatment with UV radiation. The *sir-2.1::gfp* strain was kindly provided by Heidi Tissenbaum. Fluorescent photomicrographs were taken with a confocal laser scanning microscope. **A.** to **C.** SIR-2.1::GFP expression and localization in the head region (**A**) along the body axis (**B**) and in the tail region (**C**) of a representative young adult worms. **D.** to **F.** SIR-2.2::GFP expression and localization in the head (**D**) and tail (**E**) region and gonad (**F**) of adult *C. elegans*. **G.** to **I.** SIR-2.3::GFP expression and localization in head region (**G**) and gonad (**H** and **I**) of adult *C. elegans*. Arrows point at unidentified cells in the head. **J.** to **L.** SIR-2.4::GFP expression and localization in a representative three-fold stage egg (**J**), L1 larvae (**K**) and young adult worm (**L**). Arrows indicate spermatheca. Scale bars represent level of magnification.

Overall, these results show that the expression patterns of the different *C. elegans* SIR-2 proteins are diverse. Similar to the mammalian counterparts their localization is not only restricted to the cell nucleus.

3.1.2 SIR-2.2 and SIR-2.3 expression and localization patterns partially overlap

The primary structure of SIR-2.2 is very similar to the protein sequence of SIR-2.3 (75.3% identity). The gene sequences of both proteins are located directly next to each other on chromosome X, suggesting that one gene might have evolved from the other by gene duplication. Analysis of transgenic *gfp*-reporter strains showed that not only the expression patterns of SIR-2.2::GFP and SIR-2.3::GFP were very similar, but also that both proteins localized to filamentous subcellular structures.

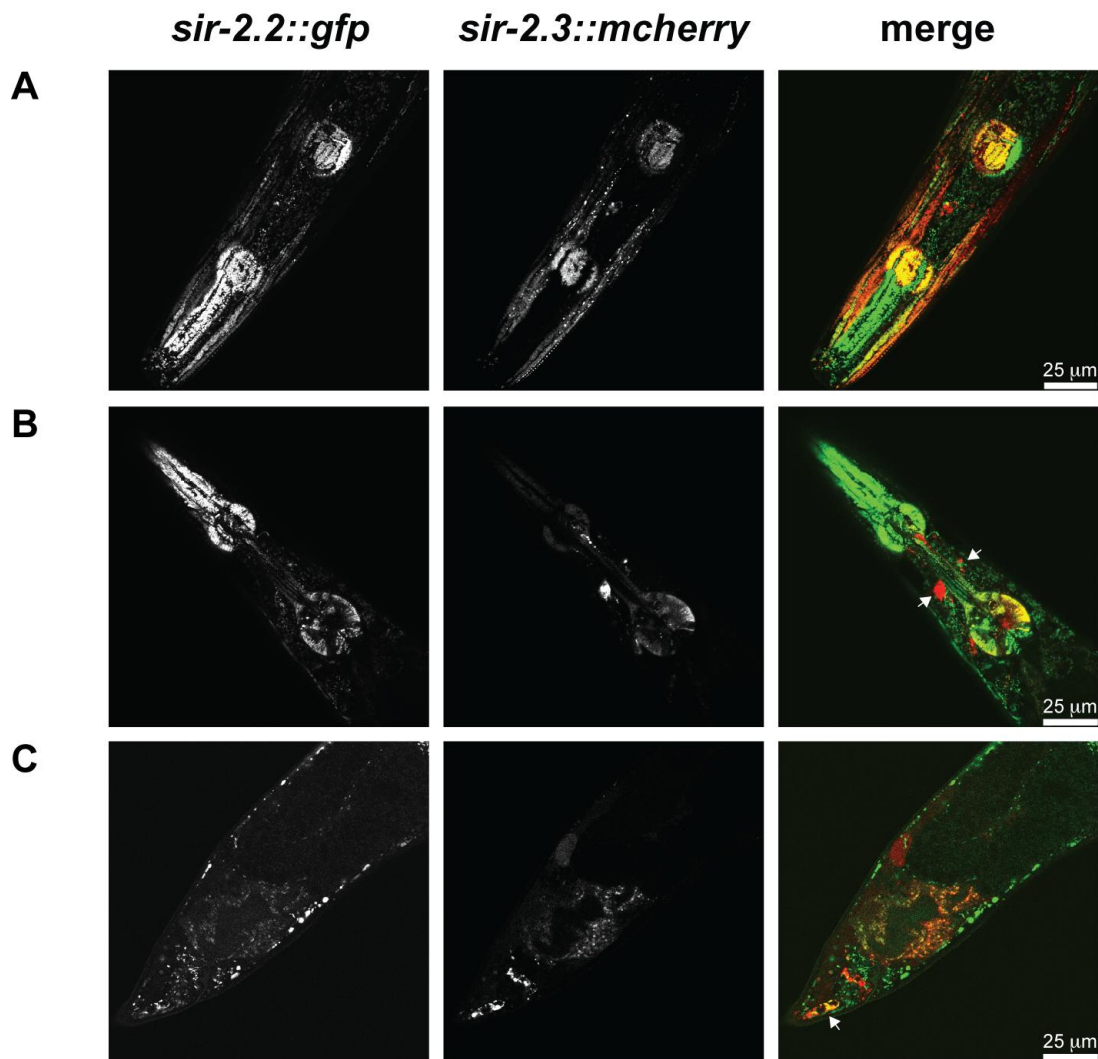


Figure 3-2: The expression and localization patterns of SIR-2.2 and SIR-2.3 partially overlap.

Double transgenic strains were generated by microinjecting a translational mCherry (C-terminal) fusion of SIR-2.3 [184] into stable integrated *sir-2.2::gfp* transgenic worms. **A.** and **B.** Representative fluorescent photomicrographs showing the head region of *sir-2.2::gfp*; *sir-2.3::mCherry* double transgenic worms. Arrows point at unidentified cells around the pharynx. **C.** Expression and localization of SIR-2.2::GFP and SIR-2.3::mCherry in the tail region of a representative worm. Arrow indicates unidentified cells in the tail. Scale bars represent level of magnification.

To analyze whether both proteins are targeted to the same subcellular structures, I generated double transgenic worms by microinjecting a translational mCherry (C-terminal) fusion of SIR-2.3 [184] into stable integrated *sir-2.2::gfp* transgenic worms. Fluorescence microscopy analysis showed that both SIR-2.3::mCherry and SIR-2.2::GFP co-localized in body wall muscle cells, the pharynx, intestine and unidentified cells (possibly neurons) in the tail (indicated by an arrow) (Figure 3-2). These findings implicate that they function at the same subcellular structures.

However, the expression patterns of SIR-2.2 and SIR-2.3 only partially overlapped and there were also differences. No prominent GFP-Signal of SIR-2.2 was observed in unidentified cells located between the two pharyngeal bulbs (Figure 3-2 B, marked with arrows). In addition I detected only for SIR-2.3 a prominent expression in the somatic gonad (Figure 3-1 I) and observed first SIR-2.3 expression earlier in embryogenesis (Figure 3-1 H).

3.1.3 Analysis of SIR-2.3 expression in head neurons by DiI staining

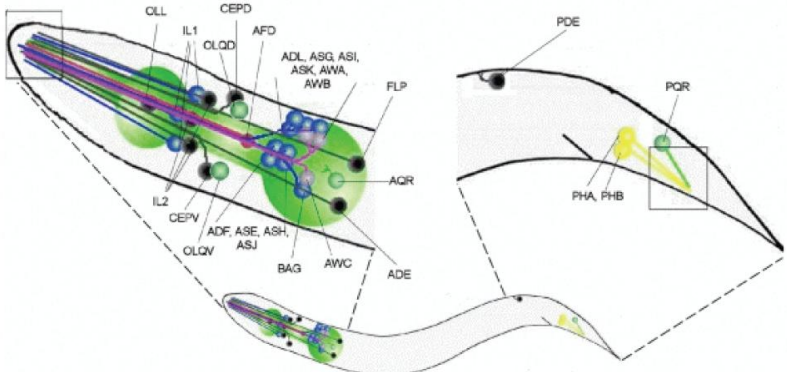
Cells of the *C. elegans* nervous system are organized in various ganglia in the head, the tail and along the ventral cord. The majority of neurons are located in ganglia of the head surrounding the pharynx between the two pharyngeal bulbs (isthmus) and forming the nerve ring with their axon bundles. A large fraction of these neurons are sensory neurons that allow *C. elegans* to perceive environmental cues such as food stimuli, oxygen levels, temperature, pH, light, or mechanic stimuli [197]. Since sirtuins are potential metabolic sensors and *sir-2.3::gfp* transgenic worms showed a prominent SIR-2.3::GFP signal in cells that might be sensory neurons, I performed dye-filling experiments with DiI. DiI is a lipophilic dye that is specifically taken up by amphid neurons (ASI, ADL, ASK, AWB, ASH, ASJ) and inner labial neurons (IL1, IL2, IL sheath and socket cells) in the head and phasmid neurons (PHA, PHB) in the tail of hermaphrodites [189] (Figure 3-3 A). *Sir-2.3::gfp* transgenic worms stained with DiI (diluted in M9 buffer) were analyzed by fluorescence microscopy. In Figure 3-3 B and C SIR-2.3::GFP expression overlapped with DiI-filled inner labial neurons, however the DiI staining did not co-localize with the prominent SIR-2.3::GFP signal present in the unidentified cells that were located also anterior of the nerve ring close to inner labial neurons (marked with arrows). SIR-2.3::GFP was also expressed in amphid neurons (Figure 3-3 D) and in phasmid neurons (Figure 3-3 E) where it showed a high expression in the PHA neuron and a rather weak expression in the PHB neuron.

In summary, this experiment showed that SIR-2.3 and SIR-2.2 (data not shown) were expressed in many head neurons and co-localized with DiI-filled inner labial neurons, amphid neurons and phasmid neurons in the tail. DiI was not sufficient to determine the identity of the cells around the pharynx with the prominent SIR-2.3::GFP expression and this will be addressed by future experiments.

Figure 3-3: DiI staining of *sir-2.3::gfp* transgenic worms.

A. Illustration of the relative positions of ciliated neurons (cells bodies and their dendritic extensions) in the *C. elegans* hermaphrodite. Figure taken from [197]. **B. to E.** *Sir-2.3::gfp* transgenic worms were stained with DiI and analyzed by fluorescence microscopy. Representative fluorescent photomicrographs of DiI stained *sir-2.3::gfp* transgenic L4 larvae, showing the head region (**B** and **C**; Arrows point at unidentified cells, which exhibit prominent SIR-2.3::GFP expression), the region around the second pharyngeal bulb (**D**) and the tail region (**E**). Scale bar represent the level of magnification.

A



sir-2.3::gfp

Dil

merge

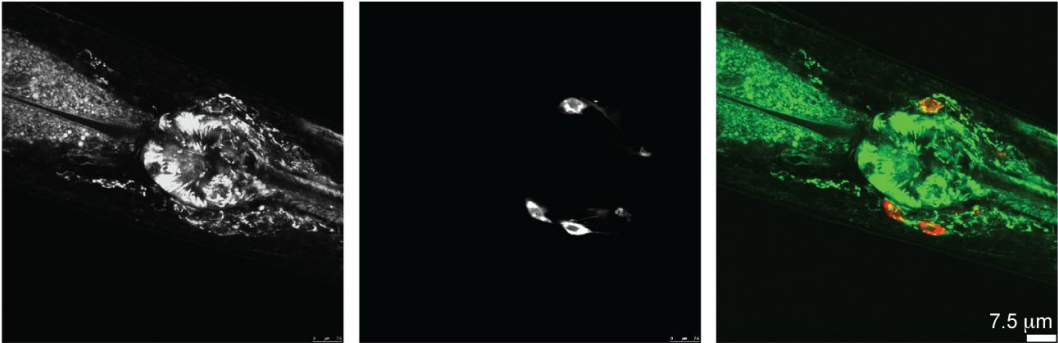
B



C



D



E



3.1.4 SIR-2.2 and SIR-2.3 localize to mitochondria

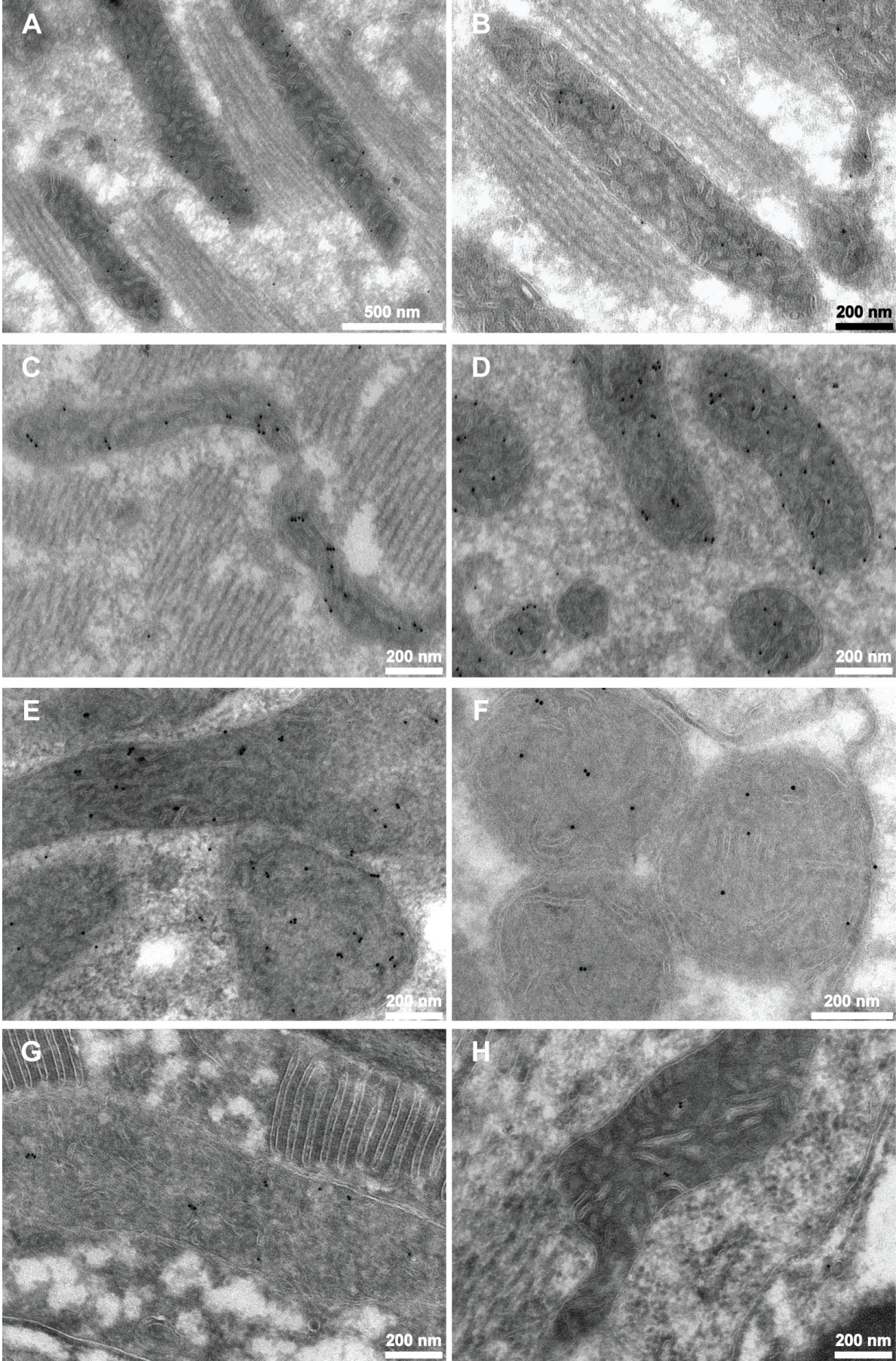
To determine the exact subcellular localization of SIR-2.2, I analyzed *sir-2.2::gfp* transgenic worms, using immunoelectron microscopy in collaboration with Dirk Wenzel from the Electron microscopy facility of the Max Planck Institute for Biophysical Chemistry (Göttingen). Immunogold labeling of cryo sections labeled with a GFP-specific antibody showed that the long filamentous structures SIR-2.2 localized to are not filaments of the cytoskeletal system but mitochondria (Figure 3-4 A and B). The mitochondrial localization of SIR-2.2 could be further confirmed by immunogold labeling of *sir-2.2::gfp* transgenic worms and wild type N2 worms with SIR-2.2-specific antibodies (Figure 3-4 C to F, for antibody characterization see Figure 2-1), demonstrating that both GFP-tagged and endogenous SIR-2.2 were targeted to mitochondria. Fluorescence microscopy analysis of *sir-2.2::gfp*, *sir-2.3::mCherry* double transgenic worms (3.1.2) indicated that both proteins localize to the same subcellular structures. Analysis of cryo sections of *sir-2.3::gfp* transgenic worms with a GFP-specific antibody showed that SIR-2.3 was also mitochondrial (Figure 3-4 G and H) and verified that both proteins are targeted to the same subcellular compartment.

To further confirm these findings, I isolated mitochondria of N2 worms by subcellular fractionation of *C. elegans*. In brief, worms were homogenized with a glass tissue grinder and the crude lysate was subjected to differential centrifugation steps. Firstly, nuclei and debris were removed by centrifugation at 800 x g (Figure 3-5 A). In a second centrifugation step mitochondria were separated from cytosolic compounds by centrifuging the post nuclear supernatant (PNS) at 12000 x g. The resulting mitochondrial pellet (MP) and post mitochondrial supernatant (PMS), as well as the post nuclear supernatant (PNS), were analyzed by Western blotting using antibodies specific for mitochondrial and non-mitochondrial marker proteins (Figure 3-5 B). SIR-2.2 was depleted from the PMS and highly enriched in the MP together with the mitochondrial markers NUO-2 (subunit of complex I), cytochrome c and the α -subunit of ATP-synthase. An antibody against histone H3 was used as a non-mitochondrial marker. During this study I could not obtain a SIR-2.3-specific antibody. Therefore, *sir-2.3::gfp* transgenic worms were fractionated and a GFP-specific antibody was used to detect the localization of SIR-2.3. Like SIR-2.2, SIR-2.3::GFP was also enriched in the MP and depleted from the PMS. Since folded GFP cannot be imported into mitochondria anymore a weak band of SIR-2.3::GFP was also detected in the PMS.

From these experiments I conclude that both SIR-2.2 and SIR-2.3 are like their mammalian homologue SIRT4 mitochondrial proteins.

Figure 3-4: Analysis of SIR-2.2 and SIR-2.3 subcellular localization by electron microscopy.

Representative cryo sections of worms were stained with an anti-GFP or the anti-SIR-2.2 antibodies and visualized with protein A-conjugated gold beads (10 nm). High-density black dots indicate the localization of SIR-2.2 and SIR-2.3 to mitochondria. **A.** and **B.** Immunogold labeling of *sir-2.2::gfp* transgenic worms with an anti-GFP antibody. **C.** to **F.** Analysis of *sir-2.2::gfp* transgenic worms (**C** and **D**) and wild type N2 worms (**E** and **F**) with the anti-SIR-2.2 antibodies. **G.** and **H.** Immunogold labeling of *sir-2.3::gfp* transgenic worms with an anti-GFP antibody. Scale bars represent level of magnification.



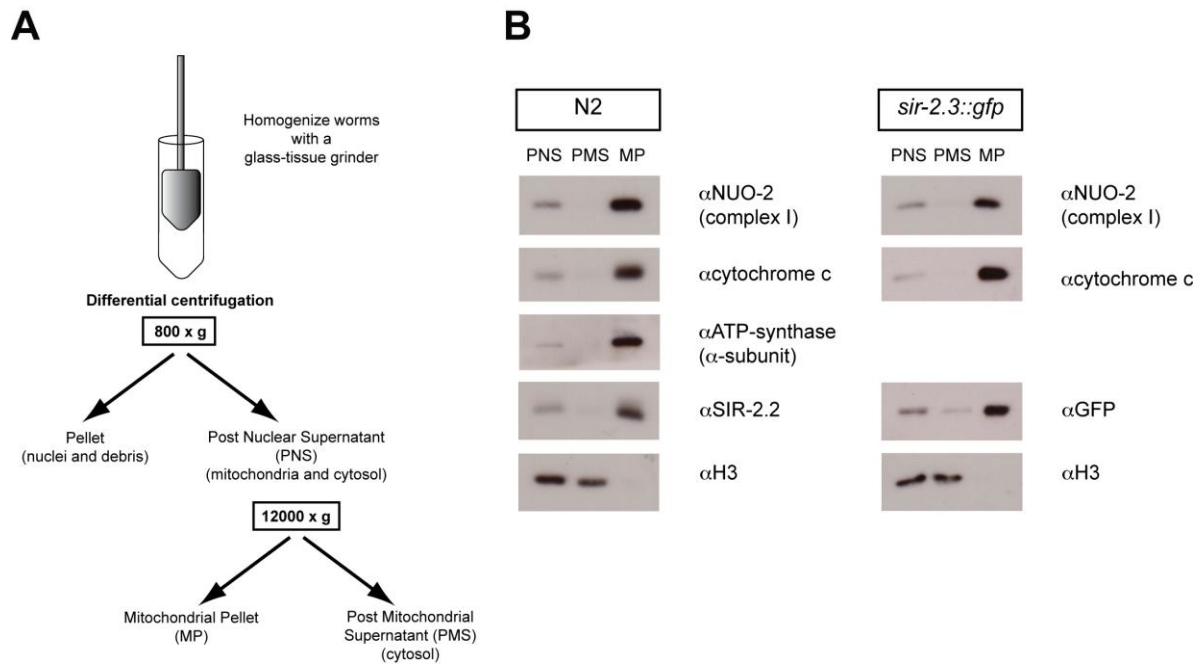


Figure 3-5: Subcellular fractionation of N2 and *sir-2.3::gfp* transgenic worms by differential centrifugation.

A. Schematic overview on the subcellular fractionation procedure to isolate crude mitochondria from *C. elegans*. **B.** Wild type N2 worms and *sir-2.3::gfp* transgenic worms were homogenized and subjected to differential centrifugation. Equal protein amounts of the post nuclear supernatant (PNS), mitochondrial pellet (MP) and post mitochondrial supernatant (PMS) were analyzed by SDS-PAGE and Western blotting, using antibodies against the complex I subunit NUO-2 (mitochondria), cytochrome c (mitochondria), the α -subunit of ATP-synthase (mitochondria), histone H3 (non-mitochondrial), SIR-2.2 and GFP.

3.2 Characterization of *sir-2.2* and *sir-2.3* deletion mutant *C. elegans* strains

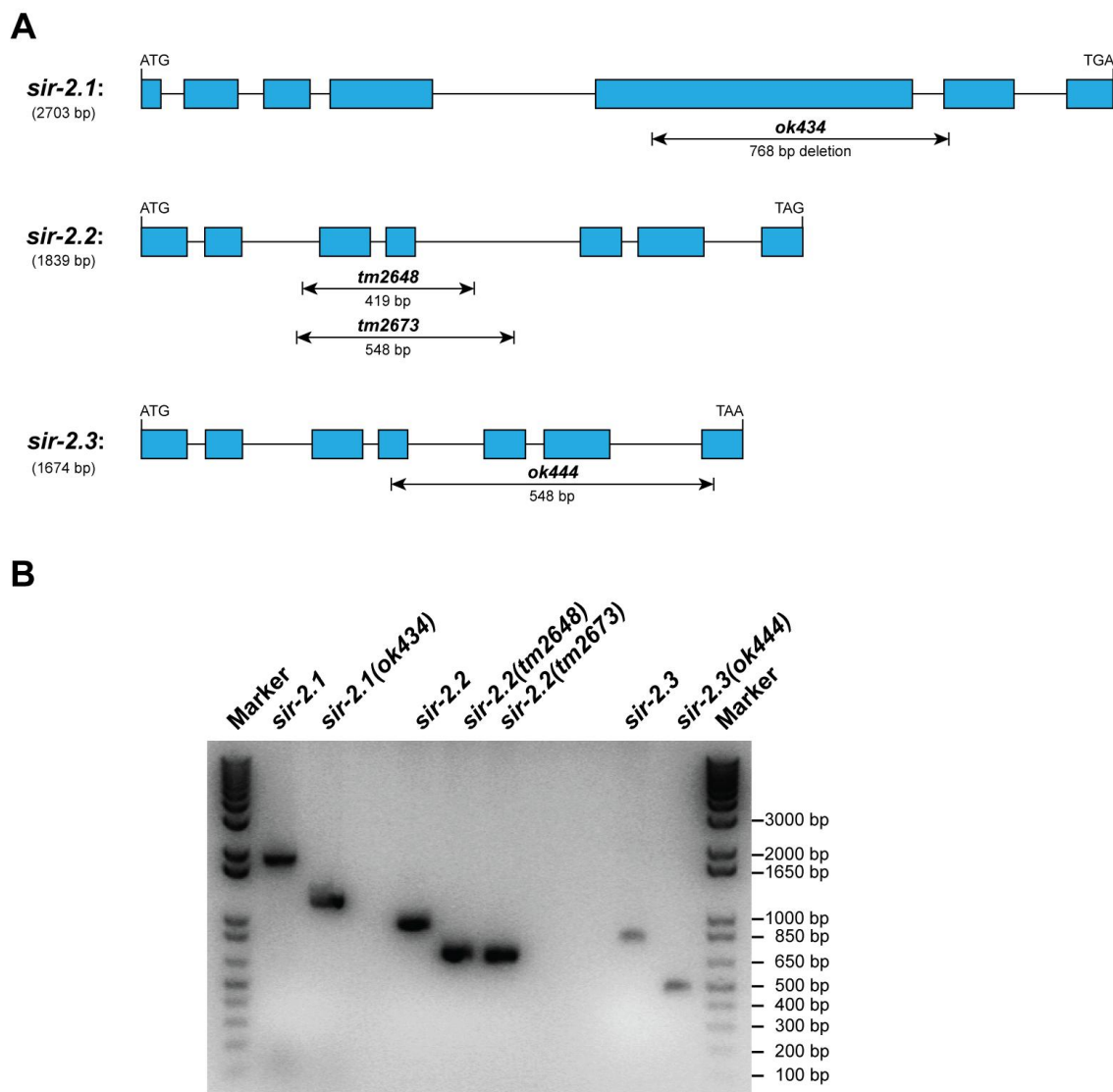
To analyze the biological function of mitochondrial sirtuins in *C. elegans*, *sir-2.2(tm2648)*, *sir-2.2(tm2673)* and *sir-2.3(ok444)* deletion mutant worm strains were phenotypically characterized.

3.2.1 *Sir-2.2* and *sir-2.3* deletion mutant worms used in this study

For all four *C. elegans sir-2* genes deletion strains were generated by the *C. elegans* Gene Knockout Consortium or the National Bioresource Project for the Experimental Animal *C. elegans* (NBRP) using chemical mutagenesis (Table 3-1). For *sir-2.2* I obtained two deletion strains (*sir-2.2(tm2648)* and *sir-2.2(tm2673)*) which had in the beginning severe developmental defects affecting growth, muscle function and germline. After crossing five times (*sir-2.2(tm2673)*) and six times (*sir-2.2(tm2648)*) to wild type N2 worms these strains did not show an obvious phenotype any more, suggesting that there were also background mutations. The mutant strains *sir-2.3(ok444)* and *sir-2.1(ok434)* kindly provided by the Caenorhabditis Genetics Center (CGC) also did not exhibit an obvious phenotype under normal growth conditions. Only worms of the *sir-2.4(tm2817)* mutant strain exhibited an embryonic lethal phenotype [198].

Table 3-1: Overview on available *sir-2* mutant deletion strains.

SIR-2 variant	Mutant strain	Source	Phenotype	BlastP Identities
SIR-2.1	<i>sir-2.1(ok434)IV</i>	<i>C. elegans</i> Gene Knockout Project	wild type	44% human SIRT1
SIR-2.2	<i>sir-2.2(tm2648)X</i> <i>sir-2.2(tm2673)X</i>	National BioResource Project (NBRP)	wild type	49% human SIRT4
SIR-2.3	<i>sir-2.3(ok444)X</i>	<i>C. elegans</i> Gene Knockout Project	wild type	42% human SIRT4
SIR-2.4	<i>sir-2.4(tm2817)I</i>	National BioResource Project (NBRP)	embryonic lethal	38% human SIRT6

**Figure 3-6: RT-PCR analysis of the *sir-2* deletion mutant alleles**

A. Schematic overview on the gene structure of the *sir-2.1*, *sir-2.2* and *sir-2.3* genes ranging from translation initiation codon (ATG) to the termination codon (TGA, TAG, TAA). Blue boxes indicate exons, black lines introns. Arrows mark the deleted regions within the deletion alleles. **B.** RNA was isolated from wild type N2 and *sir-2.1(ok434)*, *sir-2.2(tm2648)*, *sir-2.2(tm2673)*, *sir-2.3(ok444)* deletion mutant worm strains. mRNA was reverse transcribed using oligo(dT) primers, and cDNAs were amplified by standard PCR reactions using primers that specifically bind to coding start and end of each gene. Obtained PCR fragments were separated on a 1% agarose gel and visualized by ethidium bromide staining. Running positions of size markers are indicated on the right.

Since only parts and not the whole genomic sequences were deleted by chemical mutagenesis (Figure 3-6 A), it had to be determined whether these mutations result in null-mutations. I isolated RNA from *sir-2.1(ok434)*, *sir-2.2(tm2648)*, *sir-2.2(tm2673)* and *sir-2.3(ok444)* deletion mutant worms and performed reverse transcription PCR (RT-PCR) experiments using oligo(dT) primers. cDNAs were subjected to PCR reactions with primers specifically amplifying the complete coding sequence of each gene. PCR fragments were separated by agarose gel electrophoresis and visualized by ethidium bromide staining (Figure 3-6 B). mRNA encoding truncated SIR-2 protein was synthesized by all three *sir-2* deletion strains, whereas no mRNA was detected in the *sir-2.4(tm2817)* deletion strain producing a null allele [198].

Sequencing of the PCR products of the *tm2648* and *tm2673* mutant alleles showed that the 419 bp and 548 bp deletions in the genomic sequence of *sir-2.2* resulted in a loss of exons 3 and 4, and exon 2 was spliced in frame to exon 5. After translation 75 aa (encoded by exon 3 and 4) of 287 aa would be deleted in the truncated SIR-2.2 protein (212 aa) (Figure 3-7 A). To test whether truncated protein is produced, *sir-2.2(tm2648)* and *sir-2.2(tm2673)* crude protein extracts were analyzed by Western blotting using the anti-SIR-2.2-specific antibodies (Figure 3-7 C). In wild type N2 worms the antibody detected a double band at ~33 kD. This double band I also observed with protein recombinantly expressed in *E. coli*. Since mass spectrometric analysis showed that both bands were SIR-2.2 protein, SIR-2.2 might be posttranslationally modified or proteolytically processed. In the *sir-2.2(tm2648)* and *sir-2.2(tm2673)* mutant worms a protein band with the correct size of the corresponding truncated SIR-2.2 protein (~24 kD) was detected. In addition electron microscopic analysis of *sir-2.2(tm2648)* mutant worms showed that the truncated SIR-2.2 protein also localized to mitochondria, indicating that the deletion mutation did not affect the mitochondrial targeting of the protein (Figure 3-7 D).

I do not have a SIR-2.3-specific antibody for Western blot analysis. However it is possible that a truncated SIR-2.3 protein is also produced in *sir-2.3(ok444)* mutant worms.

Figure 3-7: Characterization of truncated proteins resulting from *sir-2* deletion mutant alleles.

A. Protein sequence of full-length (287 aa) and truncated SIR-2.2 (212 aa). Black box indicates the 75 aa that were deleted in the truncated protein. Residues of the catalytic sirtuin core domain are shown in blue (same for SIR-2.3 and SIR-2.1 in **B** and **E**, respectively). **B.** Protein sequence of full-length (287 aa) and hypothetical truncated SIR-2.3 protein (154 aa). In the truncated protein 141 aa (black box) were deleted and 8 aa (red) were added to the C-terminus due to the frame shift caused by the deletion. **C.** Western blot analysis of wild type N2, *sir-2.2(tm2648)* and *sir-2.2(tm2673)* crude protein extracts using the anti-SIR-2.2-specific and anti-H3 (loading control) antibodies. Running positions of the full-length and truncated SIR-2.2 protein are indicated on the right. **D.** Representative cryo section of *sir-2.2(tm2648)* deletion mutant worms immunogold labeled with the anti-SIR-2.2-specific antibodies and analyzed by electron microscopy. Scale bar represents 200 nm. **E.** Protein sequence of full-length (607 aa) and hypothetical truncated SIR-2.1 protein (381 aa). The truncated SIR-2.1 protein lacked 229 aa encoded by a part of exon 5 (black box). Exon 6 was spliced in frame to the rest of the third exon, generating five additional amino acids in between (red). **F.** Recombinant full-length and truncated SIR-2.1 as well as HP1 were assayed for HDAC activity on a [³H] peracetylated histone H4 tail peptide. Deacetylation was determined by quantifying released acetyl by scintillation counting (for details see 2.6.1). Quantitative values, indicating HDAC activity, are means of three measurements; error bars represent standard deviation.

A

MAQKFVPEAAELCENSLKKFISLIGTVDKLLVIS
GAGISTESGIPDYRSKDVGLYARIAHKPI
YFQDYMRSNRCRQR

YWSRNFLAWPRFGQAAPNINHIALSKWEAS
DRFQWLITQNV DGLHLKAGSKMVTE LHG
SALQVKCTTCDYIESRQ

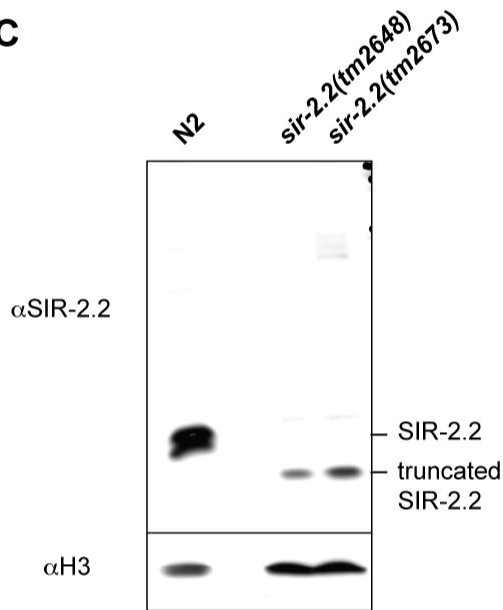
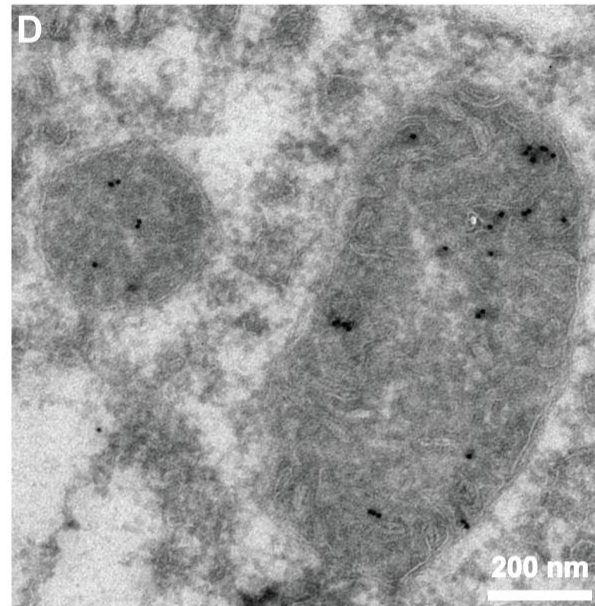
TYQDRLDYANPGFKEEHVAPGELAPDGDIIPL
GTEKGFQIPEPCSCGGLMKT DVTFFGENVNMD
KVNFCYEKVNEDGILSLGTS LAVLSGFRFIH HAN
MKKKPIFIVNIGPTRADH MATMKLDYKISDVLKEM

B

MARKYVPHTTELCENSLKKFKSLVGTVDKLLIIT
GAGISTESGIPDYRSKDVGLYTKTALEPIYFQDFMK
SKKCRQRYWSRSYLNWPRFAQALPNFNHYALSK
WEAANKFHWLITQNV DGLHLKAGSKMITELHG
NALQVKCTSCE

YIETRQTYQDRNLNANPGFKEQFVSPGQQELDAD
TALPLGSEQGFKIPECLNCGGLMKT DVTLFGEN
LNTDKIKVCGKKVNECNGVLT LGTSLEVLSGYQI
VNHAHMQNKP I FIVNIGPTRADQMATMKLDYRISD
VLKEM

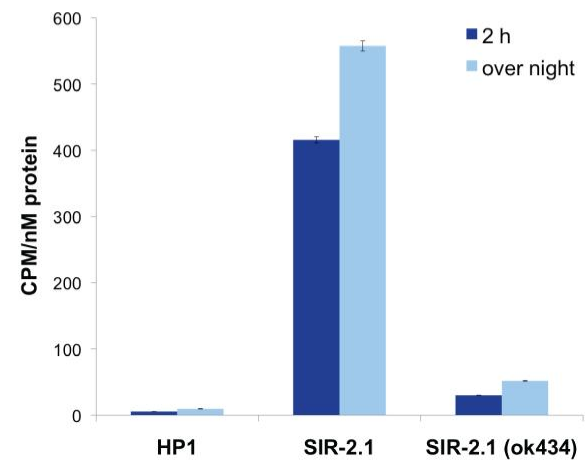
CKTNQFSS

C**D****E**

MSRDSGNDSEVAVTHGEVQEITEEN
PEIGSMHITQETDISDAPETNTDSSRQRTESTTS
VSSESWQNNDEMMSNLRRARLLDDGATPLQI
IQQIFPDFNASRIATMSENAHFALIS
DLLERAPVRQKLTNYNSLADAVELFKKKHILVLT
GAGVSVSCGIPDFRSKDG IYARLRSEFPDLP
DPTAMFDIRYFRENPAFYNFAREIFPGQFVPS
VSHRFIKELETSGRLLRNYTQNI DTLEHQ TGIKRV
VECHGSF S K C T C T R C G Q K F F L Q

YDGN E I R E E V L A M R V A H C K R C E G V I K P N I V F F
G E D L G R E F H Q H V T E D K H K V D L I V V I G S S L K V R P V A
L I P H C V D K N V P Q I L I N R E S L P H Y N A D I E L L G N C D D I
I R D I C F S L G G S F T E L I T S Y D S I M E Q Q G K T K S Q K P
S Q N K R Q L I S Q E D F L N I C M K E K R N D D S S D E P T L K
K P R M S V A D D S M D S E K N N F Q E I Q K H K S E D
D D D T R N S D D I L K K I K H P R L L S I T E M L H D N K C V A

ISAHQTVFPGAEC S F D L E T L K L V R D V H H E T H C E S S
C G S S C S S N A D S E A N Q L S R A Q S L D D F V L S D
E D R K N T I H L D L Q R A D S C D G D F Q Y E L S E T I D P E T F
S H L C E E M R I

F

Here the deletion of 548 bp in the genomic sequence of *sir-2.3* caused a partial loss of exon 4 and the complete loss of exons 5, 6 and 7. Since the fusion of the residual parts of exon 4 and exon 7 resulted in a frame shift mutation, the hypothetical truncated SIR-2.3 protein (Figure 3-7 B) would lack 154 aa of its C-terminus (black box), and 8 new aa (CKTNQFSS, shown in red) would be added before the occurrence of a stop codon. In *sir-2.1(ok434)* mutant worms 768 bp of the genomic sequence were deleted. A large region of exon 5 was gone and its residual 5' region was spliced in frame to exon 6, thereby 5 additional codons were generated in between. In the hypothetical truncated SIR-2.1 protein, therefore, 299 aa (encoded by exon 5, black box) would be missing and 5 additional aa (FFFLQ, shown in red) would be inserted at the site of the deletion (Figure 3-7 E). I also did not have a SIR-2.1-specific antibody, but an *in-vitro* histone deacetylase (HDAC) activity assay (3.4.2.1) with recombinantly expressed protein showed that the deacetylase activity was abrogated in the truncated SIR-2.1 protein (Figure 3-7 F). Therefore, the *ok434* deletion allele generates a non-functional SIR-2.1 protein. Heterochromatin protein 1 (HP1) was used as negative control in this experiment. Since full-length SIR-2.2 and SIR-2.3 (3.4.2.1) did not exhibit deacetylase activity in this HDAC assay, it is not known whether truncated SIR-2.2 and SIR-2.3 are still functional.

Interestingly, the functional null mutation in the *sir-2.1(ok434)* mutant strains did not cause an obvious phenotype in these worms under normal growth conditions. Although in the *sir-2.2* and *sir-2.3* mutant worms the deletion mutations removed large parts of the catalytic sirtuin core domain and important residues required for the NAD⁺-dependent deacetylase activity (Figure 3-7 A and B, shown in blue), no obvious phenotype was observed.

These results led me to the conclusion that there might be functional redundancy among the different SIR-2 variants in *C. elegans*.

3.2.2 Knockdown of *sir-2.2* in a *sir-2.3* mutant background leads to a very mild phenotype

To test whether there is functional redundancy among the mitochondrial SIR-2 variants, I knocked down *sir-2.2* by RNAi in a *sir-2.3(ok444)* mutant background. As the *sir-2.2* and *sir-2.3* genes are directly next to each other on chromosome X and homologous recombination is very rare in *C. elegans*, it was not possible to generate a *sir-2.2(tm2648) sir-2.3(ok444)* double mutant worm strain. Therefore, *sir-2.2* was knocked down by microinjection of *sir-2.2* dsRNA into *sir-2.3(ok444)* mutant hermaphrodites and subsequent *sir-2.2* RNAi feeding of the injected hermaphrodites and their F1 progeny. For control wild type (N2) hermaphrodites were microinjected with M9 buffer and transferred to feeding plates seeded with *E. coli* HT115(DE3) containing an empty L4440 vector.

Knock down of *sir-2.2* by RNAi in a *sir-2.3* mutant background resulted in a very weak phenotype and only 4.5% of the worms exhibited growth and egg-laying defects. As 1.9% of wild type (N2) control worms were as well dumpy (Dpy, short fat worms) and egg-laying defective (Egl), the difference were only minor and non-significant (with a p-value > 0.05 in standard Student t-test for the data presented in Table 3-2).

Loss of *sir-2.2* or *sir-2.3* as well as knock down of *sir-2.2* in a *sir-2.3(ok444)* mutant background did not cause a severe phenotype under normal growth conditions. Knockout

mice of SIRT3, SIRT4 and SIRT5 also grow and develop normally under physiological conditions [25, 92, 114]. However, mitochondrial sirtuins function in stress responses [19], suggesting that SIR-2.2 and SIR-2.3 might play a role during stress.

Table 3-2: Knock down of *sir-2.2* in *sir-2.3(ok444)* mutant worms did not cause an obvious phenotype.

Genotype	% Dpy and Egl \pm S.E.M	n (F1)
wild type (N2)	1.9 \pm 0.3	5 (518)
<i>sir-2.3(ok444); sir-2.2(RNAi)</i>	4.5 \pm 1.3	7 (1012)

For knock down, *sir-2.2* dsRNA was microinjected into *sir-2.3(ok444)* mutant hermaphrodites. Injected hermaphrodites were subsequently singled onto *sir-2.2* RNAi feeding plates. For control, wild type (N2) hermaphrodites were microinjected with M9 buffer and transferred to feeding plates seeded with *E. coli HT115(DE3)* containing an empty L4440 vector. The F1 generation was analyzed for dumpy (Dpy) and egg-laying defective (Egl) phenotypes. S.E.M: standard error of mean; n: number of microinjected hermaphrodites, F1: number of analyzed F1 generation progeny; a p-value > 0.05 (0.05003) was calculated using the standard Student t-test.

3.2.3 Sensitivity towards oxidative stress

Mitochondria are the central organelle for cellular energy production, but also the major site of ROS generation within cells. If uncontrolled, ROS can seriously damage macromolecules (DNA, protein and lipids) and cause mitochondrial dysfunction, which is thought to be a major determinant of life span (free radical theory) [199, 200]. Because of the mitochondrial subcellular localization of SIR-2.2 and SIR-2.3, I analyzed the tolerance of *sir-2.2(tm2648)* and *sir-2.3(ok444)* mutant worms to oxidative stress. Since there might be functional redundancy between *sir-2.2* and *sir-2.3*, I also performed this analysis on worms grown on *sir-2.2* or *sir-2.3* feeding plates. To test whether overexpression of SIR-2.2 and SIR-2.3 affects the sensitivity to oxidative stress, I assayed *sir-2.2::gfp* and *sir-2.3::gfp* transgenic worms that express GFP-tagged SIR-2 proteins in a wild type background as well. (For analysis of SIR-2.2 protein levels see Appendix A.1, Figure A-1.)

Oxidative stress resistance was investigated by assaying daily the survival of worms (starting with L4 larvae) on RNAi feeding plates containing paraquat, which is known to generate superoxide anions. Worms were scored as dead when they did not respond to prodding with a pick. The highest sensitivity towards oxidative stress was observed in *sir-2.2::gfp* and *sir-2.3::gfp* transgenic worms having a mean survival of 5.07 ± 0.16 (S.E.M.) and 5.16 ± 0.21 (S.E.M.), respectively, compared to wild type N2 worms 7.86 ± 0.21 (S.E.M.) (Figure 3-8 A and B). *Sir-2.2(tm2648)* (6.66 ± 0.16 (S.E.M.)) and *sir-2.3(ok444)* (6.26 ± 0.18 (S.E.M.)) mutant worms were also significantly more sensitive to oxidative stress than wild type worms (Figure 3-8 A and C). Knockdown of *sir-2.3* in *sir-2.2(tm2648)* mutant worms led to a slight increase in sensitivity (5.86 ± 0.15 (S.E.M.)). However, no increased sensitivity was observed when knocking down *sir-2.2* in a *sir-2.3(ok444)* mutant background (6.42 ± 0.18 (S.E.M.)), suggesting that there is no functional redundancy between *sir-2.2* and *sir-2.3*.

Overall, this data shows that both loss and overexpression of SIR-2.2 and SIR-2.3 leads to an increased sensitivity to oxidative stress and both proteins seem to function in oxidative stress resistance pathways.

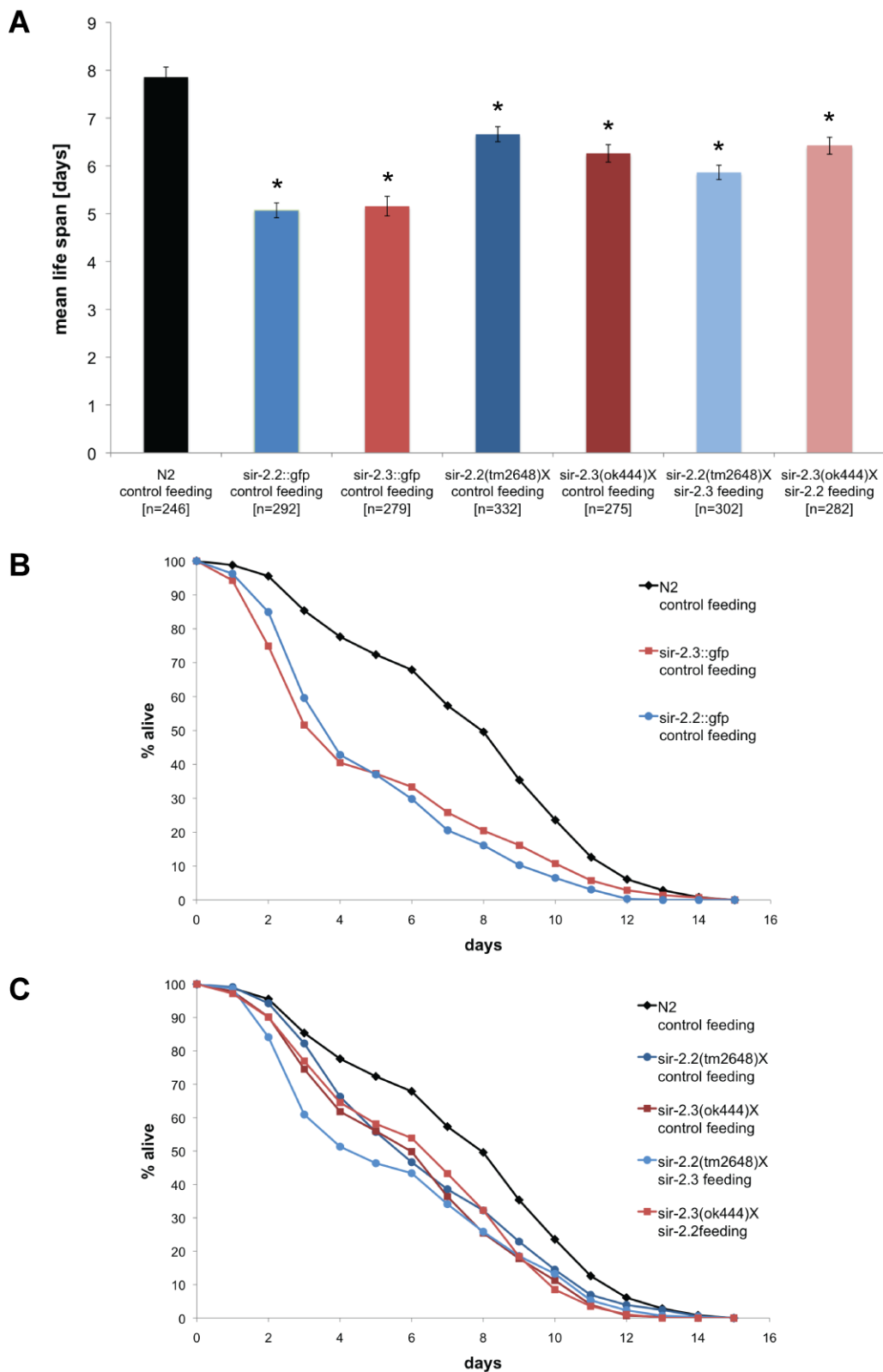


Figure 3-8: Increased sensitivity to oxidative stress in worms overexpressing or deficient in SIR-2.2 and SIR-2.3.

A. Mean life span of worms grown at 24.5°C on RNAi feeding plates containing paraquat (200 μ l of 250 mM paraquat solution/plate). At least 3 trials were conducted per strain. Error bars show standard error of mean (S.E.M.); asterisks indicate a significant difference (p -value < 0.001) to average life span of wild type (N2) worms; p -values were calculated using standard Student t -test; n : number of analyzed worms. **B.** Average survival curve of wild type (N2) and worms overexpressing SIR-2.2 (*sir-2.2::gfp*) or SIR-2.3 (*sir-2.3::gfp*). **C.** Average survival curve of wild type (N2) worms and worms deficient in *sir-2.2*, *sir-2.3* or both.

3.3 Identification of SIR-2.2 and SIR-2.3 interaction partners

3.3.1 Identification of mitochondrial biotin carboxylases as factors interacting with SIR-2.2 and SIR-2.3

To identify factors interacting with SIR-2.2, the promoter and genomic sequence of SIR-2.2 was fused to a modified version of the so-called localization and affinity purification (LAP)-tag [177] using a C-terminal Strep-GFP-tag. A stable integrated transgenic worm strain expressing SIR-2.2::Strep::GFP was generated by microinjection and UV treatment. Since the tagged protein could not be recovered from *C. elegans* lysates in sufficient amounts by Strep-tag purification (data not shown), I could not use a tandem affinity purification approach. Thus, SIR-2.2::Strep::GFP was immunoprecipitated from total worm lysates with different antibodies raised against GFP and the SIR-2.2-specific antibodies (Figure 3-9 A). Because of the mitochondrial localization of SIR-2.2 (3.1.4), I also isolated mitochondria from *C. elegans* and used mitochondrial extracts for the immunoprecipitation experiments. As a negative control immunoprecipitation experiments were performed with total worm lysates prepared from the transgenic worm strains BC15074 and BC14289 (expressing GFP under control of the endogenous *sir-2.2* promoter) and with mitochondrial lysates of the transgenic strains SJ4104 and SJ4143 (expressing GFP with a mitochondrial targeting sequence). Bound proteins were subjected to SDS-PAGE and complete lanes were analyzed by mass spectrometry in the group of Dr. Henning Urlaub (MPI of Biophysical Chemistry, Göttingen). Proteins that were identified with at least two peptides or a protein score of at least 80 and were present only in the SIR-2.2::GFP bound fraction but not in the control IP, were extracted from the data with the statistical program R (for details on the R protocol and a list of factors see Appendix A.2 and A.3). Five different immunoprecipitation experiments were performed and SIR-2.2-specific factors that showed the highest occurrence in these experiments were further analyzed. Among the identified factors D2023.2 (*pyc-1*, pyruvate carboxylase), F27D9.5 (*pcca-1*, propionyl-coenzyme A (-CoA) carboxylase alpha subunit), and F32B6.2 (ortholog to human alpha methylcrotonoyl-coenzyme A (-CoA) carboxylase 1, in this study referred to as *mccc-1*) were particularly interesting as the proteins represent the three mitochondrial members of the biotin-dependent carboxylase protein family. The best sequence coverage obtained for these proteins were 48% with 107 identified peptides for PYC-1 (Figure 3-9 B), 32% with 18 peptides for PCCA-1 (Figure 3-9 C) and 13% with 9 peptides for MCCC-1 (Figure 3-9 D).

In mammals pyruvate carboxylase (PC) has an important anaplerotic function for the tricarboxylic acid (TCA) cycle as the enzyme catalyzes the carboxylation of pyruvate to oxaloacetate, an important TCA cycle intermediate [201] (Figure 3-10). Propionyl-CoA carboxylase (PCC) is essential for the catabolism of branched chain amino acids (Thr, Val, Ile, and Met), odd-chain length fatty acids and cholesterol. Since it carboxylates propionyl-CoA to methylmalonyl-CoA, which feeds into the TCA cycle after conversion to succinyl-CoA, it is also important for anaplerosis [202, 203]. Methylcrotonyl-CoA carboxylase (MCC) catalyzes the carboxylation of 3-methylcrotonyl-CoA to 3-methylglutaconyl-CoA, the fourth step in catabolism of the essential amino acid (aa) leucine. Leucine, as a exclusively ketogenic aa, is degraded to acetoacetate and acetyl-CoA. Therefore, MCC does not function in

anaplerosis but formation of ketone bodies [203, 204]. Anaplerosis and formation of ketone bodies are essential for maintaining energy homeostasis during nutrient deprivation such as fasting. Sirtuins are potential energy sensors [19, 20] and *C. elegans* SIR-2.2 and SIR-2.3 might regulate the enzymatic activities of mitochondrial biotin-dependent carboxylases during metabolic stress. Thus, I selected mitochondrial biotin carboxylases for further studies.

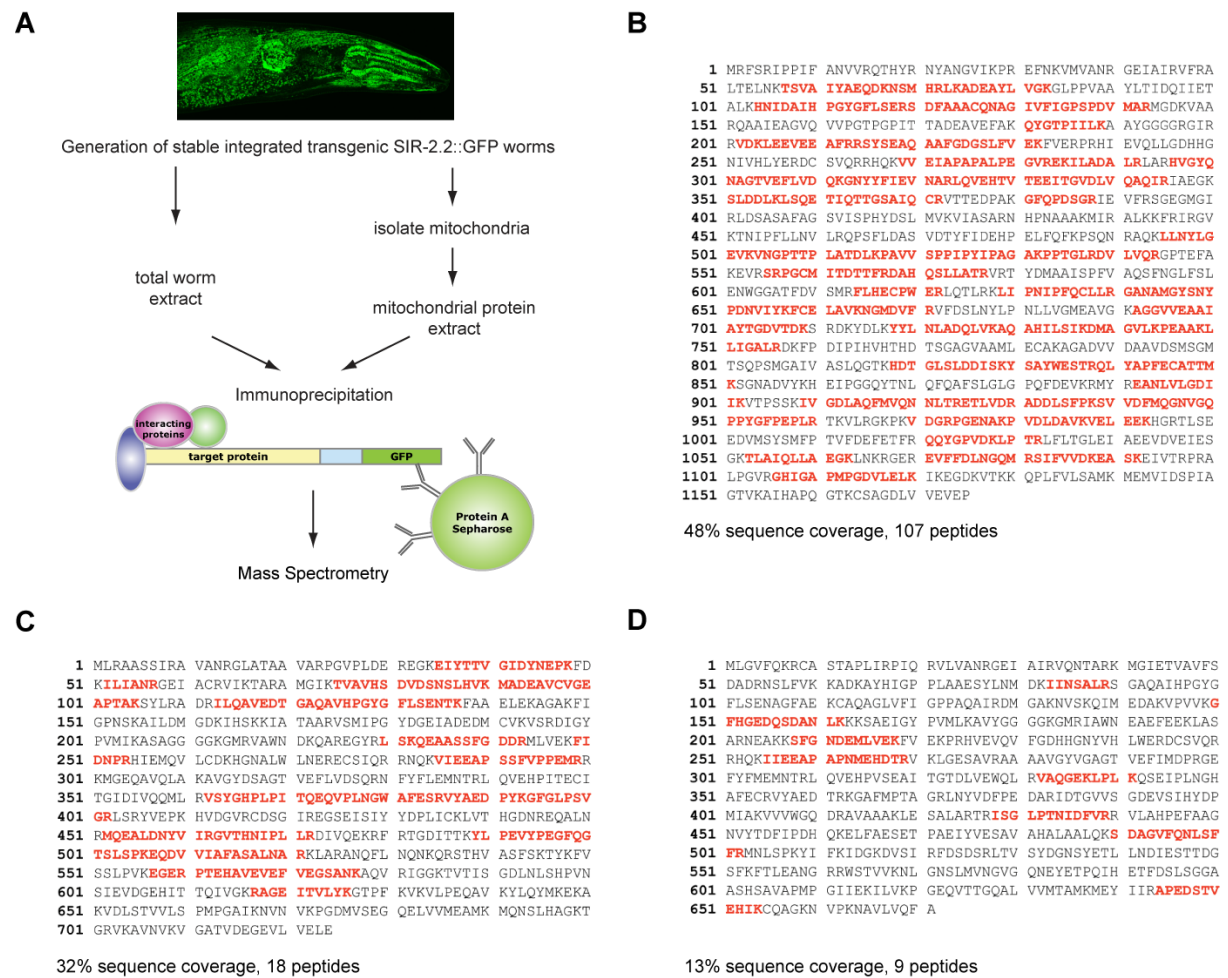


Figure 3-9: Identification of mitochondrial biotin carboxylases as factors interacting with SIR-2.2.

A. Schematic overview on strategy used to identify interaction partners of SIR-2.2. A stable integrated transgenic worm strain expressing SIR-2.2 with a C-terminal Strep-GFP-tag under control of the endogenous promoter was generated and used for extract preparation. GFP-tagged SIR-2.2 was immunoprecipitated with anti-GFP-specific antibodies or the anti-SIR-2.2-specific antibodies from total or mitochondrial worm extracts. Isolated proteins were subjected to SDS-PAGE and analyzed by mass spectrometry. **B.** Protein sequence of *C. elegans* D2023.2 (PYC-1). **C.** Protein sequence of *C. elegans* F27D9.5 (PCCA-1) **D.** Protein sequence of F32B6.2 (MCCC-1). Best sequence coverage of PYC-1, PCCA-1 and MCCC-1 and peptides identified by mass spectrometric analyses (highlighted in red) are shown.

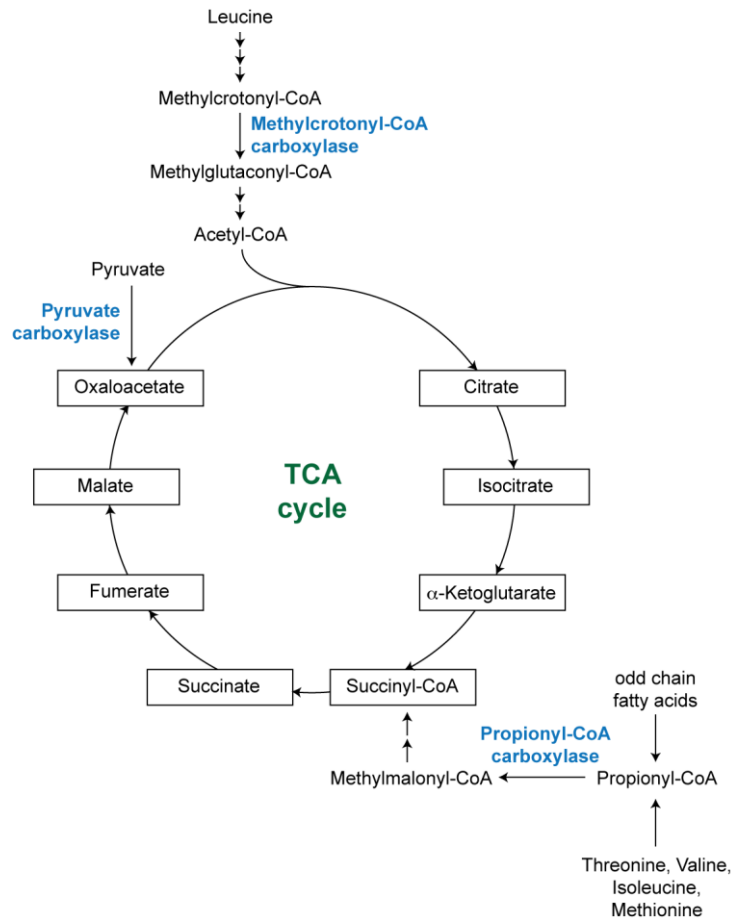


Figure 3-10: Role of mitochondrial biotin-dependent carboxylases in anaplerosis and generation of ketone bodies.

In mammals pyruvate carboxylase (PC) catalyzes the important anaplerotic reaction of carboxylating pyruvate to oxaloacetate, a TCA cycle intermediate. Propionyl-CoA carboxylase (PCC) carboxylates propionyl-CoA to methylmalonyl-CoA, which feeds into the TCA cycle after conversion to succinyl-CoA. This reaction is essential for the catabolism of branched chain amino acids (Thr, Val, Ile, and Met) and odd-chain length fatty acids. Methylcrotonyl-CoA carboxylase (MCC) catalyzes the carboxylation of 3-methylcrotonyl-CoA to 3-methylglutaconyl-CoA, the fourth step in catabolism of the essential amino acid (aa) leucine. Leucine being an exclusively ketogenic aa is degraded to acetoacetate and acetyl-CoA, which is oxidized in the TCA cycle. MCC does not function in anaplerosis but formation of ketone bodies.

Since there were no *gfp*-transgenic strains of these factors existing to verify their interaction with SIR-2.2, I cloned the cDNAs of all three biotin carboxylases into a mammalian expression vector with a C-terminal double FLAG-tag. GFP-tagged SIR-2.2 was expressed together with the corresponding FLAG-tagged proteins in HEK293 cells, immunoprecipitated with GFP-Trap[®]A, and analyzed by SDS-PAGE and Western blotting. PYC-1, PCCA-1 and MCCC-1 co-immunoprecipitated specifically with GFP-tagged SIR-2.2, but not with GFP alone (Figure 3-11 A). Importantly, the mitochondrial protein ACDH-3 (acyl-CoA dehydrogenase) and the nuclear protein HP1 β did not associate with SIR-2.2::GFP in the same experiment.

SIR-2.2 and SIR-2.3 were both mitochondrial (3.1.4) and share a high sequence homology (75.3% identity) with each other. To test whether SIR-2.3 also interacts with these factors, co-immunoprecipitation experiments were performed with GFP-tagged SIR-2.3 and FLAG-

tagged biotin carboxylases. Interestingly, SIR-2.3 also specifically interacted with the three factors. Again, no interaction with HP1 β was observed (Figure 3-11 B).

Since I was able to generate stable integrated worm strains expressing SIR-2.3 with a C-terminal HA-GFP-tag, I also performed immunoprecipitation experiments with GFP-specific antibodies and mitochondrial extracts of *sir-2.3::gfp* transgenic worms. Bound proteins were separated by SDS PAGE and analyzed by mass spectrometry (using same strategy as described above). Peptides of all three biotin carboxylases were identified in the SIR-2.3 bound protein fraction, indicating that SIR-2.3 also interacts with the endogenous proteins. The best sequence coverage obtained for these proteins are shown in Figure 3-12 (for a list of identified factors see Appendix A.3). PYC-1 was identified with a sequence coverage of 48% with 50 identified peptides (Figure 3-12A). The highest sequence coverage for PCCA-1 and MCCC-1 were 17% with 13 peptides (Figure 3-12 B) and 21% with 14 peptides (Figure 3-12 C), respectively.

In summary, mass spectrometric and Western blot analyses of immunoprecipitation experiments showed that both, SIR-2.2 and SIR-2.3, interact with the mitochondrial proteins, PYC-1, PCCA-1 and MCCC-1, which might be biological substrates of these proteins.

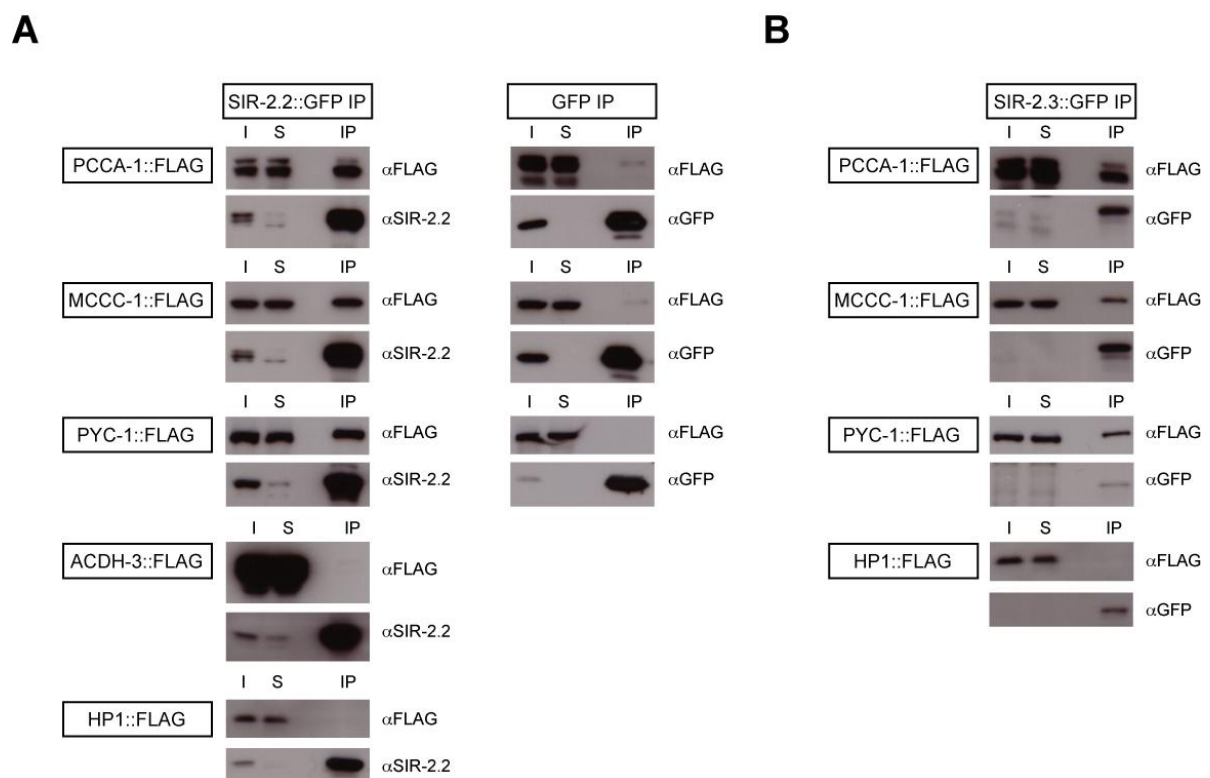


Figure 3-11: Verification of mitochondrial biotin-dependent carboxylases as interaction partners of *C. elegans* SIR-2.2 and SIR-2.3.

Expression vectors encoding SIR-2.2::GFP, SIR-2.3::GFP or GFP alone were co-transfected in HEK293 cells with an expression vector for either FLAG-tagged PCCA-1, MCCC-1, PYC-1, ACDH-3 or HP1. GFP-tagged proteins were immunoprecipitated with GFP-Trap[®] A and analyzed by SDS-PAGE and Western blotting using anti-GFP and anti-FLAG antibodies. I: input (2%), S: supernatant after IP (2%), IP: immunoprecipitated protein fraction. **A.** Representative Western blot analyses of proteins bound to immunoprecipitated SIR-2.2::GFP (left panel) and GFP (right panel). **B.** Representative Western blot analyses of proteins bound to immunoprecipitated SIR-2.3::GFP.

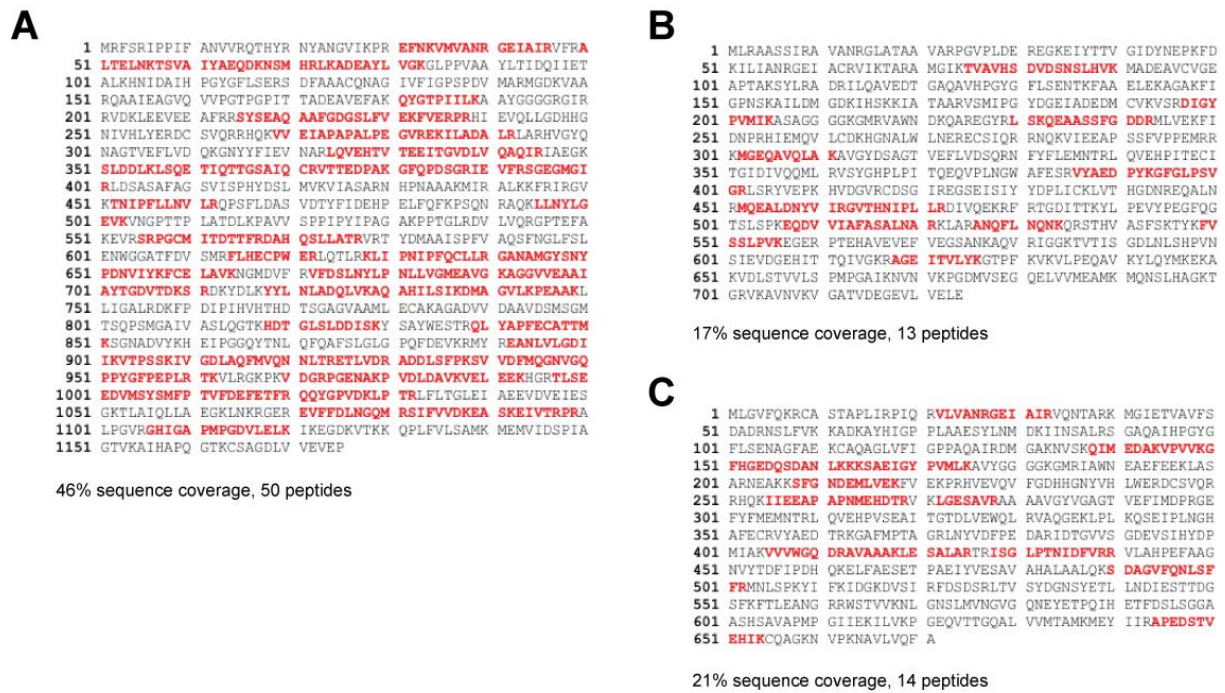


Figure 3-12: Identification of endogenous mitochondrial biotin-dependent carboxylases as interacting factors of SIR-2.3.

Immunoprecipitation experiments using mitochondrial extracts of *sir-2.3::gfp* transgenic worms and anti-GFP antibodies were performed and analyzed by mass spectrometry. Best sequence coverage of PYC-1, PCCA-1 and MCCC-1 are shown. **A.** Protein sequence of *C. elegans* D2023.2 (PYC-1). **B.** Protein sequence of *C. elegans* F27D9.5 (PCCA-1) **C.** Protein sequence of F32B6.2 (MCCC-1). Peptides identified by mass spectrometric analyses are highlighted in red.

3.3.2 Evolutionarily conserved interaction of mammalian SIRT4 with mitochondrial biotin-dependent carboxylases

Both SIR-2.2 and SIR-2.3 show high sequence similarity with the mammalian sirtuin variant SIRT4 (49% and 42% identity to human SIRT4, respectively). It has been reported that SIRT4 is targeted to the mitochondrial matrix and regulates insulin secretion by modifying glutamate dehydrogenase [25], and possibly also by interacting with the ADP/ATP carrier protein (ANT2/3) and insulin-degrading enzyme (IDE) [26]. These findings indicate an important role for SIRT4 in regulation of energy metabolism. I therefore hypothesized that mitochondrial biotin carboxylases might be as well substrates for mammalian SIRT4. To test whether the observed interaction is conserved between *C. elegans* and mammals, I performed co-immunoprecipitation experiments with GFP-tagged mouse SIRT4 (mSIRT4) and FLAG-tagged mouse propionyl-CoA carboxylase α -subunit (mPCCA), mouse methylcrotonyl-CoA carboxylase α -subunit (mMCCC-1), and mouse pyruvate carboxylase (mPC). All three mouse biotin carboxylases (as well as the *C. elegans* biotin carboxylases, data not shown) associated specifically with mSIRT4 (Figure 3-13), indicating an evolutionarily conserved interaction.

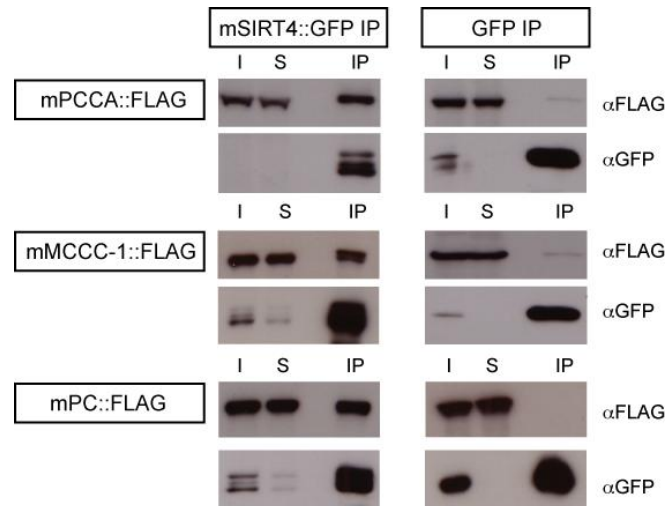


Figure 3-13: Evolutionarily conserved interaction of mammalian SIRT4 with mitochondrial biotin carboxylases.

GFP-tagged murine SIRT4 (mSIRT4) was expressed together with murine PCCA (mPCCA), MCCC1 (mMCCC1), and PC (mPC) in HEK293 cells and immunoprecipitated with GFP-Trap[®]A. Bound proteins were separated by SDS-PAGE and analyzed by Western blotting using anti-GFP and anti-FLAG antibodies. Representative Western blot analyses of proteins bound to immunoprecipitated SIRT4::GFP (left panel) and GFP (right panel) are shown. I: input (2%), S: supernatant after IP (2%), IP: immunoprecipitated protein fraction.

3.3.3 Analysis of the interaction specificity of *C. elegans* and mammalian sirtuins with mitochondrial biotin-dependent carboxylases

C. elegans SIR-2.2 and SIR-2.3 share high sequence similarity with each other. Both proteins were localized to mitochondria and interacted with mitochondrial biotin carboxylases. In contrast to SIR-2.2 and SIR-2.3, the structure of nuclear SIR-2.1 exhibits next to the conserved catalytic core domain long N-terminal and C-terminal regions, which also differ in sequence composition (Figure 3-14 A). To analyze whether there are differences in the interaction strength and specificity of different *C. elegans* SIR-2 proteins, I co-transfected FLAG-tagged biotin carboxylase expression vectors together with an expression vector for either GFP-tagged SIR-2.1, SIR-2.2, or SIR-2.3 in HEK293 cells, and performed co-immunoprecipitation experiments with GFP-Trap[®]A beads. Since SIR-2.2::GFP and SIR-2.3::GFP showed a higher protein degradation rate than SIR-2.1::GFP, equal amounts of full-length immunoprecipitated protein were loaded on SDS-PAGE gels and analyzed by Western blotting with anti-GFP and anti-FLAG antibodies (Figure 3-14 B, asterisks indicate degraded protein). GFP alone served as a negative control.

SIR-2.2 showed the strongest interaction with all three biotin carboxylases. SIR-2.3 also associated strongly with FLAG-tagged biotin carboxylases. SIR-2.1 did not interact with PCCA-1. Considerably less of MCCC-1 and PYC-1 was associated with SIR-2.1 than with SIR-2.2 and SIR-2.3. These results suggest that the regions N- and C-terminal to the catalytic core domain of SIR-2.1 seem to mainly influence the ability to interact with mitochondrial biotin carboxylases.

In *sir-2.2* and *sir-2.3* mutant worms truncated SIR-2.2 (Δ SIR-2.2::GFP) and SIR-2.3 (Δ SIR-2.3::GFP) proteins, which are encoded by the *sir-2.2(tm2648)/(tm2673)* and *sir-2.3(ok444)*

deletion alleles, different regions of the conserved sirtuin catalytic core domain (Figure 3-7 A and B) were missing. To test whether these deletions affect the interaction with mitochondrial biotin carboxylases, I also performed co-immunoprecipitation experiments with GFP-tagged truncated SIR-2.2 (Δ SIR-2.2::GFP) and SIR-2.3 (Δ SIR-2.3::GFP). Δ SIR-2.2, lacking 75 aa in the central region of the sirtuin catalytic core domain (Figure 3-14 A and Figure 3-7 A) showed like SIR-2.2 and SIR-2.3 strong interaction with PCCA-1, MCCC-1 and a weaker interaction with PYC-1. In Δ SIR-2.3 a large part (141 aa) of the catalytic core domain is deleted at the C-terminus (Figure 3-14 A and Figure 3-7 B). The interaction of Δ SIR-2.3 with all three biotin carboxylases was very weak, suggesting that aa residues located at the C-terminus of the catalytic sirtuin core domain contribute more to the interaction than aa residues located in the middle of the protein sequence of SIR-2.3 and SIR-2.2.

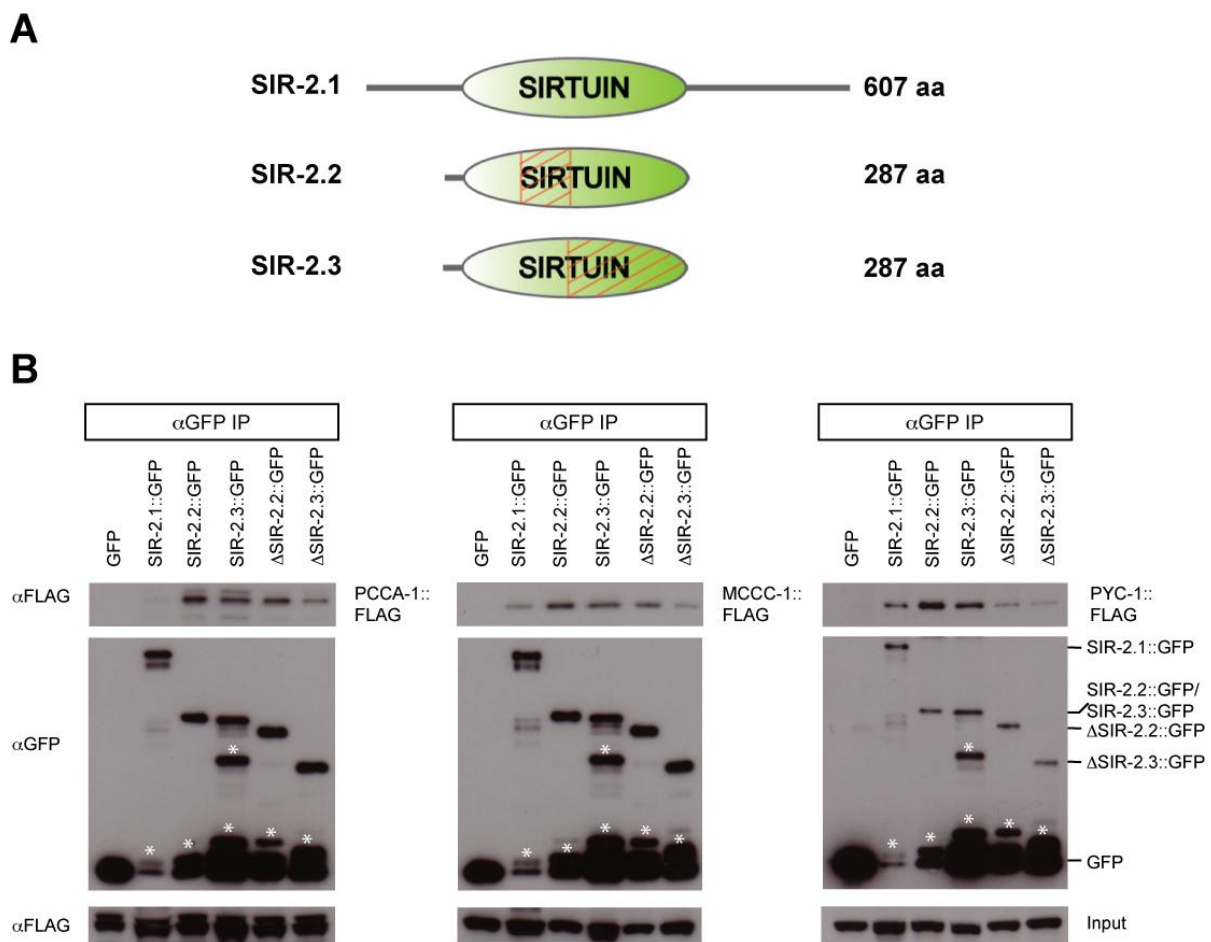


Figure 3-14: Analysis of specificity of interaction with *C. elegans* SIR-2.1, SIR-2.2 and SIR-2.3.

A. Schematic view of the structural organization of *C. elegans* SIR-2.1, SIR-2.2 and SIR-2.3. Conserved sirtuin catalytic core domain is shown in green. N- and C-terminal regions, which are variable in length and sequence composition, are represented by grey lines. Regions deleted in Δ SIR-2.2 and Δ SIR-2.3 are shaded in red. **B.** FLAG-tagged mitochondrial biotin carboxylases were expressed together with GFP-tagged SIR-2.1, SIR-2.2, SIR-2.3, Δ SIR-2.2 or Δ SIR-2.3 in HEK293 cells and immunoprecipitated with GFP-Trap[®]A. Due to the high protein degradation of SIR-2.2::GFP and SIR-2.3::GFP equal amounts of full-length immunoprecipitated protein was loaded on SDS-PAGE gels and analyzed by Western blotting with anti-GFP and anti-FLAG antibodies. The results of the co-immunoprecipitation experiments are shown in the left panel for PCCA-1::FLAG, in the middle panel for MCCC-1::FLAG, and in the right panel for PYC-1::FLAG. Running positions of GFP-tagged proteins are shown on the right side of the right panel. Inputs were loaded to confirm that FLAG-tagged proteins were expressed in each experiment. Asterisks indicate degraded protein.

Taken together, these results show that both SIR-2.2 and SIR-2.3 strongly interact with mitochondrial biotin carboxylases. The interaction seems to be mainly mediated by aa located at the C-terminus (and maybe also at the N-terminus) of their conserved sirtuin catalytic core domain.

Mammalian mitochondria possess three sirtuin variants (SIRT3 to SIRT5). To test whether SIRT4 interacts specifically with the mammalian biotin carboxylases FLAG-tagged mPC, mMCCC1 and mPCCA were expressed together with human Myc-tagged SIRT3, SIRT4 or SIRT5 in HEK293T cells. Proteins were immunoprecipitated with FLAG-M2 agarose beads and analyzed by SDS-PAGE and Western blotting using anti-Myc and anti-FLAG antibodies (Figure 3-15). SIRT4 specifically co-immunoprecipitated with FLAG-tagged mPC and mMCCC1, and no interaction with both SIRT3 and SIRT5 was detected. However, I did not observe a SIRT4-specific interaction with mPCCA. Both SIRT3 (full-length variant) and SIRT4 strongly associated with the protein, suggesting that there might be functional overlap between SIRT3 and SIRT4.

Nevertheless, SIRT4 showed strong association with all three mitochondrial biotin carboxylases, indicating that they might be as well modified by SIRT4.

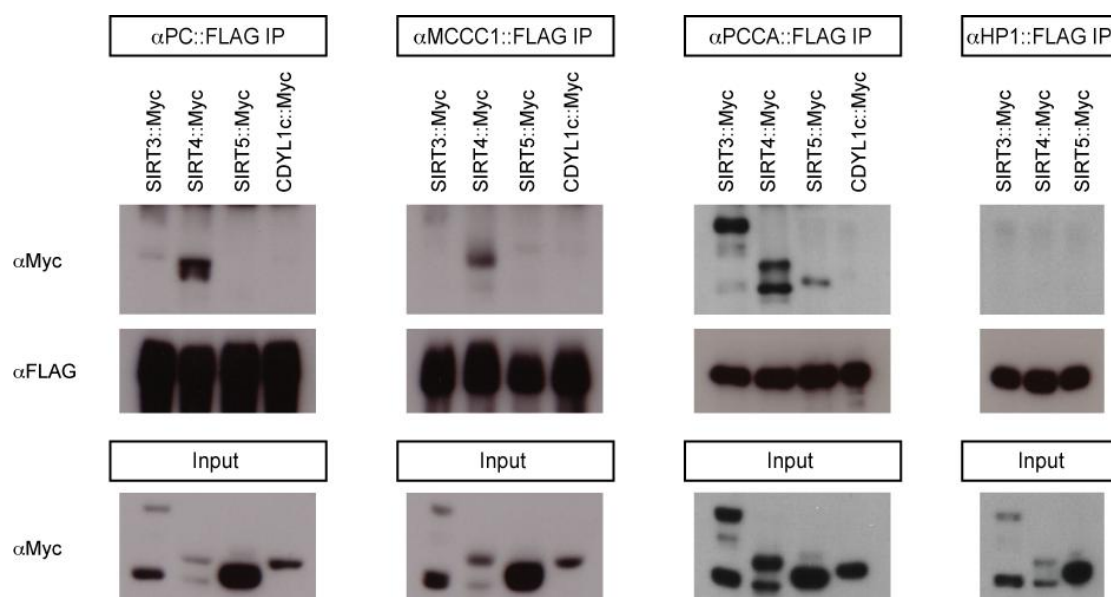


Figure 3-15: Interaction specificity of human mitochondrial sirtuins with mitochondrial biotin-dependent carboxylases.

Expression vectors for human SIRT3, SIRT4, SIRT5 and CDYL1c (Myc-tagged) were co-transfected with expression vectors encoding either murine PC, MCCC1, or PCCA (FLAG-tagged) in HEK293T cells. FLAG-tagged HP1 was used as negative control. Proteins were immunoprecipitated with FLAG-M2 agarose beads and analyzed by Western blotting with anti-Myc and anti-FLAG antibodies. Inputs were loaded to confirm that Myc-tagged proteins were expressed in each experiment. Co-Immunoprecipitation experiments with CDYL1c::Myc or HP1::FLAG served as negative controls.

3.3.4 Mapping of the biotin carboxylase domain mediating interaction with SIRT4

All three mitochondrial biotin carboxylases catalyze metabolically important carboxyl group transfer reactions and possess a highly conserved N-terminal biotin carboxylase domain and C-terminal biotin carboxyl carrier protein (BCCP) domain (Figure 3-16 A). To determine,

which domain mediates the interaction with SIRT4, various deletion constructs of mPC, mMCCC-1 and mPCCA were cloned.

In mammals PC is comprised of four identical subunits (α_4 -form) and each subunit of approximately 120-130 kD contains all three functional domains. The biotin carboxylase domain (BC) featuring a conserved ATPgrasp domain (ATP) (Figure 3-16 A) catalyzes the first step of the carboxylation reaction, i.e. the ATP-driven carboxylation of biotin to form carboxybiotin. The pyruvate carboxyltransferase domain, catalyzing the second step of the reaction (the transfer of the carboxyl group of the carboxybiotin to pyruvate), is located in the middle of the polypeptide chain. At the C-terminus the biotin carboxyl carrier protein (BCCP) domain, also referred to as the biotinyl-lipoyl domain, is found. This domain containing biotin covalently attached to a highly conserved lysine residue is present in all biotin-dependent enzymes and facilitates the carboxylation of a substrate by transferring CO₂ from one subsite to the other [203, 205].

To map the interaction domain of mPC, I generated the following five constructs with an N-terminal FLAG-tag (Figure 3-16 A):

- biotin carboxylase domain (BC)
- ATPgrasp domain (ATP)
- pyruvate carboxyltransferase domain (PCT)
- C-terminal domain containing biotin carboxyl carrier protein (BCCP) domain, BCCP domain large (BCCPL)
- biotin carboxyl carrier protein domain alone, BCCP

Each construct was expressed together with human Myc-tagged SIRT4 in HEK293T cells and co-immunoprecipitation experiments were performed with an antibody against the Myc-tag. Since the expression levels and consequently also the recovery rates of SIRT4 were not equal when co-expressed with the different mPC constructs, I subjected equal amounts of immunoprecipitated SIRT4-Myc to SDS-PAGE and Western blot analysis. Next to full-length mPC only the biotin carboxylase domain associated with SIRT4, indicating that the N-terminal region of mPC mediates the interaction with SIRT4 (Figure 3-16 B). As no binding of the ATPgrasp domain was observed, amino acid residues outside this domain must be sufficient for the interaction with SIRT4.

Both propionyl-CoA carboxylase and methylcrotonyl-CoA carboxylase are heteropolymeric enzymes with six heterodimers of one α - and one β -subunit arranged in an $(\alpha\beta)_6$ configuration [202-204]. The α -subunits contain the N-terminal biotin carboxylase (BC) domains and the C-terminal biotin carboxyl carrier protein (BCCP) domain (Figure 3-16 A). The carboxyltransferase (CT) activities catalyzed by the propionyl-CoA carboxyltransferase domain and the methylcrotonyl-CoA carboxyltransferase domain, respectively, are located on separated β -chains [203] and were not detected as binding partners of *C. elegans* SIR-2.2 in mass spectrometric analyses. To test whether the interactions of SIRT4 with mPCCA and mMCCC1 were mediated by the same conserved domain a N-terminal and C-terminal deletion construct of each protein was generated (Figure 3-16 A) and analyzed by co-immunoprecipitation experiments as described above. Figure 3-16 C and D show that binding to SIRT4 was again depending on the N-terminal BC domains of both PCCA and MCCC1 but not on the C-terminal regions containing the BCCP domain.

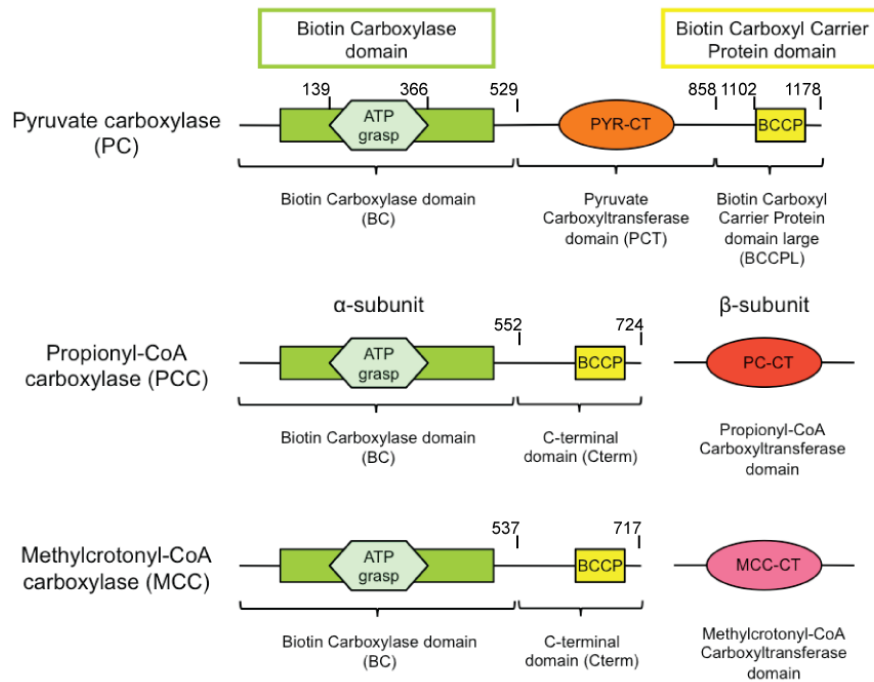
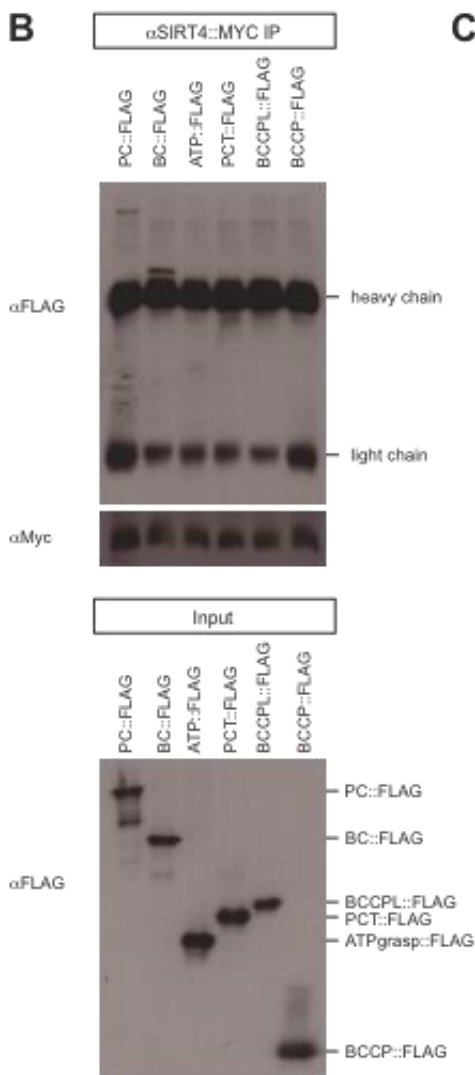
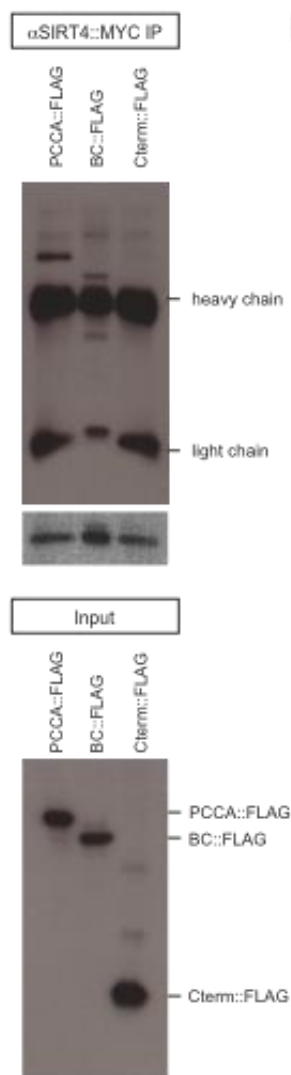
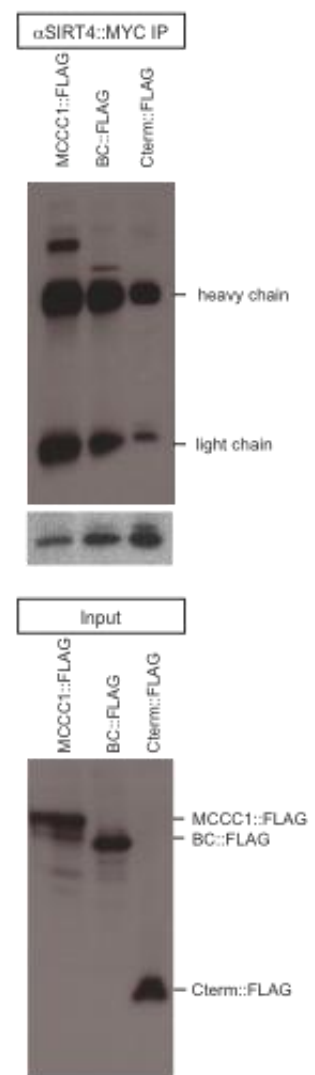
A**B****C****D**

Figure 3-16: Mapping of the domain of PC, PCCA and MCCC1 mediating interaction with SIRT4.

A. Schematic representation of the domain organization of mitochondrial biotin carboxylases. All three proteins have a highly conserved N-terminal biotin carboxylase domain (BC) and a C-terminal biotin carboxyl carrier protein domain (BCCP). The following deletion constructs were generated for mPC: biotin carboxylase (BC) domain (marked by bracket), ATPgrasp (ATP) domain, pyruvate carboxyltransferase (PCT) domain (marked by bracket), C-terminal domain containing biotin carboxyl carrier protein domain (BCCP domain large) (BCCPL, marked with bracket), biotin carboxyl carrier protein domain alone (BCCP). For both mPCCA and mMCCC1 a N-terminal construct comprising the biotin carboxylase domain (BC, indicated by brackets) and a C-terminal construct containing the BCCP domain (Cterm, indicated by brackets) were generated. Domain boundaries of the mutant proteins are indicated by the aa positions. **B.** to **D.** For co-immunoprecipitation (Co-IP) experiments, FLAG-tagged deletion constructs were expressed together with human SIRT4 (Myc-tag) in HEK293T cells. Equal amounts of immunoprecipitated Myc-tagged SIRT4 were loaded on SDS-PAGE gels and analyzed by Western blotting with anti-FLAG and anti-Myc antibodies. Inputs confirm expression of FLAG-tagged proteins in each experiment. Running positions of FLAG-tagged proteins and of the antibody's heavy and light chains are indicated on the right. Representative Western blot analyses of Co-IP experiments using full-length and mutated murine PC proteins (**B**), full-length and mutated murine PCCA proteins (**C**) and full-length and mutated murine MCCC1 proteins (**D**) are shown.

This leads to the conclusion that SIRT4 interacts with PC, PCCA and MCCC1 via the N-terminal biotin carboxylase domain. Residues located outside the ATP-grasp domain mediate the interaction.

3.4 Regulation of biotin carboxylase function by mitochondrial sirtuins

3.4.1 Mitochondrial biotin carboxylases are acetylated proteins

There has been growing evidence in recent years that lysine acetylation is an important posttranslational modification to regulate metabolic enzymes. A proteomic survey by Kim et al. [98] found that approximately 20% of all mitochondrial proteins are acetylated. Together with two other proteomic studies [99, 146] acetylation sites were identified in mitochondrial proteins of all major metabolic pathways including TCA cycle, oxidative phosphorylation, β -oxidation, amino acid catabolism and urea cycle.

As mitochondrial biotin carboxylases might be acetylated proteins, I surveyed the published candidate lists of all three proteomic screens for identified acetylated peptides of these factors. Indeed, I found three different acetylation sites in PC and one acetylation site in PCCA (marked by orange boxes, Figure 3-17 A and B). In the mouse sequence of PC these residues map to K316, K992 and K1090 [98, 99, 146]. In human PCCA K528 was acetylated [146], this residue corresponds to R549 in mouse PCCA and K545 in *C. elegans*.

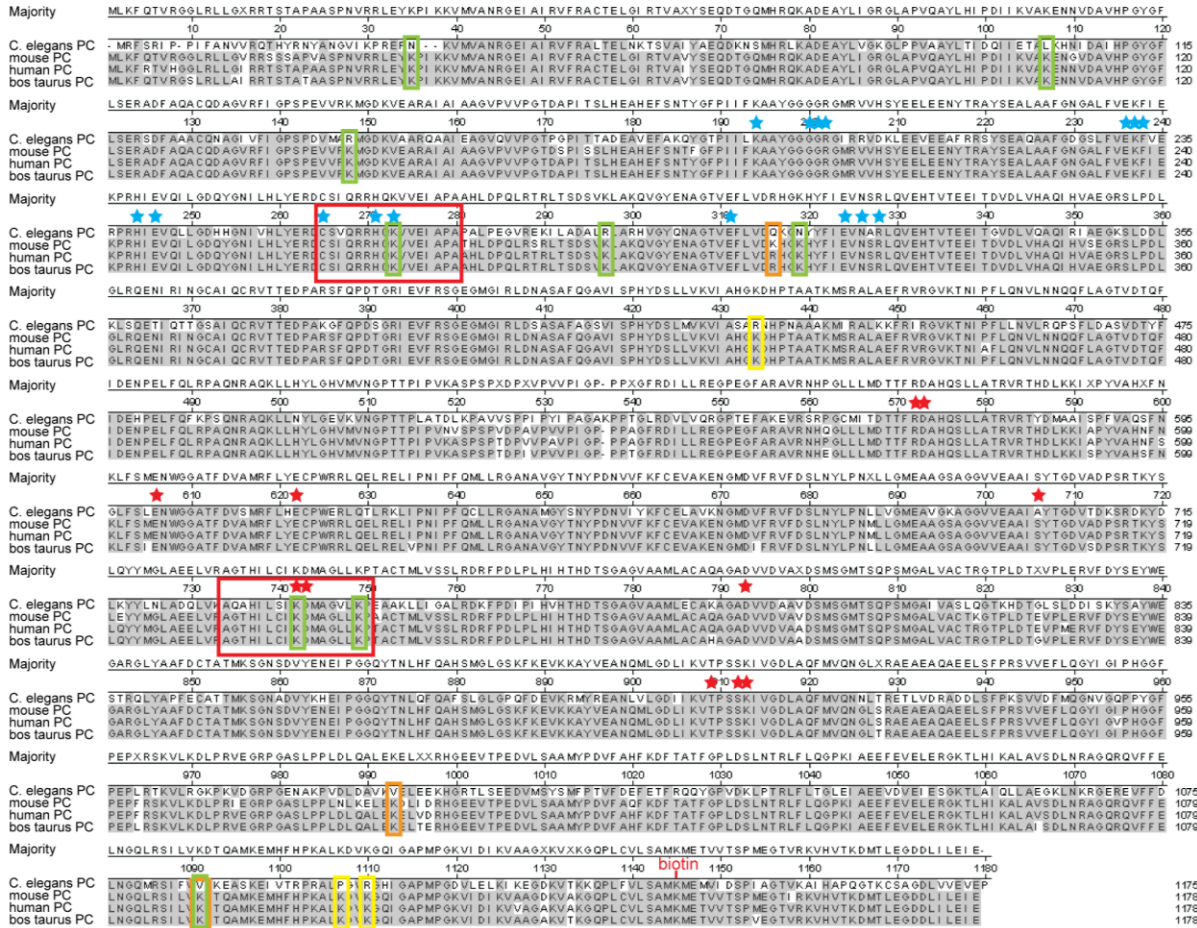
Additional acetylation sites of all three biotin carboxylases were also detected in an unpublished mass spectrometric screen performed in the laboratory of our collaborator Prof. Eric Verdin (Gladstone Institute, San Francisco, USA) (marked by yellow boxes, Figure 3-17 A, B, and C). In their screen three sites namely K434, K1106 and K1109 were found in mouse PC. Seven acetylation sites were detected in mouse PCCA (K128, K150, K223, K403, K460, K492 and K509) and two acetylation sites in mouse MCCC1 (K180 and K717).

To further map putative acetylation sites, I also obtained commercial PC isolated from bovine liver (Sigma, P7173) and analyzed it for protein acetylation (Dr. Henning Urlaub, MPI of Biophysical Chemistry, Göttingen). Nine different acetylation sites were found in bovine PC (marked with green boxes, Figure 3-17 A). These residues map to K35, K107, K148, K273, K297, K319, K741, K748 and K1090 in the sequence of mouse pyruvate carboxylase. Only

one of the sites, K1090 overlapped with findings of the previous mass spectrometric screens, which were all based on anti-acetyllysine-specific antibodies. Due to certain sequence specificities, different anti-acetyllysine pan-antibodies seem to immunoprecipitate different acetylated lysine peptides.

A

Pyruvate Carboxylase



B

Propionyl-CoA Carboxylase



C

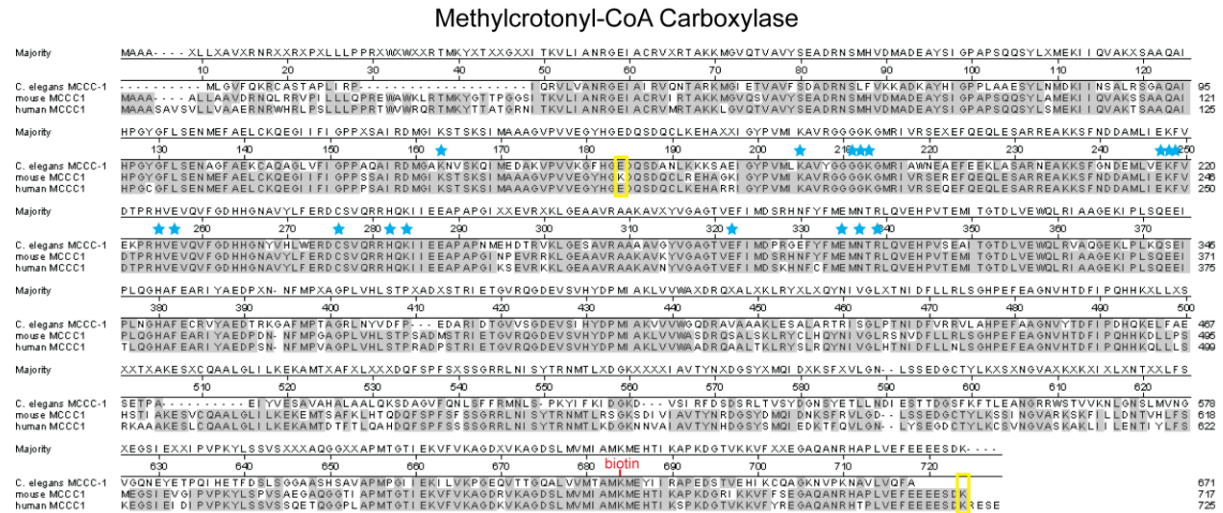


Figure 3-17: Lysine acetylation sites identified in PC, PCCA and MCCC1 by different mass spectrometric approaches.

A. Sequence alignment (Clustal W) of *C. elegans*, mouse, human and bovine pyruvate carboxylase. **B.** Sequence alignment (Clustal W) of *C. elegans*, mouse, and human PCCA. **C.** Sequence alignment (Clustal W) *C. elegans*, mouse, and human MCCC1. Matching residues are shaded with gray; acetylation sites found in published screens by [98, 99, 146] are boxed in orange; yellow boxes mark acetylation sites found by our collaborator Prof. Eric Verdin (Gladstone Institute, San Francisco, USA); green boxes label acetylation sites found in commercial bovine PC by mass spectrometric analysis; blue stars mark residues implicated in biotin carboxylase reaction [203]; red stars mark residues important for pyruvate transcarboxylase reaction [203, 205]; red boxes indicate localization of the peptides MPIG-47 and MPIG-48; biotin indicates highly conserved lysine residue to which biotin is covalently attached.

In summary, all three mitochondrial biotin carboxylases are acetylated. PC and PCCA seem to be highly acetylated protein as 14 and 8 acetylation sites, respectively, have been identified in total so far.

To further confirm these results, I investigated in collaboration with the laboratory of Prof. Eric Verdin the acetylation levels of the biotin-dependent carboxylases by Western blot analysis using anti-acetyllysine-specific antibodies (Figure 3-18). FLAG-tagged mPC, mPCCA and mMCCC1 were expressed in HEK293T cells and immunoprecipitated with FLAG-M2 agarose beads. As positive control cells were also transfected with a vector encoding FLAG-tagged acetyl-CoA synthetase 2 (AceCS2), which was shown to be acetylated and which is regulated by SIRT3 [101, 102]. Cells transfected with an empty vector served as negative control. Like AceCS2 all three proteins were detected with anti-acetyllysine-specific antibodies (α AcK) after immunoprecipitation, further supporting the finding that PC, PCCA and MCCC1 are acetylated mitochondrial proteins.

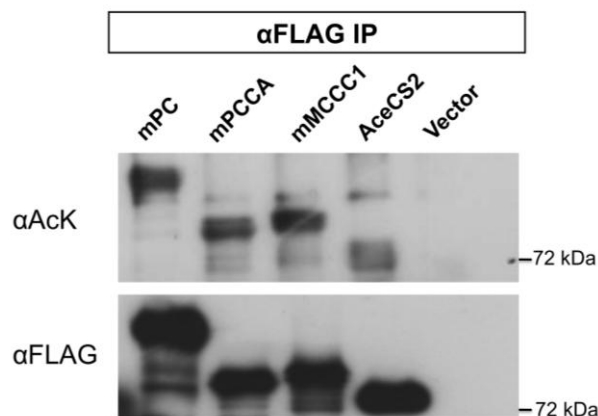


Figure 3-18: Analysis of protein acetylation levels by Western blotting with anti-acetyllysine-specific antibodies.

Expression vectors encoding FLAG-tagged mPC, mPCCA and mMCCC1 were transfected into HEK293T cells. Proteins were immunoprecipitated with FLAG-M2 beads (anti-FLAG IP) and protein acetylation levels were analyzed using anti-acetyllysine-specific antibodies (α AcK). Cells transfected with an empty vector (vector) were used for negative control. Western blot analysis using anti-acetyllysine and anti-FLAG antibodies are shown. Running position of molecular weight marker is indicated on the right.

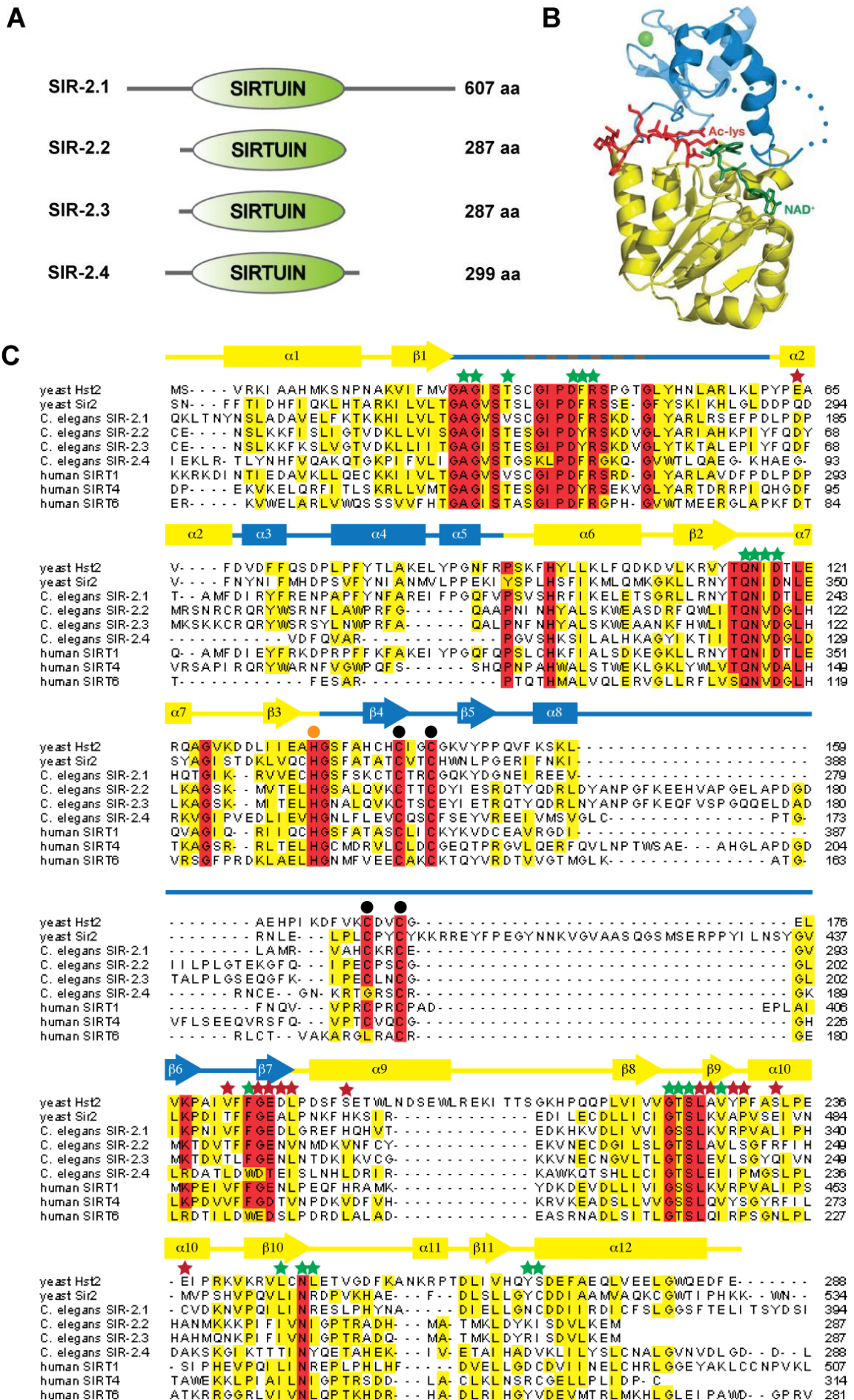
3.4.2 Analysis of the enzymatic activities of *C. elegans* SIR-2.2, SIR-2.3 and mammalian SIRT4

Mass spectrometric analyses have not only identified acetylation sites in many metabolic enzymes but also detected changes in acetylation levels upon fasting [98, 146]. Therefore, deacetylation of mitochondrial biotin carboxylases by SIRT4, SIR-2.2 and/or SIR-2.3 might be an important regulatory mechanism to modulate the activity of these enzymes and energy metabolism in response to changing energy demands.

Apart from SIR-2.1 [18], no analysis on the enzymatic activities of *C. elegans* SIR-2.2, SIR-2.3 and SIR-2.4 has been reported so far. All four sirtuins share a conserved catalytic core domain, but differ in length and sequence composition in their N- and C-terminal regions (Figure 3-19 A). This difference might contribute to their substrate specificity. The structure of SIR-2.2 and SIR-2.3 seems to be primarily made up by the sirtuin catalytic core region and exhibits only a short N-terminal region and no C-terminal region. Compared to SIR-2.1, SIR-2.4 also possesses only short N- and C-terminal regions.

Figure 3-19: Highly conserved catalytic core domain of *C. elegans* sirtuins.

A. Schematic overview of the structural organization of *C. elegans* sirtuins. All four SIR-2 proteins contain a highly conserved catalytic sirtuin core domain (shown in green), but differ in length and sequence composition in their N- and C-terminal regions (indicated by grey lines). **B.** Three dimensional structure of a sirtuin bound with an acetylated peptide (red) and NAD^+ (blue). The Rossmann-fold domain is shown in yellow, the small Zn^{2+} -binding domain in blue and the cofactor binding loop is indicated by blue dots; Green dot represents Zn^{2+} ion; Figure taken from [27]. **C.** Multiple sequence alignment (ClustalW) of the catalytic core domain of *S. cerevisiae* Hst2 and SIR2, *C. elegans* SIR-2.1, SIR-2.2, SIR-2.3 and SIR-2.4, and human SIRT1, SIRT4 and SIRT6. Conserved residues are highlighted in red; similar residues in yellow; the secondary structure elements above the sequence alignment follow the coloring of the structural domains shown in **B**; green stars: NAD^+ -binding residues; red stars: residues involved in acetyllysine peptide binding; orange dot: histidine in active site; black dots: Zn^{2+} binding residues.



A multiple sequence alignment (ClustalW) of the catalytic core domain of *C. elegans* SIR-2 proteins with *S. cerevisiae* Hst2 and SIR2 as well as human SIRT1, SIRT4 and SIRT6 showed a high degree of sequence conservation (Figure 3-19 C). Residues important for the enzymatic activity such as the active site histidine (Figure 3-19 C, marked with an orange dot) as well as the majority of residues involved in NAD⁺ and acetyllysine peptide binding were also conserved in *C. elegans* SIR-2 proteins. In addition, structurally important residues, such as the Zn²⁺ binding motif (Figure 3-19 C, indicated by black dots) located in the small domain of the sirtuin catalytic core region (Figure 3-19 B), were also present in SIR-2.2 and SIR-2.3. The high degree of sequence conservation within the catalytic sirtuin core domain of *C. elegans* SIR-2 protein suggests that these proteins also might exhibit NAD⁺-dependent deacetylase activity. To analyze the enzymatic activity of *C. elegans* sirtuins as well as SIRT4 I used several assays.

3.4.2.1 *In vitro* histone deacetylase activity (HDAC) assay

A standard assay to analyze the NAD⁺-dependent enzymatic activity of sirtuins is an *in vitro* histone deacetylase (HDAC) activity assay using a ³H-acetylated histone 4 (H4) tail peptide as substrate. While the *C. elegans* variant SIR-2.1 has been shown to possess HDAC activity [18]), the enzymatic activities of SIR-2.2, SIR-2.3 as well as SIR-2.4 still need to be determined. In collaboration with the group of Prof. Lührmann (MPI of Biophysical Chemistry, Göttingen) recombinant SIR-2 protein was expressed in wheat germ extract, a cell-free *in vitro* translation system. Since the wheat germ extract did not exhibit intrinsic deacetylase activity, *in vitro*-translated proteins were directly used for the enzymatic assay without any further purification. Reactions were incubated at 25°C for 2 h or overnight and after acidification released acetate was quantified by scintillation counting (Figure 3-20 A). HDAC activity was only detected for SIR-2.1, but not for the other three variants (Figure 3-20 B). Since stable transgenic *gfp*-strains could be generated for SIR-2.2 and SIR-2.3, I also isolated GFP-tagged protein from *C. elegans* by immunoprecipitation and performed the HDAC assay with immunoprecipitated protein bound to beads (Figure 3-20 C). Again, only SIR-2.1::GFP showed detectable HDAC activity.

Using the same HDAC assay as described above, HDAC activity could be demonstrated for human SIRT1, SIRT2, SIRT3 and SIRT5, but not for SIRT4, SIRT6 and SIRT7 [29, 91]. For a long time only ADP-ribosyltransferase activity had been reported for SIRT6 [25, 26, 30], however Michishita et al. [31] recently showed that SIRT6 is a histone 3 lysine 9 (H3K9) specific deacetylase, suggesting a high substrate specificity for these proteins. SIRT4 also has been shown to exhibit ADP-ribosyltransferase activity [25, 26], but it might also exhibit protein deacetylase activity with very strict substrate specificity. Since soluble *C. elegans* SIR-2.2 and SIR-2.3 could not be expressed recombinantly in *E. coli*, I was not able to obtain sufficient amounts of protein to test whether these proteins possess ADP-ribosyltransferase activity in [³²P]NAD⁺-labeling experiments.

In summary, I did not observe NAD⁺-dependent HDAC activity of *C. elegans* SIR-2.2 and SIR-2.3. SIR-2.2 and SIR-2.3 were localized to mitochondria (3.1.4) and an acetylated histone H4 tail peptide is not a natural substrate of these proteins. Thus, the lack of detectable HDAC activity does not allow the conclusion that *C. elegans* SIR-2.2 and SIR-2.3 as well as

mammalian SIRT4 are not true NAD^+ -dependent deacetylases. To determine, whether these proteins are NAD^+ -dependent protein deacetylases with high substrate specificity, I analyzed additional acetylated substrates for deacetylation by *C. elegans* SIR-2.2 and SIR-2.3 as well as mammalian SIRT4 in deacetylase activity assays.

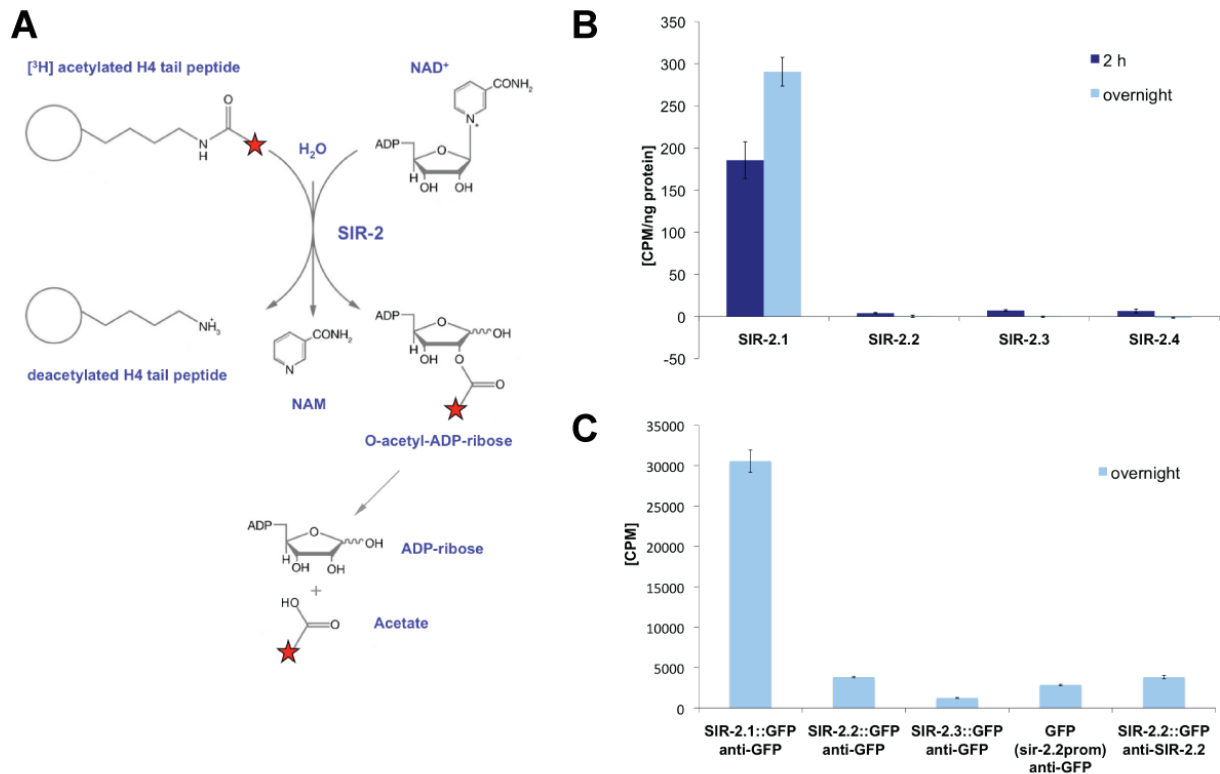


Figure 3-20: Analysis of NAD^+ -dependent HDAC activity.

A. Overview on the enzymatic reaction catalyzed by SIR-2 proteins. The deacetylation of a [³H] acetylated lysine residue on a histone H4 tail peptide is coupled to hydrolysis of NAD^+ , yielding nicotinamide (NAM) and O-acetyl-ADP-ribose. For quantification by scintillation counting, acetate is released from O-acetyl-ADP-ribose by addition of acid and extracted with organic solvent. Figure taken from [27] and further modified. **B.** All four *C. elegans* SIR-2 proteins were translated *in vitro* using wheat germ extract and analyzed for HDAC activity on a [³H] peracetylated H4 tail peptide. **C.** GFP-tagged SIR-2 proteins were immunoprecipitated from worm lysates of *sir-2::gfp* transgenic worm strains using anti-GFP antibodies (and for SIR-2.2 also the anti-SIR-2.2 antibodies). HDAC activity assays were performed with protein bound to beads and a [³H] peracetylated H4 tail peptide as substrate. Quantitative values, indicating HDAC activity, are means of three measurements; error bars represent standard deviation; overnight and 2 h incubation times of the enzymatic reactions are indicated by light blue and dark blue bars, respectively.

3.4.2.2 Mass spectrometry based *in vitro* deacetylase activity assay

Mammalian SIRT4 and *C. elegans* SIR-2.2 and SIR-2.3 interacted with mitochondrial biotin carboxylases in co-immunoprecipitation experiments. Different mass spectrometric analyses detected a total of 14 lysine acetylation sites in PC (Figure 3-17 A). Among these only three lysine residues (K273, K741 and K748, numbers are mapped to human and mouse PC) were conserved from *C. elegans* to human. Interestingly, K273, located in the biotin carboxylase domain of PC, and K741, located in the pyruvate carboxyltransferase domain, are important for the enzymatic activity of PC. I hypothesized that SIRT4, SIR-2.2 and SIR-2.3 might deacetylate these residues and thereby regulate the activity of pyruvate carboxylase. Therefore, I obtained two peptides, one with acetylated K273 (MPIG-47) and one with acetylated K741 (MPIG-48) (red boxes Figure 3-17 A) for *in vitro* deacetylase activity assays.

Myc-tagged human SIRT3, SIRT4 and SIRT5 and FLAG-tagged *C. elegans* SIR-2.1, SIR-2.2, and SIR-2.3 were expressed in HEK293T cells, immunoprecipitated and immediately subjected to *in vitro* deacetylase activity assays using the acetylated peptides as substrate. NAD⁺-dependent deacetylation of the peptides was then determined by mass spectrometry. No deacetylation of MPIG-47 (K273ac) and MPIG-48 (K741ac) was observed for SIR-2.2 (Figure 3-21 C), SIR-2.3 (Figure 3-21 D), SIRT4 (Figure 3-21 F), and SIRT5 (Figure 3-21 G) (Table 3-3). However, both peptides were deacetylated by SIR-2.1 (Figure 3-21 B) and SIRT3 (Figure 3-21 E) leading to a 42 kD reduction of the peptide mass (indicated by black arrows). SIR-2.1 being a nuclear protein also showed strong activity on H4K16ac and H3K9ac peptides (Table 3-3). Interestingly, SIRT3, although it is a mitochondrial protein, deacetylated histone 4 lysine 16 (H4K16ac) and histone 3 lysine 9 (H3K9ac) acetylated peptides as well. For negative control (Mock) deacetylase reactions were performed without immunoprecipitated protein (Figure 3-21 A, H to J).

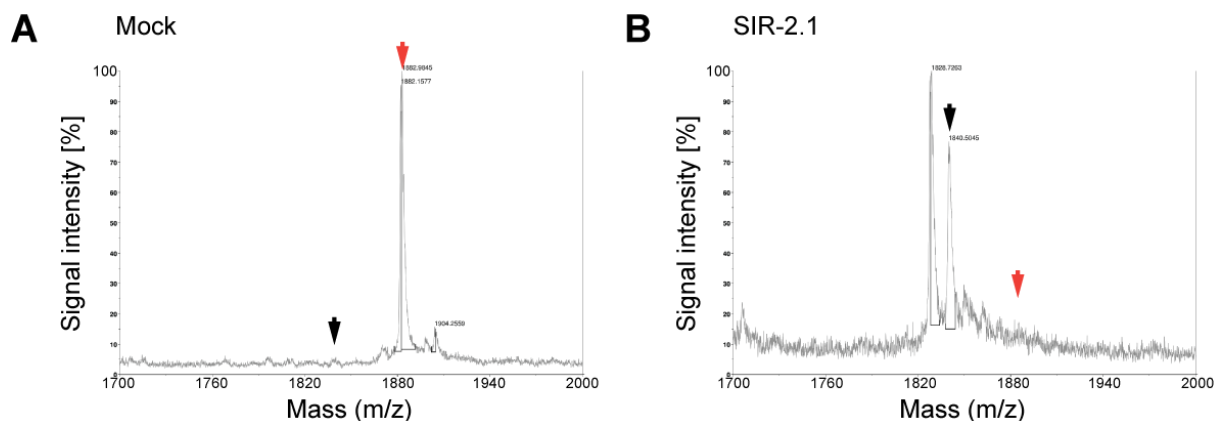
Table 3-3: Summary on observed NAD⁺-dependent deacetylase activity on acetylated peptides analyzed by mass spectrometry.

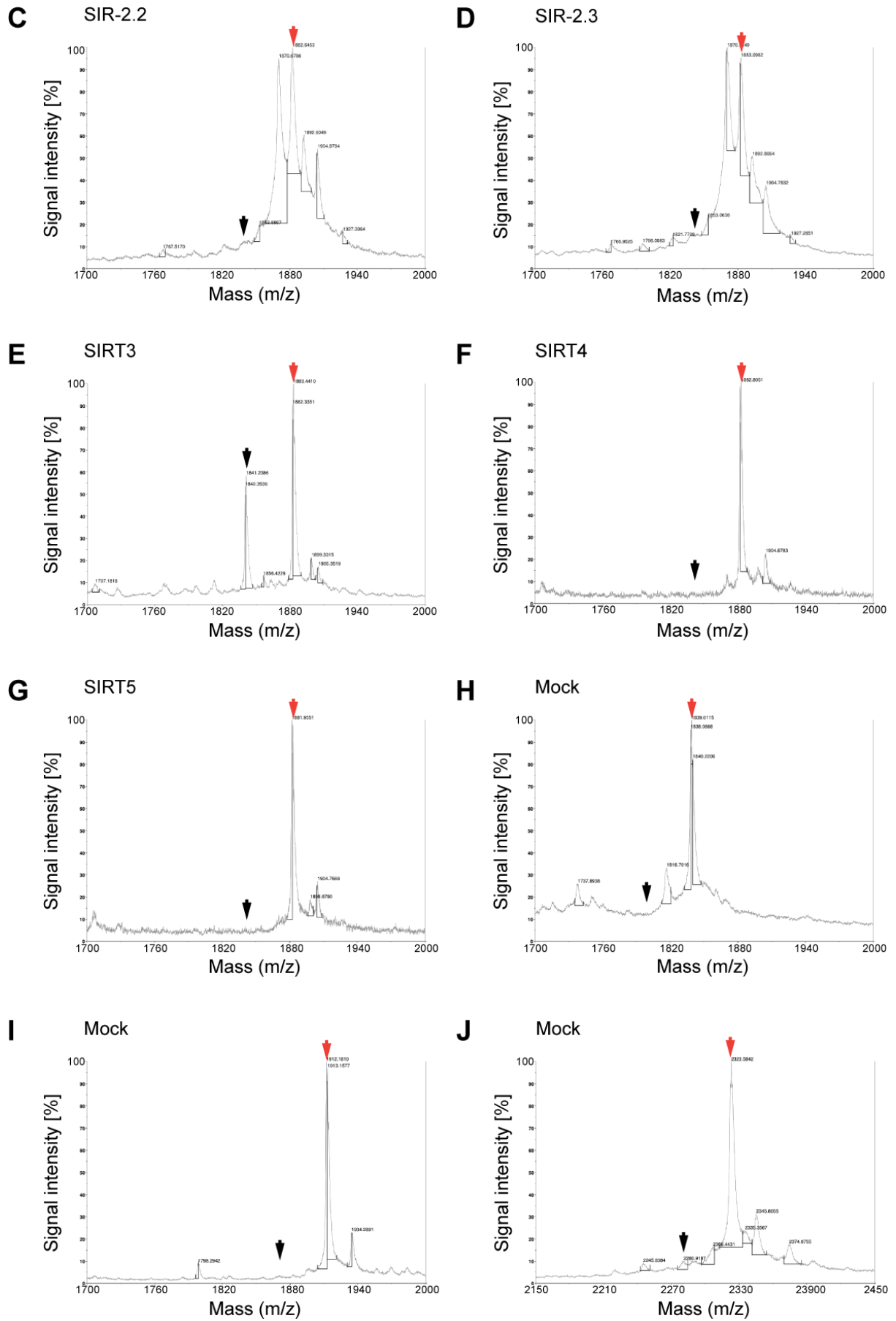
peptide	SIRT3	SIRT4	SIRT5	SIR-2.1	SIR-2.2	SIR-2.3
MPIG-47 (K273ac)	+	-	-	+	-	-
MPIG-48 (K741ac)	+	-	-	+	-	-
H4K16ac	+	-	-	+	-	-
H3K9ac	+	-	-	+	-	-

(+ indicates activity, - no activity)

Figure 3-21: Mass spectrometric analysis of *in vitro* deacetylase reactions using acetylated peptides.

Myc-tagged human SIRT3, SIRT4 and SIRT5 as well as FLAG-tagged *C. elegans* SIR-2.1, SIR-2.2, and SIR-2.3 were expressed in HEK293T cells, immunoprecipitated and immediately subjected to *in vitro* deacetylase activity assays using different acetylated peptides as substrate. For negative control (Mock) peptides were incubated in deacetylase reaction buffer without immunoprecipitated protein. NAD⁺-dependent deacetylation of the peptides was determined by mass spectrometry (MS). **A. to G.** Representative MS spectra of MPIG-47 (K273ac) peptide after deacetylase (DAC) reaction using: Mock (**A**), SIR-2.1 (**B**), SIR-2.2 (**C**), SIR-2.3 (**D**), SIRT3 (**E**), SIRT4 (**F**) and SIRT5 (**G**). **H. to J.** Representative MS spectra of MPIG-48 (K741ac) (**H**), H4K16ac (**I**) and H3K9ac (**J**) peptides after control DAC reactions. Red arrow: mass peak corresponding to the acetylated peptide; black arrow: mass peak corresponding to the deacetylated peptide; for details on aa sequence of substrate peptides see **Table 2-7** in section 2.1.7.



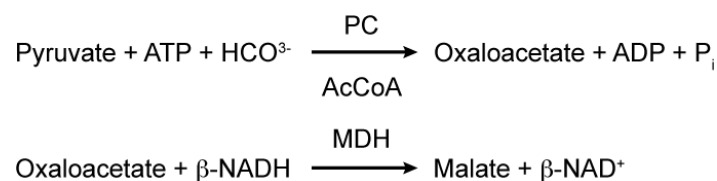


These results show that both SIR-2.1 and SIRT3 are protein deacetylases with low substrate specificity on different acetylated peptides. I did not observe deacetylase activity of SIR-2.2, SIR-2.3 and SIRT4, suggesting that acetylated K273 and K741 are not substrates of them.

3.4.3 Analysis of bovine PC activity after deacetylase reaction with *C. elegans* sirtuins

Since next to K273ac and K741ac six additional acetylated lysine residues were identified in bovine PC by mass spectrometry (Figure 3-17 A), I tested in parallel to the peptide deacetylase activity assays, whether *C. elegans* SIR-2.2, SIR-2.3 or human SIRT4 can modulate the enzymatic activity of bovine PC.

A



B

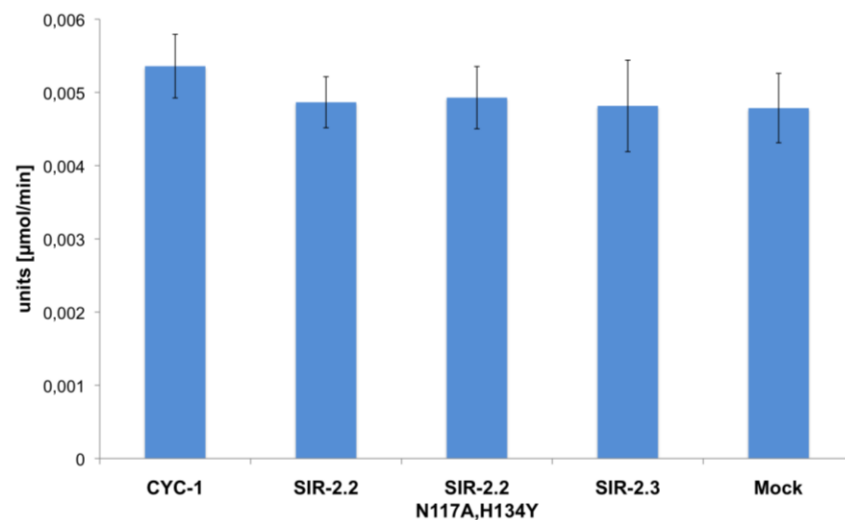


Figure 3-22: No changes in bovine PC activity after treatment with *C. elegans* SIR-2.2 and SIR-2.3.

A. Principle of the spectrophotometric assay used to assay the enzymatic activity of PC. The carboxylation of pyruvate by PC is coupled to the conversion of oxaloacetate to malate by malate dehydrogenase and recorded by measuring the decrease in NADH absorbance at 340 nm. **B.** FLAG-tagged *C. elegans* proteins were expressed in HEK293T cells and immunoprecipitated proteins bound to beads were immediately used for an *in vitro* deacetylase activity assay using bovine PC as substrate. Subsequently, the supernatants of the deacetylase reactions were analyzed for PC activity. The enzymatic activity of PC was calculated from measured reaction velocities. Mean activities were determined from four measurements of two independent immunoprecipitation experiments; error bars represent the standard deviation.

A spectrophotometric assay was used to assay the enzymatic activity of PC after incubation with mitochondrial sirtuins. FLAG-tagged *C. elegans* and Myc-tagged human proteins were expressed in HEK293T cells and immunoprecipitated. The proteins bound to beads were immediately used for an *in vitro* deacetylase activity assay using bovine PC as substrate. The supernatants of the deacetylase reactions were analyzed for PC activity using a malate dehydrogenase coupled system. The conversion of pyruvate to oxaloacetate (by PC) and finally to malate (by malate dehydrogenase) was measured by recording the decrease in absorbance at 340 nm due to oxidation of NADH (Figure 3-22 A). The enzymatic activity of PC was then determined from measured reaction velocities.

No changes in bovine PC activity were observed after incubation with SIR-2.2 and SIR-2.3 (Figure 3-22 B). PC deacetylation reactions using CYC-1 (*C. elegans* cytochrome c), SIR-2.2-N117A/H134Y carrying point mutations in residues essential for the catalytic activity of sirtuins as well as beads incubated with protein lysate of non-transfected cells (Mock) served as negative control. Treatment of bovine PC with human SIRT4 and SIRT3 (data not shown) also did not lead to changes in activity.

I could not detect reliable acetylation of bovine PC with anti-acetyllysine antibodies, and therefore I could not use Western blot analyses to investigate changes in acetylation levels of bovine PC after treatment with sirtuins. Thus, it is possible that I did not observe changes in activity because of lack of deacetylase activity. However, it is also possible that the acetylation sites, which were present in commercial bovine PC, did not have a regulatory function and affected the catalytic activity of PC.

3.4.4 Reduced acetylation levels of MCCC1 and PCCA in cells overexpressing SIRT4

It is possible that I did not observe protein deacetylase activity for mammalian SIRT4 (as well as *C. elegans* SIR-2.2 and SIR-2.3) because of non-optimal reaction conditions (e.g. buffer conditions, missing co-factor/s) present in the *in vitro* deacetylase activity assays.

Since mitochondrial biotin carboxylases, expressed in HEK293T cells, were lysine acetylated (Figure 3-18), I decided to test in collaboration with the laboratory of Prof. Eric Verdin (Gladstone Institute, San Francisco, USA) whether SIRT4 can deacetylate these proteins *in vivo*. Expression vectors encoding FLAG-tagged murine PCCA or MCCC1 were co-transfected with expression vectors for human Myc-tagged SIRT3, SIRT4, or SIRT5 into HEK293T cells. For negative control cells were co-transfected with an empty vector. FLAG-tagged PCCA and MCCC1 were immunoprecipitated with FLAG-M2 beads and acetylation levels were measured by Western blotting with anti-acetyllysine antibodies.

The acetylation levels of both mPCCA (Figure 3-23 A) and mMCCC1 (Figure 3-23 B) were specifically reduced in cells overexpressing SIRT4, but not SIRT3 or SIRT5. It remains to be tested, whether SIRT4 is also able to deacetylate mPC.

These results indicate for the first time that SIRT4 might indeed be a NAD⁺-dependent protein deacetylase that specifically deacetylates PCCA and MCCC1.

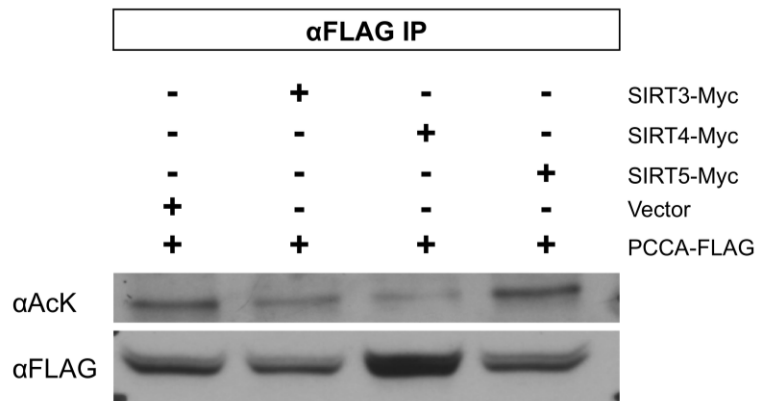
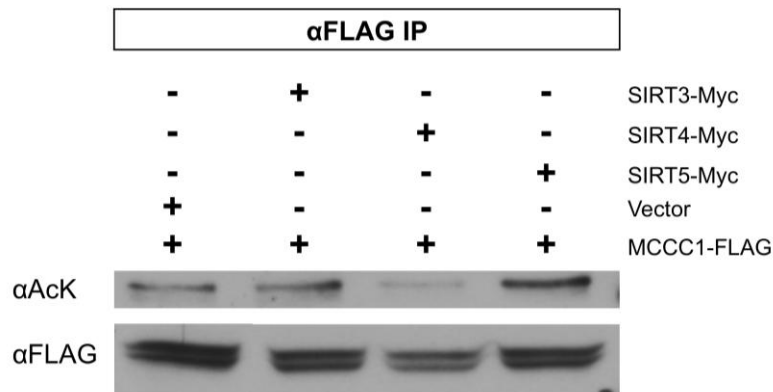
A**B**

Figure 3-23: Overexpression of SIRT4 specifically reduces the acetylation levels of PCCA and MCCC1 *in vivo*.

FLAG-tagged murine PCCA or MCCC1 were expressed together with human Myc-tagged SIRT3, SIRT4, or SIRT5 in HEK293T cells. For negative control the cells were co-transfected with an empty vector (carrying a Myc-tag). FLAG-tagged PCCA and MCCC1 were immunoprecipitated with FLAG-M2 beads and analyzed by Western blotting with anti-acetyllysine (α AcK) and anti-FLAG antibodies. **A.** and **B.** Western blot analyses of immunoprecipitated PCCA::FLAG (**A**) and MCCC1::FLAG (**B**) using anti-acetyllysine and anti-FLAG antibodies are shown. Doublet bands of PCCA::FLAG and MCCC1::FLAG in anti-FLAG Western blots correspond to full-length protein (upper band) and protein, which was proteolytically processed after mitochondrial import (lower band).

4 Discussion

4.1 SIR-2.2 and SIR-2.3 are mitochondrial proteins strongly expressed in tissue with high metabolic demand

SIR-2 proteins are a highly conserved protein family and play an important role in chromatin regulation, metabolism and aging in eukaryotes [1]. The nematode *C. elegans* possesses four different SIR-2 variants with high sequence conservation to mammalian sirtuins. Whereas the great majority of studies have focused on SIR-2.1, the other three variants remained virtually uncharacterized so far. SIR-2.2 and SIR-2.3 are most homologous to mammalian SIRT4 (49% and 42% identity), suggesting that they might also localize to mitochondria. However, in a genome wide RNAi screen SIR-2.2 was identified to be required for genome stability, next to many chromatin, DNA repair and cell cycle factors. Since these proteins are nuclear and/or cytoplasmic, SIR-2.2 might not be targeted to mitochondria and might not share conserved functions with mammalian SIRT4.

In this study I investigated for the first time the expression and localization pattern of SIR-2.2 and SIR-2.3 by generating translational *sir-2::gfp*-reporter strains, expressing SIR-2.2 and SIR-2.3 under control of the endogenous promoters. Electron microscopic analysis as well as cellular subfractionation showed that both SIR-2.2 and SIR-2.3 are targeted to mitochondria. SIR-2.2 and SIR-2.3 are highly expressed in the pharynx, body wall muscles, neurons, and intestine, which are all tissues with high energy demand. Interestingly, mammalian SIRT4 also shows higher expression levels in the major metabolic tissues including heart, liver, kidney, pancreatic β -cells, brain and skeletal muscle.

The *C. elegans* pharynx is analogous to the vertebrate heart, since both are tubular organs pumping continuously to keep the organism alive [206]. The intestine of *C. elegans* is a multifunctional organ, that not only has an enormous digestive power and is important for defecation, but is also the major organ for synthesis, storage (gut granules containing lipids, carbohydrates, and protein) and metabolism of nutrients, nurturing germ cells (particularly with produced yolk) and other tissues [207]. In mammals distinct organs including intestine, kidney, liver and adipose tissue carry out these miscellaneous functions. Insulin secretion in *C. elegans* is not executed by a specific cell type like pancreatic β -cells in mammals, but both neuronal cells as well as intestinal cells were shown to secrete insulin-like proteins [208]. *C. elegans* body wall muscles are, like mammalian skeletal muscles, striated muscle tissue important for locomotion and therefore rich in mitochondria [209].

Due to this conserved subcellular localization to mitochondria as well as the high expression in functionally equivalent tissues with high energy demand, *C. elegans* SIR-2.2 and SIR-2.3 and mammalian SIRT4 seem to have conserved functions. Therefore, analysis of SIR-2.2 and SIR-2.3 function in *C. elegans* is likely to provide insights into sirtuin function in mammals.

4.2 Is there genetic redundancy between SIR-2.2 and SIR-2.3 in *C. elegans*?

SIR-2.2 and SIR-2.3 share high sequence similarity (75.3% identity) and are located next to each other on chromosome X, suggesting that one gene might have evolved from the other by sequence duplication and that there might be genetic redundancy between *sir-2.2* and *sir-2.3*. In *C. elegans* gene duplications seem to occur with a rate of ~ 0.02 duplications per gene per million years more frequently than in *Drosophila* (~ 0.002) and yeast (~ 0.008) [210]. In the case of sirtuins *C. elegans* possesses two genes, SIR-2.2 and SIR-2.3, whereas the *D. melanogaster* genome encodes only one gene most homologous to mammalian SIRT4 [3]. Gene duplications are an evolutionarily important source for new gene functions and expression patterns. As fully functional redundant genes should not be evolutionarily stable and are not protected against deleterious mutations, duplicated genes have three possible fates during evolution: firstly, nonfunctionalization and silencing of one copy; secondly, neofunctionalization, where one copy obtains novel, beneficial functions; thirdly, subfunctionalization, where both copies become partially compromised and are necessary for the overall function provided by the single ancestral gene [210, 211].

RT-PCR experiments (Figure 3-6 B) show that both *sir-2.2* and *sir-2.3* are expressed in *C. elegans*. In case of the *sir-2.2* gene, I also know from Western blot analysis with the anti-SIR-2.2-specific antibodies (Figure 3-7 C) that protein is made. In addition, a multiple sequence alignment of *C. elegans* sirtuins with yeast and mammalian sirtuins (Figure 3-19 C) shows that residues important for the enzymatic activity are also highly conserved in both SIR-2.2 and SIR-2.3. Although I currently do not have experimental proof of enzymatic activity of SIR-2.2 and SIR-2.3, this high degree of sequence conservation and lack of detrimental mutations in important amino acid residues suggests, that both proteins most probably retained their catalytic activity. Therefore, I exclude that *sir-2.2* or *sir-2.3* became nonfunctionalized during evolution.

A variation of neofunctionalization is that both genes acquired divergent functions but still retained overlapping functions. The genes would be then maintained by selection due to their independent functions [212].

This model is supported by the observed expression patterns of SIR-2.2 and SIR-2.3. Analysis of double transgenic *sir-2.2::gfp*;*sir-2.3::mcherry* worms shows that both proteins are co-expressed in the pharynx, body wall muscle cells, neurons and intestine. However, SIR-2.3 also shows distinct prominent expression in undefined cells in the head as well as in the somatic gonad, which is not observed for SIR-2.2. Moreover, SIR-2.3 expression starts earlier in embryogenesis approximately at the 100 cell stage, whereas the first SIR-2.2 expression is observed in the three fold-stage.

Both, SIR-2.2 and SIR-2.3, seem to function in oxidative stress responses. Since knock down of either variant in a *sir-2.2(tm2648)* or *sir-2.3(ok444)* mutant background does not significantly enhance the phenotype, they do not seem to be functionally redundant and might act on different factors. SIR-2.2 and SIR-2.3 therefore might have divergent functions in mediating oxidative stress resistance. However, it might be also possible that both proteins became subfunctionalized. This would mean that the function of both, SIR-2.2 and SIR-2.3, is

needed to mediate resistance to stress. Then loss of one gene can already result in reduced stress tolerance, and this will not be further enhanced by disrupting the other gene.

SIR-2.2 and SIR-2.3 are both interacting with mitochondrial biotin carboxylases. Currently, I do not know whether either one or both proteins are able to modulate the enzymatic activity of these biotin carboxylases *in vivo*. At present the data are not sufficient to clearly define whether there is functional redundancy between SIR-2.2 and SIR-2.3, or whether both genes are required to regulate the enzymatic activities of mitochondrial biotin carboxylases.

Knock down of *sir-2.2* by RNAi was shown to augment huntingtin polyglutamine toxicity whereas *sir-2.3* RNAi did not have any effect [127]. In addition, only *sir-2.2* but not *sir-2.3* was identified in a genome wide RNAi screen to contribute to genome stability [129], demonstrating independent functions of *sir-2.2*.

No SIR-2.3-specific functions have been reported so far. However, e.g. the prominent expression of SIR-2.3::GFP in unidentified cells located between the two pharyngeal bulbs, indicates a distinct function of SIR-2.3. DiI staining alone has not been sufficient to determine the identity of these cells (Figure 3-3 B and C). (This will require more detailed analyses of all head neurons with Nomarski optics including comprehensive mapping of relative positions of neurons to DiI-filled neurons and neurons that express cell-specific transgenes.). DiI-filling labels specifically amphid, inner labial and phasmid neurons, which are chemosensory neurons, but represent only a subset of the *C. elegans* sensory nervous system. *C. elegans* hermaphrodites possess 60 ciliated neurons and also several non-ciliated neurons to perceive environmental cues, such as food stimuli, oxygen levels, pH, ambient osmolarity, temperature, light, and mechanical stimuli [197]. Both SIR-2.3 (Figure 3-3) and SIR-2.2 (data not shown) are expressed in amphid, inner labial and phasmid neurons, suggesting that both might function in chemosensation. The cells with prominent SIR-2.3::GFP expression might be sensory neurons as well, and SIR-2.3 might play a role in sensing a specific environmental cue.

Interestingly, genes involved in regulating responses to environmental stress and pathogens seem to be most prone to gene duplications in organisms that are confronted with challenging and dynamic environments [213]. This further supports the idea that sirtuins have a key function in adapting cells and tissues to changes in the environment.

In *C. elegans* mitochondrial SIR-2.2 and SIR-2.3 might be important regulators of various stress responses and in my opinion *sir-2.2* and *sir-2.3* have thereby overlapping but not completely redundant functions.

4.3 SIR-2.2 and SIR-2.3 mediate resistance to oxidative stress

Under normal growth conditions *sir-2.2(tm2648)*, *sir-2.2(tm2673)* and *sir-2.3(ok444)* deletion mutant worms do not show any obvious phenotype. To test whether there is functional redundancy, I also have knocked down *sir-2.2* in *sir-2.3(ok444)* mutant worms by RNAi (microinjection and feeding), but do not observe any obvious phenotype. Knockout mice of the mitochondrial sirtuins SIRT3, SIRT4 and SIRT5 are also viable and fertile, develop and grow normally under standard physiological conditions [25, 92, 114]. However, the functions

of SIRT3, SIRT4 and SIRT5 are important during stress [50]. Because of the mitochondrial localization of SIR-2.2 and SIR-2.3, I have tested whether they play a role during oxidative stress. Both *sir-2.2(tm2648)* and *sir-2.3(ok444)* mutant worms are more sensitive to oxidative stress than wild type worms, indicating that SIR-2.2 and SIR-2.3 regulate responses to oxidative stress. Knock down of *sir-2.2* or *sir-2.3* by RNAi in *sir-2.3(ok444)* and *sir-2.2(tm2648)* mutant worms, respectively, does not cause a significant decrease in survival. This suggests that the genes are not functionally redundant or that both genes need to be functional to mediate resistance to oxidative stress. Overexpression of both SIR-2.2 and SIR-2.3, as it occurs in the corresponding *gfp* transgenic worm strains, results in even higher sensitivity to oxidative stress and does not increase stress resistance as it might be expected. Why does both overexpression and loss of SIR-2.2 and SIR-2.3 increase the sensitivity to oxidative stress?

The catalytic activity of sirtuins requires NAD^+ as cofactor. Currently, I do not know whether GFP-tagged SIR-2.2 and SIR-2.3 are enzymatically functional. Therefore, it is possible that these proteins act as dominant negatives antagonizing the function of wild type SIR-2.2 and SIR-2.3 in mediating stress resistance.

On the other hand, it is also possible that overexpression of catalytically active SIR-2.2 and SIR-2.3, which are NAD^+ consumers, might lead to severe consumption and reduction of NAD^+ levels in mitochondria. Mitochondrial NAD^+ levels were shown to be essential for cell survival during genotoxic stress and nutrient deprivation [108]. Consistently, there is growing evidence that NAD^+ salvage pathways leading to increased cellular NAD^+ levels promote cell survival. Worms mutant for the nicotinamidase *pnc-1*, which catalyzes the first rate-limiting step of NAD^+ synthesis from NAM, are more sensitive to oxidative stress. Overexpression of *pnc-1* increases stress resistance [135].

Therefore, I think it would be interesting to test whether overexpression of *pnc-1* in *sir-2.2::gfp* and *sir-2.3::gfp* transgenic worms has opposing effects and can rescue the observed sensitivity to oxidative stress by restoring mitochondrial NAD^+ levels.

Oxidative stress might lead to an increase in mitochondrial NAD^+ levels, which activate SIR-2.2 and SIR-2.3 to trigger protective pathways. In mammals Nampt promotes increased mitochondrial NAD^+ levels and survival during stress in a SIRT3 and SIRT4 dependent manner [108]. Moreover, increased dosage of Nampt was shown to upregulate SIRT1 activity [214]. In *C. elegans* increased stress resistance of *pnc-1* overexpressing worms depends on *sir-2.1* [135], suggesting that mitochondrial *sir-2.2* and *sir-2.3* might be important as well. Thus, another intriguing question is whether the augmented oxidative stress resistance of worms overexpressing *pnc-1* depends on *sir-2.2* and *sir-2.3*.

Mass spectrometric analyses showed that 20% of mitochondrial proteins are lysine acetylated. Among these factors were proteins of the respiratory chain, antioxidant enzymes such as superoxide dismutase, heat shock proteins, and chaperones [98-100], suggesting that lysine acetylation is an important posttranslational modification in regulating stress responses. The vast majority (approximately 90%) of reactive oxygen species (ROS) is produced in mitochondria as a consequence of oxidative phosphorylation by the electron transport chain. SIRT3 was shown to deacetylate subunits of complex I and to regulate the activity of complex I [104], which notably seems to be the major source of cellular ROS together with complex

III [199]. Moreover, SIRT3 was reported to suppress ROS formation in cardiomyocytes [215], C₂C₁₂ myotubes [216] and brown adipocytes [97]. Recently SIRT3-deficient mouse embryonic fibroblasts (MEFs) were shown to exhibit increased stress-induced ROS levels and genomic instability, contributing partly to a tumor-permissive phenotype [109]. These studies implicate a key role for mitochondrial sirtuins, particularly SIRT3, in regulating oxidative stress responses. Since SIR-2.2 and SIR-2.3 also function during oxidative stress, the role of mitochondrial sirtuins in coordinating stress responses seems to be conserved from *C. elegans* to human.

Interestingly, *sir-2.2* was identified as a factor promoting genome stability [129]. There is growing evidence that mitochondrial dysfunction, caused by oxidative damage of mtDNA, proteins and lipids, leads to nuclear genomic instability [217, 218]. Therefore, *sir-2.2* might protect against mutations and genome instability by maintaining mitochondrial integrity.

4.4 Evolutionary conserved interaction with mitochondrial biotin carboxylases

Much of our understanding of sirtuin biology in mammals and *C. elegans* is based on studies of nuclear SIRT1 and *sir-2.1*. Although mitochondrial sirtuins might be key regulators of metabolic pathways, few studies have investigated their function. Glutamate dehydrogenase is the only physiological substrate that was described for mammalian SIRT4 [25]. No factors regulated by *C. elegans* SIR-2.2 and SIR-2.3 have been reported in the literature so far. Thus, it was not known whether SIR-2.2 and SIR-2.3 regulate conserved pathways in *C. elegans*. Such results could also provide insights into the biological function of mammalian SIRT4.

As described in section 3.3, I have identified mitochondrial biotin carboxylases as factors specifically interacting with both SIR-2.2 and SIR-2.3 in *C. elegans*. Because of the high sequence conservation to mammalian SIRT4, I also have tested whether the interaction is conserved and specific for mammalian SIRT4. SIRT4 also associates with pyruvate carboxylase (PC), propionyl-CoA carboxylase (PCCA) and methylcrotonyl-CoA carboxylase-1 (MCCC-1) of mammals as well as of *C. elegans* (data not shown), demonstrating that it is a highly conserved interaction. The interaction with mitochondrial biotin carboxylases seems to be SIRT4-specific with exception of PCCA. SIRT3 (full-length form) as well shows strong interaction suggesting that there might be functional overlap between SIRT3 and SIRT4. It therefore has to be tested by further immunoprecipitation experiments and Western blot analyses with antibodies specific for the endogenous proteins, whether endogenous SIRT3 and SIRT4 associate with endogenous PCCA. However, preliminary results show that only overexpression of SIRT4 reduces the acetylation levels of PCCA, suggesting that PCCA is specifically regulated by SIRT4.

In this study *C. elegans* has provided a useful model system to identify novel interaction partners of mammalian SIRT4, and is therefore a well-suited model system to analyze the biological function of mitochondrial sirtuins.

4.5 Mitochondrial biotin-dependent carboxylases are acetylated proteins

Mass spectrometric analyses and a Western blot analysis with anti-acetyllysine specific antibodies (3.4.1) show that all three mitochondrial biotin-dependent carboxylases are acetylated proteins (see also [98, 99, 146]). PC and PCCA with a total of 14 and 8 acetylation sites, respectively, seem to be highly acetylated whereas only two acetylation sites have been found for MCCC1.

There is growing evidence that lysine acetylation is an important posttranslational modification in regulating metabolic enzymes and highly abundant in mitochondrial proteins. The global identification of lysine acetylation is still not complete. All published proteomic analyses used different pan-antibodies against acetyllysine, which exhibit certain sequence specificities and which in general have lower binding affinities than anti-pan-phosphorylation antibodies [98, 99, 146]. Therefore, different anti-acetyllysine pan-antibodies seem to immunoprecipitate different acetylated lysine peptides. Moreover, not all acetylation sites might have been identified so far, especially those of proteins with lower abundance. Consistently, PC has been identified as acetylated protein by all mass spectrometric screens (Figure 3-17 A in section 3.4.1), but none of the acetylation sites, which were detected using different anti-acetyllysine antibodies, overlap. Thus, MCCC1 might be as well highly acetylated, but these sites have not been identified so far. In addition there might be more unknown lysine acetylation sites present in PC and PCCA.

PC and PCCA seem to be highly acetylated, but only few of the identified acetylated lysine residues are conserved from *C. elegans* to human. Since acetylation can also occur in a non-enzymatic manner [154, 155], not all of the identified acetylation sites will probably have a regulatory function. Mapping of acetylated lysines in substrates regulated by SIRT3 also showed that not all sites were regulated by SIRT3 [106, 107]. Nevertheless, since all three proteins interact with mitochondrial sirtuins and possess acetylated lysine residues it is very likely that their enzymatic activity is regulated by reversible lysine acetylation. Interestingly, in contrast to the cytosolic biotin-dependent carboxylase, acetyl-CoA carboxylase (ACC), PC was shown to be not regulated by phosphorylation [219].

4.6 Are mammalian SIRT4 and *C. elegans* SIR-2.2 and SIR-2.3 protein deacetylases?

SIRT4 is the only mammalian sirtuin for which no protein deacetylase activity could be demonstrated. In *C. elegans* no studies reported on the enzymatic activity of SIR-2.2 and SIR-2.3 so far. This raises the question whether SIRT4 as well as *C. elegans* SIR-2.2 and SIR-2.3 are NAD⁺-dependent protein deacetylases.

A multiple sequence alignment of the catalytic core domains (Figure 3-19 C) shows that SIRT4, SIR-2.2 and SIR-2.3 share a high degree of sequence conservation in residues important for the enzymatic activity of sirtuins, suggesting that these proteins retained activity as NAD⁺-dependent deacetylases during evolution (Figure 3-19 C).

However, no enzymatic activity of *C. elegans* SIR-2.2 and SIR-2.3 has been observed when using a chemically acetylated histone H4 tail peptide as substrate (3.4.2.1). Using the same assay, other groups could not detect histone deacetylase activity for SIRT4 either, but they observed in [³²P]NAD⁺-labeling experiments that SIRT4 can ADP-ribosylate histones, BSA and GDH [25, 26]. Because of difficulties in expressing sufficient amounts of recombinant *C. elegans* SIR-2.2 and SIR-2.3, I could not test whether these proteins also possess ADP-ribosyltransferase activity in [³²P]NAD⁺-labeling experiments.

Currently, ADP-ribosylation of GDH by SIRT4, inhibiting GDH activity, is the only reported sirtuin-catalyzed ADP-ribosylation with physiological relevance [25]. Nevertheless, there are still many open questions regarding the ADP-ribosyltransferase activity of SIRT4 and other sirtuins.

ADP-ribosylation of GDH by SIRT4 was demonstrated using [³²P]NAD⁺-labeling experiments, but the specific ADP-ribosylated residue has not been mapped and the catalytic mechanism is still unknown [21]. Analysis of the NAD⁺-dependent ADP-ribosyltransferase activity of the *T. brucei* SIR2-like protein TbSIR2rp1 showed that ADP-ribosylation by TbSIR2rp1 requires an acetylated substrate, is mainly enzymatic and only to a small extent non-enzymatic [35]. The ADP-ribosyltransferase activity of TbSIR2rp1 is approximately 5 orders of magnitude lower than its deacetylase activity raising the question whether ADP-ribosylation by sirtuins has a physiological role. A recent report doubted the physiological relevance of the ADP-ribosyltransferase activity of sirtuins (including SIRT4) due to the weak efficiency compared to a bacterial ADP-ribosyltransferase and/or their own NAD⁺-dependent deacetylase activity (if detectable) [36]. The authors suggested that the ADP-ribosyltransferase activity of sirtuins is rather an inefficient side reaction.

Initially, SIRT6 was reported to exhibit auto-ADP-ribosyltransferase activity [30], but was recently shown to specifically deacetylate H3K9ac and none of the other twelve tested peptides [31]. Therefore, it is very likely that SIRT4 acts also as NAD⁺-dependent deacetylase with very strict substrate specificity.

Mitochondrial biotin carboxylases are acetylated proteins, which might be regulated by deacetylation through SIRT4, SIR-2.2 and SIR-2.3. Although the highly conserved acetylated lysine residues K273ac or K741ac (residue numbers are mapped to human and mouse PC) were promising candidates, I could not detect NAD⁺-dependent protein deacetylase activity for mammalian SIRT4 and *C. elegans* SIR-2.2 and SIR-2.3 in an *in vitro* deacetylase activity assay (3.4.2.2). K273ac and K741ac might not be substrates of SIRT4, SIR-2.2 and SIR-2.3. However, it is also possible that I have not observed protein deacetylase activity because the reaction conditions (e.g. buffer conditions, missing co-factor/s) have not been optimal in the *in vitro* deacetylase activity assays.

Western blot analysis of lysine acetylation levels show that overexpression of SIRT4 specifically reduces the acetylation levels of both MCCC1 and PCCA *in vivo* (Figure 3-23 in section 3.4.4). These results demonstrate for the first time that SIRT4 also exhibits NAD⁺-dependent deacetylase activity.

It still needs to be determined which lysine residues of mitochondrial biotin carboxylases are specifically deacetylated by SIRT4. These might be other lysine residues than K273ac and K741ac. Interaction domain mapping shows that SIRT4 interacts specifically with all three

mitochondrial biotin carboxylases via the highly conserved N-terminal biotin-carboxylation domain. The biotin carboxylation domain contains a highly conserved ATP grasp domain and catalyzes ATP driven carboxylation of biotin, the first step of the carboxylation reaction. Next to the conserved K273 are two additional highly conserved lysines (K194, K237) within the ATP grasp domain, which are important for the enzymatic activity.

Although acetylated lysine residues within the interaction domain are not necessarily substrates, it will be interesting to test whether these can be deacetylated by SIRT4 and *C. elegans* SIR-2.2 and SIR-2.3.

In my opinion mammalian SIRT4 and *C. elegans* SIR-2.2 and SIR-2.3 are NAD⁺-dependent protein deacetylases. This study provides first evidence that SIRT4 is indeed a protein deacetylase that acts on mitochondrial biotin carboxylases and that this interaction might also modulate their enzymatic activities.

4.7 Possible physiological role of interaction

The interaction of SIRT4 and *C. elegans* SIR-2.2 and SIR-2.3 with the mitochondrial biotin-dependent carboxylases suggests that these sirtuins play a central role in regulating metabolic pathways, which maintain energy homeostasis in response to nutrient deprivation.

Glucose is the primary fuel in mammalian tissues and blood glucose concentration has to be kept within a narrow range by coordinated homeostatic mechanisms [201]. Starvation promotes glucose synthesis in liver and kidney cortex by gluconeogenic pathways to maintain serum glucose levels. PC converting pyruvate to oxaloacetate catalyzes an important anaplerotic reaction for the tricarboxylic acid (TCA) cycle in liver and kidney. Fasting induces hepatic gluconeogenesis in rats and mice by upregulating PC activity [220, 221]. Insulin secreted from pancreatic β -cells tightly regulates blood glucose levels after dietary carbohydrate uptake. Interestingly, although β -cells lack gluconeogenesis, PC is highly abundant and required for glucose-stimulated insulin secretion [201, 222].

Propionyl-CoA carboxylase (PCC) also acts in anaplerosis and catalyzes the carboxylation of propionyl-CoA to methylmalonyl-CoA that feeds into the TCA cycle after conversion to succinyl-CoA. PCC has essential functions in the catabolism of branched chain amino acids (Thr, Val, Ile and Met), odd-chain length fatty acids and cholesterol [202].

Methylcrotonyl-CoA carboxylase (MCC) carboxylates 3-methylcrotonyl-CoA to 3-methylglutaconyl-CoA which is the fourth step in catabolism of the essential amino acid leucine [204]. Leucine is a strictly ketogenic amino acid as it is degraded to acetoacetate and acetyl-CoA, which is subsequently oxidized in the TCA cycle [223]. Therefore, MCC does not function in anaplerosis, but plays a role in formation of ketone bodies under starvation conditions.

All three mitochondrial biotin carboxylases play an important role during nutrient deprivation. Since PC, PCCA and MCCC1 are acetylated proteins, it is very likely that their enzymatic activity is regulated by reversible lysine acetylation.

There is growing evidence that reversible lysine acetylation of metabolic enzymes regulates the catalytic activity and/or protein stability of metabolic enzymes and allows cells to respond

to changes in nutrient availability [146, 147]. A recent study in *Salmonella enterica* showed that reversible lysine acetylation mediates adaptation to different carbon sources [147]. Key enzymes of glycolysis and gluconeogenesis are lysine acetylated and regulated by reversible lysine acetylation/deacetylation in *S. enterica*. Whereas acetylation of proteins through the acetyltransferase Pat promotes carbon flux towards glycolysis, deacetylation through the NAD⁺-dependent protein deacetylase CobB (SIR-2-like protein) stimulates gluconeogenesis. This finding is further supported by another recent study demonstrating that nearly every enzyme of the major metabolic pathways, i.e. glycolysis, gluconeogenesis, the TCA cycle, fatty acid and glycogen metabolism was acetylated in human liver tissue [146]. Moreover, this study showed that high glucose levels inhibit amino acid catabolism and gluconeogenesis by increased acetylation of representative proteins. In the presence of high glucose concentrations argininosuccinate lyase (ASL) and phosphoenolpyruvate carboxykinase (PEPCK1) are highly acetylated, decreasing their catalytic activity and protein stability, respectively. In contrast to allosteric effects that specifically modulate the catalytic activities of individual metabolic enzymes, reversible lysine acetylation seems to be a global mechanism in coordinating energy metabolism. Two molecules closely linked to energy metabolism thereby seem to facilitate energy sensing. Acetyl-CoA, used for acetylation, is abundant during high cellular energy levels and NAD⁺, required for deacetylation, increases during nutrient deprivation [108, 147].

Since deacetylation of mitochondrial biotin carboxylases by SIRT4, SIR-2.2 and SIR-2.3 might modulate their catalytic activity during nutrient deprivation, I have established conditions to assay the enzymatic activities of all three biotin carboxylases in liver lysates. Liver tissue of starved and fed SIRT4 knockout mice will be provided by our collaborator Prof. Eric Verdin. In addition, I am also going to test mitochondrial lysates of *sir-2.2*, *sir-2.3* mutant worms and *sir-2.3*, *sir-2.2RNAi* worms for changes in biotin carboxylase activity.

In collaboration with the laboratory of Prof. Eric Verdin we observe reduced acetylation levels of PCCA and MCCC1 in cells overexpressing SIRT4. Starvation is shown to enhance the enzymatic activity of PC in mouse and rat livers [224, 225] and deacetylation of PC by SIRT4 might mediate this increase in activity.

Working hypothesis I.

Based on the findings described above, I propose the following working hypothesis for the regulation of mitochondrial biotin-dependent carboxylases by mammalian SIRT4 and *C. elegans* SIR-2.2 and SIR-2.3 (Figure 4-1).

Starvation or fasting reduces cellular energy levels and leads to an increase in mitochondrial NAD⁺ levels. Elevated NAD⁺ activates mitochondrial SIRT4 or *C. elegans* SIR-2.2 and SIR-2.3, which deacetylate mitochondrial biotin-dependent carboxylases. Deacetylation of PC, PCC and MCC increases their catalytic activities and upregulates gluconeogenesis, amino acid catabolism and fatty acid oxidation. Increased glucose and ketone body formation provides energy fuels for other tissues and promotes cell survival. In mammals this mechanism would take place in the liver and kidney cortex, in *C. elegans* probably in the intestine and muscles.

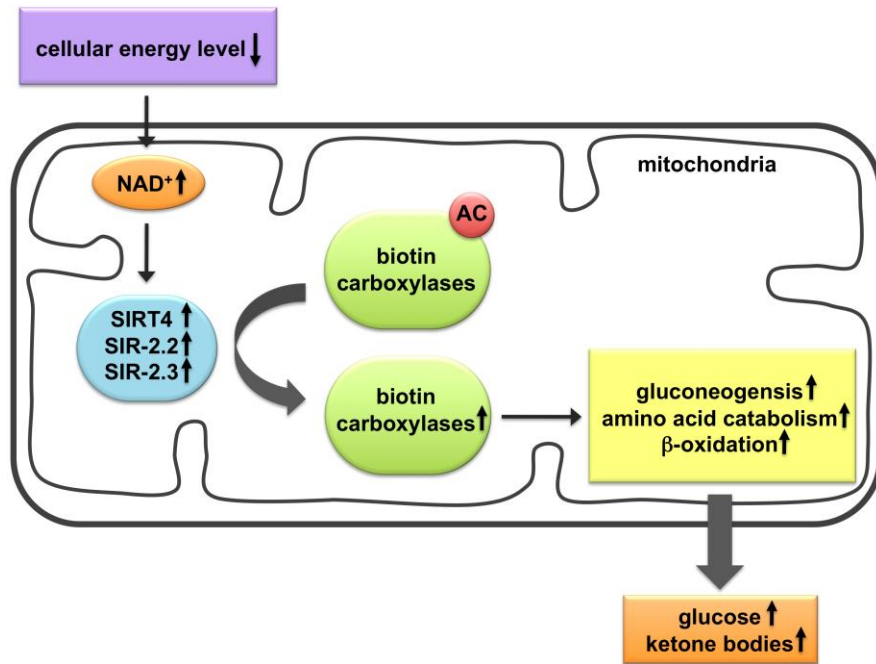


Figure 4-1: Working hypothesis I.

Deacetylation of mitochondrial biotin-dependent carboxylases by mammalian SIRT4 (in *C. elegans* SIR-2.2 and SIR-2.3) upregulates their activities and promotes gluconeogenesis and ketone body formation in liver and kidney (in *C. elegans* intestine and muscle) during nutrient deprivation. AC indicates acetylation.

Negative regulation of insulin secretion in pancreatic β -cells by SIRT4

In addition to the proposed function of SIRT4 in the liver, SIRT4 also seems to play an important role in the pancreas. This role is discussed in the following and will lead to a second working hypothesis, that complements working hypothesis I.

In the pancreas, which functions as fuel sensor, SIRT4 is highly expressed specifically in β -cells. Interestingly, pancreatic islets isolated from SIRT4 knockout mice exhibit increased insulin secretion, which is caused by augmented GDH activity increasing ATP production. SIRT4 was shown to negatively regulate insulin secretion by ADP-ribosylating and inhibiting GDH activity [25]. GDH was also reported to be lysine acetylated [98, 99]. SIRT3 deacetylates (*in vivo* and *in vitro*) [92, 106] and activates GDH (*in vitro*) [106].

There might be functional redundancy between SIRT3 and SIRT4, and SIRT4 might as well regulate GDH by protein deacetylation. However, most interestingly, interaction of GDH with SIRT3 and SIRT4 seems to have opposing consequences in different tissues. Whereas deacetylation of GDH by SIRT3 and/or SIRT4 might increase its catalytic activity in liver promoting anaplerosis, ADP-ribosylation of GDH by SIRT4 seems to repress its enzymatic activity, inhibiting insulin secretion. Mitochondrial biotin-dependent carboxylases might be as well differentially regulated. I hypothesize that SIRT4 negatively regulates insulin secretion by having contrary effects on these enzymes in pancreatic β -cells compared to liver and kidney.

Mitochondrial metabolism plays a key role in insulin secretion stimulated by fuels (secretagogues such as glucose and amino acids). The rise of intracellular ATP produced in mitochondria leads to closure of the ATP-sensitive potassium channels and to depolarization of the plasma membrane, triggering Ca^{2+} influx and exocytosis of insulin granulae.

Mitochondria also synthesize metabolites via anaplerosis that have intra- and extramitochondrial signaling functions. Next to ATP these anaplerotic metabolites are needed to couple glucose sensing to stimulation and enhancement of insulin secretion in β -cells [205, 226, 227].

PC was shown to be necessary for glucose-induced insulin secretion [201] (Figure 4-2). Although pancreatic β -cells lack cytosolic phosphoenolpyruvate carboxykinase and are not able to carry out gluconeogenesis, PC is expressed in high levels comparable to those of the gluconeogenic organs liver and kidney cortex [227]. Approximately half of glucose-derived pyruvate is converted into oxaloacetate by PC [226, 227]. Oxaloacetate provided by PC feeds into the TCA cycle, allowing rapid oxidation of pyruvate and generation of large amounts of the reducing equivalent NADH for ATP production via oxidative phosphorylation.

PC also plays an important role in generating high levels of NADPH, a metabolic coupling factor for insulin secretion. Mitochondrial oxaloacetate generated by PC can be converted into either malate or citrate, which is then exported into the cytosol via the pyruvate/malate [222] or pyruvate/citrate shuttle [228]. Conversion of malate and citrate back to pyruvate results in production of high levels of NADPH in the cytosol. Cytosolic pyruvate then re-enters the mitochondrion and can be carboxylated again by PC. This shuttle mechanism also referred to as pyruvate cycling produces more NADPH than the pentose phosphate shunt pathway and contributes significantly to glucose-stimulated insulin secretion [222, 228]. Interestingly, the rate of pyruvate carboxylation but not pyruvate oxidation correlates with the rate of insulin release in rat pancreatic islets, suggesting that anaplerosis via PC has a critical function in supporting insulin secretion [229].

Catabolism of dietary amino acids provides another energy source for ATP and anaplerotic products. PCC is involved in the catabolism of the branched chain amino acids threonine, valine, isoleucine, and methionine, which provide the anaplerotic intermediate succinyl-CoA. Succinate metabolism was shown to have an important function in insulin secretion, since methylesters of succinate, which are converted to succinate in β -cells, are as potent in stimulating insulin release as glucose. Since succinyl-CoA is thereby a key intermediate and source for the generation of the metabolic coupling factors GTP, mevalonate as well as NADPH [230, 231], the anaplerotic function of PCC seems to be also important for insulin secretion in response to amino acids.

The amino acid leucine is another potent insulin secretagogue (one third as potent as glucose) [232]. Next to allosterically activating GDH and enhancing the conversion of glutamate to α -ketoglutarate, leucine can be metabolized to α -ketoisocaproic acid (KIC), the first intermediate in leucine catabolism, and finally to acetyl-CoA and acetoacetate. Interestingly, KIC stimulates insulin secretion more potently than leucine (as potent as glucose), which in part seems to be caused by providing faster acetoacetate and acetyl-CoA. Therefore, leucine catabolism, generating acetoacetate and Acetyl-CoA, and MCC, catalyzing the fourth step in this pathway, seem to contribute to leucine-stimulated insulin release.

SIRT4 was shown to negatively regulate both glucose and amino acid stimulated insulin secretion [25, 26] and this might be mediated by modulating the enzymatic activities of PC, PCC and MCC.

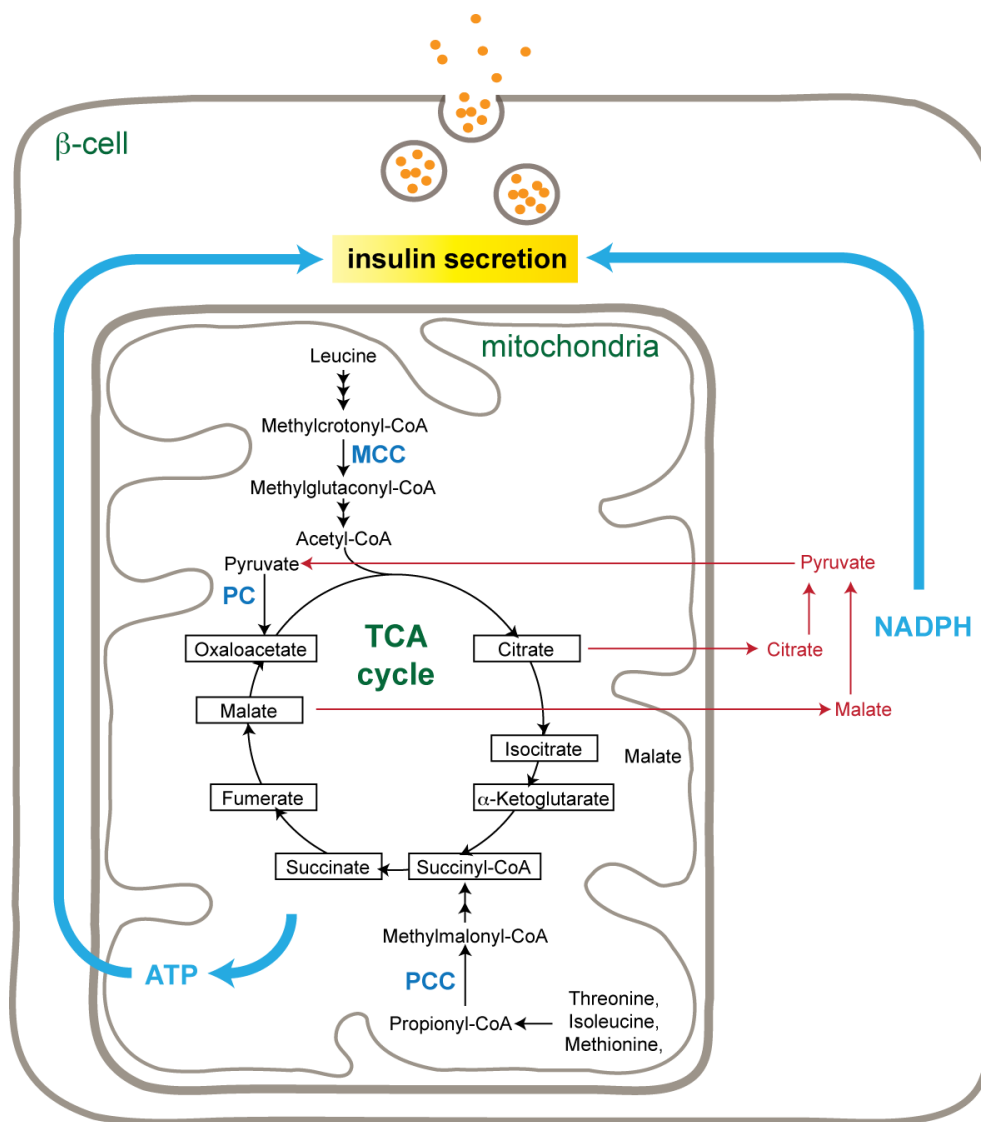


Figure 4-2: Role of mitochondrial biotin carboxylases in insulin secretion.

Pyruvate carboxylase (PC), propionyl-CoA carboxylase (PCC) and methylcrotonyl-CoA (MCC) carboxylase catalyze anaplerotic and catabolic reactions involved in insulin secretion. ATP and NADPH (shown in blue) are important coupling factors for triggering insulin release. Large amounts of ATP are produced via the TCA cycle and oxidative phosphorylation. The pyruvate/malate and pyruvate/citrate shuttle generate high levels of NADPH and are shown in red.

Working hypothesis II.

In my proposed model (Figure 4-3) absence of dietary glucose and amino acids results in increasing mitochondrial NAD^+ levels. These activate SIRT4, which subsequently inhibits mitochondrial biotin-dependent carboxylases and GDH in pancreatic β -cells. ADP-ribosylation of GDH by SIRT4 was shown to inhibit its activity [25]. In the case of mitochondrial biotin carboxylases it has to be determined whether acetylation or ADP-ribosylation downregulates their activities. It is possible that SIRT4 mediates this contrary effect on the catalytic activities of these enzymes in pancreatic β -cells and liver/kidney, by interacting with different accessory proteins or metabolites that modulate sirtuin activity. Inhibition of PC, PCC, MCC contributes together with inhibition of GDH to a decrease in ATP synthesis, anaplerosis and leucine catabolism, downregulating insulin secretion.

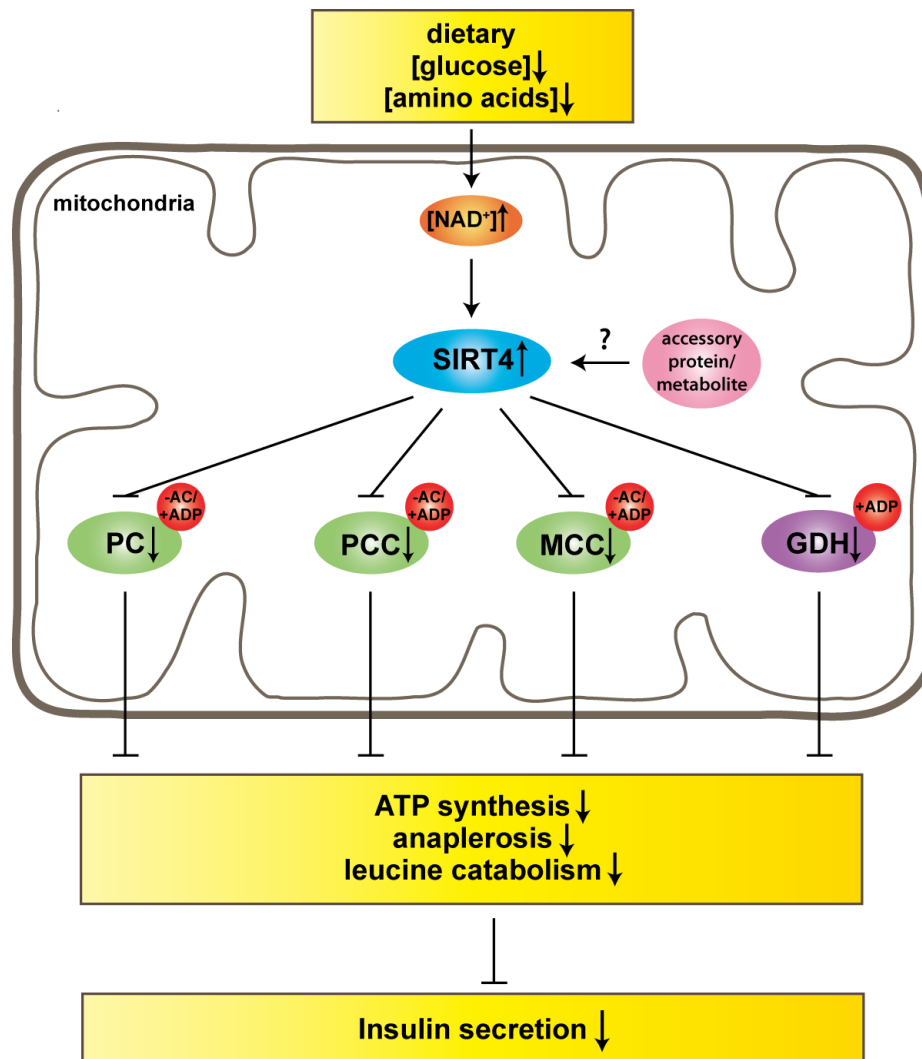


Figure 4-3: Working hypothesis II.

SIRT4 negatively regulates insulin secretion by inhibiting the catalytic activities of mitochondrial biotin-dependent carboxylases, thereby downregulating ATP synthesis, anaplerosis, leucine catabolism and consequently insulin release. Red dots indicate deacetylation (-Ac) or ADP-ribosylation (+ADP).

A gain of function mutation in GDH, rendering the protein hyperactive, causes hyperinsulinism and hyperammonemia [233]. In humans PC activity and expression was shown to be lower in individuals with type 2 diabetes [234]. Dysregulation of leucine-metabolic-induced insulin secretion also has been linked to progression of β -cell dysfunction and development of type 2 diabetes [235]. Therefore, SIRT4 interacting with biotin-dependent carboxylases and GDH might as well play a role in the pathogenesis of diabetes. SIRT4 is not the only sirtuin that has been linked to insulin secretion. Mice overexpressing SIRT1 specifically in pancreatic β -cells (BESTO) exhibit increased glucose-stimulated insulin release and improved glucose tolerance [67, 236]. Intriguingly, decreased insulin secretion in aging BESTO mice was accompanied by declined NAD^+ biosynthesis, suggesting that NAD^+ is a central molecule in modulating sirtuin activity and insulin release in pancreatic β -cells [67, 236].

SIRT1 and SIRT4 seem to have opposing effects on insulin secretion. β -cell insulin secretion involving nutrient signaling is complex and needs to be tightly regulated under a broad range of food availability [19, 25]. SIRT1 and SIRT4 might therefore function during different conditions of food limitation, such as acute starvation and chronic nutrient deprivation.

Moreover, for efficient insulin release β -cells need to synchronize mitochondrial metabolism, including ATP synthesis and anaplerosis, with cytoplasmic pathways, such as glycolysis and plasma membrane activity. Reversible protein lysine acetylation might be a potential regulatory mechanism to globally coordinate pathways that contribute to insulin release. Thereby, a potential interplay between mitochondrial SIRT4 (acting directly on metabolic enzymes) and SIRT1 (modulating transcriptional levels of metabolic enzymes) might coordinate mitochondrial metabolism with transcription and protein expression in the nucleus.

5 Summary and Conclusion

Sirtuins are highly conserved NAD⁺-dependent protein deacetylases involved in many cellular processes including genome stability, cell survival, stress responses, metabolism, and aging. Three sirtuins, SIRT3, SIRT4 and SIRT5, of the seven mammalian sirtuins are located in mitochondria and are emerging to be important energy sensors and regulators of mitochondrial metabolism.

We are just beginning to understand the role of mitochondrial SIRT4 in regulating energy metabolism. The nematode *C. elegans* possesses two genes, *sir-2.2* and *sir-2.3*, which are homologous to SIRT4, but there are no homologous genes to SIRT3 and SIRT5. In this study I have shown that both SIR-2.2 and SIR-2.3 localize to mitochondria and are highly expressed in tissues with high energy demand, suggesting conserved functions to mammalian SIRT4. Both SIR-2.2 and SIR-2.3 seem to function in oxidative stress responses. Moreover, *C. elegans* provided a useful model system to identify the mitochondrial biotin-dependent carboxylases PC, PCC and MCC as interaction partners of SIR-2.2, SIR-2.3 and mammalian SIRT4. The fact that mitochondrial biotin carboxylases play an important role in gluconeogenesis, amino acid catabolism, β -oxidation and ketone body formation, strengthens the idea that sirtuins regulate metabolic adaptations during nutrient deprivation.

All three biotin carboxylases exhibit lysine acetylation and preliminary results indicate that PCC and MCC might be the first substrates of SIRT4, where the protein displays NAD⁺-dependent deacetylase activity. Therefore, SIRT4 might be an important regulator of the enzymatic activities of mitochondrial biotin carboxylases in pancreatic β -cells and liver. SIRT4 negatively regulates insulin secretion. Insulin inhibits gluconeogenesis in the liver and β -cell activity needs to be tightly coupled to the metabolic activity of the liver for efficient utilization of energy fuels.

Based on these considerations, I propose that SIRT4 plays an important role in coordinating β -cell activity with liver metabolism. Thereby, SIRT4's interaction with mitochondrial biotin carboxylases might couple downregulation of insulin secretion in β -cells to upregulation of gluconeogenesis and ketone body formation in the liver during nutrient deprivation.

Appendix

A.1 SIR-2.2 protein levels in *sir-2.2::gfp* and *sir-2.3(ok444)*; *sir-2.2*RNAi worms

To determine the SIR-2.2 protein levels in *sir-2.2::gfp* transgenic worms (overexpressing SIR-2.2) and in *sir-2.3(ok444)*; *sir-2.2*RNAi worms (knock down of *sir-2.2*), crude *C. elegans* lysates were analyzed by Western blotting using the anti-SIR-2.2 antibodies. The protein levels of SIR-2.3 could not be analyzed, since I do not have a SIR-2.3-specific antibody.

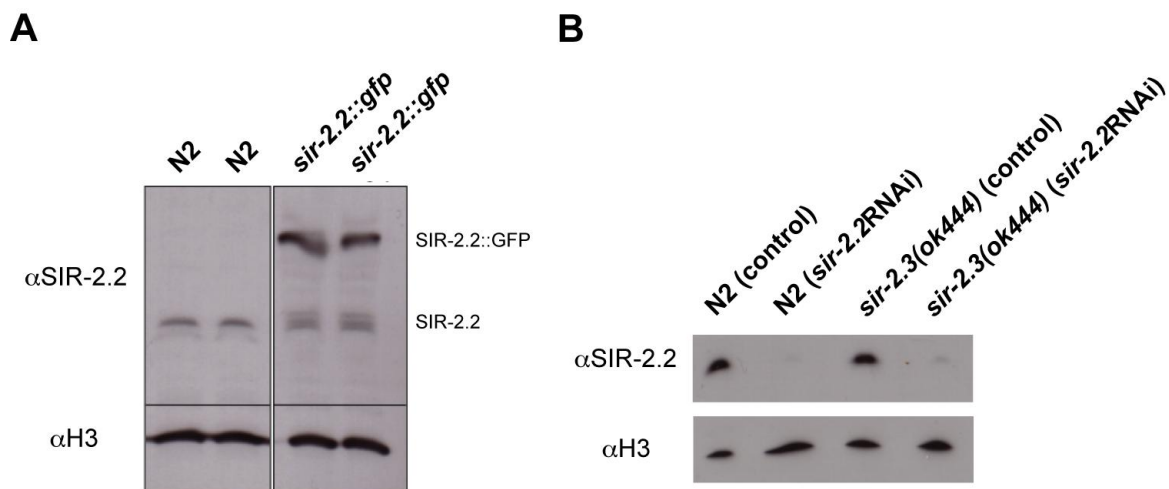


Figure A-1: Analysis of SIR-2.2 protein levels in *sir-2.2::gfp* and *sir-2.3(ok444)*; *sir-2.2*RNAi worms.

C. elegans crude lysates were separated by SDS-PAGE and analysed by Western blotting using anti-SIR-2.2 antibodies and anti-H3 antibodies (loading control). **A.** Western blot analysis of SIR-2.2 protein levels in wild type N2 and *sir-2.2::gfp* transgenic worms. Running positions of SIR-2.2 (~33 kD) and SIR-2.2::GFP (~63 kD) are indicated on the right. **B.** Western blot analysis of SIR-2.2 protein levels in wild type N2 and *sir-2.3(ok444)* mutant worms, which were grown on *sir-2.2* RNAi feeding plates or control (*E. coli* HT115(DE) containing empty L4440 vector) feeding plates.

A.2 R programming for mass spectrometry analysis

Representative program used to analyze mass spectrometric data of immunoprecipitation (IP) experiments

Open "R" (D1=IP1, D2=IP2, D3=IP3, D4=IP4)

```
> D1=read.table("/Users/mwirth/Desktop/M_Wirth_110509_L1.txt", sep="\t", header=T)
> D2=read.table("/Users/mwirth/Desktop/M_Wirth_110509_L2.txt", sep="\t", header=T)
> D3=read.table("/Users/mwirth/Desktop/M_Wirth_110509_L3.txt", sep="\t", header=T)
> D4=read.table("/Users/mwirth/Desktop/M_Wirth_110509_L4.txt", sep="\t", header=T)
> dim(D1)
> dim(D2)
> dim(D3)
> dim(D4)
> D1_D2=merge(D1,D2, by.x=1, by.y=1)
> D1_D3=merge(D1,D3, by.x=1, by.y=1)
```

```

> D1_D4=merge(D1,D4, by.x=1, by.y=1)
> dim(D1_D2)
> dim(D1_D3)
> dim(D1_D4)
> D2_unique=subset(D2,is.element(prot_acc,D1_D2$prot_acc)==FALSE)
> dim(D2_unique)
> D3_unique=subset(D3,is.element(prot_acc,D1_D3$prot_acc)==FALSE)
> dim(D3_unique)
> D4_unique=subset(D4,is.element(prot_acc,D1_D4$prot_acc)==FALSE)
> dim(D4_unique)
> D2_unique_gr80=D2_unique[D2_unique[,3]>79,]
> dim(D2_unique_gr80)
> D3_unique_gr80=D3_unique[D3_unique[,3]>79,]
> dim(D3_unique_gr80)
> D4_unique_gr80=D4_unique[D3_unique[,3]>79,]
> dim(D3_unique_gr80)
> D2gr80_D3gr80=merge(D2_unique_gr80,D3_unique_gr80, by.x=1,by.y=1)
> dim(D2gr80_D3gr80)
> D2gr80_D3gr80andD3gr80=merge(D2gr80_D3gr80,D4_unique_gr80, by.x=1,by.y=1)
> dim(D2gr80_D3gr80andD3gr80)
>write.table(D2gr80_D3gr80andD4gr80,file="/Users/mwirth/Desktop/D2_D3andD4.txt", sep="\t")

```

A.3 Mass Spectrometry results

Representative list of factors identified to interact with SIR-2.2.

(Red indicates SIR-2.2; F46G10.7a and F46G10.7b are two different splice variants of SIR-2.2; yellow marks mitochondrial biotin carboxylases)

prot_acc	prot_desc	prot_s core	pep_d ups_n umber
gi 71990482	F46G10.7a [Caenorhabditis elegans], (sir-2.2)	3822	159
gi 71990487	F46G10.7b [Caenorhabditis elegans], (sir-2.2)	3759	159
gi 17562816	PYruvate Carboxylase family member (pyc-1) [Caenorhabditis elegans]	2924	107
gi 71985184	E04F6.5a [Caenorhabditis elegans]	1660	49
gi 604515	Na,K-ATPase alpha subunit	1592	70
gi 17551436	ATP Synthase B homolog family member (asb-2) [Caenorhabditis elegans]	870	30
gi 450496	lamin [Caenorhabditis elegans]	820	34
gi 17553678	Ubiquinol-Cytochrome c oxidoReductase complex family member (ucr-1) [Caenorhabditis elegans]	795	26
gi 71994394	T22D1.4 [Caenorhabditis elegans]	729	29
gi 17536479	T24H7.1 [Caenorhabditis elegans]	654	19
gi 17561814	GEX Interacting protein family member (gei-7) [Caenorhabditis elegans]	605	24
gi 17507183	F36A2.7 [Caenorhabditis elegans]	562	27
gi 32564386	Worm AIF (apoptosis inducing factor) Homolog family member (wah-1) [Caenorhabditis elegans]	530	23
gi 1255199	sel-1 gene product	499	15
gi 17551802	B0303.3 [Caenorhabditis elegans]	490	24
gi 17555006	T12A2.2 [Caenorhabditis elegans]	471	13
gi 17553980	Tubulin, Beta family member (tbb-1) [Caenorhabditis elegans]	470	16
gi 71992778	Y105E8A.2 [Caenorhabditis elegans]	460	19
gi 1181593	elongation factor Tu homologue precursor [Caenorhabditis elegans]	452	27
gi 17557498	C02E11.1a [Caenorhabditis elegans]	450	24
gi 71982905	D2030.2a [Caenorhabditis elegans]	449	20
gi 17557316	B0250.5 [Caenorhabditis elegans]	430	13
gi 17569737	Ubiquinol-Cytochrome c oxidoReductase complex family member (ucr-2.2) [Caenorhabditis elegans]	423	17
gi 17539560	DIFferentiation abnormal family member (dif-1) [Caenorhabditis elegans]	415	19
gi 32564064	B0432.4 [Caenorhabditis elegans]	390	18
gi 17567343	Propionyl Coenzyme A Carboxylase Alpha subunit family member (pcca-1) [Caenorhabditis elegans]	384	18
gi 17569967	T22H6.2a [Caenorhabditis elegans]	377	19
gi 17535649	R53.4 [Caenorhabditis elegans]	366	17
gi 17557712	ATP synthase subunit family member (atp-5) [Caenorhabditis elegans]	362	16
gi 17554158	SERCA (Sarco-Endoplasmic Reticulum Calcium ATPase) family member (sca-1) [Caenorhabditis elegans]	358	17
gi 17570205	Ubiquinol-Cytochrome c oxidoReductase complex family member (ucr-2.1) [Caenorhabditis elegans]	339	9
gi 17534029	TuBulin, Alpha family member (tba-4) [Caenorhabditis elegans]	335	15
gi 115534052	K02F3.2 [Caenorhabditis elegans]	330	16
gi 17505833	C34B2.7 [Caenorhabditis elegans]	309	12
gi 17535181	M05D6.6 [Caenorhabditis elegans]	309	11
gi 17555336	TuBulin, Alpha family member (tba-7) [Caenorhabditis elegans]	301	13
gi 17507897	G protein,O, Alpha subunit family member (goa-1) [Caenorhabditis elegans]	297	10

gi 17536841	W10D9.5 [Caenorhabditis elegans]	296	9
gi 171994521	Y47G6A.10 [Caenorhabditis elegans]	292	11
gi 17535651	R53.5 [Caenorhabditis elegans]	283	12
gi 86563381	Y45F3A.3a [Caenorhabditis elegans]	280	9
gi 17569483	SPeCtrin family member (spc-1) [Caenorhabditis elegans]	279	16
gi 171999690	ZC410.5a [Caenorhabditis elegans]	277	10
gi 17510485	Y71F9AL.17 [Caenorhabditis elegans]	276	7
gi 25141345	F23C8.5 [Caenorhabditis elegans]	274	12
gi 71999412	Y66H1B.2a [Caenorhabditis elegans]	267	14
gi 17535117	gaLECTin family member (lec-3) [Caenorhabditis elegans]	262	13
gi 17568379	General Anaesthetic Sensitivity abnormal family member (gas-1) [Caenorhabditis elegans]	254	9
gi 3549723	calcium ATPase [Caenorhabditis elegans]	250	8
gi 17560308	fatty Acid CoA Synthetase family member (acs-2) [Caenorhabditis elegans]	239	11
gi 17556298	Y56A3A.21 [Caenorhabditis elegans]	236	8
gi 71999758	ZK550.3 [Caenorhabditis elegans]	234	15
gi 17540418	Iron-Sulfur Protein family member (isp-1) [Caenorhabditis elegans]	231	12
gi 17508157	K07G5.6 [Caenorhabditis elegans]	224	7
gi 17563944	ATP synthase subunit family member (atp-4) [Caenorhabditis elegans]	220	9
gi 71997325	ZK370.8 [Caenorhabditis elegans]	219	8
gi 72001364	DeHydrogenases, Short chain family member (dhs-24) [Caenorhabditis elegans]	218	9
gi 17536165	T09A5.11 [Caenorhabditis elegans]	217	7
gi 25146366	W02F12.5 [Caenorhabditis elegans]	216	7
gi 71983779	Disorganized Muscle family member (dim-1) [Caenorhabditis elegans]	215	6
gi 42538971	TPA: TPA_exp: ANC-1 [Caenorhabditis elegans]	204	10
gi 115534640	F07C3.2 [Caenorhabditis elegans]	203	7
gi 17556106	Y53G8AL.2 [Caenorhabditis elegans]	202	6
gi 17506651	F15D3.7 [Caenorhabditis elegans]	201	7
gi 71989417	G protein, Subunit Alpha family member (gsa-1) [Caenorhabditis elegans]	200	5
gi 25144561	NADH Ubiquinone Oxidoreductase family member (nuo-4) [Caenorhabditis elegans]	198	6
gi 482124	hypothetical protein K11H3.3 - Caenorhabditis elegans	198	10
gi 17534525	F58F12.1 [Caenorhabditis elegans]	196	6
gi 17542494	T22B11.5 [Caenorhabditis elegans]	193	8
gi 17508075	K05C4.2 [Caenorhabditis elegans]	192	7
gi 17554894	T04A8.6 [Caenorhabditis elegans]	189	6
gi 71987519	F32B6.2 [Caenorhabditis elegans] (mccc-1)	189	9
gi 17541830	HisTone variant H2AZ homolog family member (htz-1) [Caenorhabditis elegans]	188	5
gi 17508505	P-GlycoProtein related family member (pgp-2) [Caenorhabditis elegans]	187	3
gi 17555742	C.Elegans Y-box family member (cey-4) [Caenorhabditis elegans]	184	5
gi 72001668	ZK836.2 [Caenorhabditis elegans]	182	7
gi 17507937	H25P06.1 [Caenorhabditis elegans]	181	9
gi 17556552	Y76A2B.3 [Caenorhabditis elegans]	181	5
gi 17533571	F29C12.4 [Caenorhabditis elegans]	178	10
gi 17531419	C01F1.2 [Caenorhabditis elegans]	177	4
gi 17551592	F11C1.5b [Caenorhabditis elegans]	176	10
gi 17567217	F20D1.9 [Caenorhabditis elegans]	174	9
gi 17534007	F44E5.1 [Caenorhabditis elegans]	172	9
gi 17569955	T22B7.7 [Caenorhabditis elegans]	170	6
gi 17531783	steroid Alpha ReducTase family member (art-1) [Caenorhabditis elegans]	169	9
gi 17507093	Fatty Acid SyNthase family member (fasn-1) [Caenorhabditis elegans]	168	5
gi 17553312	F37C12.7 [Caenorhabditis elegans]	168	4
gi 17510401	Y65B4BL.5 [Caenorhabditis elegans]	161	8
gi 71994271	MethylMalonic Aciduria type A protein family member (mmaa-1) [Caenorhabditis elegans]	159	6
gi 17553096	DNAJ domain (prokaryotic heat shock protein) family member (dnj-10) [Caenorhabditis elegans]	158	5
gi 17543984	Y67H2A.5 [Caenorhabditis elegans]	157	8
gi 7498104	hypothetical protein D1037.4 - Caenorhabditis elegans	154	10
gi 17542998	Y17G9B.5 [Caenorhabditis elegans]	153	6
gi 17506225	C54G4.8 [Caenorhabditis elegans]	152	7
gi 17556745	Y119D3B.14 [Caenorhabditis elegans]	152	4
gi 71990971	F22B8.7 [Caenorhabditis elegans]	151	5
gi 25143253	T08G11.1a [Caenorhabditis elegans]	150	6
gi 17533397	F22B5.4 [Caenorhabditis elegans]	148	6
gi 17537937	ZK669.4 [Caenorhabditis elegans]	147	7
gi 17538400	C02B10.3 [Caenorhabditis elegans]	147	5
gi 7496641	hypothetical protein C28C12.9 - Caenorhabditis elegans	146	6
gi 5734146	beta-G spectrin [Caenorhabditis elegans]	146	5
gi 17538097	FZO (Fzo mitochondrial fusion protein) related family member (fzo-1) [Caenorhabditis elegans]	146	7
gi 17553574	Temporarily Assigned Gene name family member (tag-174) [Caenorhabditis elegans]	146	7
gi 17533517	F28A10.6 [Caenorhabditis elegans]	142	6
gi 17539680	F02H6.5 [Caenorhabditis elegans]	142	4
gi 17544682	ZK829.7 [Caenorhabditis elegans]	135	5
gi 17568881	K11G12.5 [Caenorhabditis elegans]	135	9
gi 71993767	K10C2.1 [Caenorhabditis elegans]	133	4
gi 17508985	T09B4.9 [Caenorhabditis elegans]	132	8
gi 17533543	F28C6.8 [Caenorhabditis elegans]	132	3
gi 17562026	Heat Shock Protein family member (hsp-16.1) [Caenorhabditis elegans]	131	4
gi 17557107	Temporarily Assigned Gene name family member (tag-252) [Caenorhabditis elegans]	129	4
gi 17556042	GLutaRedoXin family member (glrx-5) [Caenorhabditis elegans]	128	3
gi 17563928	T05H4.5 [Caenorhabditis elegans]	126	4
gi 133901662	NSF (N-ethylmaleimide sensitive secretion factor) homolog family member (nsf-1) [Caenorhabditis elegans]	125	3
gi 7500037	chromosome segregation protein smc1 F28B3.7 [similarity] - Caenorhabditis elegans	125	6
gi 17561272	F53C11.3 [Caenorhabditis elegans]	123	5

gi 71997968	Y54G2A.2a [Caenorhabditis elegans]	123	4
gi 17553276	ATP Synthase B homolog family member (asb-1) [Caenorhabditis elegans]	122	8
gi 32564577	T07D3.9a [Caenorhabditis elegans]	120	4
gi 32563621	NADH Ubiquinone Oxidoreductase family member (nuo-2) [Caenorhabditis elegans]	119	6
gi 17556096	Alkyl-Dihydroxyacetonephosphate Synthase family member (ads-1) [Caenorhabditis elegans]	118	4
gi 17555666	Cytochrome C Oxidase family member (cco-2) [Caenorhabditis elegans]	118	5
gi 17552648	C48B4.1 [Caenorhabditis elegans]	118	5
gi 17509233	T23H2.5 [Caenorhabditis elegans]	117	4
gi 17562364	K08D9.4 [Caenorhabditis elegans]	117	4
gi 25143064	B0205.6 [Caenorhabditis elegans]	116	6
gi 17542706	Vacuolar H ATPase family member (vha-5) [Caenorhabditis elegans]	115	6
gi 17556130	RAL (Ras-related GTPase) homolog family member (ral-1) [Caenorhabditis elegans]	114	4
gi 17562892	R04F11.2 [Caenorhabditis elegans]	112	3
gi 17550468	PeRoXisome assembly factor family member (prx-3) [Caenorhabditis elegans]	112	3
gi 17560918	F43H9.4 [Caenorhabditis elegans]	112	3
gi 17552202	C16A3.5 [Caenorhabditis elegans]	111	3
gi 71998231	Carnitine Palmitoyl Transferase family member (cpt-1) [Caenorhabditis elegans]	109	4
gi 17509681	W10C8.5 [Caenorhabditis elegans]	109	4
gi 17550124	C04C11.2 [Caenorhabditis elegans]	108	4
gi 71999501	Y69A2AR.5 [Caenorhabditis elegans]	108	3
gi 17561402	F54F3.4 [Caenorhabditis elegans]	107	3
gi 17536829	W09H1.5 [Caenorhabditis elegans]	106	5
gi 17541894	R11A8.5 [Caenorhabditis elegans]	106	4
gi 17509253	T25G3.4 [Caenorhabditis elegans]	105	6
gi 17538940	C33A12.1 [Caenorhabditis elegans]	105	5
gi 7495955	hypothetical protein C14A4.2 - Caenorhabditis elegans	104	5
gi 17510361	DNaJ domain (prokaryotic heat shock protein) family member (dnj-29) [Caenorhabditis elegans]	104	6
gi 115534188	T07E3.3 [Caenorhabditis elegans]	102	3
gi 17560096	F23H12.2 [Caenorhabditis elegans]	100	5
gi 6686276	Histone H3	100	7
gi 71983876	C41C4.10 [Caenorhabditis elegans]	100	6
gi 71998175	Y55F3AR.2 [Caenorhabditis elegans]	99	3
gi 17535241	M176.3 [Caenorhabditis elegans]	98	3
gi 17540238	F37C4.6 [Caenorhabditis elegans]	98	5
gi 17506935	Temporarily Assigned Gene name family member (tag-173) [Caenorhabditis elegans]	98	4
gi 71990294	F54B3.3 [Caenorhabditis elegans]	98	4
gi 17537053	Y38F1A.6 [Caenorhabditis elegans]	97	3
gi 7209577	kinesin like protein [Caenorhabditis elegans]	95	3
gi 71997402	T25G12.7 [Caenorhabditis elegans]	95	3
gi 17556801	Temporarily Assigned Gene name family member (tag-354) [Caenorhabditis elegans]	95	3
gi 17555956	RAB family member (rab-35) [Caenorhabditis elegans]	93	4
gi 17542570	T26C12.1 [Caenorhabditis elegans]	91	5
gi 71999402	Y66H1A.2 [Caenorhabditis elegans]	91	3
gi 17536635	Vacuolar H ATPase family member (vha-6) [Caenorhabditis elegans]	91	3
gi 17536047	T05H10.6a [Caenorhabditis elegans]	90	5
gi 17556907	UBX-containing protein in Nematode family member (ubxn-4) [Caenorhabditis elegans]	90	3
gi 71982617	Serine Palmitoyl Transferase family member (sptl-1) [Caenorhabditis elegans]	89	3
gi 72000917	TiTiN family member (ttn-1) [Caenorhabditis elegans]	89	3
gi 17564522	LiPid Depleted family member (lpd-9) [Caenorhabditis elegans]	89	4
gi 32565091	EATing: abnormal pharyngeal pumping family member (eat-3) [Caenorhabditis elegans]	88	3
gi 17554998	T10F2.2 [Caenorhabditis elegans]	88	5
gi 32565766	LLC1.3 [Caenorhabditis elegans]	86	4
gi 7507437	hypothetical protein T08B2.10 - Caenorhabditis elegans	86	4
gi 17562104	K03B4.1 [Caenorhabditis elegans]	84	3
gi 17553976	associated with RAN (nuclear import/export) function family member (ran-1) [Caenorhabditis elegans]	84	3
gi 17563798	CathePsin L family member (cpl-1) [Caenorhabditis elegans]	80	4

Representative list of factors identified to interact with SIR-2.3.

(Red indicates SIR-2.3; yellow marks mitochondrial biotin carboxylases)

prot_acc	prot_desc	prot_s core	pep_d ups_n umber
gi 17509401	UNCoordinated family member (unc-54) [Caenorhabditis elegans]	5204	86
gi 25150292	MYOsin heavy chain structural genes family member (myo-2) [Caenorhabditis elegans]	1447	22
gi 469483	CCT-1	965	24
gi 25151802	ASpartyl Protease family member (asp-1) [Caenorhabditis elegans]	895	14
gi 17562816	PYruvate Carboxylase family member (pyc-1) [Caenorhabditis elegans]	886	28
gi 14278147	Chain A, Crystal Structure Of Caenorhabditis Elegans Mg-Atp Actin Complexed With Human Gelsolin Segment 1 At 1.75 A Resolution	872	21
gi 17564182	Chaperonin Containing TCP-1 family member (cct-7) [Caenorhabditis elegans]	854	14
gi 17567771	yeast SIR related family member (sir-2.3) [Caenorhabditis elegans]	831	19
gi 17508449	LEThal family member (let-75) [Caenorhabditis elegans]	817	27
gi 71993203	PolyA Binding protein family member (pab-1) [Caenorhabditis elegans]	608	15
gi 17532603	Chaperonin Containing TCP-1 family member (cct-4) [Caenorhabditis elegans]	390	19
gi 17554158	SERCA (Sarco-Endoplasmic Reticulum Calcium ATPase) family member (sca-1) [Caenorhabditis elegans]	343	16

gi 71982858	HElicase family member (hel-1) [Caenorhabditis elegans]	318	11
gi 25144678	Chaperonin Containing TCP-1 family member (cct-6) [Caenorhabditis elegans]	305	17
gi 7496461	hypothetical protein C25A11.4a - Caenorhabditis elegans	304	10
gi 17510661	Valyl tRNA Synthetase family member (vrs-2) [Caenorhabditis elegans]	296	14
gi 71987750	human HnRNP A1 homolog family member (hrp-2) [Caenorhabditis elegans]	291	13
gi 17552356	hypothetical protein C28H8.3 [Caenorhabditis elegans]	273	13
gi 17567343	Propionyl Coenzyme A Carboxylase Alpha subunit family member (pcca-1) [Caenorhabditis elegans]	273	13
gi 25144293	hypothetical protein F35G12.2 [Caenorhabditis elegans]	271	9
gi 6744	gpd-2 gene product [Caenorhabditis elegans]	263	9
gi 212642053	Fatty Acid SynThase family member (fasn-1) [Caenorhabditis elegans]	247	7
gi 17509741	Cytokinesis, Apoptosis, RNA-associated family member (car-1) [Caenorhabditis elegans]	237	11
gi 21913108	Proteasome regulatory particle, non-atpase-like protein 2, isoform a [Caenorhabditis elegans]	231	14
gi 17509631	Temporarily Assigned Gene name family member (tag-210) [Caenorhabditis elegans]	230	7
gi 17509631	proteasome Regulatory Particle, ATPase-like family member (rpt-4) [Caenorhabditis elegans]	223	6
gi 17561814	GEX Interacting protein family member (gei-7) [Caenorhabditis elegans]	218	12
gi 17536195	hypothetical protein T10D4.3 [Caenorhabditis elegans]	211	12
gi 212656549	hypothetical protein Y48G9A.3 [Caenorhabditis elegans]	211	6
gi 32566139	MYOsin heavy chain structural genes family member (myo-3) [Caenorhabditis elegans]	211	7
gi 17555344	hypothetical protein T28D6.6 [Caenorhabditis elegans]	200	5
gi 17554638	Leucyl tRNA Synthetase family member (lrs-1) [Caenorhabditis elegans]	199	6
gi 482806	14-3-3 protein	195	6
gi 17531191	Argonaute (plant)-Like Gene family member (alg-2) [Caenorhabditis elegans]	189	8
gi 25144314	hypothetical protein F26B1.2 [Caenorhabditis elegans]	188	8
gi 17555418	UNCoordinated family member (unc-116) [Caenorhabditis elegans]	184	7
gi 17505699	hypothetical protein C25A1.4 [Caenorhabditis elegans]	182	5
gi 17544682	hypothetical protein ZK829.7 [Caenorhabditis elegans]	178	6
gi 171993870	hypothetical protein Y43F4B.5 [Caenorhabditis elegans]	177	8
gi 17535701	proteasome Regulatory Particle, Non-ATPase-like family member (rpn-9) [Caenorhabditis elegans]	171	7
gi 193211092	hypothetical protein T25C12.3 [Caenorhabditis elegans]	170	4
gi 17533087	Tudor Staphylococcal Nuclease homolog family member (tsn-1) [Caenorhabditis elegans]	168	9
gi 17554784	proteasome Regulatory Particle, ATPase-like family member (rpt-3) [Caenorhabditis elegans]	166	4
gi 17541896	Isoleucyl tRNA Synthetase family member (irs-1) [Caenorhabditis elegans]	164	8
gi 171987519	hypothetical protein F32B6.2 [Caenorhabditis elegans]	161	14
gi 17542510	RUVB (recombination protein) homolog family member (ruvb-2) [Caenorhabditis elegans]	157	8
gi 17505779	hypothetical protein C30F12.7 [Caenorhabditis elegans]	154	3
gi 17507385	Y-box family member (cey-2) [Caenorhabditis elegans]	154	3
gi 17554570	ALIX (Apoptosis-linked gene 2 interacting protein X) homolog family member (alx-1) [Caenorhabditis elegans]	154	7
gi 17554786	proteasome Regulatory Particle, ATPase-like family member (rpt-6) [Caenorhabditis elegans]	150	5
gi 17532177	hypothetical protein C30G12.2 [Caenorhabditis elegans]	149	3
gi 17507121	hypothetical protein F33D11.10 [Caenorhabditis elegans]	146	3
gi 17533517	Acyl CoA DeHydrogenase family member (acdh-9) [Caenorhabditis elegans]	144	4
gi 17563248	proteasome Regulatory Particle, ATPase-like family member (rpt-1) [Caenorhabditis elegans]	137	5
gi 193204318	PYrimidine biosynthesis family member (pyr-1) [Caenorhabditis elegans]	137	9
gi 17542008	proteasome Regulatory Particle, Non-ATPase-like family member (rpn-1) [Caenorhabditis elegans]	135	10
gi 17564550	hypothetical protein T22F3.3 [Caenorhabditis elegans]	135	6
gi 604515	Na,K-ATPase alpha subunit	131	4
gi 115532854	hypothetical protein F49C12.7 [Caenorhabditis elegans]	131	3
gi 17509919	hypothetical protein Y39G10AR.8 [Caenorhabditis elegans]	130	6
gi 171998426	Eukaryotic Initiation Factor family member (eif-3.B) [Caenorhabditis elegans]	129	5
gi 17531535	Cell Division Cycle related family member (cdc-48.1) [Caenorhabditis elegans]	123	5
gi 17541388	COP9/Signalosome and eIF3 complex shared subunit family member (cif-1) [Caenorhabditis elegans]	122	10
gi 549848	putative	122	5
gi 17558992	SKN-1 Dependent Zygotic transcript family member (sdz-8) [Caenorhabditis elegans]	118	3
gi 17508685	proteasome Regulatory Particle, Non-ATPase-like family member (rpn-8) [Caenorhabditis elegans]	118	3
gi 17506191	Importin Beta family member (imb-3) [Caenorhabditis elegans]	117	4
gi 171987092	proteasome Regulatory Particle, Non-ATPase-like family member (rpn-6) [Caenorhabditis elegans]	116	6
gi 17505955	Eukaryotic Initiation Factor family member (eif-3.H) [Caenorhabditis elegans]	112	6
gi 17508425	MAP kinase kinase or Erk Kinase family member (mek-2) [Caenorhabditis elegans]	110	3
gi 5430723	dynamin [Caenorhabditis elegans]	103	5
gi 3287963	RecName: Full=Probable coatomer subunit beta~; AltName: Full=Beta~-coat protein; Short=Beta~-COP	103	5
gi 17508687	Ribosomal Protein, Small subunit family member (rps-6) [Caenorhabditis elegans]	102	5
gi 171985061	aRginyl aa-tRNA syntheTase family member (rrt-1) [Caenorhabditis elegans]	100	5
gi 171989071	Puromycin-sensitive AMinopeptidase family member (pam-1) [Caenorhabditis elegans]	100	3
gi 32565170	hypothetical protein Y54H5A.2 [Caenorhabditis elegans]	98	5
gi 17554792	Stress Induced Protein family member (sip-1) [Caenorhabditis elegans]	95	6
gi 171982035	UDP-GALactose 4-Epimerase family member (gale-1) [Caenorhabditis elegans]	95	4
gi 17508701	proteasome Regulatory Particle, ATPase-like family member (rpt-5) [Caenorhabditis elegans]	92	5
gi 17536431	Ribosomal Protein, Large subunit family member (rpl-32) [Caenorhabditis elegans]	92	3
gi 25151863	hypothetical protein F46H5.7 [Caenorhabditis elegans]	90	3
gi 17561272	hypothetical protein F53C11.3 [Caenorhabditis elegans]	88	5
gi 17508049	eIFTwoBeta (eIF2beta translation initiation factor) family member (iftb-1) [Caenorhabditis elegans]	87	3
gi 17555742	Y-box family member (cey-4) [Caenorhabditis elegans]	86	5
gi 1181593	elongation factor Tu homologue precursor [Caenorhabditis elegans]	84	4
gi 171999412	hypothetical protein Y66H1B.2 [Caenorhabditis elegans]	84	4
gi 115533072	hypothetical protein Y67H2A.2 [Caenorhabditis elegans]	83	3
gi 7496230	hypothetical protein C17G10.8 - Caenorhabditis elegans	83	3
gi 25149807	eXPORtin (nuclear export receptor) family member (xpo-1) [Caenorhabditis elegans]	80	4

References

- [1] G. Blander, L. Guarente, The Sir2 family of protein deacetylases, *Annu Rev Biochem* 73 (2004) 417-435.
- [2] C.B. Brachmann, J.M. Sherman, S.E. Devine, E.E. Cameron, L. Pillus, J.D. Boeke, The SIR2 gene family, conserved from bacteria to humans, functions in silencing, cell cycle progression, and chromosome stability, *Genes Dev* 9 (1995) 2888-2902.
- [3] R.A. Frye, Phylogenetic classification of prokaryotic and eukaryotic Sir2-like proteins, *Biochem Biophys Res Commun* 273 (2000) 793-798.
- [4] S. Imai, C.M. Armstrong, M. Kaerberlein, L. Guarente, Transcriptional silencing and longevity protein Sir2 is an NAD-dependent histone deacetylase, *Nature* 403 (2000) 795-800.
- [5] J. Landry, A. Sutton, S.T. Tafrov, R.C. Heller, J. Stebbins, L. Pillus, R. Sternglanz, The silencing protein SIR2 and its homologs are NAD-dependent protein deacetylases, *Proc Natl Acad Sci U S A* 97 (2000) 5807-5811.
- [6] J.S. Smith, C.B. Brachmann, I. Celic, M.A. Kenna, S. Muhammad, V.J. Starai, J.L. Avalos, J.C. Escalante-Semerena, C. Grubmeyer, C. Wolberger, J.D. Boeke, A phylogenetically conserved NAD⁺-dependent protein deacetylase activity in the Sir2 protein family, *Proc Natl Acad Sci U S A* 97 (2000) 6658-6663.
- [7] K.G. Tanner, J. Landry, R. Sternglanz, J.M. Denu, Silent information regulator 2 family of NAD- dependent histone/protein deacetylases generates a unique product, 1-O-acetyl-ADP-ribose, *Proc Natl Acad Sci U S A* 97 (2000) 14178-14182.
- [8] J.C. Tanny, D. Moazed, Coupling of histone deacetylation to NAD breakdown by the yeast silencing protein Sir2: Evidence for acetyl transfer from substrate to an NAD breakdown product, *Proc Natl Acad Sci U S A* 98 (2001) 415-420.
- [9] S.M. Gasser, M.M. Cockell, The molecular biology of the SIR proteins, *Gene* 279 (2001) 1-16.
- [10] D.L. Pappas, Jr., R. Frisch, M. Weinreich, The NAD(+)-dependent Sir2p histone deacetylase is a negative regulator of chromosomal DNA replication, *Genes Dev* 18 (2004) 769-781.
- [11] Y. Tsukamoto, J. Kato, H. Ikeda, Silencing factors participate in DNA repair and recombination in *Saccharomyces cerevisiae*, *Nature* 388 (1997) 900-903.
- [12] M. Kaerberlein, M. McVey, L. Guarente, The SIR2/3/4 complex and SIR2 alone promote longevity in *Saccharomyces cerevisiae* by two different mechanisms, *Genes Dev* 13 (1999) 2570-2580.
- [13] S.J. Lin, P.A. Defossez, L. Guarente, Requirement of NAD and SIR2 for life-span extension by calorie restriction in *Saccharomyces cerevisiae*, *Science* 289 (2000) 2126-2128.
- [14] K.T. Howitz, K.J. Bitterman, H.Y. Cohen, D.W. Lamming, S. Lavu, J.G. Wood, R.E. Zipkin, P. Chung, A. Kisielewski, L.L. Zhang, B. Scherer, D.A. Sinclair, Small molecule activators of sirtuins extend *Saccharomyces cerevisiae* lifespan, *Nature* 425 (2003) 191-196.
- [15] H.A. Tissenbaum, L. Guarente, Increased dosage of a sir-2 gene extends lifespan in *Caenorhabditis elegans*, *Nature* 410 (2001) 227-230.
- [16] B. Rogina, S.L. Helfand, Sir2 mediates longevity in the fly through a pathway related to calorie restriction, *Proc Natl Acad Sci U S A* 101 (2004) 15998-16003.
- [17] S.U. Astrom, T.W. Cline, J. Rine, The *Drosophila melanogaster* sir2⁺ gene is nonessential and has only minor effects on position-effect variegation, *Genetics* 163 (2003) 931-937.
- [18] J.G. Wood, B. Rogina, S. Lavu, K. Howitz, S.L. Helfand, M. Tatar, D. Sinclair, Sirtuin activators mimic caloric restriction and delay ageing in metazoans, *Nature* 430 (2004) 686-689.
- [19] M.C. Haigis, D.A. Sinclair, Mammalian sirtuins: biological insights and disease relevance, *Annu Rev Pathol* 5 (2010) 253-295.
- [20] S. Imai, L. Guarente, Ten years of NAD-dependent SIR2 family deacetylases: implications for metabolic diseases, *Trends Pharmacol Sci* 31 (2010) 212-220.
- [21] A.A. Sauve, Sirtuin chemical mechanisms, *Biochim Biophys Acta* 1804 (2010) 1591-1603.

- [22] A.W. Tsang, J.C. Escalante-Semerena, CobB, a new member of the SIR2 family of eucaryotic regulatory proteins, is required to compensate for the lack of nicotinate mononucleotide:5,6-dimethylbenzimidazole phosphoribosyltransferase activity in cobT mutants during cobalamin biosynthesis in *Salmonella typhimurium* LT2, *J Biol Chem* 273 (1998) 31788-31794.
- [23] R.A. Frye, Characterization of five human cDNAs with homology to the yeast SIR2 gene: Sir2-like proteins (sirtuins) metabolize NAD and may have protein ADP-ribosyltransferase activity, *Biochem Biophys Res Commun* 260 (1999) 273-279.
- [24] J.C. Tanny, G.J. Dowd, J. Huang, H. Hilz, D. Moazed, An enzymatic activity in the yeast Sir2 protein that is essential for gene silencing, *Cell* 99 (1999) 735-745.
- [25] M.C. Haigis, R. Mostoslavsky, K.M. Haigis, K. Fahie, D.C. Christodoulou, A.J. Murphy, D.M. Valenzuela, G.D. Yancopoulos, M. Karow, G. Blander, C. Wolberger, T.A. Prolla, R. Weindruch, F.W. Alt, L. Guarente, SIRT4 inhibits glutamate dehydrogenase and opposes the effects of calorie restriction in pancreatic beta cells, *Cell* 126 (2006) 941-954.
- [26] N. Ahuja, B. Schwer, S. Carobbio, D. Waltregny, B.J. North, V. Castronovo, P. Maechler, E. Verdin, Regulation of insulin secretion by SIRT4, a mitochondrial ADP-ribosyltransferase, *J Biol Chem* 282 (2007) 33583-33592.
- [27] A.A. Sauve, C. Wolberger, V.L. Schramm, J.D. Boeke, The biochemistry of sirtuins, *Annu Rev Biochem* 75 (2006) 435-465.
- [28] B.C. Smith, W.C. Hallows, J.M. Denu, Mechanisms and molecular probes of sirtuins, *Chem Biol* 15 (2008) 1002-1013.
- [29] B.J. North, B.L. Marshall, M.T. Borra, J.M. Denu, E. Verdin, The human Sir2 ortholog, SIRT2, is an NAD⁺-dependent tubulin deacetylase, *Mol Cell* 11 (2003) 437-444.
- [30] G. Liszt, E. Ford, M. Kurtev, L. Guarente, Mouse Sir2 homolog SIRT6 is a nuclear ADP-ribosyltransferase, *J Biol Chem* 280 (2005) 21313-21320.
- [31] E. Michishita, R.A. McCord, E. Berber, M. Kioi, H. Padilla-Nash, M. Damian, P. Cheung, R. Kusumoto, T.L. Kawahara, J.C. Barrett, H.Y. Chang, V.A. Bohr, T. Ried, O. Gozani, K.F. Chua, SIRT6 is a histone H3 lysine 9 deacetylase that modulates telomeric chromatin, *Nature* 452 (2008) 492-496.
- [32] J.A. Garcia-Salcedo, P. Gijon, D.P. Nolan, P. Tebabi, E. Pays, A chromosomal SIR2 homologue with both histone NAD-dependent ADP-ribosyltransferase and deacetylase activities is involved in DNA repair in *Trypanosoma brucei*, *EMBO J* 22 (2003) 5851-5862.
- [33] E.L. Jacobson, D. Cervantes-Laurean, M.K. Jacobson, ADP-ribose in glycation and glyoxidation reactions, *Adv Exp Med Biol* 419 (1997) 371-379.
- [34] D. Cervantes-Laurean, D.E. Minter, E.L. Jacobson, M.K. Jacobson, Protein glycation by ADP-ribose: studies of model conjugates, *Biochemistry* 32 (1993) 1528-1534.
- [35] T.M. Kowieski, S. Lee, J.M. Denu, Acetylation-dependent ADP-ribosylation by *Trypanosoma brucei* Sir2, *J Biol Chem* 283 (2008) 5317-5326.
- [36] J. Du, H. Jiang, H. Lin, Investigating the ADP-ribosyltransferase activity of sirtuins with NAD analogues and 32P-NAD, *Biochemistry* 48 (2009) 2878-2890.
- [37] W.F. Hawse, C. Wolberger, Structure-based mechanism of ADP-ribosylation by sirtuins, *J Biol Chem* 284 (2009) 33654-33661.
- [38] K.J. Bitterman, R.M. Anderson, H.Y. Cohen, M. Latorre-Esteves, D.A. Sinclair, Inhibition of silencing and accelerated aging by nicotinamide, a putative negative regulator of yeast sir2 and human SIRT1, *J Biol Chem* 277 (2002) 45099-45107.
- [39] M.D. Jackson, M.T. Schmidt, N.J. Oppenheimer, J.M. Denu, Mechanism of nicotinamide inhibition and transglycosidation by Sir2 histone/protein deacetylases, *J Biol Chem* 278 (2003) 50985-50998.
- [40] A.A. Sauve, V.L. Schramm, Sir2 regulation by nicotinamide results from switching between base exchange and deacetylation chemistry, *Biochemistry* 42 (2003) 9249-9256.
- [41] L. Tong, J.M. Denu, Function and metabolism of sirtuin metabolite O-acetyl-ADP-ribose, *Biochim Biophys Acta* 1804 (2010) 1617-1625.
- [42] G.G. Liou, J.C. Tanny, R.G. Kruger, T. Walz, D. Moazed, Assembly of the SIR complex and its regulation by O-acetyl-ADP-ribose, a product of NAD-dependent histone deacetylation, *Cell* 121 (2005) 515-527.
- [43] G. Kustatscher, M. Hothorn, C. Pugieux, K. Scheffzek, A.G. Ladurner, Splicing regulates NAD metabolite binding to histone macroH2A, *Nat Struct Mol Biol* 12 (2005) 624-625.

- [44] B.D. Sanders, B. Jackson, R. Marmorstein, Structural basis for sirtuin function: what we know and what we don't, *Biochim Biophys Acta* 1804 (2010) 1604-1616.
- [45] M.S. Finnin, J.R. Donigian, N.P. Pavletich, Structure of the histone deacetylase SIRT2, *Nat Struct Biol* 8 (2001) 621-625.
- [46] J. Min, J. Landry, R. Sternglanz, R.M. Xu, Crystal structure of a SIR2 homolog-NAD complex, *Cell* 105 (2001) 269-279.
- [47] A. Schuetz, J. Min, T. Antoshenko, C.L. Wang, A. Allali-Hassani, A. Dong, P. Loppnau, M. Vedadi, A. Bochkarev, R. Sternglanz, A.N. Plotnikov, Structural basis of inhibition of the human NAD⁺-dependent deacetylase SIRT5 by suramin, *Structure* 15 (2007) 377-389.
- [48] K. Zhao, X. Chai, A. Clements, R. Marmorstein, Structure and autoregulation of the yeast Hst2 homolog of Sir2, *Nat Struct Biol* 10 (2003) 864-871.
- [49] K. Zhao, X. Chai, R. Marmorstein, Structure of the yeast Hst2 protein deacetylase in ternary complex with 2'-O-acetyl ADP ribose and histone peptide, *Structure* 11 (2003) 1403-1411.
- [50] J.Y. Huang, M.D. Hirschey, T. Shimazu, L. Ho, E. Verdin, Mitochondrial sirtuins, *Biochim Biophys Acta* 1804 (2010) 1645-1651.
- [51] E. Michishita, J.Y. Park, J.M. Burneskis, J.C. Barrett, I. Horikawa, Evolutionarily conserved and nonconserved cellular localizations and functions of human SIRT proteins, *Mol Biol Cell* 16 (2005) 4623-4635.
- [52] A. Vaquero, M. Scher, D. Lee, H. Erdjument-Bromage, P. Tempst, D. Reinberg, Human SirT1 interacts with histone H1 and promotes formation of facultative heterochromatin, *Mol Cell* 16 (2004) 93-105.
- [53] T. Bouras, M. Fu, A.A. Sauve, F. Wang, A.A. Quong, N.D. Perkins, R.T. Hay, W. Gu, R.G. Pestell, SIRT1 deacetylation and repression of p300 involves lysine residues 1020/1024 within the cell cycle regulatory domain 1, *J Biol Chem* 280 (2005) 10264-10276.
- [54] A. Vaquero, M. Scher, H. Erdjument-Bromage, P. Tempst, L. Serrano, D. Reinberg, SIRT1 regulates the histone methyl-transferase SUV39H1 during heterochromatin formation, *Nature* 450 (2007) 440-444.
- [55] H. Vaziri, S.K. Dessain, E. Ng Eaton, S.I. Imai, R.A. Frye, T.K. Pandita, L. Guarente, R.A. Weinberg, hSIR2(SIRT1) functions as an NAD-dependent p53 deacetylase, *Cell* 107 (2001) 149-159.
- [56] J. Luo, A.Y. Nikolaev, S. Imai, D. Chen, F. Su, A. Shiloh, L. Guarente, W. Gu, Negative control of p53 by Sir2alpha promotes cell survival under stress, *Cell* 107 (2001) 137-148.
- [57] C. Wang, L. Chen, X. Hou, Z. Li, N. Kabra, Y. Ma, S. Nemoto, T. Finkel, W. Gu, W.D. Cress, J. Chen, Interactions between E2F1 and SirT1 regulate apoptotic response to DNA damage, *Nat Cell Biol* 8 (2006) 1025-1031.
- [58] J. Nakae, Y. Cao, H. Daitoku, A. Fukamizu, W. Ogawa, Y. Yano, Y. Hayashi, The LXXLL motif of murine forkhead transcription factor FoxO1 mediates Sirt1-dependent transcriptional activity, *J Clin Invest* 116 (2006) 2473-2483.
- [59] M.C. Motta, N. Divecha, M. Lemieux, C. Kamel, D. Chen, W. Gu, Y. Bultsma, M. McBurney, L. Guarente, Mammalian SIRT1 represses forkhead transcription factors, *Cell* 116 (2004) 551-563.
- [60] A. Brunet, L.B. Sweeney, J.F. Sturgill, K.F. Chua, P.L. Greer, Y. Lin, H. Tran, S.E. Ross, R. Mostoslavsky, H.Y. Cohen, L.S. Hu, H.L. Cheng, M.P. Jedrychowski, S.P. Gygi, D.A. Sinclair, F.W. Alt, M.E. Greenberg, Stress-dependent regulation of FOXO transcription factors by the SIRT1 deacetylase, *Science* 303 (2004) 2011-2015.
- [61] A. van der Horst, L.G. Tertoolen, L.M. de Vries-Smits, R.A. Frye, R.H. Medema, B.M. Burgering, FOXO4 is acetylated upon peroxide stress and deacetylated by the longevity protein hSir2(SIRT1), *J Biol Chem* 279 (2004) 28873-28879.
- [62] F. Gao, J. Cheng, T. Shi, E.T. Yeh, Neddylation of a breast cancer-associated protein recruits a class III histone deacetylase that represses NFkappaB-dependent transcription, *Nat Cell Biol* 8 (2006) 1171-1177.
- [63] T. Takata, F. Ishikawa, Human Sir2-related protein SIRT1 associates with the bHLH repressors HES1 and HEY2 and is involved in HES1- and HEY2-mediated transcriptional repression, *Biochem Biophys Res Commun* 301 (2003) 250-257.

- [64] F. Picard, M. Kurtev, N. Chung, A. Topark-Ngarm, T. Senawong, R. Machado De Oliveira, M. Leid, M.W. McBurney, L. Guarente, Sirt1 promotes fat mobilization in white adipocytes by repressing PPAR-gamma, *Nature* 429 (2004) 771-776.
- [65] J.T. Rodgers, C. Lerin, W. Haas, S.P. Gygi, B.M. Spiegelman, P. Puigserver, Nutrient control of glucose homeostasis through a complex of PGC-1alpha and SIRT1, *Nature* 434 (2005) 113-118.
- [66] X. Li, S. Zhang, G. Blander, J.G. Tse, M. Krieger, L. Guarente, SIRT1 deacetylates and positively regulates the nuclear receptor LXR, *Mol Cell* 28 (2007) 91-106.
- [67] K.M. Ramsey, K.F. Mills, A. Satoh, S. Imai, Age-associated loss of Sirt1-mediated enhancement of glucose-stimulated insulin secretion in beta cell-specific Sirt1-overexpressing (BESTO) mice, *Aging Cell* 7 (2008) 78-88.
- [68] J.A. Baur, K.J. Pearson, N.L. Price, H.A. Jamieson, C. Lerin, A. Kalra, V.V. Prabhu, J.S. Allard, G. Lopez-Lluch, K. Lewis, P.J. Pistell, S. Poosala, K.G. Becker, O. Boss, D. Gwinn, M. Wang, S. Ramaswamy, K.W. Fishbein, R.G. Spencer, E.G. Lakatta, D. Le Couteur, R.J. Shaw, P. Navas, P. Puigserver, D.K. Ingram, R. de Cabo, D.A. Sinclair, Resveratrol improves health and survival of mice on a high-calorie diet, *Nature* 444 (2006) 337-342.
- [69] J.N. Feige, M. Lagouge, C. Canto, A. Strehle, S.M. Houten, J.C. Milne, P.D. Lambert, C. Matak, P.J. Elliott, J. Auwerx, Specific SIRT1 activation mimics low energy levels and protects against diet-induced metabolic disorders by enhancing fat oxidation, *Cell Metab* 8 (2008) 347-358.
- [70] M. Lagouge, C. Argmann, Z. Gerhart-Hines, H. Meziane, C. Lerin, F. Daussin, N. Messadeq, J. Milne, P. Lambert, P. Elliott, B. Geny, M. Laakso, P. Puigserver, J. Auwerx, Resveratrol improves mitochondrial function and protects against metabolic disease by activating SIRT1 and PGC-1alpha, *Cell* 127 (2006) 1109-1122.
- [71] J.C. Milne, P.D. Lambert, S. Schenk, D.P. Carney, J.J. Smith, D.J. Gagne, L. Jin, O. Boss, R.B. Perni, C.B. Vu, J.E. Bemis, R. Xie, J.S. Disch, P.Y. Ng, J.J. Nunes, A.V. Lynch, H. Yang, H. Galonek, K. Israelian, W. Choy, A. Iffland, S. Lavu, O. Medvedik, D.A. Sinclair, J.M. Olefsky, M.R. Jirousek, P.J. Elliott, C.H. Westphal, Small molecule activators of SIRT1 as therapeutics for the treatment of type 2 diabetes, *Nature* 450 (2007) 712-716.
- [72] Y. Yamazaki, I. Usui, Y. Kanatani, Y. Matsuya, K. Tsuneyama, S. Fujisaka, A. Bukhari, H. Suzuki, S. Senda, S. Imanishi, K. Hirata, M. Ishiki, R. Hayashi, M. Urakaze, H. Nemoto, M. Kobayashi, K. Tobe, Treatment with SRT1720, a SIRT1 Activator, Ameliorates Fatty Liver with Reduced Expression of Lipogenic Enzymes in MSG Mice, *Am J Physiol Endocrinol Metab* (2009).
- [73] B. Yang, B.M. Zwaans, M. Eckersdorff, D.B. Lombard, The sirtuin SIRT6 deacetylates H3 K56Ac in vivo to promote genomic stability, *Cell Cycle* 8 (2009) 2662-2663.
- [74] R. Mostoslavsky, K.F. Chua, D.B. Lombard, W.W. Pang, M.R. Fischer, L. Gellon, P. Liu, G. Mostoslavsky, S. Franco, M.M. Murphy, K.D. Mills, P. Patel, J.T. Hsu, A.L. Hong, E. Ford, H.L. Cheng, C. Kennedy, N. Nunez, R. Bronson, D. Frendewey, W. Auerbach, D. Valenzuela, M. Karow, M.O. Hottiger, S. Hursting, J.C. Barrett, L. Guarente, R. Mulligan, B. Demple, G.D. Yancopoulos, F.W. Alt, Genomic instability and aging-like phenotype in the absence of mammalian SIRT6, *Cell* 124 (2006) 315-329.
- [75] T.L. Kawahara, E. Michishita, A.S. Adler, M. Damian, E. Berber, M. Lin, R.A. McCord, K.C. Ongaiqui, L.D. Boxer, H.Y. Chang, K.F. Chua, SIRT6 links histone H3 lysine 9 deacetylation to NF-kappaB-dependent gene expression and organismal life span, *Cell* 136 (2009) 62-74.
- [76] O. Vakhrusheva, C. Smolka, P. Gajawada, S. Kostin, T. Boettger, T. Kubin, T. Braun, E. Bober, Sirt7 increases stress resistance of cardiomyocytes and prevents apoptosis and inflammatory cardiomyopathy in mice, *Circ Res* 102 (2008) 703-710.
- [77] E. Ford, R. Voit, G. Liszt, C. Magin, I. Grummt, L. Guarente, Mammalian Sir2 homolog SIRT7 is an activator of RNA polymerase I transcription, *Genes Dev* 20 (2006) 1075-1080.
- [78] R.R. Alcendor, L.A. Kirshenbaum, S. Imai, S.F. Vatner, J. Sadoshima, Silent information regulator 2alpha, a longevity factor and class III histone deacetylase, is an essential endogenous apoptosis inhibitor in cardiac myocytes, *Circ Res* 95 (2004) 971-980.
- [79] V. Muth, S. Nadaud, I. Grummt, R. Voit, Acetylation of TAF(I)68, a subunit of TIF-IB/SL1, activates RNA polymerase I transcription, *EMBO J* 20 (2001) 1353-1362.

- [80] B.J. North, E. Verdin, Interphase nucleo-cytoplasmic shuttling and localization of SIRT2 during mitosis, *PLoS One* 2 (2007) e784.
- [81] A. Vaquero, M.B. Scher, D.H. Lee, A. Sutton, H.L. Cheng, F.W. Alt, L. Serrano, R. Sternglanz, D. Reinberg, SirT2 is a histone deacetylase with preference for histone H4 Lys 16 during mitosis, *Genes Dev* 20 (2006) 1256-1261.
- [82] M.T. Borra, F.J. O'Neill, M.D. Jackson, B. Marshall, E. Verdin, K.R. Foltz, J.M. Denu, Conserved enzymatic production and biological effect of O-acetyl-ADP-ribose by silent information regulator 2-like NAD⁺-dependent deacetylases, *J Biol Chem* 277 (2002) 12632-12641.
- [83] V. Lennerz, M. Fatho, C. Gentilini, R.A. Frye, A. Lifke, D. Ferel, C. Wolfel, C. Huber, T. Wolfel, The response of autologous T cells to a human melanoma is dominated by mutated neoantigens, *Proc Natl Acad Sci U S A* 102 (2005) 16013-16018.
- [84] M. Hiratsuka, T. Inoue, T. Toda, N. Kimura, Y. Shirayoshi, H. Kamitani, T. Watanabe, E. Ohama, C.G. Tahimic, A. Kurimasa, M. Oshimura, Proteomics-based identification of differentially expressed genes in human gliomas: down-regulation of SIRT2 gene, *Biochem Biophys Res Commun* 309 (2003) 558-566.
- [85] T. Inoue, M. Hiratsuka, M. Osaki, H. Yamada, I. Kishimoto, S. Yamaguchi, S. Nakano, M. Katoh, H. Ito, M. Oshimura, SIRT2, a tubulin deacetylase, acts to block the entry to chromosome condensation in response to mitotic stress, *Oncogene* 26 (2007) 945-957.
- [86] W. Li, B. Zhang, J. Tang, Q. Cao, Y. Wu, C. Wu, J. Guo, E.A. Ling, F. Liang, Sirtuin 2, a mammalian homolog of yeast silent information regulator-2 longevity regulator, is an oligodendroglial protein that decelerates cell differentiation through deacetylating alpha-tubulin, *J Neurosci* 27 (2007) 2606-2616.
- [87] K. Suzuki, T. Koike, Mammalian Sir2-related protein (SIRT) 2-mediated modulation of resistance to axonal degeneration in slow Wallerian degeneration mice: a crucial role of tubulin deacetylation, *Neuroscience* 147 (2007) 599-612.
- [88] T.F. Outeiro, E. Kontopoulos, S.M. Altmann, I. Kufareva, K.E. Strathearn, A.M. Amore, C.B. Volk, M.M. Maxwell, J.C. Rochet, P.J. McLean, A.B. Young, R. Abagyan, M.B. Feany, B.T. Hyman, A.G. Kazantsev, Sirtuin 2 inhibitors rescue alpha-synuclein-mediated toxicity in models of Parkinson's disease, *Science* 317 (2007) 516-519.
- [89] F. Wang, Q. Tong, SIRT2 suppresses adipocyte differentiation by deacetylating FOXO1 and enhancing FOXO1's repressive interaction with PPARgamma, *Mol Biol Cell* 20 (2009) 801-808.
- [90] E. Jing, S. Gesta, C.R. Kahn, SIRT2 regulates adipocyte differentiation through FoxO1 acetylation/deacetylation, *Cell Metab* 6 (2007) 105-114.
- [91] B. Schwer, B.J. North, R.A. Frye, M. Ott, E. Verdin, The human silent information regulator (Sir)2 homologue hSIRT3 is a mitochondrial nicotinamide adenine dinucleotide-dependent deacetylase, *J Cell Biol* 158 (2002) 647-657.
- [92] D.B. Lombard, F.W. Alt, H.L. Cheng, J. Bunkenborg, R.S. Streeper, R. Mostoslavsky, J. Kim, G. Yancopoulos, D. Valenzuela, A. Murphy, Y. Yang, Y. Chen, M.D. Hirschey, R.T. Bronson, M. Haigis, L.P. Guarente, R.V. Farese, Jr., S. Weissman, E. Verdin, B. Schwer, Mammalian Sir2 homolog SIRT3 regulates global mitochondrial lysine acetylation, *Mol Cell Biol* 27 (2007) 8807-8814.
- [93] P. Onyango, I. Celic, J.M. McCaffery, J.D. Boeke, A.P. Feinberg, SIRT3, a human SIR2 homologue, is an NAD-dependent deacetylase localized to mitochondria, *Proc Natl Acad Sci U S A* 99 (2002) 13653-13658.
- [94] N.R. Sundaresan, S.A. Samant, V.B. Pillai, S.B. Rajamohan, M.P. Gupta, SIRT3 is a stress-responsive deacetylase in cardiomyocytes that protects cells from stress-mediated cell death by deacetylation of Ku70, *Mol Cell Biol* 28 (2008) 6384-6401.
- [95] M.B. Scher, A. Vaquero, D. Reinberg, SirT3 is a nuclear NAD⁺-dependent histone deacetylase that translocates to the mitochondria upon cellular stress, *Genes Dev* 21 (2007) 920-928.
- [96] Y. Nakamura, M. Ogura, D. Tanaka, N. Inagaki, Localization of mouse mitochondrial SIRT proteins: shift of SIRT3 to nucleus by co-expression with SIRT5, *Biochem Biophys Res Commun* 366 (2008) 174-179.

- [97] T. Shi, F. Wang, E. Stieren, Q. Tong, SIRT3, a mitochondrial sirtuin deacetylase, regulates mitochondrial function and thermogenesis in brown adipocytes, *J Biol Chem* 280 (2005) 13560-13567.
- [98] S.C. Kim, R. Sprung, Y. Chen, Y. Xu, H. Ball, J. Pei, T. Cheng, Y. Kho, H. Xiao, L. Xiao, N.V. Grishin, M. White, X.J. Yang, Y. Zhao, Substrate and functional diversity of lysine acetylation revealed by a proteomics survey, *Mol Cell* 23 (2006) 607-618.
- [99] C. Choudhary, C. Kumar, F. Gnad, M.L. Nielsen, M. Rehman, T.C. Walther, J.V. Olsen, M. Mann, Lysine acetylation targets protein complexes and co-regulates major cellular functions, *Science* 325 (2009) 834-840.
- [100] J. Zhang, R. Sprung, J. Pei, X. Tan, S. Kim, H. Zhu, C.F. Liu, N.V. Grishin, Y. Zhao, Lysine acetylation is a highly abundant and evolutionarily conserved modification in *Escherichia coli*, *Mol Cell Proteomics* 8 (2009) 215-225.
- [101] W.C. Hallows, S. Lee, J.M. Denu, Sirtuins deacetylate and activate mammalian acetyl-CoA synthetases, *Proc Natl Acad Sci U S A* 103 (2006) 10230-10235.
- [102] B. Schwer, J. Bunkenborg, R.O. Verdin, J.S. Andersen, E. Verdin, Reversible lysine acetylation controls the activity of the mitochondrial enzyme acetyl-CoA synthetase 2, *Proc Natl Acad Sci U S A* 103 (2006) 10224-10229.
- [103] I. Sakakibara, T. Fujino, M. Ishii, T. Tanaka, T. Shimosawa, S. Miura, W. Zhang, Y. Tokutake, J. Yamamoto, M. Awano, S. Iwasaki, T. Motoike, M. Okamura, T. Inagaki, K. Kita, O. Ezaki, M. Naito, T. Kuwaki, S. Chohnan, T.T. Yamamoto, R.E. Hammer, T. Kodama, M. Yanagisawa, J. Sakai, Fasting-induced hypothermia and reduced energy production in mice lacking acetyl-CoA synthetase 2, *Cell Metab* 9 (2009) 191-202.
- [104] B.H. Ahn, H.S. Kim, S. Song, I.H. Lee, J. Liu, A. Vassilopoulos, C.X. Deng, T. Finkel, A role for the mitochondrial deacetylase Sirt3 in regulating energy homeostasis, *Proc Natl Acad Sci U S A* 105 (2008) 14447-14452.
- [105] H. Cimen, M.J. Han, Y. Yang, Q. Tong, H. Koc, E.C. Koc, Regulation of succinate dehydrogenase activity by SIRT3 in mammalian mitochondria, *Biochemistry* 49 (2010) 304-311.
- [106] C. Schlicker, M. Gertz, P. Papatheodorou, B. Kachholz, C.F. Becker, C. Steegborn, Substrates and regulation mechanisms for the human mitochondrial sirtuins Sirt3 and Sirt5, *J Mol Biol* 382 (2008) 790-801.
- [107] M.D. Hirschey, T. Shimazu, E. Goetzman, E. Jing, B. Schwer, D.B. Lombard, C.A. Grueter, C. Harris, S. Biddinger, O.R. Ilkayeva, R.D. Stevens, Y. Li, A.K. Saha, N.B. Ruderman, J.R. Bain, C.B. Newgard, R.V. Farese, Jr., F.W. Alt, C.R. Kahn, E. Verdin, SIRT3 regulates mitochondrial fatty-acid oxidation by reversible enzyme deacetylation, *Nature* 464 (2010) 121-125.
- [108] H. Yang, T. Yang, J.A. Baur, E. Perez, T. Matsui, J.J. Carmona, D.W. Lamming, N.C. Souza-Pinto, V.A. Bohr, A. Rosenzweig, R. de Cabo, A.A. Sauve, D.A. Sinclair, Nutrient-sensitive mitochondrial NAD⁺ levels dictate cell survival, *Cell* 130 (2007) 1095-1107.
- [109] H.S. Kim, K. Patel, K. Muldoon-Jacobs, K.S. Bisht, N. Aykin-Burns, J.D. Pennington, R. van der Meer, P. Nguyen, J. Savage, K.M. Owens, A. Vassilopoulos, O. Ozden, S.H. Park, K.K. Singh, S.A. Abdulkadir, D.R. Spitz, C.X. Deng, D. Gius, SIRT3 is a mitochondria-localized tumor suppressor required for maintenance of mitochondrial integrity and metabolism during stress, *Cancer Cell* 17 (2010) 41-52.
- [110] D. Bellizzi, S. Dato, P. Cavalcante, G. Covello, F. Di Cianni, G. Passarino, G. Rose, G. De Benedictis, Characterization of a bidirectional promoter shared between two human genes related to aging: SIRT3 and PSMD13, *Genomics* 89 (2007) 143-150.
- [111] D. Bellizzi, G. Rose, P. Cavalcante, G. Covello, S. Dato, F. De Rango, V. Greco, M. Maggiolini, E. Feraco, V. Mari, C. Franceschi, G. Passarino, G. De Benedictis, A novel VNTR enhancer within the SIRT3 gene, a human homologue of SIR2, is associated with survival at oldest ages, *Genomics* 85 (2005) 258-263.
- [112] C.A. Stanley, Hyperinsulinism/hyperammonemia syndrome: insights into the regulatory role of glutamate dehydrogenase in ammonia metabolism, *Mol Genet Metab* 81 Suppl 1 (2004) S45-51.
- [113] B.J. North, B. Schwer, N. Ahuja, B. Marshall, E. Verdin, Preparation of enzymatically active recombinant class III protein deacetylases, *Methods* 36 (2005) 338-345.

- [114] T. Nakagawa, D.J. Lomb, M.C. Haigis, L. Guarente, SIRT5 Deacetylates carbamoyl phosphate synthetase 1 and regulates the urea cycle, *Cell* 137 (2009) 560-570.
- [115] D. Haussinger, Nitrogen metabolism in liver: structural and functional organization and physiological relevance, *Biochem J* 267 (1990) 281-290.
- [116] A.J. Meijer, W.H. Lamers, R.A. Chamuleau, Nitrogen metabolism and ornithine cycle function, *Physiol Rev* 70 (1990) 701-748.
- [117] R.T. Schimke, Differential effects of fasting and protein-free diets on levels of urea cycle enzymes in rat liver, *J Biol Chem* 237 (1962) 1921-1924.
- [118] J.E. Sulston, E. Schierenberg, J.G. White, J.N. Thomson, The embryonic cell lineage of the nematode *Caenorhabditis elegans*, *Dev Biol* 100 (1983) 64-119.
- [119] J. Ahringer, Reverse Genetics, *WormBook* (2006) 1-43.
- [120] A. Berdichevsky, M. Viswanathan, H.R. Horvitz, L. Guarente, *C. elegans* SIR-2.1 interacts with 14-3-3 proteins to activate DAF-16 and extend life span, *Cell* 125 (2006) 1165-1177.
- [121] Y. Wang, S.W. Oh, B. Deplancke, J. Luo, A.J. Walhout, H.A. Tissenbaum, *C. elegans* 14-3-3 proteins regulate life span and interact with SIR-2.1 and DAF-16/FOXO, *Mech Ageing Dev* 127 (2006) 741-747.
- [122] Y. Wang, H.A. Tissenbaum, Overlapping and distinct functions for a *Caenorhabditis elegans* SIR2 and DAF-16/FOXO, *Mech Ageing Dev* 127 (2006) 48-56.
- [123] M.A. Jedrusik, E. Schulze, Telomeric position effect variegation in *Saccharomyces cerevisiae* by *Caenorhabditis elegans* linker histones suggests a mechanistic connection between germ line and telomeric silencing, *Mol Cell Biol* 23 (2003) 3681-3691.
- [124] M.A. Jedrusik, E. Schulze, Linker histone HIS-24 (H1.1) cytoplasmic retention promotes germ line development and influences histone H3 methylation in *Caenorhabditis elegans*, *Mol Cell Biol* 27 (2007) 2229-2239.
- [125] M. Wirth, F. Paap, W. Fischle, D. Wenzel, D.E. Agafonov, T.R. Samatov, J.R. Wisniewski, M. Jedrusik-Bode, HIS-24 linker histone and SIR-2.1 deacetylase induce H3K27me3 in the *Caenorhabditis elegans* germ line, *Mol Cell Biol* 29 (2009) 3700-3709.
- [126] S. Greiss, J. Hall, S. Ahmed, A. Gartner, *C. elegans* SIR-2.1 translocation is linked to a proapoptotic pathway parallel to cep-1/p53 during DNA damage-induced apoptosis, *Genes Dev* 22 (2008) 2831-2842.
- [127] E.A. Bates, M. Victor, A.K. Jones, Y. Shi, A.C. Hart, Differential contributions of *Caenorhabditis elegans* histone deacetylases to huntingtin polyglutamine toxicity, *J Neurosci* 26 (2006) 2830-2838.
- [128] N. Bizat, J.M. Peyrin, S. Haik, V. Cochois, P. Beaudry, J.L. Laplanche, C. Neri, Neuron dysfunction is induced by prion protein with an insertional mutation via a Fyn kinase and reversed by sirtuin activation in *Caenorhabditis elegans*, *J Neurosci* 30 (2010) 5394-5403.
- [129] J. Pothof, G. van Haaften, K. Thijssen, R.S. Kamath, A.G. Fraser, J. Ahringer, R.H. Plasterk, M. Tijsterman, Identification of genes that protect the *C. elegans* genome against mutations by genome-wide RNAi, *Genes Dev* 17 (2003) 443-448.
- [130] W. Mair, S.H. Panowski, R.J. Shaw, A. Dillin, Optimizing dietary restriction for genetic epistasis analysis and gene discovery in *C. elegans*, *PLoS One* 4 (2009) e4535.
- [131] N.D.L.a.C. M.M., *Lehninger Principles of Biochemistry* (4th edition), W. H. Freeman 2005.
- [132] A.A. Sauve, NAD⁺ and vitamin B3: from metabolism to therapies, *J Pharmacol Exp Ther* 324 (2008) 883-893.
- [133] J.J. Sandmeier, I. Celic, J.D. Boeke, J.S. Smith, Telomeric and rDNA silencing in *Saccharomyces cerevisiae* are dependent on a nuclear NAD(+) salvage pathway, *Genetics* 160 (2002) 877-889.
- [134] R.M. Anderson, K.J. Bitterman, J.G. Wood, O. Medvedik, H. Cohen, S.S. Lin, J.K. Manchester, J.I. Gordon, D.A. Sinclair, Manipulation of a nuclear NAD⁺ salvage pathway delays aging without altering steady-state NAD⁺ levels, *J Biol Chem* 277 (2002) 18881-18890.
- [135] A. van der Horst, J.M. Schavemaker, W. Pellis-van Berkel, B.M. Burgering, The *Caenorhabditis elegans* nicotinamidase PNC-1 enhances survival, *Mech Ageing Dev* 128 (2007) 346-349.

- [136] J.W. Foster, Y.K. Park, T. Penfound, T. Fenger, M.P. Spector, Regulation of NAD metabolism in *Salmonella typhimurium*: molecular sequence analysis of the bifunctional nadR regulator and the nadA-pnuC operon, *J Bacteriol* 172 (1990) 4187-4196.
- [137] R.M. Anderson, K.J. Bitterman, J.G. Wood, O. Medvedik, D.A. Sinclair, Nicotinamide and PNC1 govern lifespan extension by calorie restriction in *Saccharomyces cerevisiae*, *Nature* 423 (2003) 181-185.
- [138] C.M. Gallo, D.L. Smith, Jr., J.S. Smith, Nicotinamide clearance by Pnc1 directly regulates Sir2-mediated silencing and longevity, *Mol Cell Biol* 24 (2004) 1301-1312.
- [139] L. Virag, C. Szabo, The therapeutic potential of poly(ADP-ribose) polymerase inhibitors, *Pharmacol Rev* 54 (2002) 375-429.
- [140] E.A. Gale, P.J. Bingley, C.L. Emmett, T. Collier, European Nicotinamide Diabetes Intervention Trial (ENDIT): a randomised controlled trial of intervention before the onset of type 1 diabetes, *Lancet* 363 (2004) 925-931.
- [141] T.M. Jackson, J.M. Rawling, B.D. Roebuck, J.B. Kirkland, Large supplements of nicotinic acid and nicotinamide increase tissue NAD⁺ and poly(ADP-ribose) levels but do not affect diethylnitrosamine-induced altered hepatic foci in Fischer-344 rats, *J Nutr* 125 (1995) 1455-1461.
- [142] A.C. Boyonoski, J.C. Spronck, R.M. Jacobs, G.M. Shah, G.G. Poirier, J.B. Kirkland, Pharmacological intakes of niacin increase bone marrow poly(ADP-ribose) and the latency of ethylnitrosourea-induced carcinogenesis in rats, *J Nutr* 132 (2002) 115-120.
- [143] S. Imai, The NAD World: a new systemic regulatory network for metabolism and aging--Sirt1, systemic NAD biosynthesis, and their importance, *Cell Biochem Biophys* 53 (2009) 65-74.
- [144] I.E. Scheffler, A century of mitochondrial research: achievements and perspectives, *Mitochondrion* 1 (2001) 3-31.
- [145] B. Van Houten, V. Woshner, J.H. Santos, Role of mitochondrial DNA in toxic responses to oxidative stress, *DNA Repair (Amst)* 5 (2006) 145-152.
- [146] S. Zhao, W. Xu, W. Jiang, W. Yu, Y. Lin, T. Zhang, J. Yao, L. Zhou, Y. Zeng, H. Li, Y. Li, J. Shi, W. An, S.M. Hancock, F. He, L. Qin, J. Chin, P. Yang, X. Chen, Q. Lei, Y. Xiong, K.L. Guan, Regulation of cellular metabolism by protein lysine acetylation, *Science* 327 (2010) 1000-1004.
- [147] Q. Wang, Y. Zhang, C. Yang, H. Xiong, Y. Lin, J. Yao, H. Li, L. Xie, W. Zhao, Y. Yao, Z.B. Ning, R. Zeng, Y. Xiong, K.L. Guan, S. Zhao, G.P. Zhao, Acetylation of metabolic enzymes coordinates carbon source utilization and metabolic flux, *Science* 327 (2010) 1004-1007.
- [148] B. Schwer, M. Eckersdorff, Y. Li, J.C. Silva, D. Fermin, M.V. Kurtev, C. Giallourakis, M.J. Comb, F.W. Alt, D.B. Lombard, Calorie restriction alters mitochondrial protein acetylation, *Aging Cell* 8 (2009) 604-606.
- [149] M.W. Gray, G. Burger, B.F. Lang, Mitochondrial evolution, *Science* 283 (1999) 1476-1481.
- [150] B.J. Yu, J.A. Kim, J.H. Moon, S.E. Ryu, J.G. Pan, The diversity of lysine-acetylated proteins in *Escherichia coli*, *J Microbiol Biotechnol* 18 (2008) 1529-1536.
- [151] V.J. Starai, J.C. Escalante-Semerena, Identification of the protein acetyltransferase (Pat) enzyme that acetylates acetyl-CoA synthetase in *Salmonella enterica*, *J Mol Biol* 340 (2004) 1005-1012.
- [152] V.J. Starai, I. Celic, R.N. Cole, J.D. Boeke, J.C. Escalante-Semerena, Sir2-dependent activation of acetyl-CoA synthetase by deacetylation of active lysine, *Science* 298 (2002) 2390-2392.
- [153] V.J. Starai, H. Takahashi, J.D. Boeke, J.C. Escalante-Semerena, Short-chain fatty acid activation by acyl-coenzyme A synthetases requires SIR2 protein function in *Salmonella enterica* and *Saccharomyces cerevisiae*, *Genetics* 163 (2003) 545-555.
- [154] G. Ramponi, G. Manao, G. Camici, Nonenzymatic acetylation of histones with acetyl phosphate and acetyl adenylate, *Biochemistry* 14 (1975) 2681-2685.
- [155] W.K. Paik, D. Pearson, H.W. Lee, S. Kim, Nonenzymatic acetylation of histones with acetyl-CoA, *Biochim Biophys Acta* 213 (1970) 513-522.
- [156] N. Koester-Eiserfunke, Characterization of Lin-61 methyl mark binding and its function in *C. elegans* vulva development. , PhD thesis in the Group of Chromatin Biochemistry (Goettingen, Max Planck Institute of Biophysical Chemistry) (2010).

- [157] C.C. Mello, J.M. Kramer, D. Stinchcomb, V. Ambros, Efficient gene transfer in *C.elegans*: extrachromosomal maintenance and integration of transforming sequences, *EMBO J* 10 (1991) 3959-3970.
- [158] S. Brenner, The genetics of *Caenorhabditis elegans*, *Genetics* 77 (1974) 71-94.
- [159] R. Hunt-Newbury, R. Viveiros, R. Johnsen, A. Mah, D. Anastas, L. Fang, E. Halfnight, D. Lee, J. Lin, A. Lorch, S. McKay, H.M. Okada, J. Pan, A.K. Schulz, D. Tu, K. Wong, Z. Zhao, A. Alexeyenko, T. Burglin, E. Sonnhammer, R. Schnabel, S.J. Jones, M.A. Marra, D.L. Baillie, D.G. Moerman, High-throughput in vivo analysis of gene expression in *Caenorhabditis elegans*, *PLoS Biol* 5 (2007) e237.
- [160] S.J. McKay, R. Johnsen, J. Khattra, J. Asano, D.L. Baillie, S. Chan, N. Dube, L. Fang, B. Goszczynski, E. Ha, E. Halfnight, R. Hollebakk, P. Huang, K. Hung, V. Jensen, S.J. Jones, H. Kai, D. Li, A. Mah, M. Marra, J. McGhee, R. Newbury, A. Pouzyrev, D.L. Riddle, E. Sonnhammer, H. Tian, D. Tu, J.R. Tyson, G. Vatcher, A. Warner, K. Wong, Z. Zhao, D.G. Moerman, Gene expression profiling of cells, tissues, and developmental stages of the nematode *C. elegans*, *Cold Spring Harb Symp Quant Biol* 68 (2003) 159-169.
- [161] D. Dupuy, N. Bertin, C.A. Hidalgo, K. Venkatesan, D. Tu, D. Lee, J. Rosenberg, N. Svrzikapa, A. Blanc, A. Carnec, A.R. Carvunis, R. Pulak, J. Shingles, J. Reece-Hoyes, R. Hunt-Newbury, R. Viveiros, W.A. Mohler, M. Tasan, F.P. Roth, C. Le Peuch, I.A. Hope, R. Johnsen, D.G. Moerman, A.L. Barabasi, D. Baillie, M. Vidal, Genome-scale analysis of in vivo spatiotemporal promoter activity in *Caenorhabditis elegans*, *Nat Biotechnol* 25 (2007) 663-668.
- [162] C. Benedetti, C.M. Haynes, Y. Yang, H.P. Harding, D. Ron, Ubiquitin-like protein 5 positively regulates chaperone gene expression in the mitochondrial unfolded protein response, *Genetics* 174 (2006) 229-239.
- [163] I. New England Biolabs, Catalog and technical reference. 2007/2008.
- [164] J.a.R. Sambrook, D. , Molecular Cloning. A laboratory Manual. , Cold Spring Harbour, New York: Cold Spring Harbour press 3rd ed. (2001).
- [165] A.S. Spirin, and J. R. Swartz (ed.), Cell-free protein synthesis: methods and protocols, Wiley-VCH Verlag GmbH, Weinheim, Germany (2008).
- [166] U.K. Laemmli, Cleavage of structural proteins during the assembly of the head of bacteriophage T4, *Nature* 227 (1970) 680-685.
- [167] S.R. Gallagher, One-dimensional SDS gel electrophoresis of proteins, *Curr Protoc Immunol* Chapter 8 (2006) Unit 8 4.
- [168] A. Shevchenko, M. Wilm, O. Vorm, M. Mann, Mass spectrometric sequencing of proteins silver-stained polyacrylamide gels, *Anal Chem* 68 (1996) 850-858.
- [169] F.W. Studier, Protein production by auto-induction in high density shaking cultures, *Protein Expr Purif* 41 (2005) 207-234.
- [170] K. Luger, T.J. Rechsteiner, T.J. Richmond, Preparation of nucleosome core particle from recombinant histones, *Methods Enzymol* 304 (1999) 3-19.
- [171] D.E. Smith, P.A. Fisher, Identification, developmental regulation, and response to heat shock of two antigenically related forms of a major nuclear envelope protein in *Drosophila* embryos: application of an improved method for affinity purification of antibodies using polypeptides immobilized on nitrocellulose blots, *J Cell Biol* 99 (1984) 20-28.
- [172] J.S. Duerr, D.L. Frisby, J. Gaskin, A. Duke, K. Asermely, D. Huddleston, L.E. Eiden, J.B. Rand, The cat-1 gene of *Caenorhabditis elegans* encodes a vesicular monoamine transporter required for specific monoamine-dependent behaviors, *J Neurosci* 19 (1999) 72-84.
- [173] T. Stiernagle, Maintenance of *C. elegans*, *WormBook* (2006) 1-11.
- [174] T.C. Evans, Transformation and microinjection *WormBook*, The *C. elegans* Research Community (2006).
- [175] J.A.a.F.J.F. Lewis, Basic culture methods, *Methods in Cell Biology, Caenorhabditis elegans, Modern Biological Analysis of an Organism*, E. H. F. a. S. D. C., Editor. (1995).
- [176] J. Li, T. Cai, P. Wu, Z. Cui, X. Chen, J. Hou, Z. Xie, P. Xue, L. Shi, P. Liu, J.R. Yates, 3rd, F. Yang, Proteomic analysis of mitochondria from *Caenorhabditis elegans*, *Proteomics* 9 (2009) 4539-4553.

- [177] I.M. Cheeseman, S. Niessen, S. Anderson, F. Hyndman, J.R. Yates, 3rd, K. Oegema, A. Desai, A conserved protein network controls assembly of the outer kinetochore and its ability to sustain tension, *Genes Dev* 18 (2004) 2255-2268.
- [178] S. Gandre, A.M. van der Blik, Mitochondrial division in *Caenorhabditis elegans*, *Methods Mol Biol* 372 (2007) 485-501.
- [179] J.S. Duerr, Immunohistochemistry, *WormBook* (2006) 1-61.
- [180] D.T. Stinchcomb, J.E. Shaw, S.H. Carr, D. Hirsh, Extrachromosomal DNA transformation of *Caenorhabditis elegans*, *Mol Cell Biol* 5 (1985) 3484-3496.
- [181] C.a.F. Mello, A., DNA transformation, *Methods Cell Biol* 48 (1995) 451-482.
- [182] J.M. Kramer, R.P. French, E.C. Park, J.J. Johnson, The *Caenorhabditis elegans* *rol-6* gene, which interacts with the *sqt-1* collagen gene to determine organismal morphology, encodes a collagen, *Mol Cell Biol* 10 (1990) 2081-2089.
- [183] A. Fire, R.H. Waterston, Proper expression of myosin genes in transgenic nematodes, *EMBO J* 8 (1989) 3419-3428.
- [184] O. Hobert, PCR fusion-based approach to create reporter gene constructs for expression analysis in transgenic *C. elegans*, *Biotechniques* 32 (2002) 728-730.
- [185] T. Boulin, J.F. Etchberger, O. Hobert, Reporter gene fusions, *WormBook* (2006) 1-23.
- [186] M.A. Jedrusik, E. Schulze, Analysis of germline chromatin silencing by double-stranded RNA-mediated interference (RNAi) in *Caenorhabditis elegans*, *Methods Mol Biol* 254 (2004) 35-48.
- [187] L. Timmons, A. Fire, Specific interference by ingested dsRNA, *Nature* 395 (1998) 854.
- [188] L. Timmons, D.L. Court, A. Fire, Ingestion of bacterially expressed dsRNAs can produce specific and potent genetic interference in *Caenorhabditis elegans*, *Gene* 263 (2001) 103-112.
- [189] E.M. Hedgecock, J.G. Culotti, J.N. Thomson, L.A. Perkins, Axonal guidance mutants of *Caenorhabditis elegans* identified by filling sensory neurons with fluorescein dyes, *Dev Biol* 111 (1985) 158-170.
- [190] W. Liou, H.J. Geuze, J.W. Slot, Improving structural integrity of cryosections for immunogold labeling, *Histochem Cell Biol* 106 (1996) 41-58.
- [191] D. Wenzel, G. Schauermaun, A. von Lupke, G. Hinz, The cargo in vacuolar storage protein transport vesicles is stratified, *Traffic* 6 (2005) 45-55.
- [192] I. Masse, L. Molin, L. Mouchiroud, P. Vanhems, F. Palladino, M. Billaud, F. Solari, A novel role for the SMG-1 kinase in lifespan and oxidative stress resistance in *Caenorhabditis elegans*, *PLoS One* 3 (2008) e3354.
- [193] M.D. Hirschey, T. Shimazu, J.Y. Huang, E. Verdin, Acetylation of mitochondrial proteins, *Methods Enzymol* 457 (2009) 137-147.
- [194] E. Verdin, F. Dequiedt, W. Fischle, R. Frye, B. Marshall, B. North, Measurement of mammalian histone deacetylase activity, *Methods Enzymol* 377 (2004) 180-196.
- [195] G.B. Warren, K.F. Tipton, Pig liver pyruvate carboxylase. Purification, properties and cation specificity, *Biochem J* 139 (1974) 297-310.
- [196] P.G. Okkema, S.W. Harrison, V. Plunger, A. Aryana, A. Fire, Sequence requirements for myosin gene expression and regulation in *Caenorhabditis elegans*, *Genetics* 135 (1993) 385-404.
- [197] P.N. Inglis, G. Ou, M.R. Leroux, J.M. Scholey, The sensory cilia of *Caenorhabditis elegans*, *WormBook* (2007) 1-22.
- [198] F. Paap, Molekulare und funktionale Analyse der NAD⁺-abhaengigen Histon-Deacetylase SIR-2.4 in *C. elegans*, Diploma thesis in the group of Chromatin Biochemistry (Goettingen, Max Planck Institute of Biophysical Chemistry) (2008).
- [199] R.S. Balaban, S. Nemoto, T. Finkel, Mitochondria, oxidants, and aging, *Cell* 120 (2005) 483-495.
- [200] C. Kenyon, The plasticity of aging: insights from long-lived mutants, *Cell* 120 (2005) 449-460.
- [201] S. Jitrapakdee, A. Vidal-Puig, J.C. Wallace, Anaplerotic roles of pyruvate carboxylase in mammalian tissues, *Cell Mol Life Sci* 63 (2006) 843-854.
- [202] R.A. Gravel, K.F. Lam, D. Mahuran, A. Kronis, Purification of human liver propionyl-CoA carboxylase by carbon tetrachloride extraction and monomeric avidin affinity chromatography, *Arch Biochem Biophys* 201 (1980) 669-673.

- [203] S. Jitrapakdee, J.C. Wallace, The biotin enzyme family: conserved structural motifs and domain rearrangements, *Curr Protein Pept Sci* 4 (2003) 217-229.
- [204] E.P. Lau, B.C. Cochran, R.R. Fall, Isolation of 3-methylcrotonyl-coenzyme A carboxylase from bovine kidney, *Arch Biochem Biophys* 205 (1980) 352-359.
- [205] S. Jitrapakdee, M. St Maurice, I. Rayment, W.W. Cleland, J.C. Wallace, P.V. Attwood, Structure, mechanism and regulation of pyruvate carboxylase, *Biochem J* 413 (2008) 369-387.
- [206] S.E. Mango, The *C. elegans* pharynx: a model for organogenesis, *WormBook* (2007) 1-26.
- [207] J.D. McGhee, The *C. elegans* intestine, *WormBook* (2007) 1-36.
- [208] S.B. Pierce, M. Costa, R. Wisotzkey, S. Devadhar, S.A. Homburger, A.R. Buchman, K.C. Ferguson, J. Heller, D.M. Platt, A.A. Pasquinelli, L.X. Liu, S.K. Doberstein, G. Ruvkun, Regulation of DAF-2 receptor signaling by human insulin and ins-1, a member of the unusually large and diverse *C. elegans* insulin gene family, *Genes Dev* 15 (2001) 672-686.
- [209] D.G. Moerman, B.D. Williams, Sarcomere assembly in *C. elegans* muscle, *WormBook* (2006) 1-16.
- [210] M. Lynch, J.S. Conery, The evolutionary fate and consequences of duplicate genes, *Science* 290 (2000) 1151-1155.
- [211] A. Woollard, Gene duplications and genetic redundancy in *C. elegans*, *WormBook* (2005) 1-6.
- [212] J.H. Thomas, Thinking about genetic redundancy, *Trends Genet* 9 (1993) 395-399.
- [213] O. Lespinet, Y.I. Wolf, E.V. Koonin, L. Aravind, The role of lineage-specific gene family expansion in the evolution of eukaryotes, *Genome Res* 12 (2002) 1048-1059.
- [214] J.R. Revollo, A.A. Grimm, S. Imai, The NAD biosynthesis pathway mediated by nicotinamide phosphoribosyltransferase regulates Sir2 activity in mammalian cells, *J Biol Chem* 279 (2004) 50754-50763.
- [215] N.R. Sundaresan, M. Gupta, G. Kim, S.B. Rajamohan, A. Isbatan, M.P. Gupta, Sirt3 blocks the cardiac hypertrophic response by augmenting Foxo3a-dependent antioxidant defense mechanisms in mice, *J Clin Invest* 119 (2009) 2758-2771.
- [216] X. Kong, R. Wang, Y. Xue, X. Liu, H. Zhang, Y. Chen, F. Fang, Y. Chang, Sirtuin 3, a new target of PGC-1alpha, plays an important role in the suppression of ROS and mitochondrial biogenesis, *PLoS One* 5 (2010) e11707.
- [217] F. Weinberg, N.S. Chandel, Reactive oxygen species-dependent signaling regulates cancer, *Cell Mol Life Sci* 66 (2009) 3663-3673.
- [218] K.K. Singh, Mitochondria damage checkpoint in apoptosis and genome stability, *FEMS Yeast Res* 5 (2004) 127-132.
- [219] A.B. Leiter, M. Weinberg, F. Isohashi, M.F. Utter, Relationship between phosphorylation and activity of pyruvate dehydrogenase in rat liver mitochondria and the absence of such a relationship for pyruvate carboxylase, *J Biol Chem* 253 (1978) 2716-2723.
- [220] V. Large, M. Beylot, Modifications of citric acid cycle activity and gluconeogenesis in streptozotocin-induced diabetes and effects of metformin, *Diabetes* 48 (1999) 1251-1257.
- [221] K. Hagopian, J.J. Ramsey, R. Weindruch, Caloric restriction increases gluconeogenic and transaminase enzyme activities in mouse liver, *Exp Gerontol* 38 (2003) 267-278.
- [222] M.J. MacDonald, Feasibility of a mitochondrial pyruvate malate shuttle in pancreatic islets. Further implication of cytosolic NADPH in insulin secretion, *J Biol Chem* 270 (1995) 20051-20058.
- [223] O.E. Owen, S.C. Kalhan, R.W. Hanson, The key role of anaplerosis and cataplerosis for citric acid cycle function, *J Biol Chem* 277 (2002) 30409-30412.
- [224] M.E. Bizeau, C. Short, J.S. Thresher, S.R. Commerford, W.T. Willis, M.J. Pagliassotti, Increased pyruvate flux capacities account for diet-induced increases in gluconeogenesis in vitro, *Am J Physiol Regul Integr Comp Physiol* 281 (2001) R427-433.
- [225] K. Hagopian, J.J. Ramsey, R. Weindruch, Krebs cycle enzymes from livers of old mice are differentially regulated by caloric restriction, *Exp Gerontol* 39 (2004) 1145-1154.
- [226] S. Jitrapakdee, A. Wutthisathapornchai, J.C. Wallace, M.J. MacDonald, Regulation of insulin secretion: role of mitochondrial signalling, *Diabetologia* 53 (2010) 1019-1032.
- [227] M.J. MacDonald, L.A. Fahien, L.J. Brown, N.M. Hasan, J.D. Buss, M.A. Kendrick, Perspective: emerging evidence for signaling roles of mitochondrial anaplerotic products in insulin secretion, *Am J Physiol Endocrinol Metab* 288 (2005) E1-15.

- [228] S. Farfari, V. Schulz, B. Corkey, M. Prentki, Glucose-regulated anaplerosis and cataplerosis in pancreatic beta-cells: possible implication of a pyruvate/citrate shuttle in insulin secretion, *Diabetes* 49 (2000) 718-726.
- [229] D. Lu, H. Mulder, P. Zhao, S.C. Burgess, M.V. Jensen, S. Kamzolova, C.B. Newgard, A.D. Sherry, ¹³C NMR isotopomer analysis reveals a connection between pyruvate cycling and glucose-stimulated insulin secretion (GSIS), *Proc Natl Acad Sci U S A* 99 (2002) 2708-2713.
- [230] L.A. Fahien, M.J. MacDonald, The succinate mechanism of insulin release, *Diabetes* 51 (2002) 2669-2676.
- [231] R.G. Kibbey, R.L. Pongratz, A.J. Romanelli, C.B. Wollheim, G.W. Cline, G.I. Shulman, Mitochondrial GTP regulates glucose-stimulated insulin secretion, *Cell Metab* 5 (2007) 253-264.
- [232] L.A. Fahien, M.J. MacDonald, E.H. Kmiotek, R.J. Mertz, C.M. Fahien, Regulation of insulin release by factors that also modify glutamate dehydrogenase, *J Biol Chem* 263 (1988) 13610-13614.
- [233] C. MacMullen, J. Fang, B.Y. Hsu, A. Kelly, P. de Lonlay-Debeney, J.M. Saudubray, A. Ganguly, T.J. Smith, C.A. Stanley, Hyperinsulinism/hyperammonemia syndrome in children with regulatory mutations in the inhibitory guanosine triphosphate-binding domain of glutamate dehydrogenase, *J Clin Endocrinol Metab* 86 (2001) 1782-1787.
- [234] M.J. MacDonald, M.J. Longacre, E.C. Langberg, A. Tibell, M.A. Kendrick, T. Fukao, C.G. Ostenson, Decreased levels of metabolic enzymes in pancreatic islets of patients with type 2 diabetes, *Diabetologia* 52 (2009) 1087-1091.
- [235] J. Yang, Y. Chi, B.R. Burkhardt, Y. Guan, B.A. Wolf, Leucine metabolism in regulation of insulin secretion from pancreatic beta cells, *Nutr Rev* 68 (2010) 270-279.
- [236] L. Bordone, L. Guarente, Sirtuins and beta-cell function, *Diabetes Obes Metab* 9 Suppl 2 (2007) 23-27.

Curriculum vitae

Personal information

Name: Martina Barbara Wirth
Date of birth: 17.01.1982
Place of birth: Lauingen a.d. Donau, Germany
Nationality: German

Education

1988-1992 Volksschule Bissingen (primary school)
1992-2001 Theodor-Heuss Gymnasium Nördlingen
06/2001 Theodor-Heuss Gymnasium Nördlingen
Abitur

10/2002-08/2005 Biochemistry (Bachelor of Science)
Technical University of Munich
Bachelor thesis: "ChIP analysis of STATs in macrophages"

since 10/2005 Molecular Biology
(International Max Planck Research School, MSc/PhD Program)
Georg-August-University Göttingen

since 10/2006 PhD thesis project at the Max Planck Institute for Biophysical
Chemistry, Göttingen
Thesis supervisors: Dr. W. Fischle and Dr. M. Jedrusik-Bode

Stipends

10/2005-08/2006 Stipend of the International Max Planck Research School
Georg-August-University Göttingen

International Conferences

16th International *C. elegans* Meeting, June 2007, University of California, Los Angeles, CA, USA
(Epigenome Network of Excellence travel award)

4th International PhD Student Symposium "Horizons in Molecular Biology", September 2007,
Göttingen, Germany (Organizer)

59th Mosbacher Kolloquium on "Epigenetics - Molecular Principles and Mechanisms", March 2008,
Mosbach, Germany

5th International PhD Student Symposium "Horizons in Molecular Biology", September 2008,
Göttingen, Germany (Organizer)

“Development Now”, Prof. Alvin Kaye Student-Hosted Meetings, March 2009, Weizmann Institute, Rehovot, Israel

6th International PhD Student Symposium "Horizons in Molecular Biology", September 2009, Göttingen, Germany (Organizer)

61st Mosbacher Kolloquium on "The Biology of Aging: Mechanisms and Intervention", April 2010, Mosbach, Germany

7th International PhD Student Symposium "Horizons in Molecular Biology", September 2010, Göttingen, Germany

Practical Work experience

08/2003-09/2003	Practical work Max Planck Institute for Biochemistry, Department of Structure Research, Prof. Dr. R. Huber, supervised by Dr. T. Krojer
03/2004-06/2004	Project work and student assistant Technical University of Munich, Institute of Organic Chemistry and Biochemistry, Prof. Dr. A. Bacher, supervised by Dr. B. Illarionov
08/2004-09/2004	Practical work Technical University of Munich, Institute for Medical Microbiology, Immunology and Hygiene, Prof. Dr. H. Wagner, supervised by Dr. R. Lang
04/2005-07/2005	Bachelor thesis Technical University of Munich, Institute for Medical Microbiology, Immunology and Hygiene, Prof. Dr. H. Wagner, supervised by Dr. R. Lang
01/2006-02/2006	Lab rotation Georg-August-University Göttingen, DFG Research Center for Molecular Physiology of the Brain (CMPB), Dr. D. Klopfenstein, supervised by Dr. O. Wagner
02/2006-04/2006	Lab rotation Georg-August-University Göttingen, Institute for Medical Microbiology, Prof. Dr. U. Gross, supervised by Prof. C. Lüder
05/2006-06/2006	Lab rotation Max Planck Institute for Biophysical Chemistry, Chromatin Biochemistry Group, Dr. W. Fischle, supervised by Dr. M. Jedrusik-Bode

Non-Scientific Activities

09/2001-05/2002 Work and Travel in Australia